Molecular Interactions of Zinc with the Glycine Receptor

A dissertation submitted to the University of London for the degree of Doctor of Philosophy

By

Paul Steven Miller, B.Sc.(Hons)

Department of Pharmacology
Medical Sciences Building
University College London
Gower Street
London
WC1E 6BT

October 2004

UMI Number: U592189

All rights reserved

INFORMATION TO ALL USERS
The quality of this reproduction is dependent upon the quality of the copy submitted.

In the unlikely event that the author did not send a complete manuscript
and there are missing pages, these will be noted. Also, if material had to be removed,
a note will indicate the deletion.

UMI U592189
Published by ProQuest LLC 2013. Copyright in the Dissertation held by the Author.
Microform Edition © ProQuest LLC.
All rights reserved. This work is protected against
unauthorized copying under Title 17, United States Code.

ProQuest LLC
789 East Eisenhower Parkway
P.O. Box 1346
Ann Arbor, MI 48106-1346

In memory of my Grandfather

Abstract

The ionotropic receptors including nicotinic acetylcholine (nAChR), γ-aminobutyric acid type A and C ($GABA_{A/C}$), serotonin (5HT-3) and glycine receptors (GlyR) all comprise the cys-loop receptor family. A pentameric configuration is adopted by these receptors featuring a large extra cellular domain, four transmembrane (M) spanning domains and an intracellular compartment primarily contributed from the M3-4 loop. The recent advent of an X-ray crystal structure of the related ACh binding protein from snail, *Lymnaea stagnalis,* and an electron micrograph nearing atomic resolution of the transmembrane domains for the *Torpedo* nAChR provide the opportunity to homology model the structures of all cys-loop ligand-gated receptors and investigate critical elements of receptor function with unprecedented accuracy.

By using homology modelling to guide site-directed mutagenesis in combination with whole-cell patch clamp electrophysiology, molecular elements that mediate the biphasic modulation of glycine receptors by Zn^{2+} were investigated. The structure of a previously identified low sensitivity inhibitory Zn^{2+} site was clarified revealing critical determinants of GlyR subtype selectivity for Zn^{2+} mediated inhibition. Intriguingly these experiments also revealed a novel functional asymmetry at this site suggesting that one specific side of the site directs downstream transduction of the inhibitory Zn^{2+} effect. This enabled the elucidation of a hydrophobic pathway leading directly through the core of the GlyR from the inhibitory Zn^{2+} site to the agonist binding site suggesting a mechanism for Zn^{2+} mediated inhibition.

This study also investigated the structural basis for Zn^{2+} enhancement of GlyR function. A comparative study of GlyR α1 and α2 followed by a directed mutagenesis regional scan led to the identification of a complete and novel site for Zn^{2+} potentiation. Further studies also elucidated a potential mechanism of action for this site by identifying an important gating component of the GlyR, which exhibited a strong interaction with this novel potentiation site for Zn^{2+}.

These studies demonstrate the power of a homology modelling strategy to resolve key elements of cys-loop ligand-gated receptor function. Identifying and understanding receptor modulation by allosteric effectors is a key requisite to understanding receptor function. This work describes the key structural determinants involved in the biphasic Zn^{2+} modulation of GlyRs both in terms of actual binding sites and downstream effector mechanisms.

Contents

Chapter 2 – Materials and Methods

Chapter 3 - Molecular determinants of glycine receptor αβ subunit sensitivities to Zn^{2+} inhibition

Chapter 4 - Evidence for an allosteric transduction pathway across the extracellular domain of the glycine receptor

Chapter 5 - Identification of a Zn^{2+} potentiation site in glycine receptors and a mechanism of action involving the cys-loop gating domain

List of Tables

Chapter 1

Chapter 3

Chapter 4

Chapter 5

List of Figures

Chapter 1

Chapter 2

Chapter 3

Chapter 4

Chapter 5

Chapter 6

Chapter 1
Introduction

Inhibitory neurotransmission: The glycine receptor

Of all the molecules so far identified as neurotransmitters, the simplest is glycine. This achiral amino acid is vital for all known life and is the most basic building block of all amino acids. Despite its apparent simplicity glycine forms a critical component of many cellular proteins endowing peptide backbones with extra flexibility and unique functions. This simplicity is also able to code for multiple modes of neurotransmission. Glycine can act as an agonist for strychnine-sensitive inhibitory glycine receptors (Lynch, 2004) and as a co-agonist, or modulator, of excitatory N-methyl-D-aspartic acid (NMDA) receptors (Mayer and Armstrong, 2004). Furthermore, glycine is a crucial ingredient for many metabolic processes including nucleotide biosynthesis. With regards to mammals this molecule comes under the title of a non-essential amino acid as it can be synthesised within cells and is not required from the diet. This process requires the enzyme serine hydroxymethyl transferase, which acts on another amino acid, serine, itself obtained from a glycolytic intermediate (Voet and Voet, 1996). Since the requirement for this most simple of organic building blocks began, glycine has shaped the properties of almost all proteins and been a major driving force in the progression of metabolic processes and neurotransmission.

The race to identify the chemical correlates of neurotransmission, which included glycine, came about from the initial impetus generated in the 1950s. Within this period it became clear that neurotransmission in higher vertebrates required communication between central nervous system (CNS) neurones that were not physically touching and that this process was primarily chemically mediated (Nicoll, 1988). The consensus towards glycine acting as a specific neurotransmitter was cautious due to the abundant number of cellular processes this molecule was already known to be involved in. However, opinion began to change upon the publication in 1965 of a paper by Aprison and Werman, which showed that glycine fulfilled the first criterion of any substance that is classified as a neurotransmitter. The four

requirements, listed below, are considered to be important for designating a chemical as a conventional neurotransmitter (Ottersen and Storm-Mathisen, 1990).

1. The presynaptic criterion – In order for a molecule to elicit a rapid communication event across a synaptic junction it must initially be present within the presynaptic cell.
2. Release criterion – Upon depolarisation of the presynaptic cell the neurotransmitter in question must be released in quantities sufficient for it to mediate a downstream effect.
3. Identity of action criterion – Exogenous application of the putative transmitter substance should mimic the effects on the postsynaptic neurone.
4. Removal criterion – If transmission is to retain a dynamic status then the system must reset rapidly for subsequent incoming signals and this therefore requires an efficient neurotransmitter removal service.

The landmark paper of Aprison and Werman, (1965) along with follow-up studies (Graham, Jr. and Aprison, 1966; Johnston, 1968) demonstrated the presence of both glycine and GABA at significant levels through a cross section of the cat spinal cord. This research was given further credence when measurements of the glycine content was correlated with a number of small neurones present in the spinal cord (Davidoff et al., 1967a;Davidoff et al., 1967b). Finally, the advent of autoradiography and the loading of neurones with [^{3}H]glycine allowed the distribution of this amino acid to be observed using electron microscopy, firmly establishing the presence of glycine in synaptic vesicle structures and presynaptic terminals (Hokfelt and Ljungdahl, 1971;Ljungdahl and Hokfelt, 1973;Matus and Dennison, 1971;Price et al., 1976).

Verification of the release criterion for glycine proved more difficult to attain. These techniques primarily relied upon the loading of neuronal tissue, in this case hemisected or slices of spinal cord,with [^{14}C]glycine and then electrically stimulating the tissue to evoke release. Several studies all achieved success in selectively measuring [^{14}C]glycine release over non-specific release such as that of loaded [^{3}H]insulin (Aprison, 1970a,b ; Roberts and Mitchell, 1972;Osborne et al., 1973;Mulder and Snyder, 1974). These studies, however, met with limited success perhaps as a result of the efficient reuptake of this neurotransmitter upon synaptic release (Mulder and Snyder, 1974).

The postsynaptic action criterion, was demonstrated using electrical recordings accompanied by iontophoretic applications of exogenous glycine. Early studies demonstrated that stimulation of presynaptic cells from the lumbosacral spinal cord produced membrane responses in motoneurones directly comparable to those elicited by exogenous glycine application (Werman et al., 1967;Werman et al., 1968). The measurements using applied glycine produced a fall in membrane resistance, a rapid membrane hyperpolarisation and an inhibition of electrogenesis, all of which are now attributed to actions via the GlyR. Latter studies reproducing these results also revealed that β-alanine, another agonist of the GlyR, could also act in a similar fashion, though at the time it was not known that its action was mediated via the same receptor (Curtis et al., 1968;ten Bruggencate and Sonnhof, 1972).

With regards to a rapid removal system for glycine from the synaptic cleft after its release, initial evidence supported a selective reuptake mechanism. Neal (1969) reported a rapid uptake of labelled glycine by rat spinal cord slices. Furthermore, in keeping with the observation that the spinal cord seemed to possess far higher levels of glycine than the brain (Kelly and Krnjevic, 1969) it was revealed that the spinal cord maintained both high and low affinity glycine reuptake processes while the brain retained only a low affinity uptake mechanism (Johnston and Iversen, 1971;Logan and Snyder, 1972). The rate of this uptake in the spinal cord was measured using [U-^{14}C]glycine into synaptosomes and was shown to occur against a large concentration gradient suggesting an active uptake mechanism (Aprison and McBride, 1973). Thus by the middle of the 1970s all four criteria for glycine as a neurotransmitter had been established to a sufficient level to strongly implicate glycine as a genuine chemical neurotransmitter.

It should also be noted that these studies were complimented by experiments demonstrating a selective blockade of the GlyR. Such a selective blockade of spinal cord motoneurones mediating inhibitory synaptic transmission was identified early on in response to the application of the alkaloid strychnine. This naturally occurring molecule is derived from the Indian tree *Strychnos nux vomica* and was shown to selectively inhibit the response elicited via GlyRs, only inhibiting $GABA_AR$ mediated responses at much higher concentrations (Davidoff et al., 1969;Curtis et al.,

1971). This important discovery enabled receptor distribution studies using [^{3}H]strychnine, which revealed comparable staining patterns to those for the agonist glycine at postsynaptic inhibitory locations in the spinal cord and brain stem (Young and Snyder, 1973;Young and Snyder, 1974). Eventually this high affinity ligand was used to initiate the first direct selective purification of GlyRs via affinity purification columns paving the way for biochemical characterisation and subsequent cloning studies (discussed later).

The physiology of glycine receptors

Distribution

The spinal cord was the ideal preparation for many of the original distribution studies for GlyRs. However, even early glycinergic neurotransmission studies eluded to the possibility that active GlyRs may exist elsewhere, most notably the hindbrain, including the medulla oblongata, and the pons (Werman et al., 1968; Aprison et al., 1968;Aprison et al., 1969;Galindo et al., 1967;ten Bruggencate and Sonnhof, 1972). Meanwhile the presence of glycine and therefore the prospect of putative glycinergic transmission appeared low in higher brain regions including the cerebral cortex (Kelly and Krnjevic, 1969). Distribution studies of mRNA levels across a range of developmental stages up to adulthood revealed that the GlyR family exhibits a broad distribution of potentially functional receptors throughout the CNS (Kuhse et al., 1991;Malosio et al., 1991a;Nikolic et al., 1998). The relative importance of these receptors in synaptic communication is likely to vary between tissue preparations with studies identifying direct inhibitory synaptic responses mediated by GlyRs in cerebellar golgi cells, retinal ganglion cells and auditory pathway medial superior olive cells (Dieudonne, 1995;Protti et al., 1997;Tian et al., 1998;Smith et al., 2000). Whereas, other reports have only validated functional GlyR responses following exogenous agonist application with the significance of synaptic receptors not addressed, such as in cortical and amygdala neurones, and oligodendrocytes (Belachew et al., 1998;Okabe et al., 2004;Danober and Pape, 1998). At the other extreme, recordings from hippocampal neurones and rat dopaminergic neurones of the substantia nigra suggest GlyRs from these regions are exclusively extrasynaptic with no spontaneous activity observed and whole-cell glycinergic currents are only recorded in response to exogenous agonist application (Mangin et al., 2002;Mori et al., 2002). The synaptic GlyR expression patterns are also in close agreement with

the reported distribution of the two selective plasma membrane glycine transporter proteins. These sodium/chloride-dependent transporters, GLYT1 and GLYT2 (Guastella et al., 1992;Liu et al., 1993), are localised to the spinal cord and the brain stem with GLYT1 also present in the diencephalon and retina and GLYT2 expressed in the cerebellum (Kim et al., 1994;Zafra et al., 1995).

The role of the glycine receptor

Given the prevalence of this receptor in interneurones and motoneurones throughout the spinal cord and brain stem this suggested that the GlyR played an important role in the coordination of skeletal muscle movements. Most notably, lamina Ia spinal interneurones, which are regulated via a strong glycinergic input, play a critical role in mediating reciprocal inhibition in stretch reflex circuits allowing for relaxation of the antagonist muscle (Lodge et al., 1977;Kandel et al., 2000). A role for a glycinergic component in motor control circuits is demonstrated by selective disruption upon consumption of strychnine, a potent convulsing agent, and also in the rare hereditary disease, hyperekplexia. This disorder is a result of detrimental mutations within the GlyR protein family leading to dysfunctional glycinergic neurotransmission, which is manifest in patients as an overly pronounced startle response to unexpected stimuli (Rajendra and Schofield, 1995a). The patient startle response stereotypically involves facial grimacing, hunching of shoulders, flexure of arms and clenching of fists, most notably this is due to an increase in muscle rigidity, known as hypertonia throughout the body of the patient. Animal models of this syndrome also exist, which are again due to faulty glycinergic signalling following receptor mutations. These include the *oscillator, spasmodic* and *spastic* mouse lines and myoclonus in dogs, horses and cows, all of which feature a loss of muscle coordination and hypertonia (Holland et al., 1970;Lane et al., 1987;Gundlach et al., 1988;Gundlach et al., 1993;Buckwalter et al., 1994).

Besides the important contribution of GlyRs to motor coordination these receptors also play significant roles in other neuronal pathways. The GlyR is expressed throughout the lateral and medial superior olive and the medial nucleus of the trapezoid body, and evidence suggests this glycinergic circuitry is critical for tonotopic map formation and sound localisation by the auditory apparatus (Kungel and Friauf, 1997;Smith et al., 2000;Kapfer et al., 2002;Kim and Kandler, 2003). In

addition, motor coordination is not the only process that obtains feedback via the spinal cord as the peripheral sensation pathways including those that mediate pain also communicate with higher brain regions in this manner. GlyRs are prevalent in spinal cord lamina I and II, where modification of the inhibitory apparatus can alter the strength of the mediated chronic inflammatory pain response and it has recently been shown that a specific GlyR plays a vital role in this process (Ahmadi et al., 2002;Ji et al., 2002;Harvey et al., 2004).

In addition to an inhibitory neurotransmitter role for glycine, a large body of evidence now suggests GlyRs also play important roles in neuronal development by regulating differentiation and neurite outgrowth, via an excitatory action of the GlyR. Due to the depolarised nature of the chloride equilibrium potential in embryonic tissues, GlyRs elicit depolarising potentials at these stages. An electrophysiological study using microelectrodes on hemisected spinal cords demonstrated the strongest excitatory effect by GlyRs and $GABA_ARs$ at embryonic day 16 (E16), with gradual weakening and finally a reversal of excitation by postnatal day 2 (P2) (Wu et al., 1992). This excitatory effect may instigate downstream developmental processes via activation of Ca^{2+} transients as activation of GlyRs in neocortical cells and in neonatal lateral superior olive cells caused elevations of intracellular Ca^{2+} (Flint et al., 1998;Kullmann et al., 2002) and excitatory embryonic spinal cord GlyRs have also been shown to influence both intracellular calcium and neurite outgrowth (Tapia et al., 2001). It has not yet been possible though to show that differentiation and neurogenesis is a direct consequence of GlyR modulation of Ca^{2+} transients. Studies investigating the differentiation of retinal photoreceptor precursor cells and cortical neurogenesis suggest GlyRs acting via this depolarising mechanism may contribute crucially to these developmental events (Zhou, 2001;Young and Cepko, 2004;Flint et al., 1998).

Glycine receptor synaptic signalling partners

Experiments to address how glycinergic inhibitory neurotransmission is integrated within the vast complexity of neuronal systems have revealed a number of interesting ways in which this neurotransmission may be modulated. Perhaps of most significance is the potential partnership that exists between the GlyR and the $GABA_AR$. Both these receptors are present in lamina I and II of the spinal cord, the

brain stem and in cerebellar Golgi cells. In each case they are capable of co-localising at the same synapses to induce mixed inhibitory postsynaptic potentials with mixed decay components, a faster glycinergic decay and a slower GABAergic decay (Jonas et al., 1998;Chery and de Koninck, 1999;O'Brien and Berger, 1999;Donato and Nistri, 2000;Dumoulin et al., 2001;Keller et al., 2001;Russier et al., 2002). This suggests that these two receptor families may work together to coordinate and regulate motor control. This supposition is supported by the effective treatment of patients with hyperekplexia upon administration of phenobarbitone or clonazepam, both enhancers of $GABA_AR$ function (Andermann and Andermann, 1988). The mechanism of GlyR and $GABA_AR$ synergy may not always be exactly equivalent across different tissue preparations. In lamina I of the spinal cord, GlyRs are localised on the postsynaptic membrane directly opposing the presynaptic terminals while $GABA_ARs$ are positioned further away in the periphery around the GlyRs (Chery and de Koninck, 1999). In the case of retinal photoreceptor cell maturation, which again requires the activation of both GlyRs and $GABA_ARs$, the two receptor types are instead thought to be activated by the common agonist, taurine (Young and Cepko, 2004). Another interaction identified between the GlyR and the $GABA_AR$ is a negative feedback loop whereby activation of one receptor type will reduce the amplitude and increase the rate of desensitisation of the subsequently activated alternate receptor type. In the spinal cord dorsal horn this inhibition is phosphorylation dependent and is asymmetric with pre-activation of GlyRs inhibiting subsequent activation of $GABA_ARs$ more strongly than *vice versa* (Li et al., 2003).

The interaction between the neurotransmitters GABA and Gly is not only restricted to the postsynaptic membrane however, with presynaptic $GABA_BRs$ of the auditory brainstem nucleus able to attenuate the amplitude of postsynaptic glycinergic potentials by reducing glycine release (Lim et al., 2000). On the other hand presynaptic spinal GlyRs in the dorsal commissural nucleus and metabotropic glutamate receptors from rat hypoglossal motoneurones have been shown to enhance the amplitude and frequency of glycinergic postsynaptic transmission, respectively (Donato and Nistri, 2000;Jeong et al., 2003). Interestingly though, type II mGluRs have also been shown to reduce the frequency of glycinergic transmission in mechanically dissociated rat spinal cord neurones (Katsurabayashi et al., 2001). Finally, GABA neurotransmission is unlikely to be the only factor influencing

glycinergic neurotransmission as activation of presynaptic purinergic $P2X_2$ receptors has also been suggested to enhance the frequency of postsynaptic glycinergic signalling in a Zn^{2+} dependent manner (Laube, 2002a).

Intracellular signalling interactions with the glycine receptor

Besides a rapid extracellular modulation of glycinergic neurotransmission postsynaptic GlyR function can also be regulated by a number of intracellular processes. One of these is phosphorylation. The GlyR was first demonstrated to be a substrate for both cAMP-dependent protein kinase (PKA) and protein kinase C in 1990 (Song and Huang, 1990). PKA has been shown to significantly enhance the amplitude of GlyR mediated responses (Ruiz-Gomez et al., 1991;Katsurabayashi et al., 2001) and both protein tyrosine kinases and calcium-calmodulin dependent protein kinase II are capable of enhancing glycinergic neurotransmission (Xu et al., 1999;Caraiscos et al., 2002). Interestingly, the GlyR also appears capable of directly interacting with a G-protein βγ dimer, which increases the channel open probability in response to glycine, potentially allowing GlyR modulation by a whole host of G-protein coupled receptors (Yevenes et al., 2003). Another potential contribution to GlyR enhancement may arise via an as yet unreported cytoplasmic factor, which can mediate the effects of Ca^{2+} influx to increase the apparent affinity of the GlyR (Fucile et al., 2000). These modulatory processes are presumably of physiological significance, though their exact role remains unreported.

GlyR subtypes: Their respective distributions, properties and functions

Isolation of glycine receptor subtypes

The isolation of the first pure component of the glycinergic signalling pathway was achieved in 1982 when Pfeiffer et al purified a glycine receptor complex from the spinal cord using affinity chromatography. The purification, using a strychnine derivative bound to a column, yielded a protein complex comprising of three different molecular weights, 48 kD, 58 kD and 93 kD. Subsequent analysis revealed that the 48 kD component retained properties consistent with GlyRs from native tissues, namely a high affinity for the antagonist strychnine and displacement of this binding by three GlyR agonists, glycine, β-alanine and taurine.

Molecular cloning of a GlyR subunit from the rat followed five years later revealing that the GlyR α1 shared significant sequence homology with the nAChR family (Grenningloh et al., 1987b) and the $GABA_A$ receptor family (Grenningloh et al., 1987a). Owing to the conserved presence of two cysteine residues at a fixed distance of 13 amino acids apart, the three families were consigned to a new receptor superfamily known as the cys-loop family of ligand-gated ion channel receptors (Karlin and Akabas, 1995). Subsequent studies identified the human (h) GlyR α1 orthologue and another hGlyR variant designated α2, which retained 76 % amino acid sequence identity to its α1 counterpart (Fig 1.1; Grenningloh et al., 1990a). These studies were further complimented when the rat cDNA sequence corresponding to the 58 kD protein was determined (Grenningloh et al., 1990b) and later verified in human form (Handford et al., 1996). This subunit had a significantly increased molecular weight and lacked the ability to bind strychnine (Pfeiffer et al., 1982). Unsurprisingly therefore, this protein had a lower sequence identity to the α1 subunit of 47 % and was therefore classified as GlyR β.

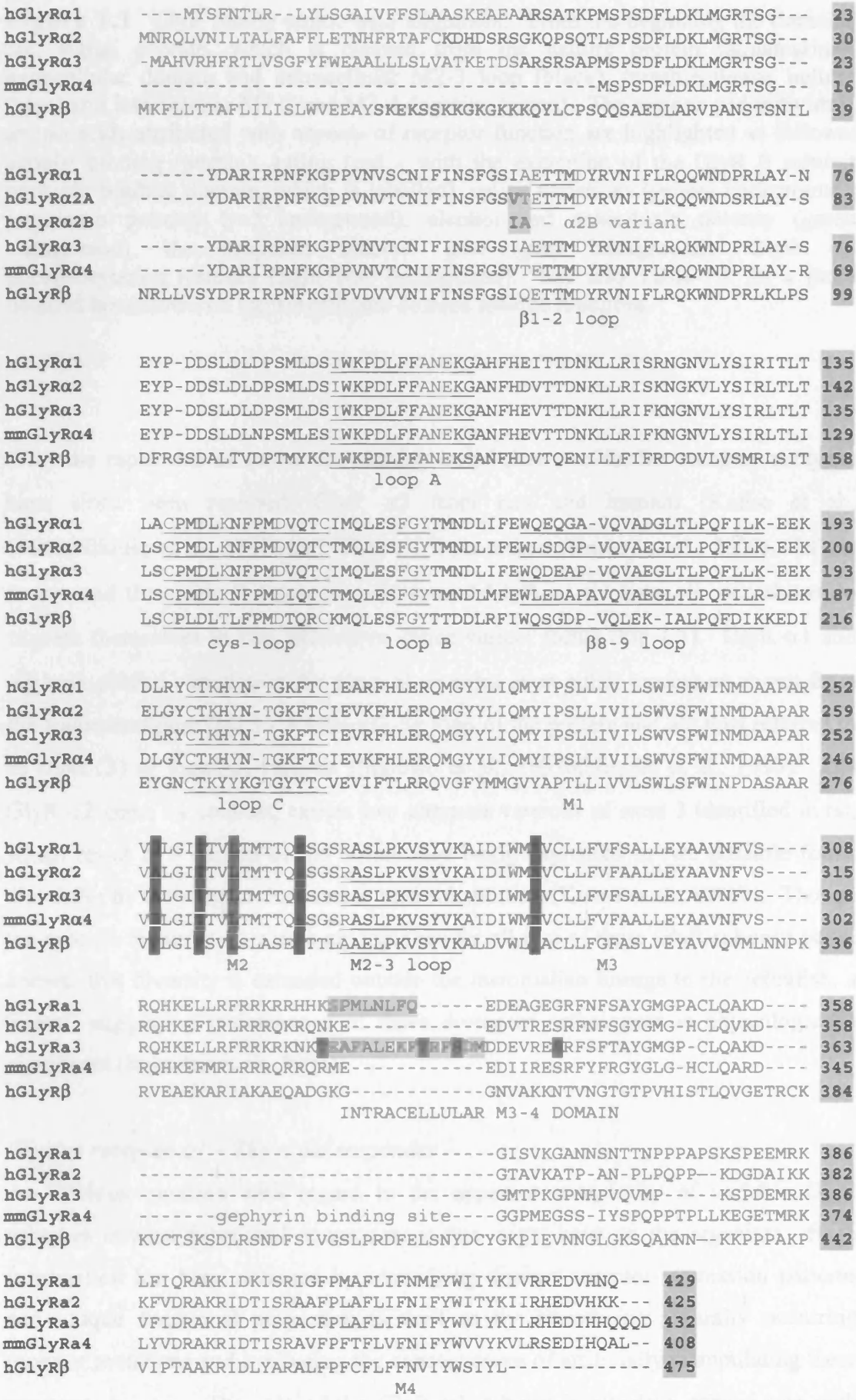
hGlyRα1 ----MYSFNTLR--LYLSGAIVFFSLAASKEAEAARSATKPMSPSDFLDKLMGRTSG--- 23
hGlyRα2 MNRQLVNILTALFAFFLETNHFRTAFCKDHDSRSGKQPSQTLSPSDFLDKLMGRTSG--- 30
hGlyRα3 -MAHVRHFRTLVSGFYFWEAALLLSLVATKETDSARSRSAPMSPSDFLDKLMGRTSG--- 23
mmGlyRα4 ----------MSPSDFLDKLMGRTSG--- 16
hGlyRβ MKFLLTTAFLILISLWVEEAYSKEKSSKKGKGKKKQYLCPSQQSAEDLARVPANSTSNIL 39
hGlyRα1 ------YDARIRPNFKGPPVNVSCNIFINSFGSIAETTMDYRVNIFLRQQWNDPRLAY-N 76
hGlyRα2A ------YDARIRPNFKGPPVNVTCNIFINSFGSVTETTMDYRVNIFLRQQWNDSRLAY-S 83
hGlyRα2B IA - α2B variant
hGlyRα3 ------YDARIRPNFKGPPVNVTCNIFINSFGSIAETTMDYRVNIFLRQKWNDPRLAY-S 76
mmGlyRα4 ------YDARIRPNFKGPPVNVTCNIFINSFGSVTETTMDYRVNVFLRQQWNDPRLAY-R 69
hGlyRβ NRLLVSYDPRIRPNFKGIPVDVVVNIFINSFGSIQETTMDYRVNIFLRQKWNDPRLKLPS 99
β1-2 loop
hGlyRα1 EYP-DDSLDLDPSMLDSIWKPDLFFANEKGAHFHEITTDNKLLRISRNGNVLYSIRITLT 135
hGlyRα2 EYP-DDSLDLDPSMLDSIWKPDLFFANEKGANFHDVTTDNKLLRISKNGKVLYSIRLTLT 142
hGlyRα3 EYP-DDSLDLDPSMLDSIWKPDLFFANEKGANFHEVTTDNKLLRIFKNGNVLYSIRLTLT 135
mmGlyRα4 EYP-DDSLDLNPSMLESIWKPDLFFANEKGANFHEVTTDNKLLRIFKNGNVLYSIRLTLI 129
hGlyRβ DFRGSDALTVDPTMYKCLWKPDLFFANEKSANFHDVTQENILLFIFRDGDVLVSMRLSIT 158
loop A
hGlyRα1 LACPMDLKNFPMDVQTCIMQLESFGYTMNDLIFEWQEQGA-VQVADGLTLPQFILK-EEK 193
hGlyRα2 LSCPMDLKNFPMDVQTCTMQLESFGYTMNDLIFEWLSDGP-VQVAEGLTLPQFILK-EEK 200
hGlyRα3 LSCPMDLKNFPMDVQTCIMQLESFGYTMNDLIFEWQDEAP-VQVAEGLTLPQFLLK-EEK 193
mmGlyRα4 LSCPMDLKNFPMDIQTCTMQLESFGYTMNDLMFEWLEDAPAVQVAEGLTLPQFILR-DEK 187
hGlyRβ LSCPLDLTLFPMDTQRCKMQLESFGYTTDDLRFIWQSGDP-VQLEK-IALPQFDIKKEDI 216
cys-loop loop B β8-9 loop
hGlyRα1 DLRYCTKHYN-TGKFTCIEARFHLERQMGYYLIQMYIPSLLIVILSWISFWINMDAAPAR 252
hGlyRα2 ELGYCTKHYN-TGKFTCIEVKFHLERQMGYYLIQMYIPSLLIVILSWVSFWINMDAAPAR 259
hGlyRα3 DLRYCTKHYN-TGKFTCIEVRFHLERQMGYYLIQMYIPSLLIVILSWVSFWINMDAAPAR 252
mmGlyRα4 DLGYCTKHYN-TGKFTCIEVKFHLERQMGYYLIQMYIPSLLIVILSWVSFWINMDAAPAR 246
hGlyRβ EYGNCTKYYKGTGYYTCVEVIFTLRRQVGFYMMGVYAPTLLIVVLSWLSFWINPDASAAR 276
loop C M1
hGlyRα1 VALGITTVLTMTTQSSGSRASLPKVSYVKAIDIWMAVCLLFVFSALLEYAAVNFVS---- 308
hGlyRα2 VALGITTVLTMTTQSSGSRASLPKVSYVKAIDIWMAVCLLFVFAALLEYAAVNFVS---- 315
hGlyRα3 VALGITTVLTMTTQSSGSRASLPKVSYVKAIDIWMAVCLLFVFSALLEYAAVNFVS---- 308
mmGlyRα4 VALGITTVLTMTTQSSGSRASLPKVSYVKAIDIWMAVCLLFVFAALLEYAAVNFVS---- 302
hGlyRβ VALGISVMSLASETTLAAELPKVSYVKALDVWLAACLLFGFASLVEYAVVQVMLNNPK 336
M2 M2-3 loop M3
hGlyRa1 RQHKELLRFRRKRRHHKSPMLNLFQ------EDEAGEGRFNFSAYGMGPACLQAKD---- 358
hGlyRa2 RQHKEFLRLRRRQKRQNKE----------EDVTRESRFNFSGYGMG-HCLQVKD---- 358
hGlyRa3 RQHKELLRFRRKRKNKSEAFALEKPTRFSRMDDEVREWRFSFTAYGMGP-CLQAKD---- 363
mmGlyRa4 RQHKEFMRLRRRQRRQRME----------EDIIRESRFYFRGYGLG-HCLQARD---- 345
hGlyRβ RVEAEKARIAKAEQADGKG----------GNVAKKNTVNGTGTPVHISTLQVGETRCK 384
INTRACELLULAR M3-4 DOMAIN
hGlyRa1 ----------GISVKGANNSNTTNPPPAPSKSPEEMRK 386
hGlyRa2 ----------GTAVKATP-AN-PLPQPP--KDGDAIKK 382
hGlyRa3 ----------GMTPKGPNHPVQVMP-----KSPDEMRK 386
mmGlyRa4 -------gephyrin binding site----GGPMEGSS-IYSPQPPTPLLKEGETMRK 374
hGlyRβ KVCTSKSDLRSNDFSIVGSLPRDFELSNYDCYGKPIEVNNGLGKSQAKNN--KKPPPAKP 442
hGlyRa1 LFIQRAKKIDKISRIGFPMAFLIFNMFYWIIYKIVRREDVHNQ--- 429
hGlyRa2 KFVDRAKRIDTISRAAFPLAFLIFNIFYWITYKIIRHEDVHKK--- 425
hGlyRa3 VFIDRAKKIDTISRACFPLAFLIFNIFYWVIYKILRHEDIHHQQQD 432
mmGlyRa4 LYVDRAKRIDTISRAVFPFTFLVFNIFYWVVYKVLRSEDIHQAL-- 408
hGlyRβ VIPTAAKRIDLYARALFPFCFLFFNVIYWSIYL---------- 475
M4

Figure 1.1 GlyR family amino acid alignment. From the beginning the domains are; signal peptide, which is cleaved from the mature protein (aquamarine), extracellular domain and extracellular M2-3 loop (black), transmembrane helices (blue) and intracellular M1-2 and M3-4 domains (green). The regions and individual amino acids attributed with aspects of receptor function are highlighted as follows: agonist binding (purple), gating (red – with the exception of the GlyR β subunit gephyrin binding domain, which is labelled), splice variations (yellow background), picrotoxin potency (red background), alcohol and anaesthetic potency (green background), the proposed channel gate (grey background), GlyR α3 phosphorylation residues (light blue background). See also Table 1.1 for a more detailed breakdown on transmembrane domain residue functions.

With the rapid rise of molecular cloning techniques two further receptor subtypes have since been reported, GlyR α3 from rats and humans (Kuhse et al., 1990a;Nikolic et al., 1998) and GlyR α4 from mouse (Harvey et al., 2000). Of the four α and the single β genes now discovered GlyR α1 - 3 have all been shown to express themselves in two alternative splice variant forms (Fig 1.1). GlyR α1 and α3 both exhibit variation in the form of an extra exon either present, or absent, from the transmembrane (M) 3 - 4 intracellular loop of the protein and are thus referred to as short (S) or long (L) variants (Malosio et al., 1991b;Nikolic et al., 1998). The GlyR α2 gene, by contrast, carries two alternate versions of exon 3 identified in rat, which result in a section of the N-terminus being expressed in two possible forms that differ by a divergent dual amino acid substitution (Kuhse et al., 1991b). Though the specific requirement within an organism for all five of these GlyR subunits is not known, this diversity is extended outside the mammalian lineage to the zebrafish, a teleost, suggesting maintenance of these divergent orthologues is physiologically significant (Imboden et al., 2001).

Glycine receptor α1 – The rapid responder

An obvious question with regard to the apparent complexity of variable GlyR subtypes is what functional consequences this might have on the organism. Such information has been obtained by identifying distinct receptor expression patterns and unique functional properties as well as by discovering naturally occurring receptor mutations and evaluating the consequences of artificially manipulating these receptors *in vivo*. The role of the GlyR α1 subunit is clearly a critical one with

several naturally occurring mutations being responsible for the genetic condition of hyperekplexia (Zhou et al., 2002;Lynch, 2004). The broad expression pattern of this subunit within the spinal cord and certain brain regions (Malosio et al., 1991a) along with the absence to date of naturally occurring mutations in any of the other α subunits, suggests that GlyR α1 may be the predominant functional isoform in mammals. Furthermore, the auxiliary nature of the β subunit and its almost ubiquitous expression throughout the central nervous system suggests this variant is unlikely to be able, by itself, to confer functional specificity. However, despite these observations recent evidence does point to specific roles for the other α subunits *in vivo*.

Several studies have suggested there is a developmental switch around the time of birth from an embryonic expression pattern where GlyR α2 and α4 predominate to the predominant postnatal forms, GlyR α1 and α3. This raises the possibility that differing receptor isoforms may perform specific roles during development. These initial studies were collated from RNA *in situ* hybridisation experiments on GlyR α1-3 (Malosio et al., 1991a;Watanabe and Akagi, 1995) and protein quantification comparing the relative amounts of the 48 kD (α1) and 49 kD (α2) species (Becker et al., 1988) during development. However, further support was also obtained from a functional study by Takahashi et al, (1992) where single channel studies revealed distinct distributions of amplitudes and open times for recombinant rat GlyR α1 and α2, which correlated with those recorded from native GlyRs in the juvenile P16 and embryonic E18 rat, respectively. These observations were tentatively linked to a shift in the kinetics of evoked IPSCs with embryonic tissues exhibiting a more diffuse IPSC that displayed slower rates of onset and offset compared to evoked IPSCs in more mature tissues. This may mean that the embryonic GlyR α2 is not as suited to the rapid response dynamics required for receptors positioned at the synapse (Mangin et al., 2003) and therefore during post-natal development, where the organism requires more precise and rapid movement, the spinal cord up regulates to the more rapidly responsive GlyR α1. Another prime example of the requirement for a highly coordinated and rapid signalling complex is provided by the central auditory system, a system which receives a strong regulatory control from GlyRs and where GlyR α1 is not expressed until birth when it undergoes rapid up regulation at the

protein level according to immunostaining with a selective α1 antibody (mAb 2b) (Kungel and Friauf, 1997).

A recent study by Mangin et al (2003) analysing recombinant GlyR α2 in a synaptic context, by rapidly applying brief 1 ms pulses of Gly to macropatches, revealed that even at 1 mM concentrations, GlyR α2 was only able to activate minimally within this time scale. This suggested that the GlyR α2 subtype is not capable of supporting rapid transmission at synapses and indeed may not be localised to the synapse. Though the slow activation kinetics of GlyR α2 makes this receptor unsuitable for dynamic synaptic integration it is unlikely that the GlyR α2 subunit is entirely extrasynaptic. Takahashi et al (1992) electrically evoked glycinergic IPSCs, presumed to be mediated by α2 receptors, in embryonic tissue. Even as early as E16, acute recordings from the rat dorsal root exhibited glycinergic synaptic activity (Wu et al., 1992). Furthermore rat spinal cord cultures, that are known to undergo only a minimal transition from the α2 to α1 subtype during maturation (Hoch et al., 1989;Hoch et al., 1992), still exhibit robust synaptic activity (Bloomenthal et al., 1994;Laube, 2002a). The auxiliary β-subunit is, however, highly expressed during culture maturation and this subunit is also an important anchoring protein to ensure efficient expression of GlyRs (Moss and Smart, 2001). In certain systems such as the basolateral amygdala the receptor subtype is predominantly α2 and its pharmacology is mostly in keeping with expression as an α2β heteromer (McCool and Farroni, 2001). Thus it may be that the β subunit can co assemble with α2 receptors and increase their activation kinetics (unfortunately not tested by Mangin et al., 2003) sufficiently to be operable at the synapse, though probably still less responsive than the GlyR α1 (Takahashi et al., 1992).

Glycine receptor α2 – The developmental subunit

Any advantage that the GlyR α1 subunit offers over α2 in mature tissues must presumably be complimented by a beneficial effect conferred by α2 receptors in the embryo. With regards to the proposed suitability of GlyR α2 to extrasynaptic localisation at embryonic stages this may indeed have important consequences for neuronal development in response to tonic stimuli. The presence of extrasynaptic

GlyRs in cortical plate neurons during embryonic development has been electrophysiologically validated in the neocortex with taurine the most likely agonist responsible (Flint et al., 1998). A subsequent study combining RT-PCR and electrophysiology confirmed these cortical receptors to be GlyR α2 (Okabe et al., 2004). Previously, taurine deprivation of kittens *in utero* has been shown to cause an apparent disruption of normal cortical migration and differentiation (Sturman, 1986), in accord with a developmental role for GlyRs. Indeed, taurine acting via GlyR α2 encourages differentiation of precursor cells into rod photoreceptors in retinal cultures (Young and Cepko, 2004). Developmental regulation by GlyR α2 subunits may also potentially be fine tuned by varying the relative expression of the two α2 receptor splice variants, which exhibit a 4-fold variation in their sensitivity to taurine regardless of co-expression with the β subunit (Miller et al., 2004). This is a particularly tantalising hypothesis as neurones possess two genes encoding NOVA-1 and 2 spread across the spinal cord and brain, which have the capacity to control the relative ratios of receptor splice variants, including GlyR α2A and 2B (Jensen et al., 2000;Ule et al., 2003).

Although GlyR α2 is the predominant receptor during embryogenesis it may also play some specialised roles in adult tissues. Though the receptor subtype has not been validated, non synaptic GlyR mediated tonic noise, a role seemingly suited to GlyR α2, has been demonstrated in the postnatal hippocampus from P7 onwards (Mori et al., 2002). Additionally, RT-PCR studies in the amygdala demonstrate that GlyR α2 is the predominant GlyR in this adult preparation (McCool and Farroni, 2001). Thus it would appear that GlyR α2 can remain in certain adult tissues, a suggestion supported by the identification of GlyR α2 transcripts that are retained at least until juvenile stages of rat spinal cord progression (Jensen et al., 2000).

Glycine receptor α3 – The bearer of great pain

The expression pattern of GlyR α3 is highly localised using *in situ* hybridisation and Northern blot studies detecting mRNA transcripts in adults at low levels in the cerebellum, frontal lobe, temporal lobe and putamen and no evidence of α3 in the spinal cord (Malosio et al., 1991a;Nikolic et al., 1998). Two further non-functional studies have both revealed that GlyR α3 is also localised to the adult mammalian

retina (Greferath et al., 1994;Haverkamp et al., 2003). It has a distinct staining pattern from the α1 subunit suggesting that α3 may mediate specific retinal pathways *in vivo*, though this function can be compensated by apparent up regulation of other GlyR subunits in the α3 knockout animal (Haverkamp et al., 2003). Of most significance though is a recent study demonstrating that despite previous mRNA studies (Nikolic et al., 1998) GlyR α3 is in fact expressed at the protein level in a highly localised manner in spinal cord lamina II of the dorsal horn (Harvey et al., 2004). This region plays an important role in mediating inflammatory pain and allodynia (Basbaum, 1999). GlyR α3, which retains a unique serine residue in the intracellular domain, underwent phosphorylation in response to activation of the PGE_2 signalling cascade and the α3 mediated inhibitory input was subsequently attenuated (Harvey et al., 2004). GlyR α3 knockout mice retained significant GlyR mediated IPSC input at lamina II but failed to down regulate the inhibitory input in response to PGE_2 mediation with the result that these mice were resistant to inflammatory pain when the PGE_2 pathway is activated (Harvey et al., 2004). This pain-induced pathway was shown in a previous overlapping study to be selective specifically to the prostaglandin PGE_2 (Ahmadi et al., 2002). Another study, which interfered with anionic homeostasis in nearby lamina I also supports the importance of inhibitory input into the dorsal horn for responsiveness to neuropathic pain (Coull et al., 2003). Thus it would appear that there is a specific role for GlyR α3 in mammals and this role cannot easily be compensated for by other ligand-gated receptors.

Glycine receptor α4 – The enigma

The α4 subunit has, as yet, received only an elementary functional analysis demonstrating that the recombinant homomer bears similarity with α1 GlyRs (Harvey et al., 2000). The same study went on to show with mRNA *in situ* hybridisation that this receptor has an embryonic distribution akin to α2 and is localised primarily to the spinal cord and sympathetic neurones, as well as the testis, suggesting it may contribute to the development of sensory and motor pathways.

Gephyrin and the glycine receptor β-subunit

Evidence to support a specific functional role for the β-subunit in GlyR physiology currently revolve around its ability to interact with a synaptic anchoring protein called gephyrin allowing the β subunit to selectively target αβ GlyR heteromers to inhibitory synapses (Meyer et al., 1995;Kneussel et al., 1999;Moss and Smart, 2001). When the GlyR was initially isolated, it was part of a complex featuring a cytoplasmic protein component with mass 93 kD (Pfeiffer et al., 1982). This component, named gephyrin, was found to exist in at least 5 different splice variant mRNA products in the brain (Prior et al., 1992) though 7 have now been detected in the spinal cord (Meier et al., 2000) and 10 neuronal isoforms have been found in humans (Rees et al., 2003). Even more may exist in both neuronal and non-neuronal tissues since 8 of its 29 exons so far verified from cDNA sequencing, have the potential to generate splice variants (Ramming et al., 2000). As suggested from the potential wide array of variant isoforms, expression analysis of gephyrin transcripts reveals a tissue distribution far beyond that of the GlyR (Prior et al., 1992;Kirsch and Betz, 1993;Ramming et al., 2000). This is in agreement with proposed additional roles for gephyrin in molybdoenzyme activity in non-neuronal tissues (Feng et al., 1998) and providing a critical interaction with RAFT1 (rapamycin and FKP12 target 1) for rapamycin immunosuppressant mediated signalling (Sabatini et al., 1999).

Also of interest, expression of the β subunit in αβ heteromers halves single channel conductance (Bormann et al., 1993) and reduces sensitivity to picrotoxin (Pribilla et al., 1992), though this has not yet been attributed with any functional significance.

Kinetics and desensitisation

Kinetics

Studies of the kinetics of ion channels usually either attempt to measure parameters of burst openings, closures and conductance states using single channel recordings, or to evaluate the rates of current onset and offset when using ultrafast perfusion systems on small receptor populations in macropatches. The first kinetic studies on GlyRs utilised single channel studies from neuronal systems owing to the lack of ultrafast perfusion techniques and molecular cloning strategies available to attain pure GlyR populations of receptors. These early studies focused on the channel conductance and revealed that GlyRs could adopt a number of different conductance states, always at least two, and though there was a large variation in the sizes of the

conductance states due to variations in holding potentials and driving forces the most commonly occurring conductance state was generally the largest, in the range 80 – 90 pS (Hamill et al., 1983;Bormann et al., 1987;Twyman and Macdonald, 1991). Although these studies used spinal cord neurones, multiple conductance states with the predominant one being the largest have now been obtained in recombinant systems (Takahashi et al., 1992;Grewer, 1999;Lewis et al., 2003;Beato et al., 2002;Beato et al., 2004). Intriguingly, the most recent and thorough studies to date suggests that multiple conductance states are far less prolific in pure recombinant populations, with the largest conductance being predominant for over 80 % of all channel openings and the second smaller conductance state being rarely visited (Beato et al., 2002;Beato et al., 2004;Lewis et al., 2003). Thus, variable conductance states might primarily reflect receptor heterogeneity in native tissue.

The first quantitative single channel study to attempt to elucidate an activation scheme for spinal cord GlyRs using open-shut time durations within bursts was carried out by Twyman and Macdonald (1991). This study, using low agonist concentrations, revealed three different mean open times within bursts, an observation reproduced in rat spinal cord slices and in zebrafish homomeric α1 receptors (Takahashi et al., 1992;Fucile et al., 1999). Furthermore, for both rat and zebrafish GlyRs, the mean open time durations remained the same but the frequency of the longer burst duration relative to the shortest burst duration increased with increasing glycine concentrations (Twyman and Macdonald, 1991;Fucile et al., 1999). Recently, an extra very short open-time duration, has been revealed for the homomeric GlyR α1 (Beato et al., 2002). In addition, only the frequency of channel openings again increased with agonist concentration with unchanged mean open time durations over a 30-fold concentration range. This property is consistent with a kinetic scheme where each individual liganded state switches between open and closed but the open states are discrete, i.e. a sequential binding model (Fig 1.2).

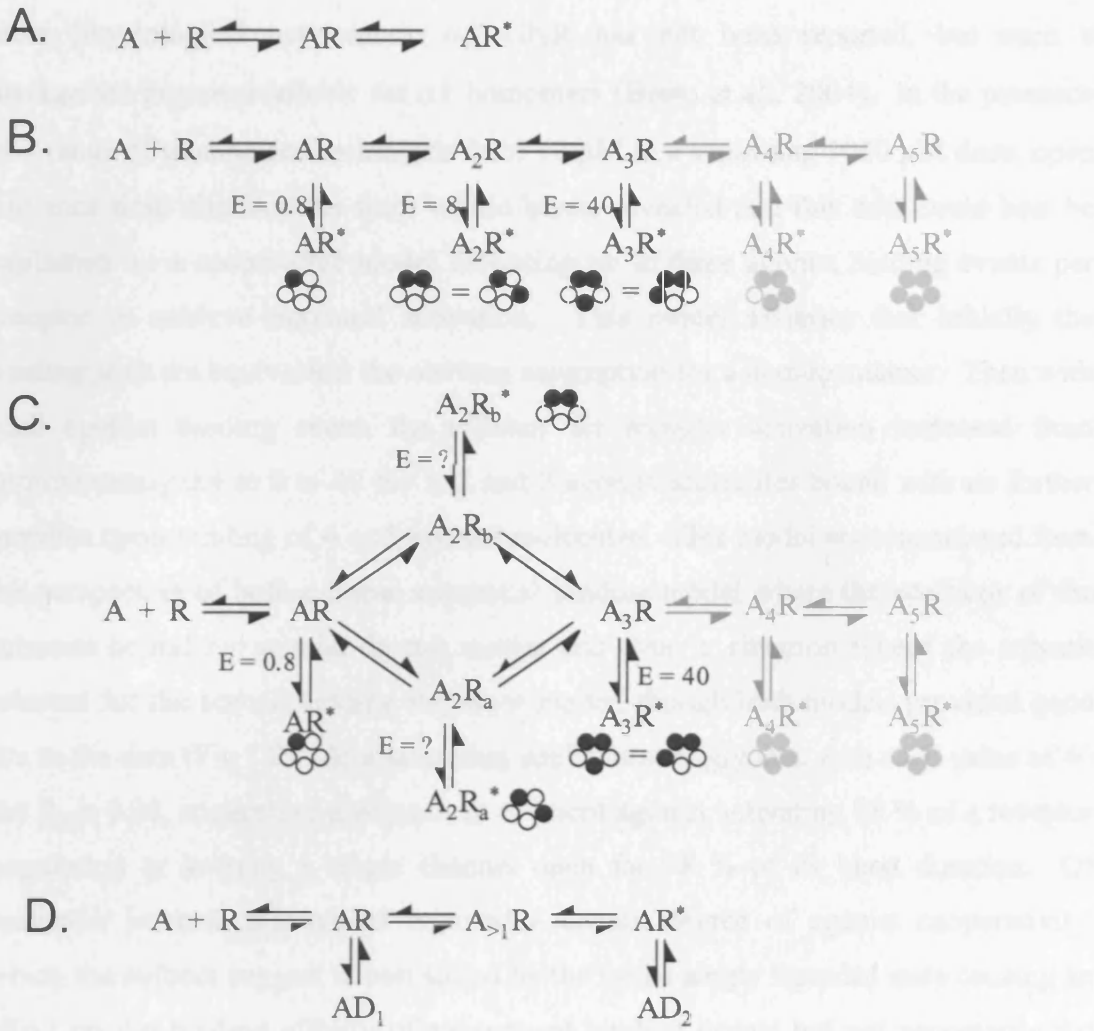

Figure 1.2 Kinetic schemes of GlyR activation. *A*, The simplest Markov model of receptor activation, which assumes that either there is only one activated state (AR*) for the receptor, or that all activated states are equivalent (AR represents the bound inactive state). *B*, A sequential binding model, which assumes that different numbers of agonist molecules bound to a receptor induce discrete activation states, reflected in single channel recordings by distributions composed of multiple open durations. *C*, The complex sequential binding model (Beato et al, 2004) where activation states with the same number of agonists bound are not necessarily phenotypically equivalent, dependent on the positions of the sites occupied by agonist. This suggests that the receptor displays allostery i.e. that binding of an agonist molecule may influence the affinity of subsequent binding events. *D*, A modified Markov model with one activation state and two desensitised states as proposed for GlyR α2 by Mangin et al, 2003. AD_1 represents a fast desensitised state that can occur before the receptor activates and is dependent on a receptor with a low number of agonist molecules bound, while AD_2 represents the standard desensitisation that the GlyR may undergo after activation. Note that desensitised states were not included in the other schemes as this process is poorly understand and cannot be accurately accounted for in these schemes.

To date an in depth single channel study to elucidate the activation mechanism of the more physiological heteromeric αβ GlyR has not been reported, but such a mechanism is now available for α1 homomers (Beato et al., 2004). In the presence of a range of glycine concentrations from 10 μM to a saturating 1000 μM dose, open and shut time distributions from within bursts revealed that this data could best be explained by a cooperative model favouring up to three agonist binding events per receptor to achieve maximal activation. This model assumes that initially the binding sites are equivalent, the obvious assumption for a homopentamer. Then with each agonist binding event, the efficacy for receptor activation increased from approximately 0.4 to 8 to 40 for 1, 2 and 3 agonist molecules bound with no further increase upon binding of 4 or 5 agonist molecules. This model was considered from the perspective of both a linear sequential binding model where the positions of the subunits bound by agonist do not matter and from a situation where the subunit selected for the second binding step does matter, though both models provided good fits to the data (Fig 1.2). At a saturating application of glycine, with an E value of 40 the P_o is 0.98, suggesting glycine is an efficient agonist activating 98 % of a receptor population or keeping a single channel open for 98 % of its burst duration. Of particular interest, this model required a certain degree of agonist cooperativity, which the authors suggest is best suited by the initial singly liganded state causing an effect on the binding affinity of subsequent binding events but not necessarily the second binding event affecting the third. Though it was not possible to determine the exact nature of any allostery even whether it was positive, or negative, depending on where and how the agonists bind, this study is important as it supports cooperativity in GlyRs and suggests 3 agonist bindings are maximally efficacious for homopentameric receptors. It should be noted that prior studies assessing the kinetic scheme for GlyR α1 activation applied a sequential kinetic model where there is effectively just one activation state (a Markov model; Fig 1.2) to simplify matters (Walstrom and Hess, 1994;Grewer, 1999;Laube et al., 2000). However both Twyman and Macdonald, (1991) and Beato et al, (2002 and 2004), demonstrated that the GlyR clearly contains 3 distinct open states representative of a sequential activation model. Additionally, studies using exponential curve fits of current onsets in response to ultrafast drug applications are unlikely to be able to attain the resolution necessary to predict all the exponential components within the rising phase

of the macroscopic activation, particularly the fastest component (Grewer, 1999). Therefore the study of Beato et al (2004) is to date the highest temporal resolution study addressing the activation dynamics of the GlyR.

This activation mechanism may provide a guide for the GlyR αβ heteromer as the α subunit is thought to directly bind the agonist and so it is possible that the binding sites could remain equivalent. Current studies to elucidate a kinetic model for the heteromeric GlyR have resulted in the proposal of a model with two open states and a reluctant gating step (Legendre, 1998). This proposal, which adopted ultrafast macroscopic perfusion techniques to record from M-cells in zebrafish that predominantly express αβ heteromers (Legendre, 1997) will, however, be an oversimplification as single channel studies on presumed αβ heteromers has previously revealed that 3 separate open states exist (Twyman and Macdonald, 1991). Certainly, from a macroscopic point of view, the evidence suggests that the β subunit does not affect activation, or inactivation rates, with these two parameters remaining comparable for α1 homomers and αβ heteromers using ultrafast perfusion studies on macropatches (Mohammadi et al., 2003). This is also supported by comparisons of recombinant α1 single channel burst durations, which when summated could be directly overlaid with presumed αβ native receptor IPSCs (Takahashi et al., 1992;Legendre, 1998).

Kinetic experiments have also recently been carried out to compare the mechanism of action elicited by the three primary GlyR agonists, glycine, β-alanine and taurine using both ultra-fast perfusion techniques and single-channel analysis (Lewis et al., 2003). These studies, on GlyR α1 homomers, also revealed three distinct open states that were distinguishable for all three agonists. Whilst the open time durations and amplitudes did not vary between the agonists the closed time durations did vary. This was reflected in the ultrafast macroscopic currents by slower activation and faster relaxation rates of currents evoked by saturating concentrations of β-alanine and taurine compared to glycine. As the mean open time durations, a direct reflection of the closing rate, did not differ, this suggested that the closing rate constants represented an intrinsic property of the receptor. In addition to this relative

estimates of the agonist efficacies were obtained with glycine, β-alanine and taurine having E values of 16, 8 and 3.4.

As has been previously mentioned an ultrafast perfusion study carried out on GlyR α2 revealed that this receptor exhibits a slower activation rate compared to studies on α1 (Takahashi et al., 1992;Legendre, 1998;Mangin et al., 2003). In addition, the relaxation and desensitisation rates were also slower and, of particular interest, an estimate of glycine efficacy at the GlyR α2 revealed a high value of 200, 5-fold higher than that for GlyR α1 (Lewis et al., 2003;Beato et al., 2004). This suggests that α1 and α2 have significant differences in terms of their kinetics, a fact supported by the delayed GlyR α2 channel openings after exposure to agonists, which were suggested to represent transitions between a ligand bound-closed state and a desensitised closed state prior to channel opening (Fig 1.2; Mangin et al., 2003). This delayed opening, which occurred at low agonist concentrations suggesting it represented low-level liganded receptors, was absent at a saturating concentration of agonist, presumably due to multiple agonist binding events occurring before the receptor could desensitise. Thus in this higher liganded state the receptor would always open (Mangin et al., 2003).

Desensitisation

The reason and mechanism for receptor desensitisation remains enigmatic. Most studies show that desensitisation consists of two components at high glycine concentrations but just one component at lower agonist concentrations (Mohammadi et al., 2003). A proposed physiological role for GlyR desensitisation has so far been suggested to be unlikely with the time course of both desensitisation components being too slow to impact on IPSC kinetics. Even with rapid re-stimulation using ultrafast perfusion techniques akin to a train of GlyR IPSCs, no paired-pulse desensitisation is observed (Legendre, 1998;Lewis et al., 2003). This is in contrast to certain $GABA_A$ receptor subtypes and nAChRs which exhibit much more rapid rates of desensitisation capable of influencing physiological functions (Burkat et al., 2001;Pidoplichko et al., 1997). Studies to recreate recombinant GlyR populations more representative of their neuronal counterparts have shown that incorporation of the β subunit does cause a significant increase in the rate of desensitisation

(Mohammadi et al., 2003) as does inducing the clustering of receptors using gephyrin (Legendre et al., 2002) raising the possibility that this process could have some impact physiologically.

Structure-Function studies

General topology

The general topology of the GlyR was originally predicted using hydropathy analysis and was placed in the context of a common general architecture shared by all cys-loop ligand-gated ion channels. The α and β subunits contain approximately 420 and 470 amino acids respectively. Starting from the N-terminus the structures comprise a large extracellular domain of around 200 – 250 residues, four transmembrane domains (M1–M4) and a sizable 80 – 100 amino acid intracellular loop between M3–M4 (Fig 1.1; Grenningloh et al., 1987b). Also consistent with the proposed quaternary structure of other cys-loop receptors, the GlyR is predicted to co-assemble into a pentamer. This was initially based on sedimentation analysis and treatment with chemical cross-linking reagents. The molecular weight measured was 260, 000, which is best accounted for by the inclusion of three 48 kD α subunits and two 58 kD β-subunits into the pentamer (Langosch et al., 1988). Evidence in support of this general tertiary and quaternary topology is based on medium and high resolution electron micrographs at 9Å, 4.6Å and 4Å levels of whole *Torpedo* nAChRs (Miyazawa et al., 1999;Miyazawa et al., 2003;Unwin, 1993;Unwin, 1995). Here globular centres of electron density based around a pseudo 5-fold axis of symmetry were observed corresponding to the five extracellular domains of the receptor pentamer. This perimeter allowed for the presence of a large central water filled vestibule, through which ions could easily gain access to the extracellular side of the membrane lining ion channel. In each subunit, 4 predicted α-helical transmembrane domains could also be distinguished as well as a globular intracellular domain. The intracellular domains appeared to link together to form a basin such that ionic conductance was proposed to occur via pores present at the side interfaces between each of the subunits (Fig 1.3). The great challenge for structure-function studies is to decipher how this general topological representation encodes for the principal functional properties of agonist binding, receptor activation, modulation desensitisation, ion conductance and selectivity.

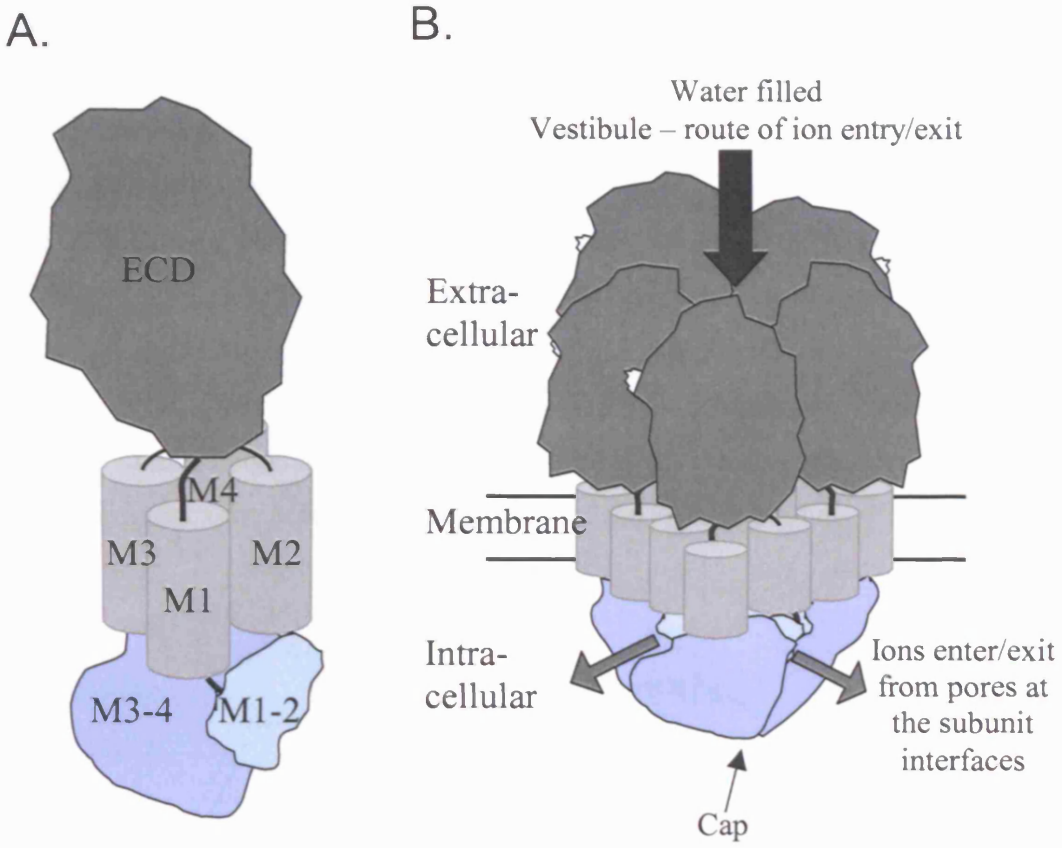

Figure 1.3 Representative model of the monomeric (*A*) and pentameric (*B*) GlyR. *A*, Each subunit consists of an N-terminal extracellular domain (ECD) of approximately 200 – 250 amino acids, four transmembrane regions (M1–M4) of approximately 20 amino acids, and two intracellular loops, M1-M2 (approximately 10 amino acids) and M3–M4 (approximately 80 - 100 amino acids). *B*, Each monomer co-assembles into a functional pentameric receptor. The pentamer draws together the five M2 domains into the interior of the protein at the level of the membrane to form a functional gate and channel to control ion influx, or efflux. The most likely routes for ion entry and exit through the solution exposed components of the GlyR are via the large extracellular vestibule, and on the intracellular side, via gaps between the subunit side interfaces (marked by arrows).

The agonist binding site

Preliminary experiments to isolate the important protein determinants of agonist binding used the technique of peptide mapping in conjunction with [^{3}H]strychnine. The assumption made in these experiments was that glycine and the competitive antagonist strychnine bind to the same part of the receptor. Modelling studies reveal that despite the obvious structural disparity between these two compounds they do share a common element allowing them to potentially interact with some of the same binding site residues (Fig 1.4, Aprison et al., 1987). Moreover [^{3}H]strychnine was able to displace glycine binding (Young and Snyder, 1973). Focusing on the ligand binding α-subunit, covalent incorporation of [^{3}H]strychnine occurred between amino acids 170 and 220 of the N-terminal extracellular domain (Graham et al., 1983;Ruiz-Gomez et al., 1990). Subsequent site-directed mutagenesis studies, targeting residues in and neighbouring this region, identified two discrete domains that were able to influence the potency and selectivity of the agonist binding site.

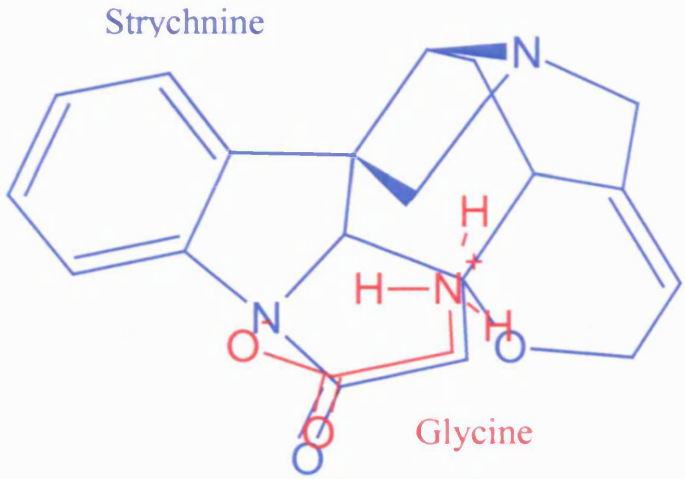

Figure 1.4 Chemical groups present in glycine and strychnine, highlighting the structural similarity of glycine (red) with one subsection of the strychnine molecule (blue), which might explain the ability of strychnine to act as a competitive antagonist at the GlyR.

In the first discrete motif, subsequently termed loop B, substitution of GlyR α1 G160 and Y161 with Glu and Ala mutations respectively, produced receptors with substantially reduced sensitivity to strychnine (Vandenberg et al., 1992a). An equivalent G167E substitution in α2 generated a receptor with a dramatically reduced glycine and strychnine potencies (Kuhse et al., 1990b). It was also demonstrated that introduction of conserved equivalents from the $GABA_AR$, to create GlyR α1 F159Y and Y161F mutated subunits, shifted the relative order of agonist potencies from; glycine > β-alanine > taurine for the wild-type receptor to one where β-alanine was most potent and the GABA potency was also enhanced (Schmieden et al., 1993). This suggested that these three agonists bind to a common site, as was already suspected from their common structural determinants. Furthermore the ability of F159 and Y161 to determine agonist selectivity makes these residues ideal candidates to face into the agonist-binding site. In accordance with this hypothesis, which infers that G160 may instead be acting as a structural linker, introduction of a more conserved alanine instead of a glutamate at G160 does not significantly alter glycine, or strychnine, potency (Vandenberg et al., 1992a). Additionally, though substantial perturbation of this FGY motif reduces the potency of strychnine, the more subtle F159Y and Y161F mutations do not, suggesting this domain can influence strychnine binding but not to the same degree as for the agonists (Schmieden et al., 1993).

The second discrete domain, termed loop C, encompasses residues between GlyR α1, C198 and C209, a cys-loop bridge domain unique to GlyRs. This is not the same as the absolutely conserved cys-loop present in all cys-loop ligand-gated receptors (Fig 1.1 – discussed later). Replacement of either of the bridging residues with chemically similar serines produced non-functional receptors. Thus, the unique ability of cysteine residues to form a disulphide bridge in this region would appear to be critical for receptor function (Rajendra et al., 1995b). The introduction of alanine residues at the even numbered positions K200, Y202 and T204 severely attenuated agonist and antagonist binding. Substitution of K200 reduced strychnine binding, perturbation of Y202 reduced strychnine and glycine binding, and mutation of T204 selectively reduced glycine potency (Vandenberg et al., 1992b;Rajendra et al., 1995b). In addition to this, chemical evaluation of the candidate residues labelled by

[^{3}H]strychnine identified two potential tyrosines as prime candidates, Y197 and Y202. As disruption of Y197 does not affect strychnine potency (Vandenberg et al., 1992b) this strengthens the supposition that the loop including Y202 is physically capable of ligand binding (Ruiz-Gomez et al., 1990). Also of interest is the pattern of disruption with only alternate mutations between C198 and the potential 'kinking' residue G205 affecting agonist and antagonist potency. This is consistent with a β-strand orientation for these residues.

Though [^{3}H]strychnine covalently labelled residues in the region α1 170 – 220, a third and final loop, positioned earlier on in the primary sequence and so termed loop A, has also been implicated in agonist binding. This region spans from I93 to G105 in the GlyR α1 subunit and the individual residue substitutions, I93A, A101H and N102A, caused reductions in glycine potency (Vafa et al., 1999). Furthermore the most significant reductions in agonist potency, involving substitutions of A101 and N102 did not reduce the maximal currents of the lower potency agonist taurine, suggesting this effect was selective to binding, not gating. The potency of strychnine was only moderately reduced suggesting this loop participates primarily in agonist binding. A follow-up study also demonstrated that an N102C mutant exhibited a drastically reduced agonist potency. However an A101C mutation failed to attenuate agonist potency and instead cysteine substitution of the opposing neighbour E103 induced a disruptive effect on receptor function (Han et al., 2001). This suggests that N102 is the primary binding residue in this loop. In the case of I93, a mutation to cysteine was not tested, but the previously reported I93A mutation also reduced agonist maximal currents suggesting this residue may be exerting other secondary effects rather than being engaged in agonist binding (Vafa et al., 1999).

To further strengthen the role of loops A-C in agonist binding, there is good agreement between the GlyR studies and those carried out on other cys-loop receptors, most notably the $GABA_AR$ and the nAChR. Identified residues in the *Torpedo* nAChR α1 subunit loop B include W149 and Y151, which align perfectly with GlyR α1 F159 and Y161. In loop C, prime binding site candidates for the nAChR α1 include Y190, C192 and C193, which are analagous to GlyR α1 K200, Y202 and T204, (Fig 1.5). These five nAChR residues can all be covalently tagged

in response to photoaffinity labelling with the competitive antagonist (N,N-dimethyl) aminobenzenediazonium fluoroborate (DDF) (Dennis et al., 1988;Galzi et al., 1990;Galzi et al., 1991a). In the case of the $GABA_AR$ β subunit, comparable residues Y157 and T160 from loop B and T202 and Y205 from loop C also exhibit properties consistent with roles in ligand binding (Fig 1.5; Amin and Weiss, 1993). Finally, regarding loop A, the GlyR α1 N102 may play a similar role to W86 and Y93 in the α1 nAChR (Cohen et al., 1991;Galzi et al., 1990;Galzi et al., 1991d;Galzi et al., 1991b), and to H101 of the $GABA_AR$ α1 (Wieland et al., 1992;Duncalfe et al., 1996) and R100 of $GABA_AR$ α6 subunits (Korpi and Seeburg, 1993), as well as Y97 and L99 of the $GABA_AR$ β2 subunit (Boileau et al., 2002; Fig 1.5). These potential agonist binding site residues in the nAChR are also thought to play a direct role in agonist coordination (Mu et al., 2003;Sullivan and Cohen, 2000;Celie et al., 2004).

The experiments discussed here provide evidence for a conserved set of loops, A-C, that are involved in agonist binding by cys-loop ligand-gated receptors. However, in the case of nAChR, $GABA_AR$ and $5HT_3R$ there is evidence for the existence of five to six loops involved in agonist binding (for reviews see Cromer et al., 2002;Reeves et al., 2003). These loops contribute to an intersubunit binding site. For example, in the case of a $GABA_AR$ containing α and β subunits, residues are contributed from loops A-C on the β subunit and loops D-F on the α subunit (Cromer et al., 2002). Currently for GlyRs, a contribution from loops D-F, in α and β subunits, to the agonist binding process has not been reported and it may be that the agonist glycine is small enough such that loops A-C from the α-subunit are wholly sufficient to mediate the necessary binding interactions.

Figure 1.5 Cys-loop receptor family amino acid alignment. The conserved locations of the agonist binding residues in loops A–C are highlighted; GlyR α1 in yellow, nAChR α in blue, $GABA_AR$ β2 in purple.

Such functional studies support a conserved location for the agonist-binding site in the cys-loop family of receptors; however, they do little to increase our understanding of the structure of this site, or inform us how each residue contributes to the binding process. Medium resolution electron micrographs of the *Torpedo* nAChR revealed the presence of a potential agonist pocket located about halfway up the extracellular domain of each subunit. This pocket was surrounded by twisted β-sheet strands at the interface of neighbouring subunits but was not of sufficient resolution to determine the locations of binding loops A, B and C (Fig 1.6*A*)(Miyazawa et al., 1999). These data have since been superseded by what is unquestionably the most significant breakthrough in our understanding of the structure of cys-loop receptors. Brejc et al, published in 2001, a high 2.6Å resolution crystal structure of a cys-loop receptor related protein known as the acetylcholine binding protein from the snail *Lymnaea stagnalis*. This soluble protein shares a low but significant 20 % homology with the N-terminal, extracellular domain of the cys-loop receptor family and importantly it places loops A, B and C in proximity to act as ideal coordinators of agonist binding (Fig 1.6*B,C* & 1.7*A,B*). The location of this site is equivalent to the previously identified pocket in medium resolution electron micrographs suggesting that the AChBP does retain a comparable overall topology to the extracellular domain of cys-loop receptors. This structure presents the extracellular domain as an initial α-helix, which then runs into two parallel sheets of β-strands where the two sets of β-strands run perpendicular to each other (Fig 1.6*A* & 1.7*A,B*). In the case of the AChBP it has been possible to crystallize this protein coordinated to three different ligands including the agonists, carbamylcholine and nicotine, to give precise insight into the exact structural interactions that occur during agonist binding (Celie et al., 2004). Due to the low homology this protein shares with the GlyR it is not possible to gain such an exact insight into the glycine binding site, however this homology model has already served as a powerful structural guide in future studies to determine the importance of domains spread throughout the cys-loop receptor extracellular regions.

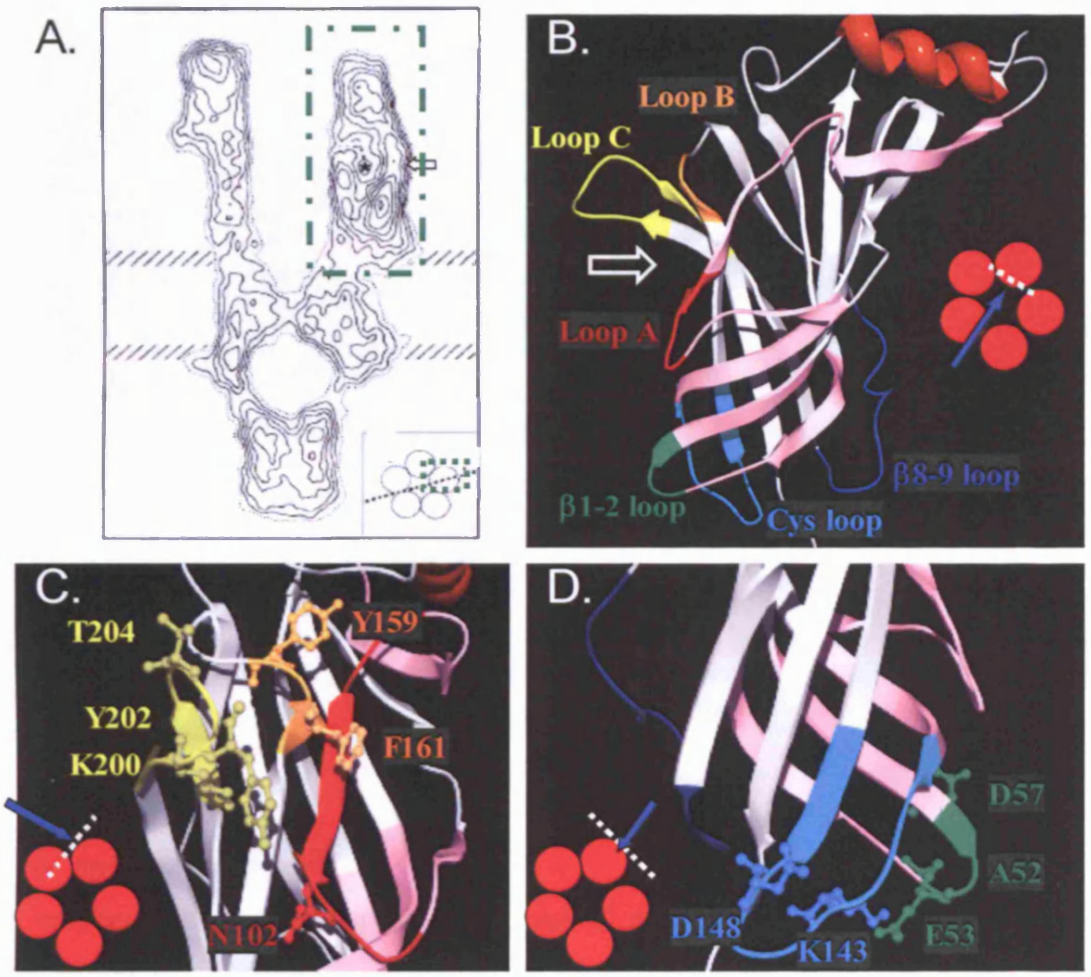

Figure 1.6 Current structural assumptions that can be made about the GlyR extracellular domain. *A*, A longitudinal section through an intermediate resolution structure (4.6 Å electron micrograph) of the *torpedo* nAChR α subunit. The highlighted extracellular domain (dashed green box) of a potential ligand binding cavity half-way up the domain from the membrane (arrow; adapted from Miyazawa et al, 1999). *B*, A homology model (see Materials and Methods) from the inside face (from the vestibule; see inset) of the GlyR α1 subunit based on the crystal structure of AChBP (Brejc et al, 2001). Starting with an initial helix (brown) this structure then forms two parallel sheets of β-strands, which run perpendicular to each other creating inside (pink strands) and outside (white strands) facing sheets. Notable features include; the agonist binding domain consisting of loop A (red), loop B (orange) and loop C (yellow), again predicted to reside half way up the extracellular domain (arrow); the gating domain consisting of the β1-2 loop (green), cys-loop (light blue) and β8-9 loop (dark blue). *C* and *D*, Close-up of the agonist binding domain from a side on perspective (*C*; see inset) and gating domain from the outside face perspective (*D*; see inset) with important residues displayed and labelled. Colour schemes of ribbons are as in (*B*). For reference, alternate nomenclature from Brejc, et al, is as follows; β1-β2 – L2, cys-loop – L7, β8-β9 – L9.

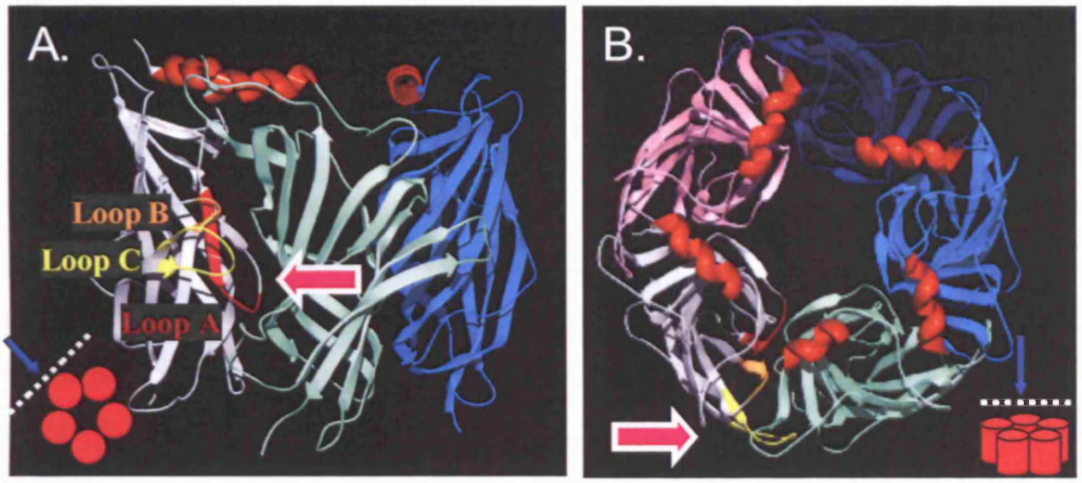

Figure 1.7 Position of the agonist binding site in the pentameric extracellular homology model. *A*, Three neighbouring subunits (white, green and blue) from a pentamer, viewed from the outside face (see inset). The binding site from the white subunit consists of loop A (red), loop B (orange) and loop C (yellow). The agonist-binding site is most likely accessed from the outer face of the subunit and at the intersubunit boundary (marked by arrow). *B*, Profile of the whole pentamer, viewed from above (see inset), displaying the same information.

The transduction process

Deciphering components specifically involved in the receptor activation process has benefited significantly from the availability of the AChBP crystal structure. This is due to the difficulties that arise in differentiating between components that are influencing the initial agonist-binding event to the closed receptor and those which determine the subsequent effectiveness of channel opening. Thus, a structural appreciation of the receptor aids in predicting and isolating residues that have a genuine significance in ligand-binding and channel-gating. Unfortunately, no unliganded crystal structures of the AChBP have so far been resolved (Celie et al., 2004). This means there is no measurement yet of the movements that loops A to C undergo upon agonist binding. However, medium resolution electron micrographs of the *Torpedo* nAChR have been obtained in the agonist-bound and unbound states (Miyazawa et al., 1999;Unwin, 1993;Unwin, 1995). These studies revealed that the agonist-bound α-subunit experiences a 'local disturbance' of the binding site. In addition the extracellular domain underwent a set of small axial rotations presumably to transmit activation to the channel region. Of particular interest was the realisation

that the α subunit transition, upon binding ligand, converted it to an orientation similar to that already assumed by the β and γ subunits, which experienced only minimal reorganisation during receptor activation. This situation may be analogous to the GlyR where the α subunit is also the principal agonist binding subunit and so the GlyR β subunit may remain conformationally stationary at least from the perspective of its extracellular domain (Fig 1.8*A,B*). Using the AChBP crystal structure, a more recent study has attempted to map the movements that occur in the extracellular domain during agonist activation by fitting the most conserved β-strand regions to the 4.6Å electron micrographs of the nAChR extracellular domains. This study revealed that the AChBP crystal structure, which has the putative agonist HEPES bound and therefore may be in the activated conformation already, could be overlaid with a good fit to the β, γ and δ subunits, but not the α subunit of the unbound-closed nAChR (Unwin et al., 2002). This is also most consistent with the non-ligand binding β, γ and δ subunits existing in a conformation close to that of the activated state for the extracellular domain, whilst the α subunit does not. It was possible to overlay the AChBP with the nAChR α subunit surface topology by simply reorienting the set of β-strands that are on the inside face of the subunit relative to those on the outer face of the subunit. This simple 15 – 16 ° rotation of the inner face strands consequently means that the '-' interface of the subunit undergoes a greater degree of movement compared to the '+' interface of the subunit (nomenclature of Fu and Sine, 1996; Fig 1.8*A,B*). This reorientation may therefore be the driving force for downstream communication with the channel. Currently there is no such evidence to validate this information in the GlyR. Furthermore, these studies were unable to address the primary movements that occur in the immediate vicinity of the agonist binding site due to the more flexible nature of the loops A to C. With regards to these initial movements the information is relatively speculative, though a mutation in the $GABA_AR$ β subunit in a position equivalent to GlyR α1 A101 of loop A does produce a spontaneously open receptor (Boileau et al., 2002). Also of interest is a Psi value analysis of a nine amino acid segment overlapping with and immediately following on from the A loop in nAChR α subunits. This technique attempted to measure the order of domain movements during receptor activation and revealed that the nine amino acid segment moves early on in the activation process

(Chakrapani et al., 2003). Thus it may be that the A loop is the actuator that enables downstream extracellular movements.

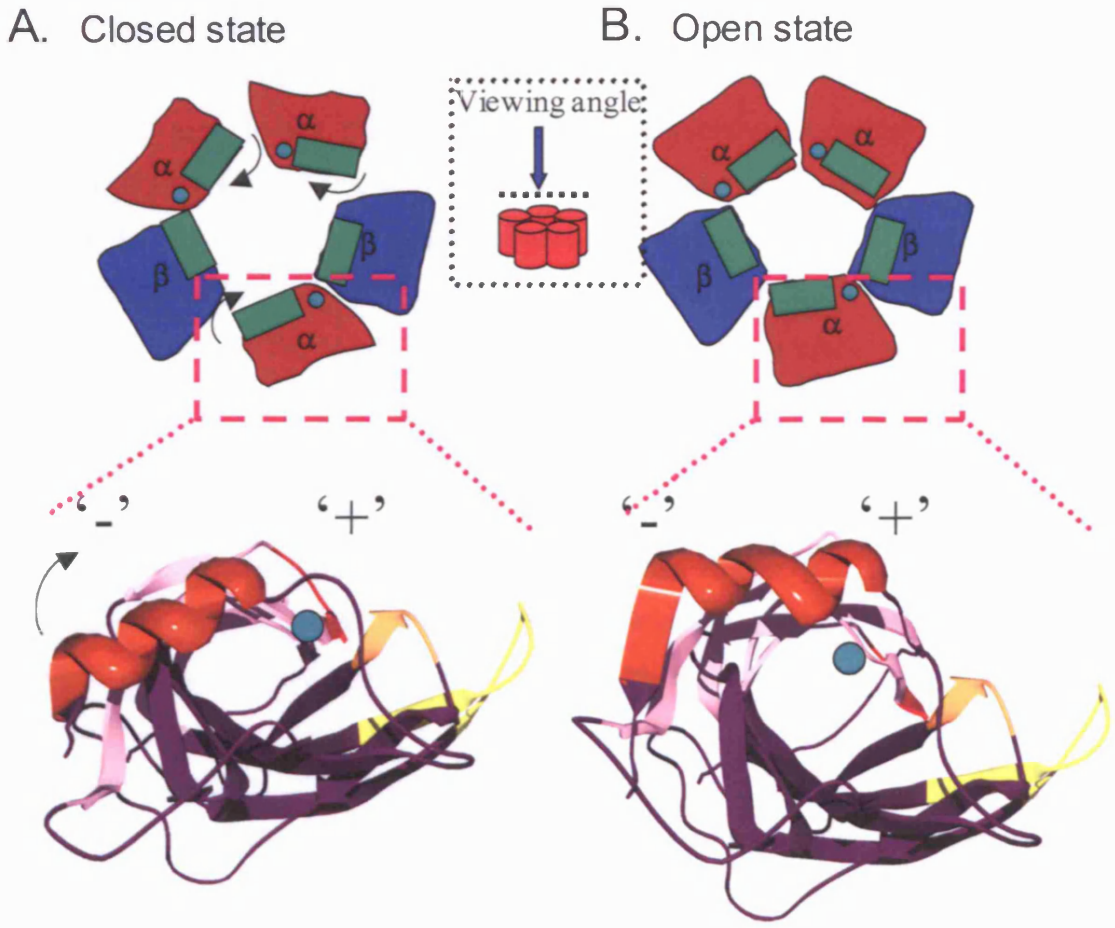

Figure 1.8 Hypothesis for cys-loop receptor activation, based on rotation of the extracellular agonist binding α subunit of the GlyR. *A*, Closed and *B*, Open conformations of the GlyR. The pentamers, viewed from above the receptor, represent cartoons of the rotation that is undertaken specifically by the agonist binding a subunit (red). The non-ligand binding β subunits (blue) are proposed to already reside in the active conformation. The green rectangles denote the α-helix present in each extracellular subunit domain for extra definition of each subunits orientation. The green circles represent the approximate axis of rotation for the α subunits during activation. The homology models reflect enlargements of a single α1 subunit from the cartoon pentamer in the same alignment (red box; also viewed from above). The green circles represent the axis of rotation and demonstrate that during the 15 – 16 ° rotation of the inner sheet relative to the outer sheet (indicated by black arrow), the internal '-' side of the subunit will undergo a greater movement than the internal '+' side of the subunit. This rotation of the extracellular domain of the GlyR α subunit is proposed to transmit downstream to the helical bundle and induce channel opening.

One limitation of the combined AChBP-electron micrograph analysis is that it does not indicate which are the critical regions for transmitting the agonist binding effect down to the channel. Initial mutagenesis experiments targeted residues predicted to reside close to the transmembrane interface based on primary sequence due to the absence of a high-resolution structural model. Likely candidates to mediate communication from this interface to the extracellular domain consist of the section immediately prior to M1, the M2-M3 linker domain or the C-terminal tail from M4. The significant size of the 12-13 amino acid M2-M3 linker, its apparent central location and its direct link to two membrane segments including M2, the pore lining helix (discussed later) makes this the most likely candidate. Early functional studies did indeed point to the M2-M3 linker as part of the gating mechanism. Initially a naturally occurring mutation was identified in patients with the human startle disease that replaced a positively charged GlyR α1 R271 with an uncharged leucine or glutamine (see review Rajendra, 1995a). Subsequent functional studies revealed that these receptors had significantly reduced sensitivities to glycine and the higher single channel conductance states were abolished sufficient to reduce whole-cell currents by 90 % (Langosch et al., 1994;Rajendra et al., 1995c). Furthermore the cell surface receptor expression levels, assessed by [^{3}H] strychnine binding, were not reduced and glycine binding, as assessed by its ability to displace [^{3}H]strychnine, was only reduced by 50 – 100 fold, in comparison to glycine potency, which was reduced by 230 – 410 fold. Further evidence supporting a role for this arginine residue in gating was the abolition of β-alanine and taurine evoked currents. By contrast, the sensitivity of the receptor to these compounds, measured in terms of their ability to inhibit glycine mediated currents, was unaffected suggesting that the efficacy of β-alanine and taurine had been reduced to such an extent that they were now unable to activate the receptor (Rajendra et al., 1995c). Since identification of R271, a functional scan of the M2-M3 loop has identified further residues that influence receptor function in a manner consistent with an involvement in gating (Lynch et al., 1997). Moreover, substituted cysteine accessibility mutagenesis (SCAM) experiments in this region on the open and closed receptor conformations revealed a differential pattern of accessibility supporting a movement of this domain during activation (Han et al., 2001). In the context of the original structural evidence on nAChRs, suggesting the ligand binding α and structural β subunits do not undergo

comparable movements during receptor activation, a second SCAM study on the GlyR β-subunit yielded no obvious effects on receptor potency when β subunit M2-M3 residues were mutated to cysteines. In addition there were no obvious effects on function upon application of a cys-modifying reagent in the open, or closed, receptor conformations to αβ heteromeric receptors containing Cys mutated β subunits in the M2-M3 region (Shan et al., 2003). In accord with the evidence that the M2-M3 linker is a critical gating component, naturally occurring mutations and site-directed mutagenesis studies on this domain in nAChRs and $GABA_A$Rs also revealed impaired receptor function in a manner consistent with an influence on gating (Campos-Caro et al., 1996;Kusama et al., 1994;Sigel et al., 1999;Baulac et al., 2001). Also of interest is the characterisation of two nearby GlyR α1 residues Q266 and S267, both present on the extracellular side of the M2 domain. These residues when mutated to create Q266H and S267Q GlyRs impair function in a manner consistent with gating (Moorhouse et al., 1999;Findlay et al., 2003).

Due to the juxtaposition of the M2-M3 linker to the channel it is easy to appreciate how this domain can influence receptor activation but prior to resolving the AChBP structure it was not clear how components of the extracellular ligand-binding domain communicate across to the M2-M3 linker. The AChBP crystal structure provided a possible solution as the β-strands and loops located at the base of this structure could now be identified and would be in an ideal location to interact with the transmembrane segments and the M2-M3 loop (Brejc et al., 2001) (Fig 1.9*A,B*). A recent study proposed an electrostatic interaction between two loops at the base of the extracellular domain and the M2-M3 linker (Kash et al., 2003a). Charge reversals at $GABA_A$R α1 D57 from the β1-2 loop, D149 from the cys-loop and K279 from the M2-M3 linker, all disrupted receptor function in a manner consistent with gating. However, paired charge reversal of the M2-3 linker, K279D, with either the β1-2 loop D57K, or the cys-loop D149K mutation, the $GABA_A$R regained a large degree of receptor function. This suggested that these domains interacted regardless of charge orientation. Since this study a high 3Å resolution electron micrograph of the M1-M4 segments including the M2-M3 linker has been reported (Miyazawa et al., 2003). This structure was paired up with the extracellular domain and predicted

that the β1-2 loop, the cys-loop and the M2-M3 linker are in prime orientation for communication (Fig 1.9*A,B*).

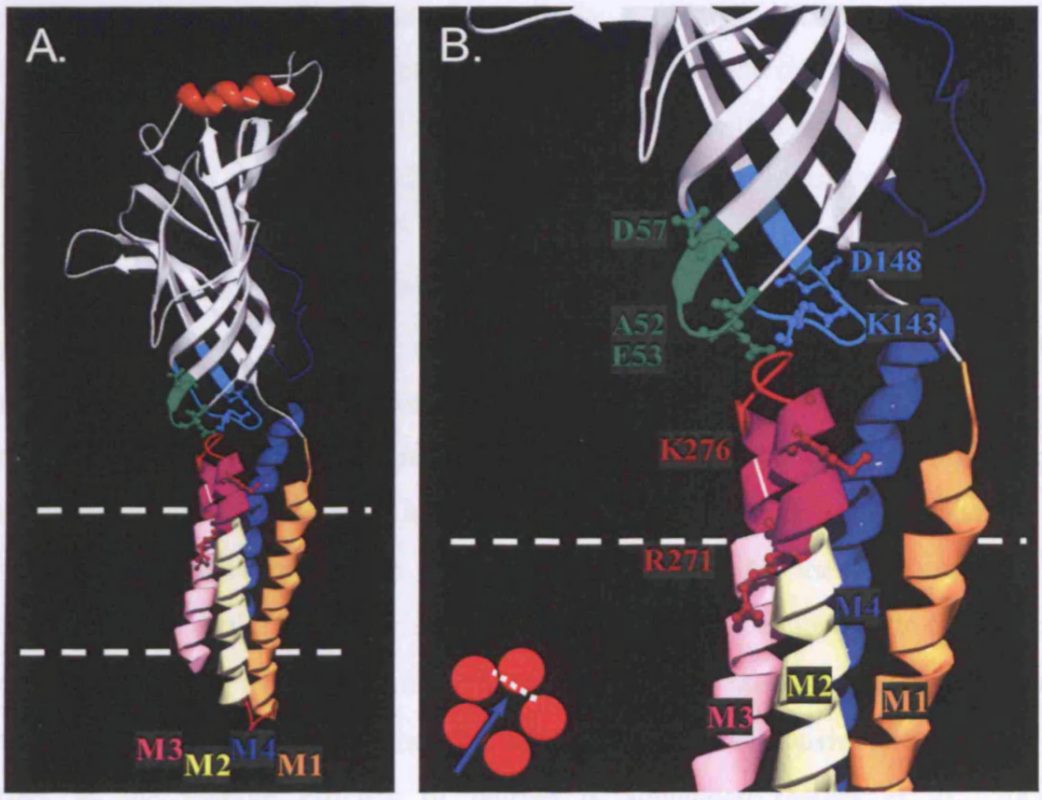

Figure 1.9 Interactions between the extracellular domain and the transmembrane domains. The structure is based on a homology model of the AChBP (Brejc et al, 2001) and the *torpedo* nAChR transmembrane domains (Miyazawa et al, 2003) paired together. *A*, Whole subunit and *B*, close-up of the gating interactions. The β1-2 loop (green) and the cys-loop (light blue) of the extracellular domain are closely apposed to the M2-3 loop (red) and the top two turns of the M2-3 helices (purple; individual helices are labelled on the diagram) which rise out above the membrane (white dashed line). Residues in the interacting domains that influence receptor properties consistent with gating are displayed and labelled.

In the context of the GlyR individual alanine substitutions have been made throughout the cys-loop domain. This approach identified a number of residues including α1 D148 (corresponding to $GABA_AR$ α1 D149), that significantly reduced glycine potency and maximal currents, as well as taurine potency and relative efficacy, consistent with an effect on channel gating (Schofield et al., 2003;Schofield et al., 2004). Charge reversals introduced at the GlyR α1 β1-2 loop E53 and D57 residues, also disrupted receptor function in a manner consistent with gating (Absalom et al., 2003). Furthermore a K143 residues in the cys-loop was shown to change its accessibility pattern in a SCAM study suggesting this domain, like the M2-M3 linker can change its conformation during activation (Absalom et al., 2003).

However, it is unlikely that electrostatic communication between the β1-2 loop, the cys-loop and the M2-M3 linker can be generalised throughout the cys-loop receptor families as attempts to reproduce a similar correlation in the $GABA_AR$ β_2 subunit and in the GlyR, failed (Absalom et al., 2003;Kash et al., 2003b). Also non-charge related substitutions in the β1-2 loop can cause subtle effects on receptor potency as was originally discovered for the *spasmodic* mouse, which has the A52S mutation in GlyR α1 (Ryan et al., 1994;Saul et al., 1994). This same location in the α2 subunit, which is the source of splice variance between α2A and α2B (Fig 1.1) also causes a reduction in glycine potency at the α2A subunit in a manner consistent with a gating effect as the relative efficacy of taurine is attenuated (Miller et al., 2004). Furthermore, a recent chimeric study generated a non-functional cys-loop receptor by pairing the extracellular domain of the AChBP to the transmembrane segments of the $5\text{-}HT_{3A}R$. Function was then restored to this receptor by progressively substituting each of the three loops at the base of the extracellular domain, the β1-2 loop, the cys-loop and the β8-9 loop, with those of the $5\text{-}HT_{3A}R$. Only when all three of these loops, not just the two identified previously by Kash et al (2003a) were restored, was there an effective return of the receptor's gating properties (Bouzat et al., 2004). In the case of the nAChR, the hydrophobic V44 from the β1-2 loop is predicted to be in close apposition with the M2-M3 domain (Miyazawa et al., 2003). These authors propose that this residue docks into a hydrophobic pocket at the end of the M2-3 loop and upon activation the rotation of the extracellular domain twists this residue

exerting an effect on the M2-M3 loop to induce channel opening. Together this evidence suggests that the gating process is most likely a combination of charged polar and apolar interactions that can occur between the three base loops of the extracellular domain and the M2-M3 linker.

The ion channel and its opening mechanism

A large body of evidence, accumulated from the nAChR, supports the view that the M2 domain of cys-loop receptors is responsible for forming the channel and contains the gate responsible for opening and shutting of this channel (for review see Devillers-Thiery et al., 1993). The M2 segment of the cys-loop receptor family is the most conserved domain between subunits, highlighting the important nature of its role. For GlyRs, a mutagenesis study identified a residue on the intracellular cusp of M2 that is critical for determining the maximal conductance state. A G254A substitution in GlyR α1 increased its maximal conductance state in symmetrical chloride solutions from 86 pS to 107 pS bringing it in line with GlyR α2 and α3, which have an alanine at this position and have maximal conductance states of 111 and 105 pS, respectively (Bormann et al., 1993). One major difference between the channels of the GlyR and the nAChR is their ionic selectivity. Whilst the nAChR favours cation conductance, the GlyR channel has an anion permeability sequence of $SCN^->I^->NO_3^->Br^->Cl^->HCO^->$acetate$>F^->$propionate (Bormann et al., 1987) and the responsible M2 residues have now been identified (Galzi et al., 1992;Keramidas et al., 2000). It is beyond the scope of this introduction to describe the multitude of experiments that have been carried out to discern the architecture of the channel and its ability to determine selectivity of anionic conductance in the GlyR (for review see Rajendra et al., 1997;Lynch, 2004). However, from the perspective of receptor activation and possible allosteric modulation there are a number of relevant points to be raised. The general structure of the pore for the *Torpedo* nAChR suggests that M1-4 exist as membrane spanning α-helices with M2 positioned on the interior face such that the pentamer contains an inner ring of five M2 helices (Fig 1.10*A,B*; Miyazawa et al., 1999;Miyazawa et al., 2003). These M2 helices are 40 Å long with two turns of each helix rising out above the extracellular membrane face. These are connected via a short M2-M3 linker to the M3 segment, which also protrudes above the membrane face by two turns of an α-helix (Fig 1.9*A,B*; Miyazawa et al., 2003).

Each of the five subunits align the M2 helices to display residues of the corresponding location at the same position thus creating rings of residues in register spanning across the membrane. The exact location of the gate is still contentious but is probably located just over halfway down the pore towards the intracellular side, corresponding to an 8 Å stretch of helix, where the pore diameter is less than 3.5 Å. This section includes a critically conserved ring of hydrophobic leucines (nAChR α1 L251; GlyR α1 L261 in Fig 1.10*A,B*) and just over one helical turn above this a ring of Val 255 residues (Labarca et al., 1995;Miyazawa et al., 2003). In this context the location L251 in the closed state, represents a ring of residues that form what is effectively a 'hydrophobic girdle' between the M2 helices. This hydrophobic girdle operates by creating an energetic barrier for ion permeation as ions must shed their hydrated water shell before being able to fit through such a small pore.

With regards to the activation mechanism, the current hypothesis is that the gate, and therefore the location of the leucine and valine rings, opens up through a sideways rotation of each M2 helix (Miyazawa et al., 2003;Unwin, 1995). This may arise through each M2 segment moving individually to gradually weaken the stable closed channel state, or a synchronised group movement of all the M2 domains together. The basis of this hypothesis was in part due to the presence of two predicted flexible loops, the M1-M2 linker and M2-M3 linker, at either end of the pore lining helix (Fig 1.10*B*). The relevance of the GlyR M1-M2 loop in gating is apparent from a hyperekplexia autosomal recessive mutation (I244N) that was identified in this region (Fig 1.10*C*; Rees et al., 1994). Mutant receptors exhibited decreased sensitivity to glycine and smaller maximal current responses, which could in part be attributed to an effect on channel gating. Thus it would seem that both flexible loops at either end of M2 can influence gating and may be acting as hinges. One potential problem with this hypothesis is that if the M2 leucine residues do form a tightly enclosed gate then where does the space arise from for the helices to each rotate to the side? Fortunately, the structural data does predict the presence of a sizeable water filled pocket on the back of M2 between M2 and M3 (Fig 1.10*D*), which allows space for M2 movement. In addition, experiments investigating a putative

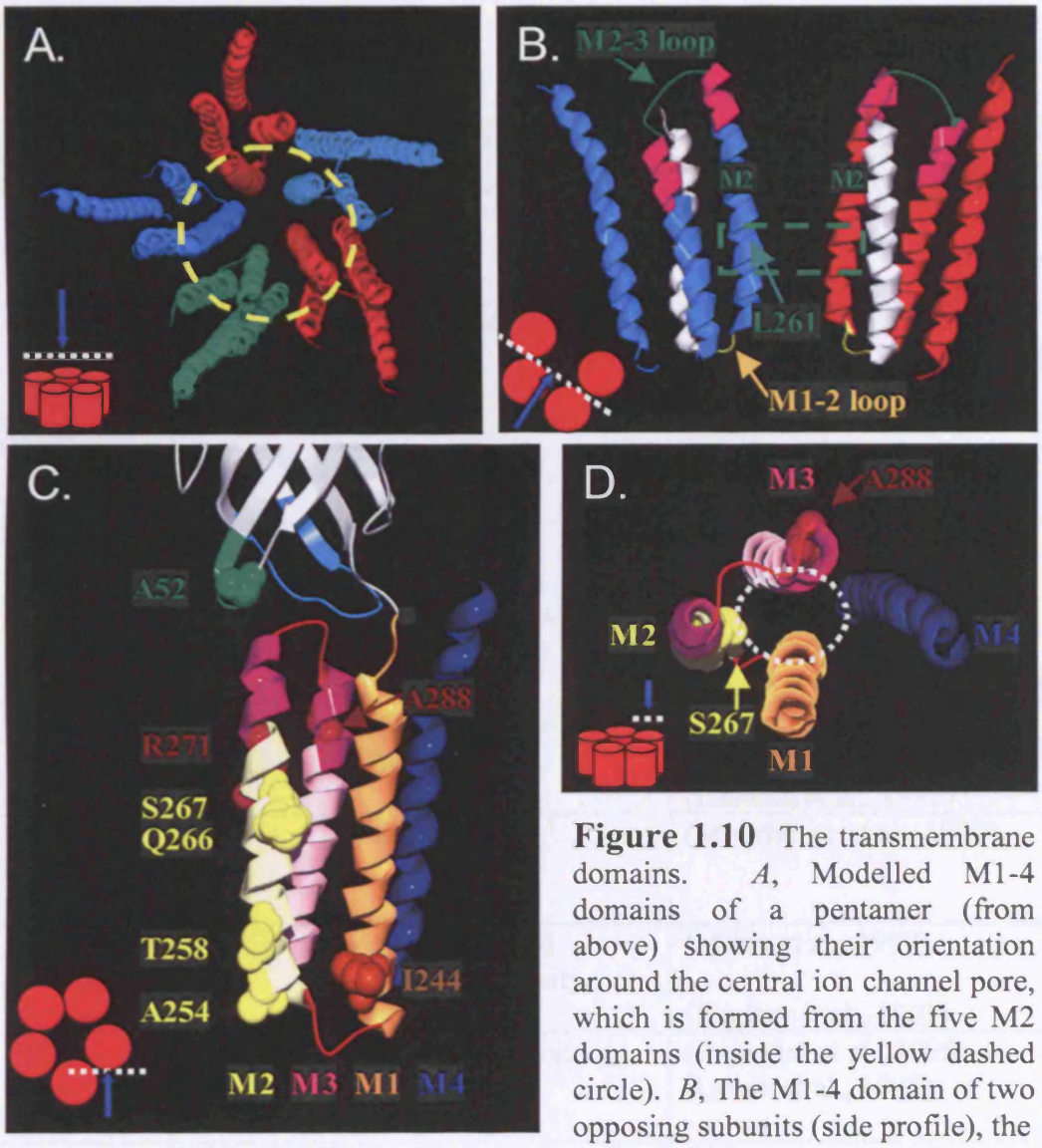

Figure 1.10 The transmembrane domains. *A*, Modelled M1-4 domains of a pentamer (from above) showing their orientation around the central ion channel pore, which is formed from the five M2 domains (inside the yellow dashed circle). *B*, The M1-4 domain of two opposing subunits (side profile), the green box highlights the hydrophobic girdle, which represents the gate approximately two thirds of the way down the channel in the M2 domains, corresponding to L261 in GlyR α1. At either end of M2 is the M1-M2 (yellow) and M2-M3 (green) loops proposed to act as two hinges that allow the M2 domain to rotate sideways and open the channel. *C*, Identification of residues involved in gating, conductance, desensitisation and sensitivity to alcohols, anaesthetics, picrotoxin and cyanotriphenylborate. The helices are colour coded and labelled (side profile). Due to the multiple roles of most of these residues, their functions are presented in Table 1.1. *D*, View from above of the four helices from a single subunit, highlighting the location of the water filled vestibule behind the pore lining M2 domain (white dashed circle). The two residues implicated in determination of alcohol and anaesthetic potency are also presented.

GlyR α1 residue	Location	Influential roles	References
A52	β1-2 loop	PTX sensitivity, Gating	(Miller et al., 2004) (Ryan et al., 1994;Saul et al., 1994;Miller et al., 2004)
L142, F145, P146, D148	cys-loop	Anaesthetic sensitivity, Gating	(Schofield et al., 2004) (Absalom et al., 2003;Schofield et al., 2003;Schofield et al., 2004)
I244	M1	Desensitisation, Gating	(Breitinger et al., 2001) (Breitinger et al., 2001)
A254	M2, (2')	Conductance, Desensitisation CTB sensitivity, PTX sensitivity	(Bormann et al., 1993) (Zhang et al., 1994) (Rundstrom et al., 1994) (Pribilla et al., 1992) (ffrench-Constant et al., 1993)
T258	M2, (6')	PTX sensitivity	(Gurley et al., 1995)
L261	M2, (9')	Channel gate	(Unwin, 1993) (Labarca et al., 1995)
Q266	M2,	Gating	(Moorhouse et al., 1999)
S267	M2, (15')	Anaesthetic and alcohol sensitivity, Gating	(Mihic et al., 1997) (Findlay et al., 2003)
R271	M2,	Conductance/Gating, PTX efficacy	(Rajendra et al., 1995) (Lynch et al., 1995)
A288	M3	Anaesthetic and alcohol sensitivity	(Mihic et al., 1997)

Table 1.1 The functions associated with residues in the GlyR transmembrane domains. Nearby residues from the β1-2 loop and cys-loop that influence the pharmacology of antagonists linked to the membrane region are also included. See Fig 1.10*C,D* for structural information on the location of these residues.

binding site for alcohols between M2 and M3 revealed that altering the size of amino acid side chains present on M2 and M3 controls the 'cutoff' point for the size of alcoholic molecules that are able to enhance receptor function. This suggests that the size of the channel lumen is determined by the side chain moieties present (Wick et al., 1998). Another experimental observation that is consistent with the M2 rotation hypothesis was determined by labelling the nAChR β subunit at A267 of M2 (equivalent to GlyR α1 Q266, Fig 1.10*C*) with a fluorophore tetramethylrhodamine. Upon agonist evoked receptor activation there was a shift in the fluorescence emission peak to lower wavelengths in accord with the fluorophore entering a more hydrophobic environment (Dahan et al., 2004). This is consistent with the M2 domain twisting to move the A267 into a more hydrophobic location near M3 and M4. It is worth mentioning that although the GlyR β subunit may have a limited effect on gating via its M2-M3 linker (Unwin et al., 2002;Shan et al., 2003), the experiment above suggests that the M2 domains in the non-ligand binding subunits still undergo a conformational shift during receptor activation. In support of this, the mutation L285T, in the leucine gate of the GlyR β M2 domain, increases the glycine potency, presumably by destabilising the closed conformation (Shan et al., 2003).

The intracellular domain

The intracellular domain is associated with the most uncertainty as regards its structure. The only available insight into its structure is from a medium resolution 4.6 Å electron micrograph (Miyazawa et al., 1999) but this is of insufficient resolution to pinpoint individual amino acids. However, it does suggest that the intracellular domain is ordered and projects inwards from each subunit to form a cap with significant apertures between the sides of the subunit interfaces through which ions could flow (Fig 1.3). These apertures, though sizeable, may at least in the case of the 5-HT_3R, control channel conductance (Kelley et al., 2003).

For the GlyR, the intracellular domain has been attributed with three functions. Firstly, the β-subunit contains an 18 amino acid insert in this region that is vital for gephyrin binding and receptor anchoring (Meyer et al., 1995;Kneussel et al., 1999); secondly, both GlyR α1 and α3 have variable splice insertions in the M3-M4 intracellular loop, which contain consensus phosphorylation sites capable of

modulating channel function. In this regard, an M2-M3 S346 residue in the GlyR α3 subunit is such a consensus, for PKA, which is vital for determining sensitivity to the PGE_2 pain induced pathway (Harvey et al., 2004). Finally, the two intracellular M1-M2 and M3-M4 domains have also been shown to have an important influence on the rate of receptor desensitisation. This is supported by the fact that phosphorylation can modulate the rate of desensitisation for GlyR α1 (Gentet and Clements, 2002). In addition, α3 splice variants, which are distinguished by the presence or absence of a 15 amino acid insert in the M3-4 intracellular domain, have different desensitisation profiles. This property was primarily attributed to the presence of three hydroxyl groups within this domain located at T325, Y334 and S337 (Breitinger et al., 2002). Furthermore a study on residues throughout the M1-M2 loop shows that disruptions in this region influence the rate of receptor desensitisation (Breitinger et al., 2001).

In summary, the structure-function studies seem to support the presence of a localised agonist-binding domain formed by, in the case of the GlyR, loops A-C. The subsequent activation event from this site may possibly be mediated via loop A and the end result of this is a downstream predicted 15° rotation of the internal face of the extracellular domain GlyR α subunit. This rotation exerts its effect on the three base loop regions, β1-2, the cys-loop and β8-9, which in turn reorganise the M2-M3 linker and this twists the M2 domain into an open conformation made easier by the flexible M1-M2 loop at the other end of M2 and a water filled lumen at the back of M2. As should be realised, this overall scheme remains relatively speculative and the fine details are only partially described. One aspect that is particularly evident from these studies is the limited identification of molecular components responsible for the different functional properties amongst GlyR subtypes. While studies now suggest that the GlyR α1 and 2 subtypes activate at different rates (Mangin et al., 2003) there have been no reports elucidating the molecular components responsible for this. Furthermore, though intracellular domains may be able to influence desensitisation there is no structural data on these regions and it is impossible to even speculate how this process is induced. In terms of single channel studies, residues have been identified which can account for subtype variations in the main conductance states, however there have been no

molecular correlations to elucidate the residues responsible for different GlyR open-closed times and agonist efficacies. Thus, a vast repository of data is still required before those properties that enable receptors to exert unique physiological effects are determined from a molecular aspect and linked to the receptor activation process. In addition, relatively little is known about how principle GlyR modulators such as alcohols, anaesthetics, picrotoxin and Zn^{2+} exert their effects (Laube et al., 2002b). It is the job of structure-function studies to now attempt to decipher the molecular correlates of subtype specificity and modulator action and to place these in the context of the newly elucidated receptor binding-activation pathway. As the focus of this study is on the modulator Zn^{2+}, and how it can interplay with receptor function, the next section will deal with a few of the prime GlyR modulators and what is known of their mechanisms of action.

Pharmacology

Alcohols and anaesthetics

Anaesthetics and alcohols are able to potentiate both $GABA_A$Rs and GlyRs. This potentiation can occur at low nanomolar concentrations dependent on alcohol or anaesthetic structure (Downie et al., 1996; Wick et al., 1998). The evidence suggests these two classes of compound may act via a common site. Indeed, two critical determinants in the GlyR α1 subunit, S267 from M2 and A288 from M3, can determine whether or not alcohols and anaesthetics potentiate GlyRs (Mihic et al., 1997). These two residues are located towards the extracellular side of the membrane and on either side of the predicted water filled lumen between M2 and M3, an ideal location for a binding site (Miyazawa et al., 2003; Fig 1.10*C,D*). The presence of this region as a binding site for modulators is strengthened by the phenomenon of alcoholic 'cutoff'. This is characterised by an increased potency for the n-alcohols, as the chain length increases, which reaches a ceiling (Wick et al., 1998) after which the potency stays unchanged, or begins to drop with longer chain lengths. This 'cutoff' varies between cys-loop receptors with the cutoff occurring earlier on the $GABA_A$R ρ subunit than for the GlyR (Mascia et al., 1996;Mihic and Harris, 1996) and can be reversed by switching the differential identities of GlyR α1 S267 and A288 with the equivalent residues from the $GABA_A$R ρ subunit (Wick et al., 1998). This suggested that these residues altered the size of the cavity,

supporting its potential as a binding site. From the location of this putative binding site it would seem sensible that in order for anaesthetics and alcohols to mediate their potentiating effects these molecules would facilitate the movement of the M2 domain either directly, or by aiding the M2-3 hinge movement. SCAM experiments of residues from the α1 GlyR, including S267 and A288, revealed that the accessibility of both these residues increased upon receptor activation suggesting that this lumen does indeed undergo a conformational change during activation and that alcohols and anaesthetics could perhaps facilitate this process (Lobo et al., 2004). Intriguingly, individual alanine substitutions across the whole of the neighbouring GlyR cys-loop revealed a number of positions where potentiation by the anaesthetics halothane and isofluorane was ablated (Schofield et al., 2004). Thus, several facets of the GlyR gating apparatus appear to be able to influence anaesthetic modulation.

Picrotoxin (PTX) and cyanotriphenylborate (CTB)

These two molecules are both antagonists at GlyRs (Pribilla et al., 1992;Rundstrom et al., 1994;Miller et al., 2004) and highlight the caution that must be taken when ascribing a mechanism of action for an inhibitor based on the location of residues that determine its sensitivity. Originally, residues in M2 were identified that affected antagonist potency in both cases. The high sensitivity of GlyR α1 to CTB, compared to α2, was reversed by substituting G254 for the α2 alanine counterpart (Fig 1.10*C*)(Rundstrom et al., 1994). Similarly for PTX, replacing part of the β subunit M2 domain with a corresponding portion from the α1 subunit, markedly increased the sensitivity of αβ heteromers to PTX (Pribilla et al., 1992). The inhibition by CTB was in keeping with a direct action at M2 as CTB was use-dependent, uncompetitive, and the block was enhanced at positive membrane potentials (Rundstrom et al., 1994). The original conclusion for PTX also suggested this molecule was partially inhibiting receptor function by channel blockade (Pribilla et al., 1992). However the mechanism of PTX action at GlyR α1 has since been shown to act in a manner more consistent with competitive antagonism (Lynch et al., 1995). Furthermore, $GABA_A$ receptors are rendered picrotoxin insensitive by introduction of the GlyR β residue F282 located towards the base of M2 (Gurley et al., 1995), which is a threonine in $GABA_A$ receptors and in the high sensitivity GlyR α1 (T258; Fig 1.10*C*). This suggests these two receptors share similar components

for PTX action and also in $GABA_A$Rs, PTX does not have the profile of an open channel blocker. Another residue from the $GABA_AR$ corresponding to GlyR α1 G254 located at the base of the channel beneath GlyRβ F282, also influences the potency of PTX action by up to 100-fold (ffrench-Constant et al., 1993). This $GABA_AR$ residue has also been shown to be important in desensitisation (Zhang et al., 1994) and it has been proposed that PTX may act via an allosteric mechanism, preferentially binding activated receptors and stabilising them in agonist-bound closed conformations (for review see Hosie et al., 1997). In support of the M2 region being a possible PTX binding site, SCAM studies on these residues showed that the $GABA_AR$ equivalent to GlyR α G254 is less accessible in the presence of PTX (Xu et al., 1995). Despite this, disruption of the GlyR α1 R271 residue at the other end of M2 (Fig 1.10*C*) can also influence PTX modulation by switching the properties of PTX from competitive to non-competitive and even to a potentiator of glycine evoked responses at low concentrations (Lynch et al., 1995). Furthermore a residue in the extracellular gating domain β1-2 loop of the GlyR α2 receptor has also been shown to modestly influence the PTX potency (Fig 1.10*C*)(Miller et al., 2004). It should be noted that PTX is in fact a mixture of two separate components, picrotoxinin and picrotin, both of which have the same potency at the GlyR suggesting they mediate their effects in a similar manner (Pribilla et al., 1992).

Zinc

The molecular basis of Zn^{2+} modulation of glycine receptors

The first study to investigate the modulation of GlyRs by Zn^{2+}, carried out by Bloomenthal et al, (1994) revealed a biphasic profile such that Zn^{2+} exerted potentiation at low 0.1-10 μM concentrations and inhibition at higher concentrations. This profile was directly comparable between homomeric GlyR α2 and heteromeric GlyR α2β and was also similar for native GlyRs from rat spinal cord cultures (Bloomenthal et al., 1994). This data was later reproduced for GlyR α1 showing that the inhibitory site was selective for Zn^{2+} over Ca^{2+} and Mg^{2+} with only Ni^{2+}, from the metal ions tested, able to replicate the Zn^{2+} mediated inhibition process (Laube et al., 1995). Since these original reports, independent studies have verified the biphasic profile of modulatory Zn^{2+} on native GlyRs in various neuronal preparations

indicating that this phenomenon is most likely retained throughout the majority of, if not all, glycinergic systems (Li and Yang, 1999;Han and Wu, 1999).

The follow-up study by Laube et al (2000) identified a putative GlyR α1 D80 residue as a plausible coordinating residue for Zn^{2+} potentiation (Laube et al., 2000;Laube et al., 2002b; Fig 1.11). Though this moiety is acidic and is therefore one of the favoured chemical groups for Zn^{2+} coordination at binding sites, a subsequent independent study demonstrated that this residue only ablated Zn^{2+} enhancement of glycine evoked responses and not those of another endogenous GlyR agonist taurine, believed to bind to the same site as glycine (Lynch et al., 1998). This suggested that D80 is unlikely to form part of a single Zn^{2+} site necessary for agonist enhancement and instead is somehow linked either to glycinergic or zincergic transduction. In addition to this, the study by Lynch et al (1998) identified a number of residues in the GlyR M2-M3 linker region that also abolished Zn^{2+} enhancement. Though these residues did not bear the traits of classical Zn^{2+} binding moieties their location in the M2-M3 linker believed to be a pertinent component of the agonist gating apparatus (Lynch et al., 1997;Han et al., 2001;Kash et al., 2003a) suggested that Zn^{2+} potentiation may mediate its effect by influencing receptor gating. This assertion is also supported by the demonstration that Zn^{2+} was able to enhance the relative efficacy of the partial agonist taurine but did not increase the maximal response for the full agonist glycine, which as discussed previously has a P_o of 0.98 (Laube et al., 2000).

Whilst advances in determining the molecular basis of Zn^{2+} enhancement have essentially stagnated since these studies, reports to identify components of Zn^{2+} mediated inhibition have continued to make progress. The first such study used the histidine scanning technique to individually replace these potential Zn^{2+} binding residues in the extracellular ligand binding portion of the protein with non-Zn^{2+} coordinating alanines. This led to the critical identification of GlyR α1 H107 and H109, as both GlyR $\alpha1^{H107A}$ and GlyR $\alpha1^{H109A}$ were resistant to 1 mM Zn^{2+} when co-applied with glycine (Harvey et al., 1999; Fig 1.11). Another report complemented these findings by demonstrating that alanine substitution of the nearby GlyR α1 T112, and also less profoundly E110, reduced the sensitivity of

GlyR α1 to Zn^{2+} mediated inhibition (Laube et al., 2000; Fig 1.11). Interestingly, the molecular basis of proton inhibition appears to overlay to some extent with the inhibitory site as Zn^{2+} inhibition has a lower potency when the concentration of protons is increased at pH 5.4 suggesting the two ions compete with each other for the same site (Harvey et al., 1999). A more recent study has identified GlyR α1 H109 and T112 as the critical components for proton inhibition, but not H107, suggesting that though the sites overlap, the reliance on certain residues such as H107 is different (Chen et al., 2004).

Figure 1.11 Residues identified in the extracellular domain that influence Zn^{2+} potentiation and inhibition. Homology model from the inside face (see inset) of two neighbouring GlyR α1 subunit extracellular domains. Residues implicated in Zn^{2+} mediated potentiation, D80, and Zn^{2+} mediated inhibition H107, H109, E110 and T112, are displayed and labelled. For ease of comparison with other characterised domains the extracellular domain is presented in a similar manner to previously as two parallel plates of β-strands, which run perpendicular to each other, the inside face in pink and the outside face in white. The agonist binding domain is also shown, consisting of loop A (red), loop B (orange) and loop C (yellow), as well as the gating domain, β1-2 loop (green), cys-loop (light blue) and β8-9 loop (dark blue).

Critically the importance of GlyR α1 H107, H109 and T112 in Zn^{2+} mediated inhibition have all been independently verified in the most up to date study on Zn^{2+} inhibition (Nevin et al., 2003). This report used a GlyR structural model based on the homologous AChBP protein (Brejc et al., 2001). The resultant model predicted that the inhibitory Zn^{2+} site between H107 and H109 could in fact form at the interface between two subunits (Fig 1.11) and the authors produced evidence in support of this by demonstrating that co-expression of $\alpha1^{H107A}$ and $\alpha1^{H109A}$ recovered near wild-type sensitivity to Zn^{2+} mediated inhibition. If the binding site was located solely within the confines of each individual subunit then co-expressing these mutated receptors to form mixed pentameric complexes would not recover Zn^{2+} inhibition as each individual site would still lack one of the Zn^{2+} binding residues. However if the site were interfacial then mixed pentameric complexes would produce receptors where some of the sites contained two non-binding alanines whilst others retained the full Zn^{2+} binding apparatus and could mediate Zn^{2+} inhibition. In addition to this the authors were unable to reproduce these results in the context of GlyR α1 T112 leading to the postulate that this residue has only an indirect bearing on the site of Zn^{2+} inhibition.

Zn^{2+} as a potential endogenous modulator of glycine receptors

Neurotransmitter release from a single synapse is generally considered to be a selective pairing between a specific neurotransmitter and its ligand-gated receptor; however in some circumstances, communication may be more complex. Such a situation can arise from the synaptic co-release of different neurotransmitters e.g. GABA and glycine in the spinal cord, which occasionally work together to simultaneously activate two types of postsynaptic receptors. This co-release property can also be extended to the paired release of a neurotransmitter with a receptor modulator, e.g., co-release of the NMDA receptor agonist glutamate and its synergistic partner, glycine (Johnson and Ascher, 1987;Corsi et al., 1996). A slight modification of this theme exists where the slow diffuse release of a modulator allows for long term modulation of postsynaptic receptors, e.g., in neurosteroid modulation of $GABA_A$ receptors (Belelli and Herd, 2003;Lambert et al., 2003;Stell et al., 2003). One prime candidate for the role of an endogenous modulator of neurotransmission is the transition metal cation Zn^{2+}. The significance of this cation

in neurotransmission and whether it participates in fast synaptic co-release, a slow diffuse release, or even simply exists as a background modulator present at a constant concentration as a 'cationic veneer' across the plasma membrane, is still debated.

The initial evidence favouring Zn^{2+} as a physiologically relevant synaptic modulator relied on histochemical studies using Zn^{2+} staining reagents such as Timms' sulphide (Danscher, 1981), sodium selenite (Danscher, 1982) and fluorescent probes, to establish the presence of Zn^{2+} across many discrete brain regions (Danscher, 1984;Danscher et al., 1985;Danscher, 1996;Frederickson et al., 1987;Frederickson, 1989;Frederickson et al., 1992). Further studies revealed that Zn^{2+} is selectively packaged into numerous particular cell types, including: fibres from the perirhinal cortex to the neocortex and septum; amygdala (Perez-Clausell et al., 1989;Perez-Clausell, 1996); neurones of the dorsal cochlear nucleus (Frederickson et al., 1988), cerebellum, thalamus (Mengual et al., 2001), brain stem, spinal cord, retina and olfactory bulb (see Frederickson, 1989;Frederickson et al., 2000). The most famous example is the hippocampal mossy fibre innervation from the dentate gyrus to the CA3 pyramidal neurones (Haug et al., 1971;Crawford and Connor, 1972;Slomianka, 1992). Though the concentration of free intracellular Zn^{2+} is believed to be very low, possibly picomolar for most cell types (Simons, 1991), the labelled 'zinc-containing neurones' (Frederickson et al., 2000) revealed intense Zn^{2+} staining in a pattern consistent with the packaging of Zn^{2+} into synaptic vesicles in axonal terminal boutons. This fits with the principal characteristic required for Zn^{2+} to act as a dynamic neuromodulator, its presence in a loosely bound, mobile form available for rapid release at the synapse (Frederickson et al., 2000).

In keeping with a zincergic action at synapses, an efficient reuptake and repackaging pathway is required. Though the exact molecular components of the initial reuptake stage from the extracellular space have not been determined a relatively high sensitivity, 0.3 – 20 μM saturable transport has been reported (Howell et al., 1984;Wensink et al., 1988; Colvin et al., 2000a;Colvin et al., 2000b). The sensitivity of this process is unlikely to be relevant to the estimated nanomolar to picomolar background levels of extracellular Zn^{2+} (Kay, 2003) but may be sufficient to have an

impact at the synapse where concentrated Zn^{2+} release could presumably reach much higher concentrations. Likely candidates for the downstream protein machinery of Zn^{2+} repackaging have, however, been elucidated with Zn^{2+} proposed, upon cellular re-entry, to bind proteins such as metallothionein III, which may facilitate Zn^{2+} translocation to synaptic vesicles for sequestration via the Zn^{2+} transporter, ZnT-3 (Palmiter et al., 1996). ZnT-3 is specific to the nervous system and testis and a ZnT-3 knockout mouse exhibits a complete absence of histologically-reactive vesicular Zn^{2+} in the brain (Palmiter et al., 1996;Cole et al., 1999;Wenzel et al., 1997).

Whilst the evidence so far suggests Zn^{2+} is located and packaged at synapses, experiments to detect a genuine neuronal release and subsequent functional consequence mediated by Zn^{2+} have proved difficult to obtain. Initial studies attempting to address this issue loaded the hippocampal mossy fibre system with $^{65}Zn^{2+}$ and measured subsequent release into the superfusate upon depolarisation using high K^+, kainate (Assaf and Chung, 1984), or electrical stimulation (Howell et al., 1984). Measurements of the Zn^{2+} concentration after such chronic treatment suggested this cation could attain 300 μM in the synaptic cleft. Further fluorescent assay based studies and atomic absorption spectroscopy suggested that depolarisation caused Zn^{2+} to reach significant levels in the extracellular media (Budde et al., 1997;Thompson et al., 2000;Li et al., 2001; Varea et al., 2001;Ueno et al., 2002). One report using the highly sensitive fluorescent Zn^{2+} probe, FluoZin-3, in hippocampal slice preparations does, however, suggest that the levels of Zn^{2+} released during synaptic transmission are far lower, even of the order 1 – 10 nM (Kay, 2003). This study even suggests that Zn^{2+} release may not be significant as a dynamic process and instead Zn^{2+} exists at a low background level accumulated on extracellular membranes in the form of a veneer, which could modulate highly sensitive ligand-gated receptors. Functional studies using electrophysiology to address whether Zn^{2+} is actually present at the synapse modulating neuronal receptors generally supports the assertion that indeed the concentrations of Zn^{2+} are likely to be low, mainly because there is little evidence available for a Zn^{2+} mediated effect. Two independent functional studies looking at synaptic Zn^{2+} release in the hippocampus suggest that postsynaptic NMDA receptors can undergo modulation by

synaptic Zn^{2+} that is possibly co-released with glutamate (Ueno et al., 2002;Vogt et al., 2000). Given the nanomolar sensitivity of some NMDA receptor subtypes in these studies to Zn^{2+} mediated inhibition, this suggests the concentrations of Zn^{2+} released are also in this range. An additional study of Zn^{2+} modulation of tonic $GABA_AR$ mediated currents, possibly by overspill of Zn^{2+} into the extrasynaptic space, also supported the claim that Zn^{2+} can exist as a modulator of neuronal receptors (Ruiz et al., 2003). The sensitivity of these extrasynaptic $GABA_A$ receptors can be variable, suggesting Zn^{2+} concentrations of high to low micromolar (Brickley et al., 1999;Draguhn et al., 1990;Hosie et al., 2003). Furthermore, the likely physiological relevance of synaptic Zn^{2+} is in keeping with a modest role for this cation in neuromodulation as the Zn-T_3 knockout mouse, which lacks synaptic vesicular Zn^{2+}, is devoid of any obvious phenotype (Cole et al., 1999;Cole et al., 2001). This suggests that either this phenomenon is unimportant or that receptors can compensate for this normally subtle effect and that the reliance on Zn^{2+} is only realised under certain confined circumstances (Cole et al., 2000).

With regards to any specific role this potential cationic modulator may play in GlyR synaptic activity, there are currently no direct functional studies to support such a claim. However, the receptor sensitivity, at least for Zn^{2+} mediated enhancement of recombinant GlyR responses, is high at 0.1 – 10 μM. This would be relevant to synaptic Zn^{2+} release, especially as the onset of potentiation is rapid (Suwa et al., 2001). In addition to this, zinc-containing neurones are present throughout the spinal cord, the most concentrated home of the GlyR, and these zinc-containing vesicles have been identified side-by-side with glycine containing vesicles at presumed glycinergic axonal boutons (Birinyi et al., 2001;Jo et al., 2000;Velazquez et al., 1999;Wang et al., 2001). It has also been shown in the zebrafish hindbrain that glycinergic IPSC currents maintain this high sensitivity to Zn^{2+} enhancement as application of a Zn^{2+} chelator increased the decay rate of the IPSC responses (Suwa et al., 2001). This suggested very low, submicromolar concentrations of Zn^{2+} are sufficient to enhance glycinergic neurotransmission by extending the IPSC decay phase, though it does not prove that Zn^{2+} was released synaptically as contaminating nanomolar concentrations of Zn^{2+} in the saline used are sufficient to account for this effect (Paoletti et al., 1997;Wilkins and Smart, 2002).

Aims of the present study

Whilst some available data hints at potential regions of the GlyR that may be important for Zn^{2+} modulation of GlyRs there are still large gaps in our understanding of both the Zn^{2+} binding sites and any possible transduction pathways by which this modulator may act. Given the possible significance of Zn^{2+} as an endogenous modulator of GlyRs and the insight that determining the molecular basis of such events might bring, both in terms of how the GlyR operates and also how other cys-loop receptors may be allosterically modulated, this study aims to elucidate these specific molecular correlates. The techniques adopted revolve primarily around the established stratagem of site-directed mutagenesis to elucidate the function of specific amino acids with regard to Zn^{2+} binding and transduction. This approach was undertaken with structural homology modelling of the GlyR based on the homologous AChBP crystal structure, a tool that vastly enhanced the power of the site-directed mutagenesis strategy. In some cases, additional SCAM experiments were implemented to assess the accessibility of potential Zn^{2+} binding sites. Furthermore pharmacological characterisations of spinal cord culture GlyRs were also carried out to link any recombinant pharmacological observations with *in vivo* receptor populations.

These techniques and tools have revealed a surprising wealth of information regarding Zn^{2+} modulation of GlyRs from both a binding and transduction standpoint. Firstly, the molecular basis of subtype divergence in sensitivity to both Zn^{2+} inhibition and enhancement was revealed. Secondly, original and novel candidates of the Zn^{2+} inhibition site were characterised and evaluated for their relative likely contributions to direct binding and transduction of Zn^{2+} inhibition. Thirdly, the study uncovered a family of Zn^{2+} activated receptors, and through this discovery, it was possible to isolate a direct and specific hydrophobic pathway through the core of the GlyR α subunit that could mediate transduction of the inhibitory Zn^{2+} site to reduce glycine binding and receptor activation. Fourthly, upon determining the molecular basis of a differential potency for Zn^{2+} between GlyR α1 and α2 it was possible to identify a specific area of the GlyR as a strong candidate for a Zn^{2+} potentiation site. As a consequence of this, a critical control element of

this site was also determined, which implied that the Zn^{2+} potentiation site is able to exert its enhancement by affecting the cys-loop gating domain to increase the efficacy of the receptor.

Whilst these results will be of interest to those engaged in structure-function determinations of the GlyR and also other cys-loop receptor family members, this data unexpectedly offered potentially more than just an insight into the action of Zn^{2+} itself. The hydrophobic pathway identified in this study and the nature of the process by which Zn^{2+} is proposed to mediate its inhibitory effect suggest that this transduction pathway is an ideal structure to mediate the initial downstream conformational shift by which the GlyR and other cys-loop receptors may activate. Under such a proposition, agonist binding would induce a downstream collapse of the hydrophobic pathway allowing for destabilisation of polar interactions between the '+' and '-' subunit faces and subsequent twisting open of the extracellular domain of the receptor. In keeping with previous evidence, this twisting would move loops of the proposed extracellular gating domain which would impinge on the M2-M3 loop and transmit to the M2 pore lining to elicit channel opening (Miyazawa et al., 2003;Unwin et al., 2002;Kash et al., 2003b;Bouzat et al., 2004). Identification of such a candidate pathway was totally unexpected and highlights the importance of such studies as modulatory domains undoubtedly feed into agonist processing at some stage and therefore always offer insight into mechanisms of agonist action.

Chapter 2
Materials and Methods

Reagents

All laboratory reagents were purchased from Sigma and tissue culture reagents were purchased from GIBCO unless stated otherwise. Water for use in electrophysiology was filtered through an ELGA PURELAB Prima machine, whilst molecular biology grade water underwent a further purification process through an ELGA PURELAB *ultra* to remove trace ionic and organic impurities.

Molecular biology: Glycine receptor cDNAs

The work carried out in this project relied on the initial availability of a number of wild-type cys-loop ligand-gated receptor clones. Human (h) GlyR α1L, hGlyR α2A and rat (r) GlyR α3S cDNAs were cloned into the vector pCIS2 (obtained from Dr. R.J. Harvey). pCIS2 is a non-commercially available plasmid vector originally developed by H. Betz (Grenningloh et al., 1990) and this is a low copy number plasmid that contains an ampicillin resistance coding region. The splice variants selected for study from each GlyR subtype, α1L (long) and α3S, contain or omit respectively, an intracellular TM3-4 loop amino acid insert compared to their spliced partners (Malosio et al., 1991b;Nikolic et al., 1998). This selection is unlikely to influence the subject of this study, the extracellular modulation by Zn^{2+}, which previous evidence and the data presented here suggest is mediated through the extracellular domain of the protein. In the case of GlyR α2A, this splice variant does differ from its α2B counterpart in the extracellular domain by a two amino acid substitution. However the functional consequences of this substitution have been examined previously and do not have any obvious bearing on the property of Zn^{2+} modulation of GlyRs (Miller et al., 2004). The human GlyR β cDNA was cloned into $pcDNA_{3.1+}$ and provided by Dr. P.J. Groot-Kormelink. All other cDNAs used, namely murine (m) $m5\text{-}HT_{3AL}$ was cloned into pRK5. Also, jellyfish enhanced green fluorescent protein (EGFP; in pEGFP-1) was obtained from Clontech. The GlyRβ subunit was used in a different vector ($pcDNA_{3.1+}$) so that high yields could be obtained upon purification, as highly saturating levels of this plasmid were required in transfections to ensure homogeneous expression of GlyR αβ heteromers.

Site-directed mutagenesis

During the course of this project more than 100 GlyRs containing single, or multiple, point mutations were generated and tested therefore only general details of the specific mutations made, or the oligonucleotide primers used, are included here. To insert an amino acid point mutation into a protein it is necessary to first substitute the corresponding nucleotide bases at the DNA level. This is done by hybridising a synthetic DNA primer containing the mutated base(s) of interest to a wild-type cDNA in a plasmid and then extending the primer with a polymerase to make a copy of the rest of the cDNA in its vector. This process is repeated in a manner similar to the cycling in PCR to amplify the vector containing the directed point mutant to sufficient levels for detection using bacterial cloning (scheme highlighted in Fig 2.1).

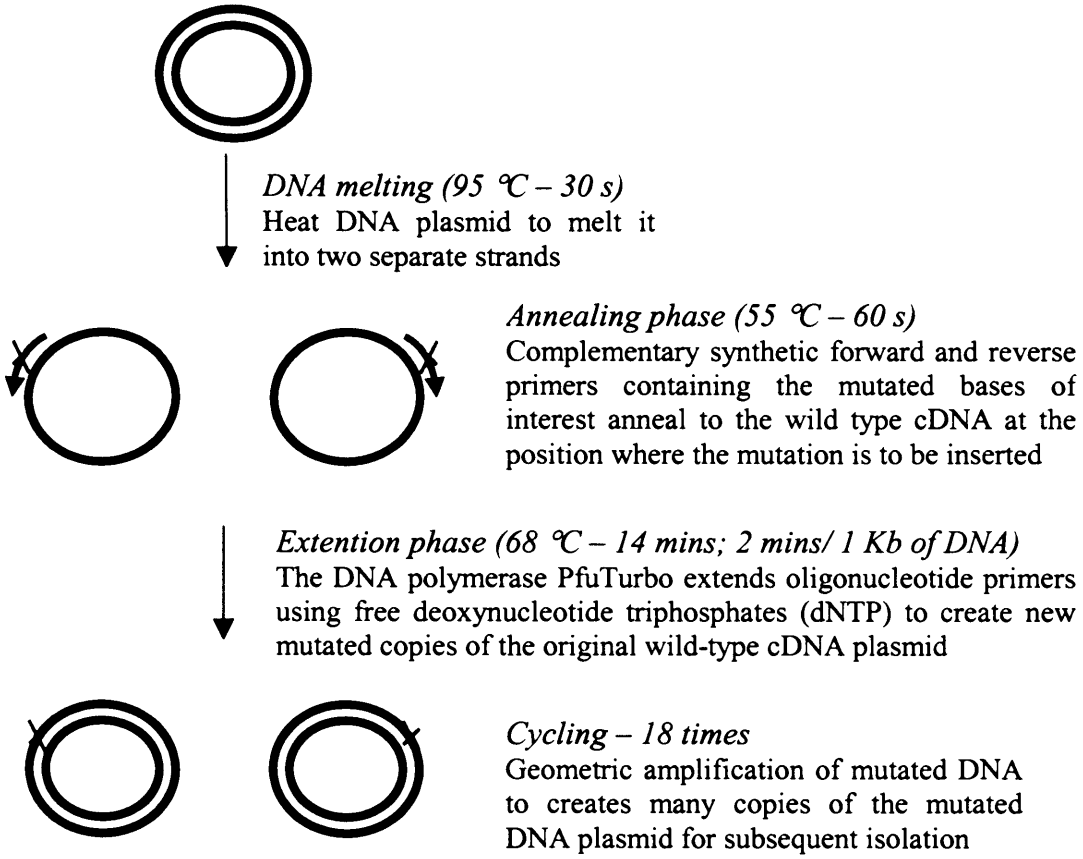

Figure 2.1 Schematic of the site-directed mutagenesis technique. Mutated cDNAs, which will later yield proteins with targeted amino acid substitutions for structure-function studies are generated by a three stage PCR amplification strategy involving DNA melting, primer annealing and extention of the mutated primer in a cycle repeated 18 times.

Oligonucleotide primers (Invitrogen) were designed to be 24 – 34 nucleotides in length, ending and starting with cytosine or guanosine to improve the efficiency of hybridisation surrounding the unmatched region. At least six matching bases encompassed either side of the mutated base(s) of interest and where possible primers were designed to contain an even mixture of each of the four bases, dATP, dCTP, dGTP and dTTP, avoiding long stretches of any one base and possible sequences that may allow for hairpin loop formation within the oligonucleotide. In some instances an automated online oligonucleotide design engine was used, available from Stratagene (web address - http://labtools.stratagene.com//Forms/SVLogin.php).

The site-directed mutagenesis protocol was modified from the Quikchange kit recipe (Stratagene):

PCR reaction mixture

5 µl of 10 × reaction buffer (Stratagene)

1 µl of 100 ng/µl double stranded cDNA plasmid template

1 µl of 100 ng/µl forward synthetic mutated oligonucleotide primer

1 µl of 100 ng/µl reverse synthetic mutated oligonucleotide primer

1 µl of 40 mM dNTP mix (dATP, dCTP, dGTP and dTTP)

40.5 µl dH_2O

0.5 µl of *PfuTurbo* DNA polymerase (Stratagene)

This reaction mixture underwent the following PCR cycling process in a ThermoHybaid PCR machine (Thermo Life Sciences Ltd) with a preheated lid element negating the need for any mineral oil overlay:

Cycle 1 – 95 °C for 30 seconds (*PfuTurbo* activation phase)

Cycle 2-18 - 95 °C for 30 seconds (melting phase)

- 55 °C for 1 minute (hybridisation phase)

- 68 °C for 14 minutes (extention phase)

Successful PCR mutagenesis was verified by the presence of a significant band of DNA (of approximately 7 Kb in size corresponding to amplified cDNA plasmid) when 10 µl of PCR product, mixed with 4 µl gel loading buffer, was run on a 1.5 % agarose gel (BDH) in TAE buffer (0.04 M Tris-acetate, 0.001 M EDTA) with 1 µl/100 ml ethidium bromide at 100 mV for 1 hour alongside a 1 kB DNA ladder

(Invitrogen). Unsuccessful mutagenesis reactions, as verified by the absence of a clear band, were repeated by varying either the hybridisation temperature, adding 0.5 µl of 10 mg/ml bovine serum albumin (BSA; New England Biolabs), or adding 1 µl 50 mM $MgSO_4$. If mutagenesis was still unsuccessful then fresh oligonucleotides varying in sequence were ordered. All mutagenesis reactions were subsequently successful.

The PCR product was incubated with 1 µl of *Dpn* I (New England Biolabs) at 37 °C for 2 hours. This selectively digests methylated DNA, in this case the original parent cDNA strands, which are methylated by bacteria during cloning. The PCR amplified templates however are unmethylated as these were generated from individual unmethylated nucleotide bases with *PfuTurbo* during the PCR amplification stage. The digested PCR product is then transformed into chemically competent TOP10 *E.coli* bacteria (Invitrogen – in exact accordance with the manual). Final transformed bacterial aliquots were plated onto ampicillin Lb agar plates (12.8 g Lb agar powder/ 400 ml molecular biology grade water + 100 µg/ml ampicillin spread across twenty 10 cm Petri dishes under sterile conditions) as all the vectors used in this project contained an ampicillin resistance coding region.

Subsequent successful mutagenesis experiments typically yielded 10 - 200 colonies per plate of which 2 colonies were picked and pipetted into separate 5 ml aliquots of Lb broth (20 g Lb broth powder/ 1000 ml molecular biology grade water + 100 µg/ml ampicillin) to be grown overnight for 15 hours at 37 °C in an Orbital Shaker S150, shaking at 250 rpm. DNA was purified using the Qiagen miniprep kit and then sequenced externally by Wolfson Institute of Biomedical Research where only the initial provision of a small DNA aliquot and some sequencing oligonucleotide were required. Receptors that yielded results deemed to be important, or which had unexpected properties, were re-sequenced across the full length of the cDNA region. Correctly generated mutated receptor cDNA constructs were grown in bulk using the Qiagen maxiprep kit in accordance with the recommended protocol to concentrations of 500 – 1000 µg/ml ready for transfection into mammalian cells.

Basic stocks of all wild-type receptor clones and point-mutated receptors were maintained by the subsequent transformation and cloning of remaining DNA into DH5α *E.coli* bacteria (Invitrogen) followed by the selection of a bacterial colony to bulk up and maxiprep into fresh DNA as and when required.

Cell culture and transfection

HEK cells (ATCC CRL1573) were grown in Dulbecco's modified Eagle's medium (DMEM) supplemented with 10 % foetal calf serum (FCS), 2 mM glutamine, 100 units/ml penicillin G and 100 μg/ml streptomycin, incubated at 37 °C in 95 % air - 5 % CO_2 (Smart et al., 1991) and were passaged two to three times weekly. Cells (passage no.10–25) transfected by one of two methods depending on requirements.

1) Electroporation technique: One 50% confluent, 10 cm sterile Petri dish of HEK cells was washed with and resuspended in Optimem (final 0.5 ml volume) taking care to wash away any trace FCS as this disrupts the electroporation process. The 0.5 ml cell aliquot, supplemented with DNA plasmid for transfection in a cuvette, was electroporated at 400 V, infinite resistance, 125 μF using a Biorad Gene Electropulser II. Cells were subsequently shaken over a 10-minute period and then plated to achieve 20 % confluence on poly-L-lysine (100 μg ml^{-1}) coated 35 mm coverslips (BDH) and used for electrophysiology the next day. This technique was used in Chapter 3 with plasmids containing GlyR α cDNA clones co-transfected 1:1 (3 μg:3 μg) with a reporter plasmid expressing the EGFP, final volume approximately 6 μl. Also this method was applied to situations where large quantities of DNA were required such as co-expression of GlyR αβ heteromers, which need high concentrations of the GlyR β-subunit to ensure its efficient incorporation into an αβ heteromeric complex. The GlyR β subunit expression construct was mixed with GlyR α subunit plasmids at a 30:1 ratio (30 μg: 1 μg, plus 2 μg EGFP), final volume approximately 20 μl.

2) Calcium Phosphate technique; reaction mix:

   1.5 to 3 μg cDNA plasmid plus 1 μg EGFP in final 4 μl aliquot

   20 μl $CaCl_2$ (from 340 mM filtered stock)

24 µl 2 × HBSS solution (280 mM NaCl, 2.8 mM Na_2HPO_4, 50 mM HEPES, pH 7.2 with NaOH and filtered)

This was incubated at 4 °C for 1 hour and then pipetted onto HEK cells plated 4 hours previously at 20 % confluence on poly-L-lysine (100 µg ml^{-1}) coated 35 mm coverslips. Cells were then used for electrophysiology the next day (more than 18 hours later).

Neuronal spinal cord cell culture preparation

E15 embryos were extracted immediately from terminally anaesthetised and cervically dislocated Sprague-Dawley rats by Caesarean section and placed in ice-cold phosphate-buffered saline (PBS). Up to four spinal columns (not more than four so that the speed of the culture preparation was maximised to give healthier cultures) were excised and separated from the meninges and dorsal root ganglia. Spinal cords were cut into four sections and treated with 0.25 % w/v trypsin in Earle's balanced salt solution (EBSS) for 15 mins at 37 °C. The tissue was then washed three times in EBSS to remove residual trypsin and sequentially triturated three times using polished Pasteur pipettes of narrowing tip diameter. Spinal cord cell suspensions were then centrifuged at 500 g for 5 mins and resuspended in MEM plating media supplemented per 100 mls with 5 ml FCS, 5 ml horse serum (HS), 0.6 % w/v L-Glucose (Sigma) and 0.04 % w/v $NaHCO_3$. Cells were plated at a density of 5 x 10^5 (approximately one third of an E15 spinal cord) per 35 mm coverslip coated either with poly-L-lysine or also with an astrocyte monolayer. High quality coverslips were used (Assistent) stored in 100 % ethanol and coated in poly-L-lysine that was suspended in a borate buffer (50 mM boric acid, 12.5 mM sodium tetraborate, pH 8.5 – Banker and Goslin, 1998) in an attempt to reduce the toxicity of poly-L-lysine to spinal cord neurones. The coverslips were washed three times in sterile distilled water to remove excess poly-L-lysine. The next day the primary culture media was 50 % replaced with Neurobasal media supplemented with 1 % v/v B-27 nutrient additive, 0.25 % v/v of 200 mM L-glutamine, 1 ng/ml recombinant rat ciliary neurotrophic factor (CNTF, Peprotech, London) and 100 pg/ml recombinant glial cell-line derived neurotrophic factor (GDNF; Peprotech, London). This media was replaced again by 75 % with fresh Neurobasal at the end of the same day. Subsequently, this medium was then replenished twice weekly. Astrocytic cultures

were prepared from rat cortex by Dr. P. Thomas or Miss H. Da Silva in accordance with an original protocol derived from Banker and Goslin, (1998). Astrocytes were maintained in astrocyte maintenance media (AMM) made up in 100 ml stocks consisting of 77.67 ml Earle's MEM (without glutamine); 20 % FCS; 0.6 % (w/v) D-Glucose; 100 U/ml Pen/Strep. Astrocytic cultures were washed twice weekly to replenish the cells with fresh AMM and to wash away any contaminating lymphocytes. Astrocytes were passaged once every two weeks until the time they were required as monolayers for spinal cord cultures. A glass scrapper was used to resuspend astrocytes after pre-treatment for 1 hour with 5 ml trypsin/EDTA per 10 cm dish (0.5 g trypsin, 0.2 g NaEDTA/L in HBSS without Ca^{2+} and Mg^{2+}) at 37 °C. Cells were then triturated and either plated in AMM to achieve 10 % confluence for passaging later, or plated onto 35 mm coverslips at 100 % confluence ready for the addition of spinal cord cultures in 7 days time. (* see end of methods)

Solutions

The internal patch pipette solution contained (mM): 140 KCl, 2 $MgCl_2$, 1 $CaCl_2$, 10 HEPES, 11 EGTA, and 2 ATP. The pH was adjusted to 7.11 for HEK cells and 7.3 for spinal cord primary cultures using 1M NaOH, (≈ 300 mOsm). The external saline solution consisted of (mM): 140 NaCl, 4.7 KCl, 1.2 $MgCl_2$, 2.5 $CaCl_2$, 10 HEPES, and 11 D-Glucose. The pH was adjusted to 7.4 using 1M NaOH (≈ 300 mOsm). Primary cultured neuronal cells were superfused in external saline that also contained 10 μM bicuculline, 0.5 μM tetrodotoxin (TTX), 20 μM 5-aminophosphovalerate (AP5) and 10 μM 6-cyano-2,3-nitroquinoxalinedione (CNQX) to remove $GABA_A$ and glutamate receptor synaptic activity and all action potentials, during glycinergic whole-cell recordings.

Experiments requiring absolute control of low (1 nM – 10 μM) concentrations of free Zn^{2+} ions were carried out in the presence of a Zn^{2+} buffering agent. Tricine was selected as the optimal buffering agent available due to its relatively low K_D for Zn^{2+}, estimated at around 10^{-5} M (Paoletti et al., 1997). For those studies to elucidate the Zn^{2+} potentiation site of the GlyR family (Chapter 5) a concentration of 10 mM tricine was used, allowing: 0.26, 0.78, 2.6, 7.8, 26, 77.5, 254 and 775 μM total Zn^{2+} to provide effective free Zn^{2+} concentrations of: 1, 3, 10, 30, 100, 1000 and 3000 nM

Zn^{2+}, respectively (Suwa et al., 2001). For those experiments investigating a potential Zn^{2+} transduction pathway from the inhibitory Zn^{2+} site (Chapter 4) the requirement for tricine based recordings was far more extensive, therefore a lower 2.5 mM concentration was used as this allowed for the health of the HEK cells to be maintained for longer recording sessions (unpublished observation). To calculate free Zn^{2+} concentrations in 2.5 mM tricine, WINMAXC 2.40 was used (http://www.stanford.edu/cpatton). The properties for tricine were entered manually into the program ($K_D = 10^{-5}$; Paoletti et al., 1997) and other parameters such as temperature (20 °C) and pH (7.4) could also be accounted for. WINMAXC 2.40 was also used to evaluate the final free Zn^{2+} concentrations in the presence of the high affinity Zn^{2+} chelator TPEN, 100 μM, (*N,N,N',N'*-tetrakis-(2-pyridylmethyl)-ethylenediamine; $K_D = 10^{-15.6}$; Paoletti et al., 1997) at pH 6.4, 7.4, and 8.4. TPEN properties were already predefined in the WINMAXC 2.40 database. Both 2.5 and 10 mM Tricine reduced the pH of the Krebs solution, which was therefore titrated back to pH 7.4 using 1M NaOH. TPEN had no observable effect on the pH of Krebs at the 100 μM concentrations used.

Cysteine accessibility experiments made use of 2-aminoethyl methane sulphonate (MTSEA) in the form of a hydrobromide salt (Insight Biotechnology Ltd). This agent covalently modified accessible Cys residues on the GlyR after incubation of transfected HEK cells for 1 minute in a 3 mM concentration of MTSEA. Frozen powdered MTSEA, dissolved in saline was applied directly to cells within 2 minutes.

Electrophysiology

An Axopatch 200B amplifier (Axon instruments) was used to record whole-cell currents from single HEK cells or spinal cord primary cultures using the patch-clamp technique. HEK cells exhibited resting potentials between –10 and –40 mV and were voltage clamped at a –40 mV holding potential. Recordings were only attempted from ideally single, or occasionally doublets, of HEK cells to ensure effective space clamp of the cells as these cells maintain gap junction communication networks. Healthy spinal cord neurones were judged on the basis of robust dendritic networking (7 days *in vitro* (DIV) and above), resting potentials of –40 to –60 mV and steady holding currents. These cells were clamped at –70 mV. Cells were visualised with a differential interference contrast Nikon microscope with

epifluorescence attachment to identify EGFP transfected cells. A Y-tube was used to rapidly apply drugs and Krebs solutions (exchange rate i.e. 10 - 90 %, rise time of a maximal saturating glycine concentration was approximately 7 - 20 ms) to patch-clamped cells. Patch electrodes were fabricated from borosilicate glass (GC150T-10 from Harvard Apparatus Limited) using a Narashige PC-10 puller with resistances after polishing of 4 - 5 MΩ. All recordings were performed in constantly perfusing Krebs at room temperature (20 - 22 °C).

Data acquisition and analysis

All recorded current signals were filtered using a low pass Bessel filter set to 3 kHz (-36dB per octave). Data were recorded in 20 s acquisition periods directly to a Pentium IV, 1.8 GHz computer running Clampex 8.0 via a Digidata 1322A (Axon instruments) interface sampling at 200 μs intervals. All digitised currents were analysed offline using Axoscope 8.2. Acquisition periods included an initial triplet of -10 mV steps to monitor the residual capacitance transients (after initial compensation) and also the cell access resistance between acquisition periods. Any change of greater than 10 % in the height of the capacitance transients between acquisition periods led to the data being discarded. Experimental run-up and run-down was also monitored by the regular application of a submaximal concentration of glycine corresponding approximately to 50 % of the maximal Gly response i.e. application of an EC_{50} agonist dose. In the case of agonist dose response curves, the EC_{50} 'monitor' dose would be applied before and after application of 4 – 6 different doses of agonist. When modulators such as Zn^{2+} or inhibitors such as strychnine, were being tested, control EC_{50} monitor doses to check for wash out of the modulator/inhibitor and run-up/run-down were applied before and after every 2 - 4 test doses. If response amplitude run-up or run-down was not observed, or was less than 15 %, then the test responses were normalised by linear interpolation between the two surrounding control agonist EC_{50} response amplitudes. The maxima of EC_{50} dose response curves for taurine (Fluka biochemicals) and β-alanine, which were demonstrated to be partial agonists in some cases, were determined from concentration response curves normalised with respect to the current activated by a maximal concentration of glycine (usually 10 mM) measured in the same cell. Inhibition dose response experiments with picrotoxin (initially dissolved in dimethyl

sulphoxide (DMSO) forming concentrated stock solutions), strychnine, or Zn^{2+}, involved pre-incubating the HEK cell with a dose of the inhibitor for 15 s to ensure full equilibration, and then co-applying the same inhibitor dose with an EC_{50} concentration of agonist. For experiments using the GlyR inhibitor sodium cyanotriphenylborate (CTB – Pfaltz & Bauer Inc), pre-incubation was not used as this molecule is an open channel blocker (Rundstrom et al., 1994).

The biphasic curves, describing the Zn^{2+} concentration response data, were generated using a non-linear least squares routine according to the following modified Hill equation which assumes Zn^{2+} binds to two distinct sites, one producing potentiation and the other inhibition of the glycine-activated membrane current (Harvey et al., 1999). For simplicity this equation assumes only one of each site per receptor rather than the actual five predicted to be present in a homomeric pentamer:

$$I = I_{min} + (I_{max} - I_{Min}) ([1 / (1 + (EC_{50}/B)^{n_H})] - [1 / (1 + (IC_{50}/B)^{m_H})]), \qquad \textbf{(1)}$$

where I and I_{max} represent the modulated peak glycine-activated currents by a concentration of Zn^{2+}, B, and by a saturating concentration of Zn^{2+} respectively. I_{min} represents the control glycine current in the absence of the modulator and was set to 100 %. EC_{50} and IC_{50} define the Zn^{2+} concentrations producing a half maximal potentiating effect and a 50% inhibition of the maximally potentiated current, respectively. Both n_H and m_H represent the respective Hill coefficients. Where this equation (1) was unable to provide good estimates of the EC_{50} and IC_{50} with acceptable errors, due to limited resolution of parts of the Zn^{2+} dose-response curves, the IC_{50} values were evaluated from curve fits to the inhibitory components of the curve (equation 2). For these curve fits, the peak potentiation was taken as the maximum of the curve and the IC_{50} measured as the point where 50 % inhibition relative to this peak was attained.

The agonist concentration response curves were fitted with the Hill equation:

$$I / I_{max} = [(1 / 1 + (EC_{50} / A)^n)], \qquad \textbf{(2)}$$

The EC_{50} represents the concentration of agonist (A) inducing 50 % of the maximal current evoked by a saturating concentration of agonist and 'n' is the Hill coefficient. This curve was also used to fit IC_{50} plots for the inhibitors picrotoxin, strychnine and also for Zn^{2+} in cases where mutated GlyRs lacked the competing Zn^{2+} potentiation component, or where equation (1) provided inadequate fits. In some cases mutated GlyRs exhibiting clear biphasic inhibition by Zn^{2+} were observed, these inhibitory dose response curves were fitted with a biphasic inhibitory curve generated by the equation:

$$I/I_{max} = 1 - (a \times A^n / (A^n + IC_{50}^n)) + (b \times A^n / (A^n + IC_{50}^n)) \qquad \textbf{(3)}$$

All values are as previously stated but 'a' and 'b' represent proportionality constants reflecting the contribution to total inhibition provided by each of the two inhibitory components.

Where parallel agonist dose response profiles were evaluated in the presence of incrementing concentrations of inhibitory Zn^{2+}, the potency of inhibition could be more thoroughly evaluated to obtain a pA_2 value according to the method devised by Schild (Arunlakshana and Schild, 1959;Rocha E Silva and Schild, 1949). Full concentration response curves for glycine were obtained in each HEK cell and then at least one but usually more glycine curves were repeated in the presence of incrementing Zn^{2+} concentrations (50, 100, 200 and 500 μM). The curves were assessed for their parallel nature and the dose-ratios (r) for Zn^{2+} were measured at the glycine EC_{50} concentrations. The mean dose-ratios for each Zn^{2+} concentration were then fitted with the Schild equation:

$$r\text{-}1 = B / K_B,$$

where K_B is the Zn^{2+} dissociation constant. The Schild equation was logarithmically transformed to:

$$\log (r\text{-}1) = \log B - \log K_B,$$

The Schild plot of log(r-1) versus log(B) was linear and if the slope of the line was judged to be not significantly different to unity, then the slope was constrained to one and the intercept on the abscissa used to determine, $-\log K_B$, which equates to the pA_2* for Zn^{2+}, a measure of Zn^{2+} affinity for the receptor. The best curve fits to the (* $pA_2 = K_D$)

experimental data were achieved by applying a non linear least squares fitting routine running in Origin (version 6.0).*[2]

Structural modelling

The mature N-terminal extracellular domain (ECD) of the human GlyR α1 subunit was modelled on the crystal structure of the acetylcholine binding protein (AChBP; (Brejc, 2001 89 /id)) using the freeware program SwissProt DeepView 3.7 available from http://ca.expasy.org/spdbv/. The AChBP crystal structure was downloaded as a PDB file labelled 1I9B from http://www.rcsb.org/pdb/ and loaded into SwissProt DeepView 3.7, under main header File → Open PDB file. The GlyR protein sequence was uploaded in a simple text format into DeepView 3.7, under main header SwissModel → Load Raw Sequence to Model (Fig 2.2*A*). The GlyR sequence was then aligned with AChBP in the alignment window (Fig 2.2*A*) under main header Window → Alignment, in accordance with a ClustalW protein alignment (Fig 2.2*B*). This alignment was submitted for modelling via the program interface of Deepview, under main header SwissModel → Submit Modelling Request. Upon submission a dialog box opened and the file was saved with an appropriate name in html format. Upon saving the file a SwissModel website window opens where the user e-mail details were entered and the location of the previously saved html file was provided so the website could access the modelling request. The results were requested in the Swiss-PDB Viewer mode and then the details were sent.

The GlyR transmembrane domains M1-3, and separately M4, were aligned using ClustalW and modelled on the atomic structure of the Torpedo nicotinic acetylcholine receptor (nAChR) chain A (PDB label, 1OED; Miyazawa et al., 2003) and imported into SwissProt DeepView in the same manner to that described above. The final GlyR ECD and M1-4 structures were then empirically docked to ensure that the C-terminus of the ECD linked with the N-terminus of TM1; the TM2-3 loop was closely apposed to the base of the N-terminal Cys loop; and that the N-terminal domains did not sterically hinder each other when assembled in a pentameric complex. The finalised models, required for presentation purposes, were processed

using a 3D rendering freeware program called POV-ray 3.5 for improved image quality (available from http://www.povray.org/).

Statistics

All statistical analysis was carried out using the Student's t-test in Microsoft Excel. Comparisons of data sets recorded in the same cell were considered paired whilst those from separate cells were treated as unpaired. The analysis compared all data under a two-tail hypothesis and quantified significance to the 5 or 1 % levels, stated in the text.

*Animals were anaethetised in a chamber using halothane in accordance with the Scientific Procedures Act (1986). Animals were obtained from the University College London pharmacology animal house, where animals were kept in accordance with the government guidelines on animal housing.

*[2] Exponential curves for decay components of desensitisation traces (Chapter 3) and for rates of action of glycine EC_{50} currents (Chapter 5) were fitted using Igor Pro version 4.01.

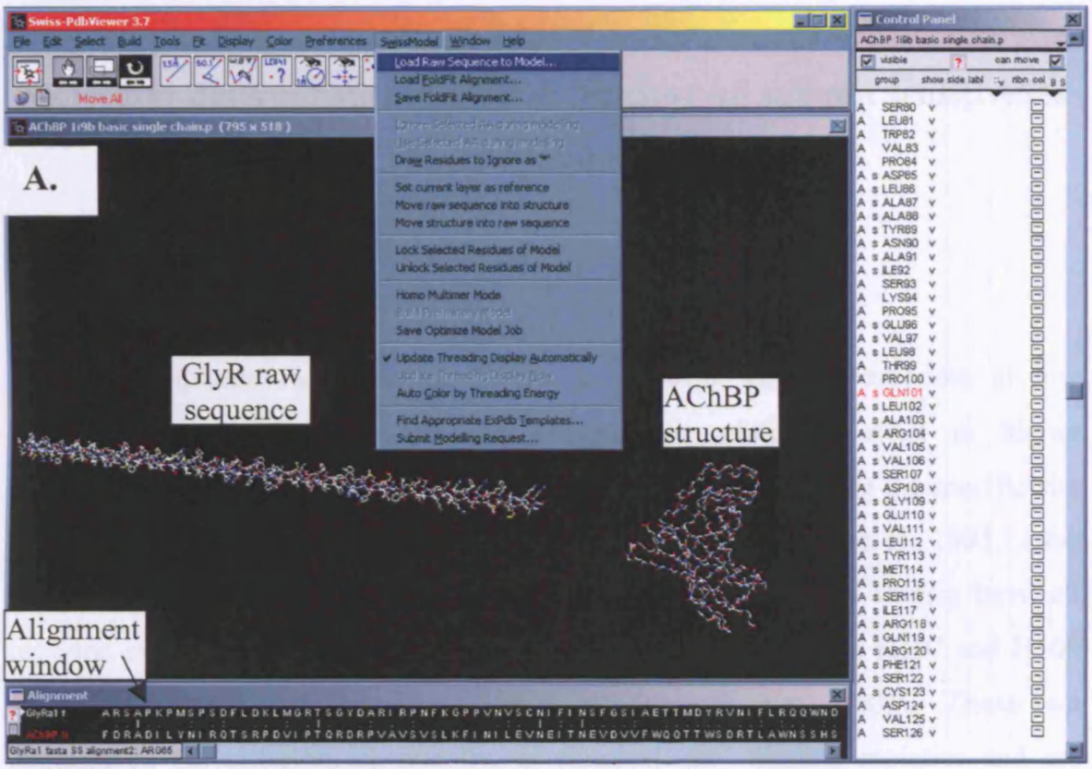

B.

```
hGlyR α1L    ----MYSFNT--LRLYLSGAIVFFSLAASKEAEAARSATKPMSPSDFLDKLMGRTSG---
hGlyR α2A    MNRQLVNILTALFAFFLETNHFRTAFCKDHDSRSGKQPSQTLSPSDFLDKLMGRTSG---
hGlyR β      MKFLLTTAFLILISLWVEEAYSKEKSSKKGKGKKKQYLCPSQQSAEDLARVPANSTSNIL
AChBP        ---------------------------------------------LDRADILYNIRQT---

hGlyR α1L    ------YDARIRPNFKGPPVNVSCNIFINSFGSIAETTMDYRVNIFLRQQWNDPRLAYNE
hGlyR α2A    ------YDARIRPNFKGPPVNVTCNIFINSFGSVTETTMDYRVNIFLRQQWNDSRLAYSE
hGlyR β      NRLLVSYDPRIRPNFKGIPVDVVVNIFINSFGSIQETTMDYRVNIFLRQKWNDPRLKLPS
AChBP        ------SRPDVIPTQRDRPVAVSVSLKFINILEVNEITNEVDVVFWQQTTWSDRTLAWNS

hGlyR α1L    YPDDSLDL--DPSMLDSIWKPDLFFANEKGAHFHEITTDNKLLRISRNGNVLYSIRITLT
hGlyR α2A    YPDDSLDL--DPSMLDSIWKPDLFFANEKGANFHDVTTDNKLLRISKNGKVLYSIRLTLT
hGlyR β      DFRGSDALTVDPTMYKCLWKPDLFFANEKSANFHDVTQENILLFIFRDGDVLVSMRLSIT
AChBP        SH-SPDQV--SVP-ISSLWVPDLAAYN-AISKPEVLTPQ--LARVVSDGEVLYMPSIRQR

hGlyR α1L    LACPMDLKNFPMDVQTCIMQLESFGYTMNDLIFEWQEQGAVQVADGLTLPQF-ILKEEKD
hGlyR α2A    LSCPMDLKNFPMDVQTCTMQLESFGYTMNDLIFEWLSDGPVQVAEGLTLPQF-ILKEEKE
hGlyR β      LSCPLDLTLFPMDTQRCKMQLESFGYTTDDLRFIWQSGDPVQLEK-IALPQFDIKKEDIE
AChBP        FSCDVSGVDTESG-ATCRIKIGSWTHHSREISVDPTTENSDDSEYFSQYSRFEILDVTQK

hGlyR α1L    LRYCTKHYN-TGKFTCIEARFHLERQM
hGlyR α2A    LGYCTKHYN-TGKFTCIEVKFHLERQM
hGlyR β      YGNCTKYYKGTGYYTCVEVIFTLRRQV
AChBP        KNSVTYSCC-PEAYEDVEVSLNFRKKG
```

Figure 2.2 SwissProt modelling program interface and amino acid homology alignment of hGlyR N-termini with the AChBP. The alignment was based on a ClustalW multiple sequence alignment and required mild manual optimisation. Grey boxed residues represent critically conserved residues present through the cys-loop receptor family.

Chapter 3

Molecular determinants of glycine receptor αβ subunit sensitivities to Zn^{2+} inhibition

Introduction

Zn^{2+} is a biphasic modulator of GlyRs, potentiating agonist responses at low concentrations (0.1 – 10 μM) and eliciting an inhibitory effect at higher concentrations (Bloomenthal et al., 1994;Laube et al., 1995). Whilst the specific site of Zn^{2+} potentiation has to date remained difficult to define (Laube et al., 1995;Laube et al., 2000;Lynch et al., 1998), three pivotal structure-function studies have all reported evidence supporting a clear role for GlyR α1 amino acids H107 and H109 in Zn^{2+} mediated inhibition (Harvey et al., 1999;Nevin et al., 2003). These two residues fit the criterion, chemically, of classical Zn^{2+} binding moieties and are predicted to reside in close apposition on a GlyR structural model (Nevin et al., 2003), ideal for the formation of a discrete Zn^{2+} inhibitory site.

Despite this progress there have been no clearly defined studies investigating any potential GlyR subtype dependence that may exist for Zn^{2+} mediated inhibition. This is of interest as it may reveal novel insight into structure-function properties of the site and may identify Zn^{2+} as a useful pharmacological tool to distinguish between GlyR subtypes for which there are currently few selective antagonists (Laube et al., 2002b). In the original study by Laube et al, (1995) GlyR α1 and α2 were both shown to retain a comparable sensitivity to Zn^{2+} mediated inhibition, whilst a recent study suggests the auxiliary GlyR β subunit is not important for the inhibitory effect (Nevin et al., 2003). Additionally, a comparison between the GlyR α2A and α2B splice variants, which differ by a dual amino acid substitution in the extracellular N-terminal domain, revealed similar sensitivities to Zn^{2+} modulation, (Miller et al., 2004). The comparable sensitivity of α1 and α2 to inhibitory Zn^{2+} suggested by Laube et al, (1995) is surprising as an amino acid alignment of GlyR α1-4 plus GlyR β encompassing the specified Zn^{2+} binding site region of interest revealed that α1 differs crucially from all other GlyR subtypes at the putative Zn^{2+} binding residue

H107 (Fig 3.1). This unique histidine is replaced by an Asn in GlyR α1-3 and GlyR β, a residue not known for its chemical capacity to coordinate Zn^{2+} ions (Auld, 2001). Previous studies to compare the subtype dependence in $GABA_A$ receptors for Zn^{2+} inhibition have already shown that potential Zn^{2+} binding residues, which vary between $GABA_A$ subunits, appear to impart on these subunits differing sensitivities to inhibitory Zn^{2+} (Smart et al., 1991;Draguhn et al., 1990;Hosie et al., 2003). Therefore, it follows that if GlyR α1 H107 is a genuine Zn^{2+} binding residue, it should alter the receptor's sensitivity to inhibition by this divalent cation when compared to other GlyR subtypes where this histidine is absent.

This chapter aims to investigate what role, if any, GlyR α1 H107 plays in subtype sensitivity to inhibitory Zn^{2+}. This influence is investigated for potential physiological relevance by assessing the impact of co-expression of α-subunits with the GlyR β subunit on Zn^{2+} inhibition and also by the measurement of Zn^{2+} inhibitory potency in a spinal cord culture preparation. Furthermore, attempts were made to isolate additional variable elements that might be responsible for contributing to the differential sensitivity observed between GlyR subtypes. These studies were supplemented by an investigation using the β subunit, which can enforce a fixed stoichiometry of Zn^{2+} binding sites upon GlyR heteromers, to elucidate information about any asymmetry of function that may exist within the GlyR inhibitory Zn^{2+} site.

```
GlyR α1 PDLFFANEKGAHFHEITTDNKLLRISR  122
GlyR α2 PDLFFANEKGANFHDVTTDNKLLRISK  129
GlyR α3 PDLFFANEKGANFHEVTTDNKLLRIFK  122
GlyR α4 PDLFFANEKGANFHEVTTDNKLLRIFK  115
GlyR β  PDLFFANEKSANFHDVTQENILLFIFR  145
```

Fig 3.1 Primary amino acid sequence alignment of the GlyR family highlighting the unique nature of H107 (underlined), a candidate residue in the inhibitory Zn^{2+} binding site, in the GlyR α1 subtype. Another important residue for Zn^{2+} mediated inhibition, H109 (blue background), is conserved throughout the family.

Results

Differential Zn^{2+} sensitivity between GlyR α1 and GlyR α2 subunits

A comparison of the sensitivities of GlyRs to Zn^{2+} mediated inhibition was initiated since one of the key Zn^{2+} binding residues, H107, is present in the GlyR α1 but not the GlyR α2 subtype. Modulation by Zn^{2+} was examined using two different protocols. The first involved co-application of varying concentrations of Zn^{2+} with a half-maximally effective (EC_{50}) concentration of glycine. The degree of inhibition was measured for the peak glycine response (I_{peak}) and 4s into the co-application (I_4) to reveal a delayed onset of inhibition (Fig 3.2*A-C*). The second protocol utilised a pre-incubation of Zn^{2+} and only the peak glycine responses were measured as pre-incubation allowed Zn^{2+} to equilibrate with the GlyR (Fig 3.2*D*). Irrespective of the protocol, all Zn^{2+} concentration response curves exhibited a biphasic shape due to the potentiating and inhibitory effects of Zn^{2+} on GlyRs. However, contrary to a previous report (Laube et al., 1995), a clear difference in the potency of inhibitory Zn^{2+} was observed between GlyR α1 and GlyR α2 subunits. This was most distinct using the pre-incubation protocol, with a 25-fold reduction in Zn^{2+} potency apparent from an IC_{50} of 15 ± 2 μM, (n = 5) for GlyR α1 to an IC_{50} of 360 ± 40 μM, (n = 11) for GlyR α2 ($P < 0.05$; Table 3.1). All subsequent experiments therefore utilised the pre-incubation protocol with Zn^{2+}.

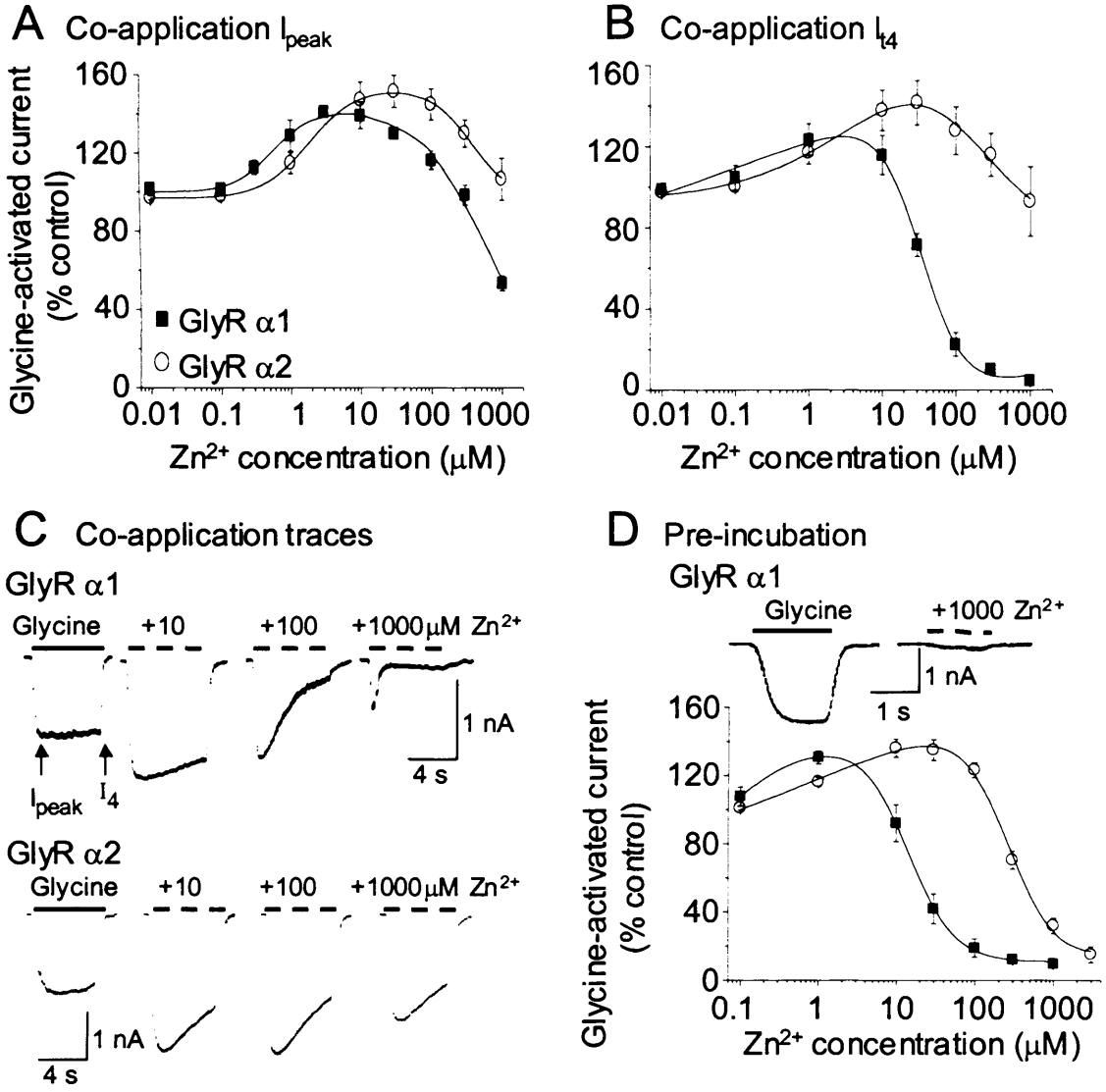

Figure 3.2 Differential inhibition of glycine-activated currents by Zn^{2+} at GlyR α1 and GlyR α2 using whole-cell patch-clamp recordings from HEK cells. *A*, Zn^{2+} modulation concentration response curves of 50 % maximal glycine-evoked currents measured at the peak (I_{peak}) of a 4 s co-application of glycine and Zn^{2+}. *B*, Zn^{2+} concentration response curves as in (*A*) but responses measured at the end of the co-application (I_4). *C*, Example membrane currents comparing glycine-activated I_{peak} and I_4 for GlyR α1 (top) and GlyR α2 (bottom) after applying 50 % maximal glycine concentrations in the absence and presence of co-applied 10, 100 and 1000 μM Zn^{2+}. *D*, Glycine-activated current following co-application of 50 % maximal doses of glycine with Zn^{2+} after prior incubation for 15 s with an equivalent concentration of Zn^{2+} for GlyR α1 and GlyR α2. The inset shows a typical 50 % maximal glycine-activated current for GlyR α1 in the absence and presence of 1000 μM Zn^{2+} under the pre-incubation protocol. $N = 6 - 13$ for all experiments.

Histidine 107 determines the differential Zn^{2+} sensitivity between GlyR α subunits

Comparing the N-terminal extracellular domains of the GlyRs reveals that GlyR α2, like all other α variants except GlyR α1, retains an asparagine (N114) residue at the homologous position to the putative Zn^{2+} binding residue, H107, in the GlyR α1 subunit (Fig 3.1). If H107 coordinates Zn^{2+}, then the divergent N114 in GlyR α2 could be responsible for the differential sensitivity to Zn^{2+} as asparagines are poor coordinating partners for Zn^{2+} (Auld, 2001). This was examined by exchanging residues between the GlyR α1 and α2 subunits at the equivalent positions of H107 (α1) and N114 (α2) to generate $\alpha1^{H107N}$ and $\alpha2^{N114H}$. This exchange reversed the sensitivities of the GlyR α1 and α2 subunits with regard to Zn^{2+} inhibition, such that $\alpha1^{H107N}$ (IC_{50}, 230 ± 40 μM, n = 5) was now approximately 8-fold less sensitive to Zn^{2+} compared to $\alpha2^{N114H}$ (29 ± 2 μM, n = 4; $P < 0.05$, Fig 3.3*B*, Table 3.1). Taken together this strongly suggests that H107 not only forms part of the inhibitory Zn^{2+} binding site but also it is largely responsible for the different sensitivities of the GlyR α1 and GlyR α2 subunits to Zn^{2+} inhibition.

GlyR α3 exhibits low sensitivity to inhibition by Zn^{2+}

To further establish the significance of H107 in the subtype sensitivity to Zn^{2+} inhibition, the GlyR α3 subunit, which possesses an asparagine residue at the homologous 107 position, was also examined in this regard to its sensitivity to Zn^{2+} inhibition. This is of particular relevance as currently there are no selective pharmacological blockers to distinguish between the two adult GlyR subtypes, α1 and α3. Consistent with the data for GlyR α2, the potency of Zn^{2+} was also substantially reduced on GlyR α3 (IC_{50} = 150 ± 10 μM, n = 4). In accord with GlyR α2 subunits, replacing N107 with histidine in GlyR α3 subunits ($\alpha3^{N107H}$) increased the potency of Zn^{2+} mediated inhibition (IC_{50} = 26 ± 7, n = 3; $P < 0.05$, Fig 3.3*B*).

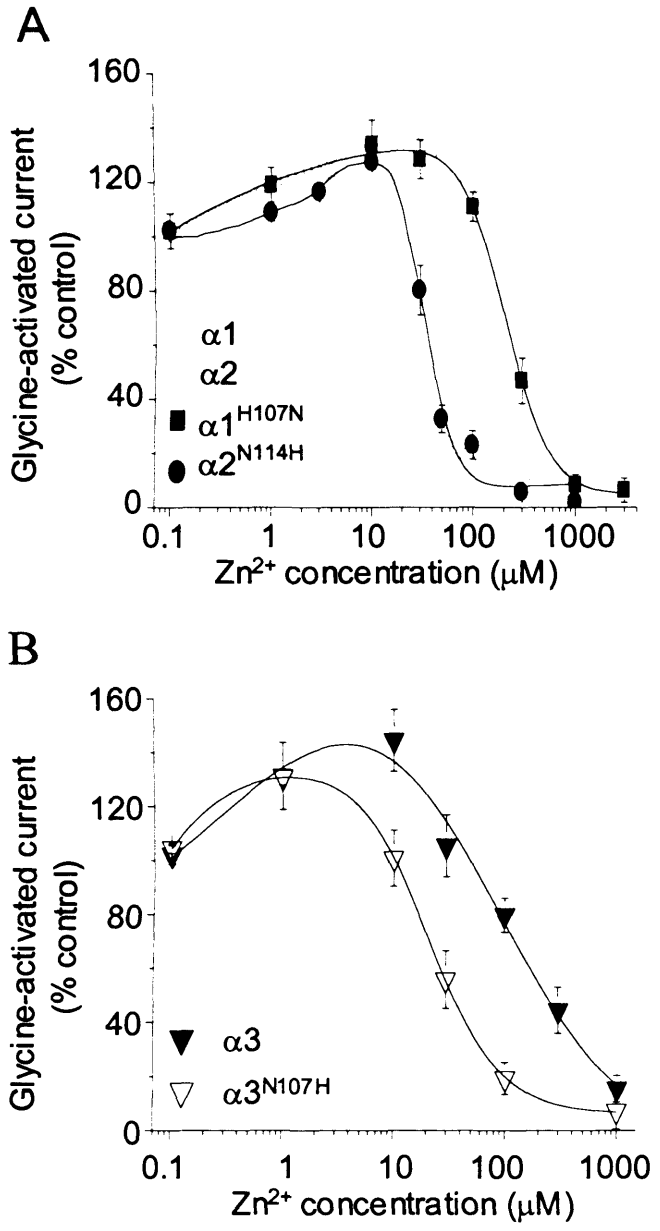

Figure 3.3 Reversal of GlyR α subunit sensitivities to Zn^{2+} mediated inhibition. *A*, GlyR $\alpha1^{H107N}$ and GlyR $\alpha2^{N114H}$ mutants and *B*, GlyR α3 and GlyR $\alpha3^{N107H}$ Zn^{2+} concentration response curves for modulating 50 % maximal glycine-activated currents. The current peaks were compared for 50 % maximal glycine responses in the absence and presence of varying concentrations of Zn^{2+} after 15 s pre-incubation with an equivalent Zn^{2+} concentration. Curves for wild-type GlyR α1 and GlyR α2 Zn^{2+} modulatory profiles are included for comparison in *A* (taken from Figure 3.2*D*). $N = 4 - 5$ for all experiments.

Mechanism for Zn^{2+} inhibition on GlyR α1 and GlyR α2 subtypes

The proposed mechanism of Zn^{2+} inhibition has not been fully investigated, although glycine concentration response curves determined in the presence of a single concentration of Zn^{2+} show no depression in the maximum response which is in accord with an apparent competitive mechanism of inhibition (Laube et al., 2000;Han and Wu, 1999). The mode of Zn^{2+} inhibition was characterised for both GlyR α1 and GlyR α2 subtypes by generating glycine concentration response curves in the presence of several inhibitory concentrations of Zn^{2+} (Fig 3.4*A,B*). For both GlyR α1 and α2 subunits the glycine curves were displaced by Zn^{2+} in a parallel manner without any significant reduction in the maximal current elicited by saturating concentrations of glycine, consistent with an apparent competitive mode of inhibition. Due to the relatively high sensitivity of GlyR α1 to Zn^{2+} inhibition it was possible to pre-incubate at several different inhibitory Zn^{2+} concentrations and achieve measurable separation between each of the glycine concentration response curves. This was not possible for the less sensitive GlyR α2 subunit without incurring solubility problems due to the high concentrations of Zn^{2+} required. This series of parallel glycine curves were transformed into a Schild plot for the evaluation of a pA_2 value for Zn^{2+} as an antagonist at the GlyR α1 subtype (Fig 3.4*C*). The Schild plot slope was not significantly different from one, and the constrained slope, with a gradient of 1, provided a pA_2 value that was 4.44 ± 0.14, yielding a dissociation constant for Zn^{2+} from the inhibitory site of 27.5 ± 0.87 μM, (n = 7).

Rate of onset of Zn^{2+} inhibition at GlyR α1 and α2

From the data presented in Fig 3.2, a pre-incubation protocol using 1000 μM Zn^{2+} caused a substantial amount of inhibition at both GlyR α1 (90 ± 2.4 %, n = 6) and GlyR α2 (78 ± 4.4 %, n = 11). During co-application protocols however, the level of inhibition induced by 1000 μM Zn^{2+} was dramatically different between the two subtypes of receptor (compare raw data traces Fig 3.2*C*). To assess the rates of onsets of Zn^{2+} inhibition at GlyR α1 and α2, potency matched doses of Zn^{2+} (40 and 1000 μM respectively) corresponding to approximately 70 % inhibition under pre-incubation conditions, were instead co-applied with 50 % maximal Gly doses for a prolonged 60 s period to allow Zn^{2+} inhibition to reach a steady-state. A prolonged

60 s application of Gly alone revealed a directly comparable biphasic desensitisation profile for both GlyR α1 and α2, with initial fast desensitisation components of 4.1 ± 0.2 s, (n = 6) and 5.6 ± 1.3 s, (n = 5), and secondary slow desensitisation components of 45.7 ± 7.8 s, (n = 6) and 49.5 ± 7.6 s, (n = 5) respectively (Fig 3.5*A,C*). As observed previously for the co-application protocol, during the initial activation phase for Gly plus Zn^{2+} responses, the current was in fact enhanced for both α1 and α2 due to the rapid onset of Zn^{2+} potentiation on GlyRs. In the case of the slow activating GlyR α2 subtype (Mangin et al., 2003) the initial Zn^{2+} enhancement caused a significant decrease in the 10 - 90 % rise time to reach steady-state from 1.4 ± 0.4 s, (n = 5) in the absence of Zn^{2+} to 0.5 ± 0.1 s, (n = 5) in the presence of Zn^{2+} ($P < 0.05$; Fig 3.5*A,B*). The GlyR α1 subtype, however, shows a faster activation time in the absence of Zn^{2+} compared to α2 and this did not experience a significant increase in activation rate for the 40 μM dose of Zn^{2+} tested (Fig 3.5*A,B*). The delayed inhibitory component of Zn^{2+} modulation observed during co-application of equivalent doses of Gly with potency matched doses of Zn^{2+} revealed that the rate of onset of inhibition is in fact indistinguishable between the two receptors. In both cases the slow desensitisation phase was completely ablated leaving only a fast decaying component. This fast phase exhibited a modest 1.5 to 2-fold increase in the rate of decay to steady state compared to the previously identified fast desensitisation in the absence of Zn^{2+}, from 4.1 ± 0.2 s to 2.8 ± 0.4 s, (n = 6) for GlyR α1 and 5.6 ± 1.3 s, to 3.1 ± 0.3 s, (n = 5) for GlyR α2 (Fig 3.5*A,C*). The total amount of inhibition after 60 s in 40 and 1000 μM Zn^{2+} compared to in the absence of Zn^{2+} was not significantly different between the two receptors. GlyR α1 was inhibited by 63 ± 7 %, (n = 6) and α2 was inhibited by 57 ± 13 %, (n = 5) indicating that the potencies of inhibition were accurately matched. The data therefore suggest that the substitution of α1 H107 with α2 N114 does not interfere with the rate at which Zn^{2+} can access the inhibitory site, or the rate at which Zn^{2+} can mediate its effect. (* Note that desensitisation time constants were measured by fitting decay components with single or double exponential curve fits as appropriate).

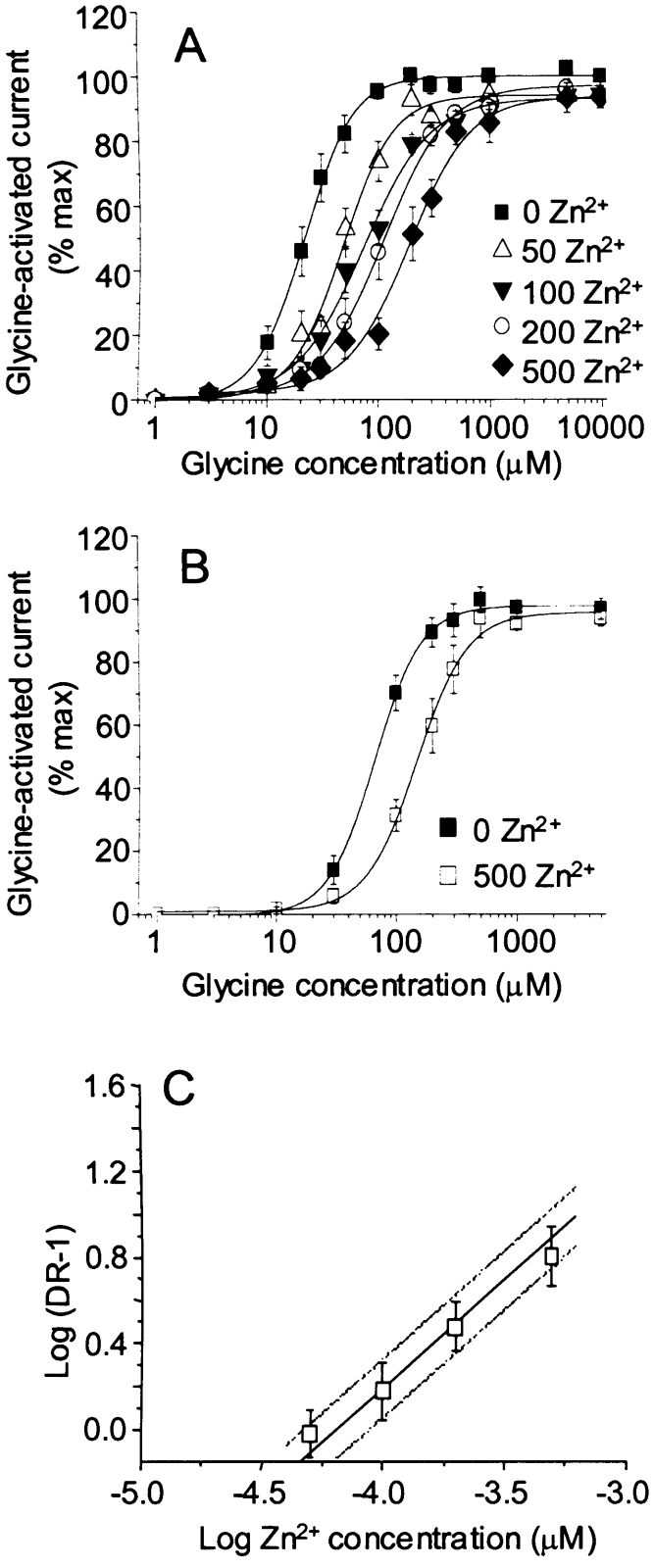

Figure 3.4 Zn^{2+} exhibits a competitive mode of inhibition at GlyR α1 and GlyR α2. Glycine concentration response curves for both α1 (*A*) and α2 (*B*) GlyRs exhibit clear parallel rightward shifts in the presence of Zn^{2+} without any decrease in the maximum response. In all cases Zn^{2+} was co-applied with the agonist glycine after a 15 s pre-incubation with an equivalent concentration of Zn^{2+}. Glycine curves for GlyR α1 were measured in the absence and presence of 50, 100, 200 and 500 μM Zn^{2+}; and for GlyR α2 in the absence and presence of 500 μM Zn^{2+}. *C*, Schild plot generated from the GlyR α1 dose-ratios taken from the curves in (*A*). A solid line indicates the constrained unity slope with 95 % confidence intervals assigned by dashed lines. All experiments were from an *n* of 6 – 13.

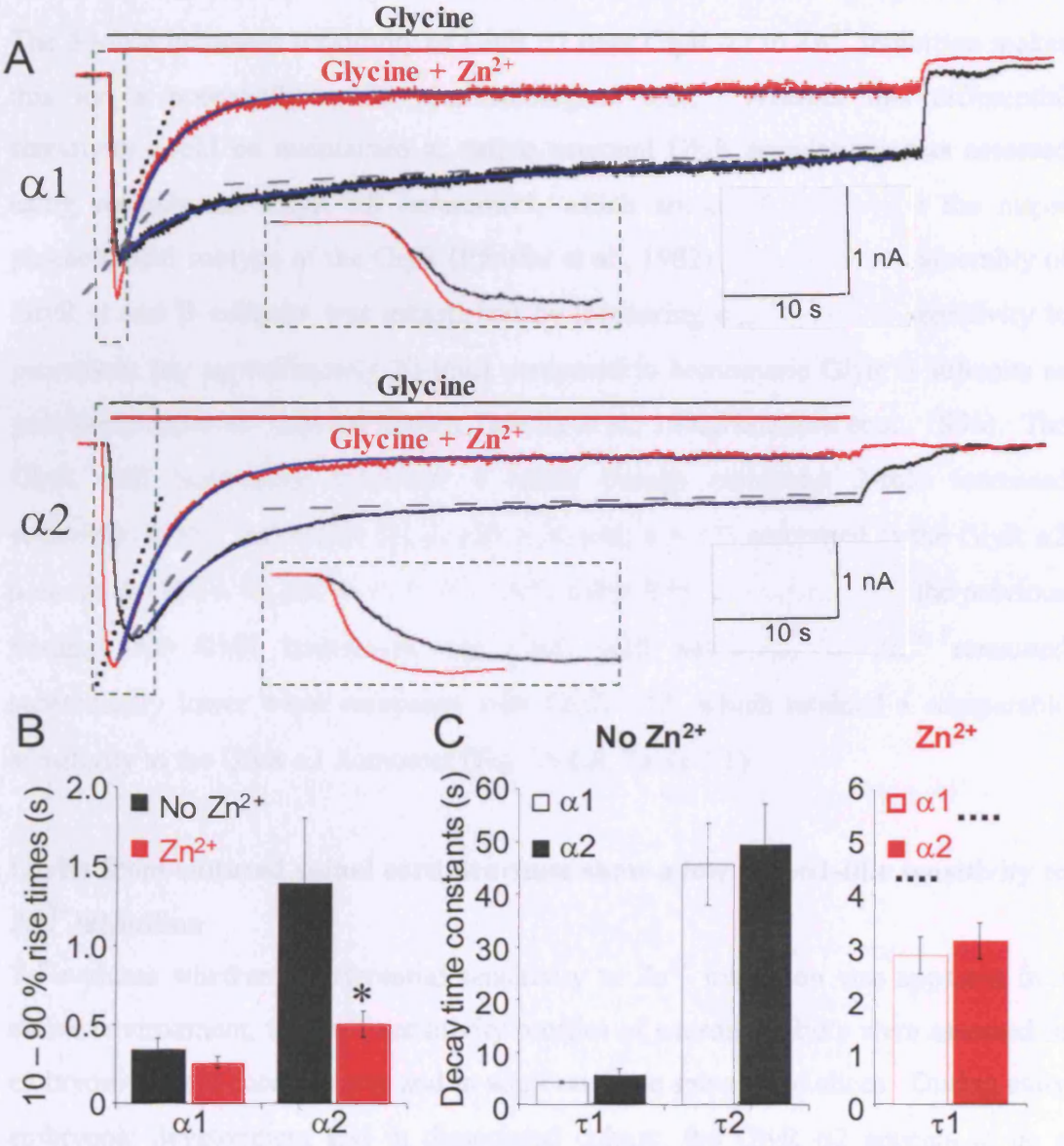

Figure 3.5 The effect of co-applied Zn^{2+} on the decay time constants of 50 % maximal Gly responses for GlyR α1 and α2. *A*, Typical raw data traces showing prolonged 60 s application of 50 % maximal doses of Gly in the absence (black) and presence (red) of potency matched doses of Zn^{2+}, 40 and 1000 μM for GlyR α1 and α2 respectively. *B*, 10 – 90 % rise-times in the absence and presence of the same Zn^{2+} concentrations, highlighted and enlarged in dashed green boxes in (*A*). The time for the slower activating macroscopic current of GlyR α2 to reach steady state is markedly reduced whilst the rate for α1 is unaffected by Zn^{2+}. *C*, Barcharts revealing that GlyR α1 and α2 have comparable desensitisation time constants in the absence and presence (red bars) of Zn^{2+}. In the absence of Zn^{2+} traces decay with two time constants, fast (4 - 5 s) and slow (40 – 50 s). In the presence of Zn^{2+} decay with only a fast time constant (approximately 3 s), dotted black lines denote the speed of the original fast decay time constant in the absence of Zn^{2+}. $N = 3 – 6$.

Differential sensitivity to Zn^{2+} inhibition is unaffected by the GlyR β subunit

The 30-fold increased sensitivity of GlyR α1 over GlyR α2 to Zn^{2+} inhibition makes this ion a potentially useful pharmacological tool. Whether this differential sensitivity could be maintained at native neuronal GlyR populations was assessed using recombinant GlyR αβ heteromers, which are considered to be the major physiological subtype of the GlyR (Pfeiffer et al., 1982). Successful co-assembly of GlyR α and β subunits was established by measuring a reduction in sensitivity to picrotoxin (by approximately 20-fold) compared to homomeric GlyR α subunits as previously reported (data not shown; Pribilla et al., 1992;Handford et al., 1996). The GlyR α2β heteromers exhibited a subtle though consistent 2-fold increased sensitivity to Zn^{2+} inhibition (IC_{50}, 180 ± 30 μM, n = 13) compared to the GlyR α2 homomers (360 ± 40 μM, n = 11; $P < 0.05$; Table 3.1). Consistent with the previous findings for GlyR homomers, the GlyR α2β sensitivity to Zn^{2+} remained substantially lower when compared with GlyR α1β, which retained a comparable sensitivity to the GlyR α1 homomer (Fig 3.6*A,B*, Table 3.1).

GlyRs from cultured spinal cord neurones show a low non-α1-like sensitivity to Zn^{2+} inhibition

To evaluate whether a differential sensitivity to Zn^{2+} inhibition was apparent in a native environment, the Zn^{2+} sensitivity profiles of neuronal GlyRs were assessed in embryonic spinal cord cultures and in adult rat acute spinal cord slices. During early embryonic development and in dissociated culture, the GlyR α2 appears to be a predominant α subtype, with a limited up-regulation of GlyR α1 during the course of culture maturation (Hoch et al., 1989;Hoch et al., 1992). This becomes more evident *in vivo* during late embryonic to early postnatal development when neurons substantially up regulate the GlyR α1 subtype (Becker et al., 1988;Takahashi et al., 1992;Watanabe and Akagi, 1995). Whole-cell recordings from 90 % of rat spinal cord cultured neurones responded to exogenously applied glycine and multipolar neurones at 7 days *in vitro* (DIV) or older, displayed robust glycinergic synaptic activity (example recording Fig 3.7*A*). The three age groups that were selected for study at, 5, 7 and 10 - 14 DIV, showed an overall low sensitivity to Zn^{2+} with 5 DIV neuronal cultures especially exhibiting a pharmacological profile consistent with a

low sensitivity GlyR subtype in accord with the GlyR α2 subtype (Fig 3.7*B*, Table 3.1).

Growing spinal cord cultures on an astrocyte monolayer has been shown to enhance the development of GABAergic and glutamatergic synaptic inputs during the first week of development (Li et al., 1999). We examined whether this co-culture may accelerate glycinergic maturation and perhaps drive the development of cultures into expressing α1 subunits as occurs *in vivo* (Becker et al., 1988;Takahashi et al., 1992;Watanabe and Akagi, 1995). Astrocytic co-cultures did accelerate the formation of synaptic activity with 5 DIV co-cultures exhibiting both a substantially higher frequency of synaptic events and also larger amplitude events, compared to 5 DIV monocultures. (5 DIV on astrocytes; mean synaptic amplitude, 450 ± 280 pA, frequency = 4.8 Hz: 5 DIV monoculture; mean synaptic amplitude, 250 ± 280 pA, frequency = 1.8 Hz; Fig 3.8*A*). However, development of spinal cord cultures on astrocyte monolayers failed to produce a noticeable increase in the sensitivity to Zn^{2+} mediated inhibition from 5 DIV to 7 DIV, or when compared to spinal cord cultures not grown on astrocytic monolayers (Fig 3.8*B*, Table 3.1).

This work was directly complemented by following the period during which GlyR expression switches *in vivo*. To do this, electrophysiological recordings were made from neurones in acute spinal cord slices at P0 and P18. Whole cell recordings using pre-incubation with 30 μM Zn^{2+} exhibited only a partial inhibition at P0, of 36 ± 4 %, (n = 19) consistent with a possible mixed GlyR α1 and α2 population; however, a profound inhibition, 69 ± 4 %, (n = 13), was exhibited at P18 in accord with a progressive developmental transition to the adult GlyR α1 subtype (Fig 3.9*A,B*). These experiments were performed in collaboration with M.Beato.

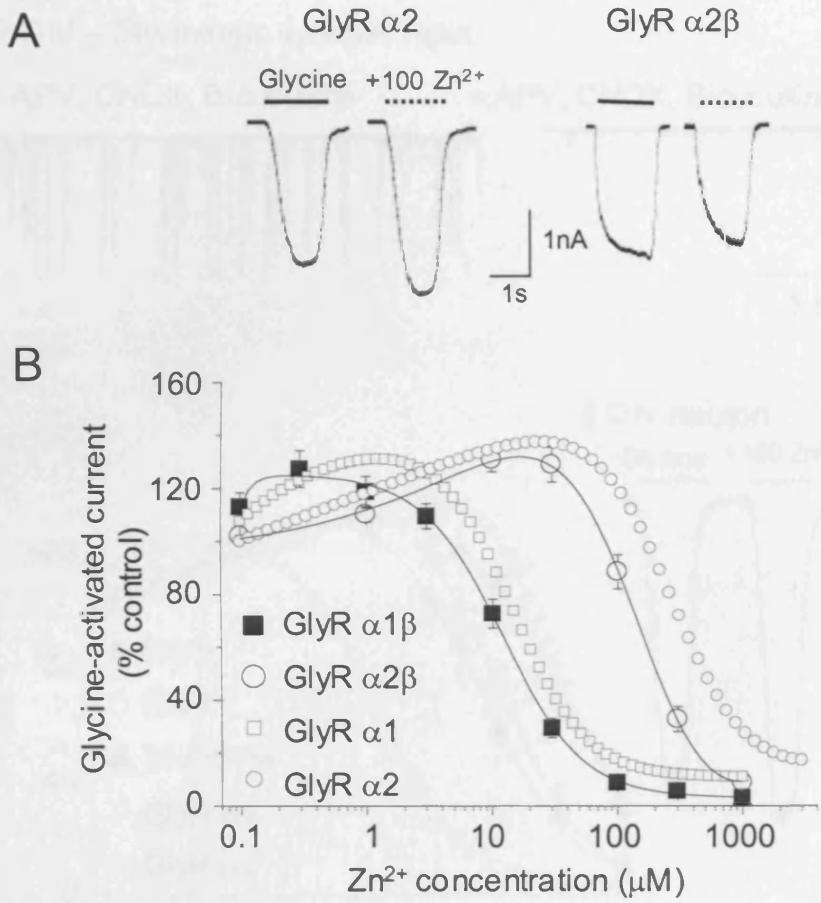

Figure 3.6 Differential sensitivity to inhibitory Zn^{2+} is retained in physiologically relevant recombinant GlyR αβ heteromers. *A*, Typical 50 % maximal currents evoked by application of an EC_{50} dose of glycine, on GlyR α2 and GlyR α2β respectively, in the absence (solid line) and presence (dashed line) of 100 μM Zn^{2+}. This shows there is a modest though not profound difference in the potency of inhibitory Zn^{2+} between the homomeric and heteromeric GlyR α2. *B*, Zn^{2+} concentration response curves for the modulation of 50 % maximal glycine responses on GlyR α1β and GlyR α2β heteromers in the presence of varying concentrations of Zn^{2+} after 15 s pre-incubation with the same concentration of Zn^{2+}. For comparison, the Zn^{2+} sensitivities of recombinant GlyR α1 and GlyR α2 homomers are shown (taken from the curve fits in Figure 3.2*D*). $N = 3 - 7$.

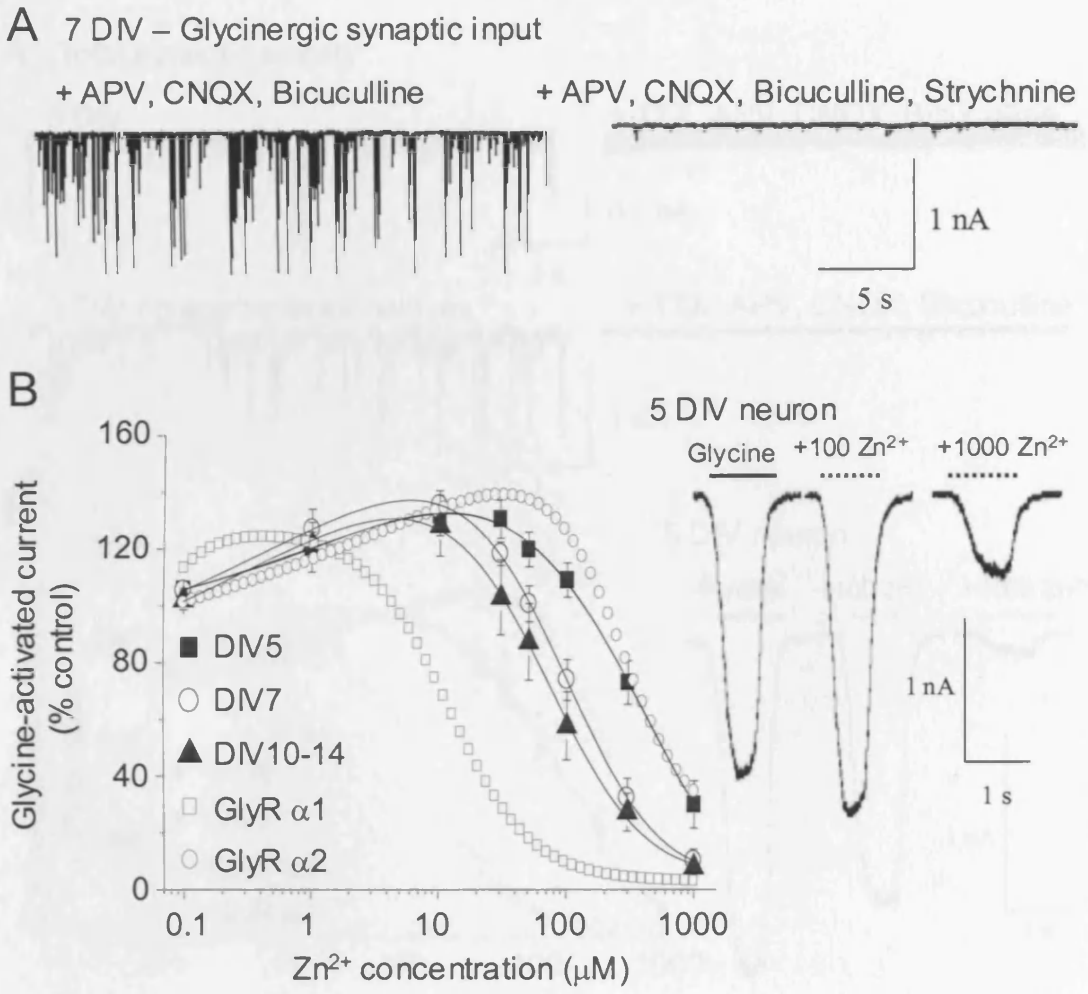

Figure 3.7 Native GlyRs from primary cultures of spinal cord neurones exhibit a low sensitivity to Zn^{2+} mediated inhibition. *A,* A selected epoch of synaptic activity from a 7 DIV neurone demonstrating that they receive robust glycinergic input. This was assessed by monitoring synaptic activity in the presence of 10 μM bicuculline, 20 μM AP5 and 10 μM CNQX to inhibit $GABA_A$, NMDA and AMPA receptors respectively (left panel) and then ablating this activity in the presence of a GlyR selective inhibitor, 1 μM strychnine (right panel). *B,* Native receptors from rat spinal cord cultures at 5, 7 and 10-14 DIV exhibit a low sensitivity to inhibitory Zn^{2+} consistent with the expected predominant presence of GlyR α2 in the embryonic spinal cord. Again, for comparison, the curve fits for the recombinant GlyR α1 and GlyR α2 homomers are shown (from 3.2*D*). The inset raw data traces illustrate, on a 5 DIV neuron, modulation by 100 and 1000 μM pre- and then co-applied Zn^{2+} with a 50 % maximal dose of glycine. $N = 8$.

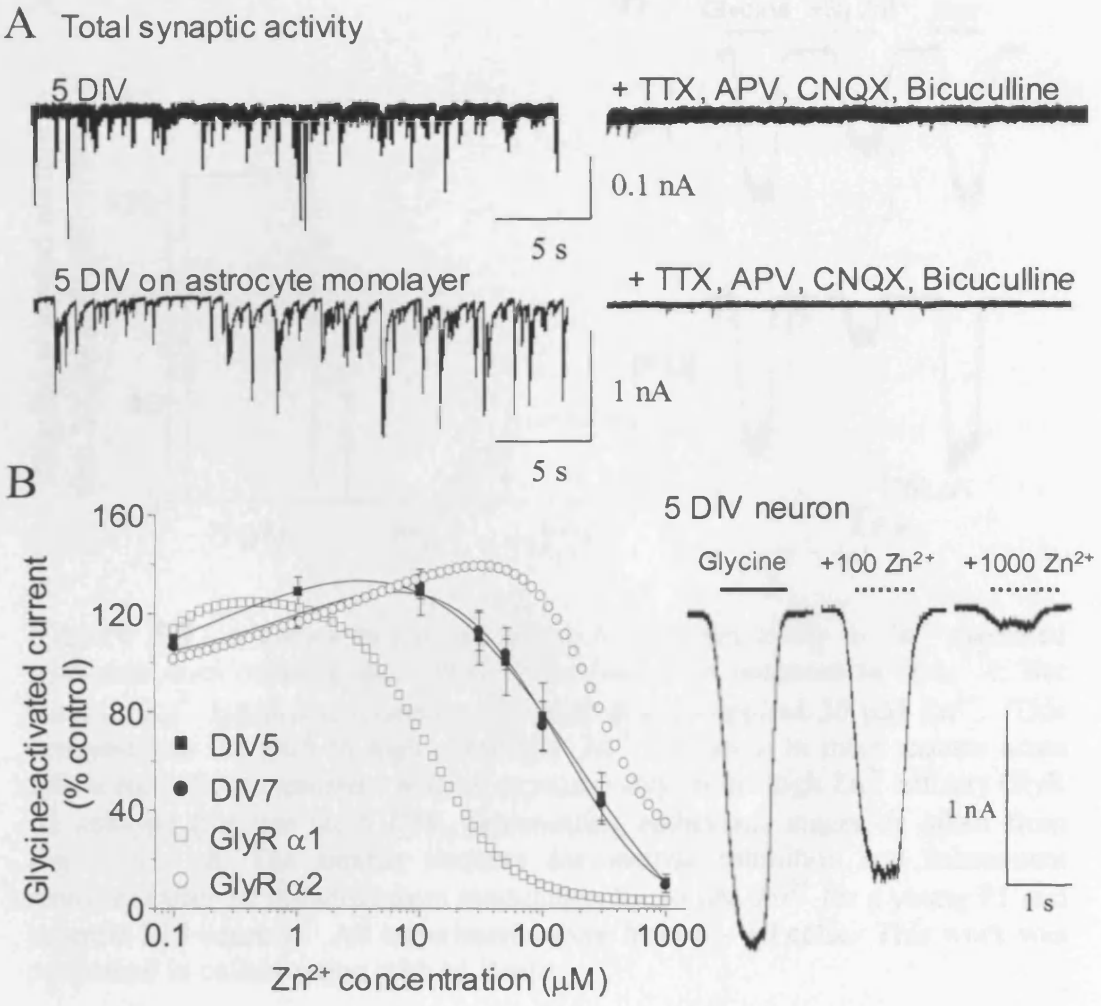

Figure 3.8 Spinal cord neurones plated on astrocytic monolayers exhibit a low sensitivity to Zn^{2+} mediated inhibition. *A,* Synaptogenesis occurred significantly earlier for astrocytic co-cultures (lower panels), which received robust synaptic input by 5 DIV (up to 2 nA currents; compare with 7 DIV neurones in Fig 3.7*A*) whilst 5 DIV spinal cord monocultures (upper panels) had less frequent and smaller synaptic currents (< 200 pA). Whole-cell exogenous glycinergic responses were measured in the presence of 10 μM bicuculline, 20 μM AP5 and 10 μM CNQX to inhibit $GABA_A$, NMDA and AMPA receptors respectively plus TTX to effectively block all synaptic input including spontaneous glycinergic events (right panel). *B,* Despite accelerated synaptogenesis of rat spinal cord cultures on astrocytic monolayers these neurones retained a low sensitivity to inhibitory Zn^{2+} at 5 and 7 DIV. Comparison of inhibition curves for recombinant GlyR α1 and GlyR α2 homomers are included (from 3.2*D*). The inset raw data traces illustrate, on a 5 DIV neurone, modulation by 100 and 1000 μM pre- and then co-applied Zn^{2+} with a 50 % maximal dose of glycine. $N = 8$.

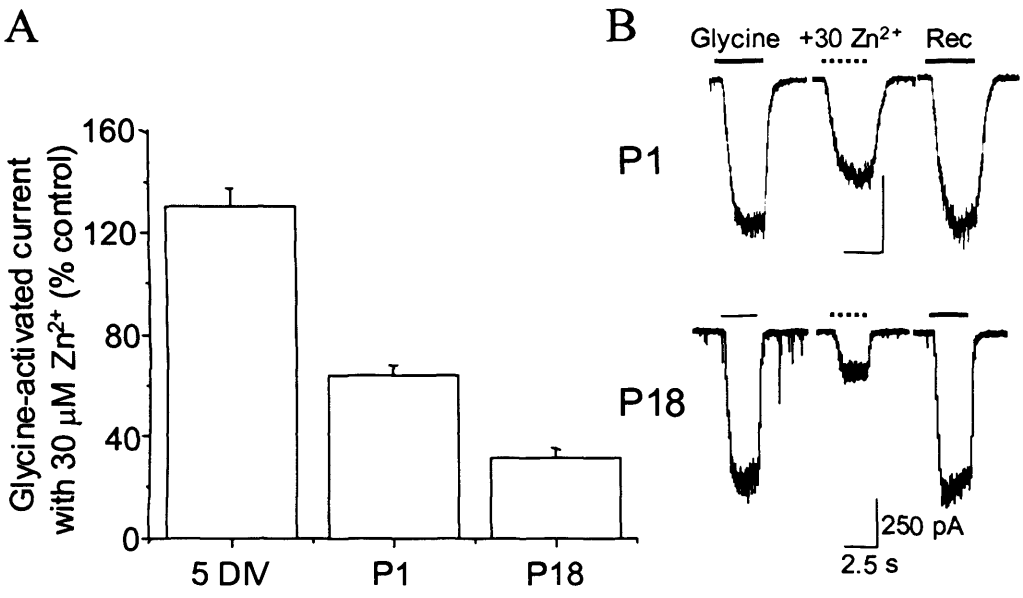

Figure 3.9 A switch to the high GlyR α1-like sensitivity to Zn^{2+} mediated inhibition does occur in rat ventral horn spinal cord neurones *in vivo*. *A*, Bar chart of Zn^{2+} inhibition following pre- and then co-applied 30 μM Zn^{2+}. This demonstrates the shift to high sensitivity Zn^{2+} inhibition in more mature acute spinal cord slices consistent with an expected shift to the high Zn^{2+} affinity GlyR α1 subtype (the bar for 5 DIV, representing embryonic stages, is taken from Fig 3.7*B*). *B*, The sample currents demonstrate inhibition and subsequent recovery (after 10 minutes) from modulation by 30 μM Zn^{2+} for a young P1 and juvenile P18 neurone. All experiments were from 8 – 19 cells. This work was performed in collaboration with M.Beato.

Identification of the structural elements required for Zn^{2+} inhibition

Inspecting the aligned primary sequences of GlyR α and β subunits reveals that the GlyR β subunit, like the α2 subunit, retains the low affinity asparagine residue at the homologous position to the Zn^{2+} binding GlyR α1 subunit H107. This is curious since co-expression of the β subunit with the GlyR α2 subunit in this study caused a modest increase in the sensitivity of this homomer to Zn^{2+} inhibition. This suggested that perhaps contrary to previous reports, the β subunit may actually contribute to the Zn^{2+} binding site. Such a β subunit dependent increase in sensitivity was not observed with the α1β heteromer, presumably because the α1 subunit has the highest subtype sensitivity to Zn^{2+} realised through the presence of its unique residue, H107. A directed comparative scan was therefore made of the α2 and β subunit primary

amino acid sequences guided by modelling the GlyR N-terminal domains on the crystal structure of the homologous acetylcholine binding protein (AChBP; Brejc et al., 2001). This approach identified specific amino acid differences in the predicted vicinity of the GlyR α1 H107 and H109 based Zn^{2+} inhibitory binding site. Of these, only two residues differed that might impact on Zn^{2+} coordination at this site. In GlyR α2 subunits, G112 (α1 G105) and T140 (α1 T133) are replaced in the β subunit by S128 and S156, respectively (Fig 3.10*A,B*). In view of their proximity to the Zn^{2+} inhibitory site, the β subunit residues were switched for their α2 subunit counterparts using the mutations, GlyR β^{S128G} and β^{S156T}, in an attempt to remove and therefore elucidate, the cause of the β subunit induced increase in GlyR α2 sensitivity to Zn^{2+} inhibition. However, neither GlyR β'^{S128G} nor β'^{S156T} removed the ability of the β subunit to increase GlyR α2 sensitivity to Zn^{2+} inhibition (Fig 3.10*C*; Table 3.1). In the absence of other suitable β subunit residues capable of interacting with the Zn^{2+} inhibitory site, the effect of the β subunit on GlyR α2 may instead be an indirect structural effect. Such a role has been suggested for T112 in the GlyR α subunit (Nevin et al., 2003), which also affected GlyR sensitivity to Zn^{2+} inhibition (Laube et al., 2000).

Further structural comparisons of the GlyR α1 subunits revealed that the T133 residue is located on β strand 6 (according to the nomenclature of Brejc et al, 2001), which is predicted to reside directly below H109 on β strand 5. Moreover, another threonine in GlyR α1, T135, is also located on β strand 6 directly below H107 (Fig 3.10*A,B*). Since GlyR α1 T133 and T135 residues are ideally located as potential coordinating ligands for Zn^{2+}, lying just below the putative Zn^{2+} binding H109 and H107 respectively, these threonines were assessed for their role in Zn^{2+} inhibition by individual mutation to alanines. Although GlyR $\alpha1^{T135A}$ exhibited a comparable Zn^{2+} IC_{50} (29 ± 2 μM, n = 3) to the wild-type GlyR α1 subunit, the GlyR $\alpha1^{T133A}$ mutation ablated Zn^{2+} inhibition up to 1 mM (n = 5, Fig 3.10*D*, Table 3.1).

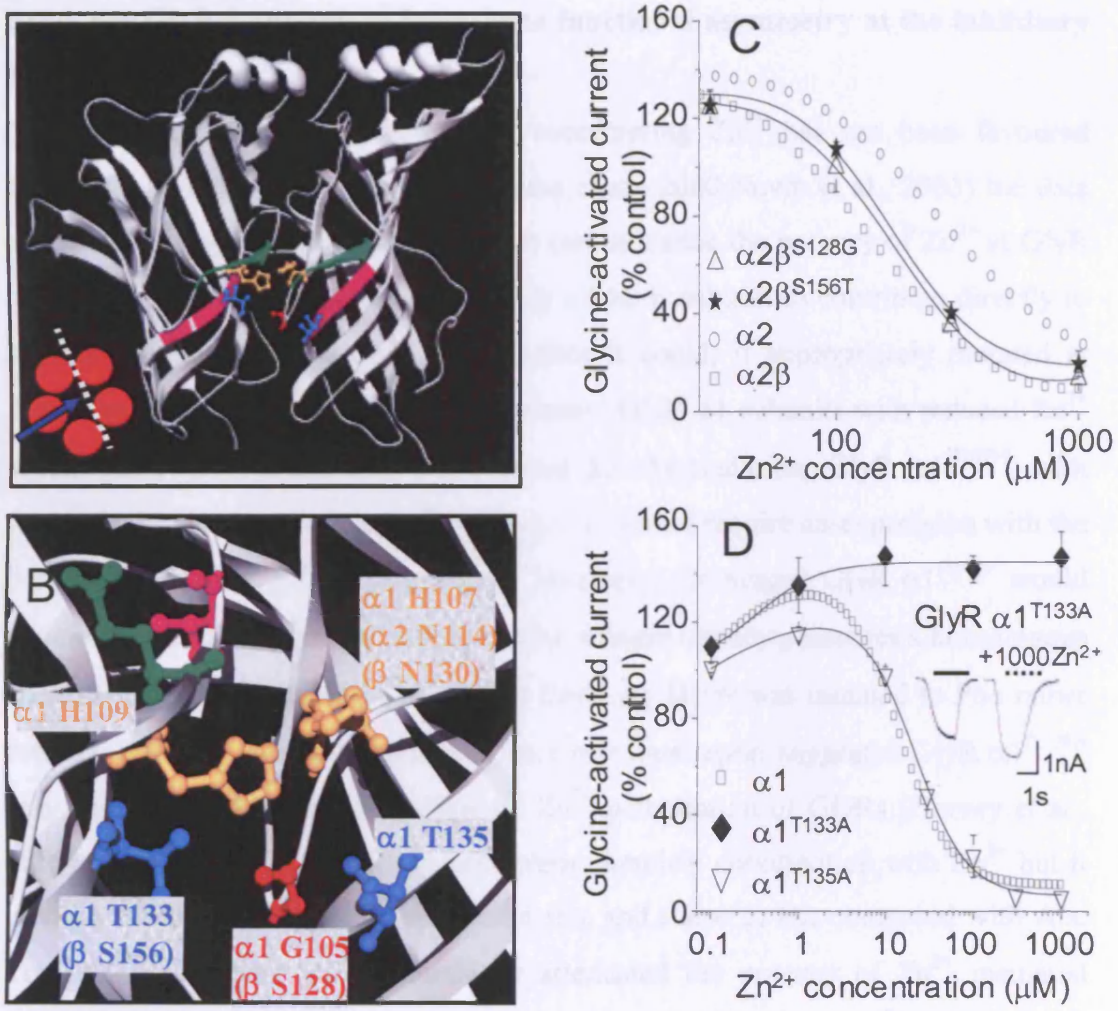

Figure 3.10 Evaluation of potential binding residues in the immediate vicinity of the inhibitory Zn^{2+} site. *A*, Two neighbouring GlyR α1 subunits modelled on the AChBP, expanded in *B*, to highlight inhibitory Zn^{2+} binding site residues, H107 and H109 (orange) and two newly-identified potential Zn^{2+} binding residues, T133 and T135 (blue). An additional variant residue, in the β subunit S128, is also shown (red). In (*A*) β-strand 5 (green) containing H107 and H109 is presented directly above β-strand 6 (pink) containing T133 and T135. *B*, Homologous residues are shown in parentheses. For reference, GlyR α1 E110 (green) and T112 (pink), previously shown (Laube et al., 2000) to influence Zn^{2+} mediated inhibition, are included and are both predicted to face away from the site, suggesting the side chains of these residues could not directly coordinate Zn^{2+}. *C*, Assessment of potential β-subunit variants that may induce the modest increase in sensitivity to Zn^{2+} mediated inhibition on the GlyR α2 subtype by measuring Zn^{2+} modulation of 50 % maximal glycine responses (using pre- and then co-applied Zn^{2+}) on GlyR $\alpha2\beta^{S128G}$ and GlyR $\alpha2\beta^{S156T}$ heteromers. Comparison with recombinant GlyR α2 and GlyR α2β curves (originally from 3.2*D* and 3.6*B*) show that these substitutions do not account for the β-subunit influence on α2. *D*, Zn^{2+} concentration response curves for modulation of 50 % maximal glycine responses at GlyR $\alpha1^{T133A}$ and GlyR $\alpha1^{T135A}$ with wild-type GlyR α1 present for comparison (from 3.2*D*). Inset shows raw data traces demonstrating the resistance of glycine responses on GlyR $\alpha1^{T133A}$ to inhibition by 1000 μM Zn^{2+}. $N = 3 - 6$.

Using the GlyR β subunit to investigate functional asymmetry at the inhibitory Zn^{2+} binding site

Although a role for the β subunit in coordinating Zn^{2+} has not been favoured previously (Bloomenthal et al., 1994;Laube et al., 2000;Nevin et al., 2003) the data presented here suggested that this subunit can influence the potency of Zn^{2+} at GlyR α2β heteromers. We addressed the ability of the β subunit to contribute directly to the Zn^{2+} binding site by examining whether it could, if appropriately mutated at homologous positions, compensate for mutated GlyR α1 subunits with reduced Zn^{2+} sensitivities. For example, to compensate for the mutation, GlyR $\alpha1^{H107N}$, with regard to the sidedness of the Zn^{2+} binding site, would require co-expression with the β subunit mutation, β^{N130H} (Fig 3.11*B*). Similarly, the mutant GlyR $\alpha1^{H109F}$ would require a pairing with wild-type β, since this subunit already possesses a homologous H109 (β H132). It should be noted that GlyR α1 H109 was mutated to Phe rather than the typical Ala usually employed, as a previous report suggested GlyR $\alpha1^{H109A}$ may exert a complicating side effect on Zn^{2+} potentiation of GlyRs (Harvey et al., 1999). The Phe moiety also does not favour chemical coordination with Zn^{2+} but it is more similar in terms of its side chain size and shape to His compared with Ala. This $\alpha1^{H109F}$ receptor still dramatically attenuated the potency of Zn^{2+} mediated inhibition but maintained wild-type levels of responsiveness to Zn^{2+} enhancement (Fig 3.11*B*). Finally, the novel GlyR $\alpha1^{T133A}$ mutant could be compensated by the β^{S156T} mutation (Fig 3.11*B*). GlyR α1 E110 and T112, previously found to influence Zn^{2+} inhibition (Laube et al., 2000), were not investigated in this study as GlyR $\alpha1^{E110A}$ exerted only a modest 5-fold increase in Zn^{2+} IC_{50} (67 ± 4 μM, n = 3, data not shown) and is predicted to face away from the H107/H109 based Zn^{2+} binding site, whilst T112 (also facing away from the site; Fig 3.10*A,B*) has properties consistent with an indirect effect on binding (Nevin et al., 2003).

For the GlyR α1 subunit mutations, H109F and T133A, both of which reside on the same '-' face (nomenclature from Fu & Sine, 1996; Fig 3.11*B*) of the inhibitory Zn^{2+} binding site, no recovery of Zn^{2+} potency was observed when either of these subunits were co-expressed with the compensating GlyR β subunits including either H132 or S156T, respectively (IC_{50}s > 1 mM, n = 3; Fig 3.11*B*). Furthermore, we investigated this face of the Zn^{2+} binding site from the perspective of the GlyR α1 T133 residue

and found that co-expression of the wild-type GlyR α1 subunit with a β^{S156A} mutant also had no effect on the receptor sensitivity to Zn^{2+} inhibition (IC_{50} = 17 ± 7 μM, n = 3). These data, accrued from one face (-) of the Zn^{2+} binding site, concur with the previously reported lack of effect of co-expressing GlyR α1 with β^{H132A} on Zn^{2+} mediated inhibition (Nevin et al., 2003).

By contrast, when the GlyR $\alpha1^{H107N}$ mutant, which is present on the opposing '+' face of the Zn^{2+} binding site to H109 and T133, was co-expressed with the GlyR β^{N130H} subunit, a dramatic recovery in the sensitivity to Zn^{2+} was observed almost reaching wild-type GlyR α1β sensitivity (IC_{50} = 24 ± 3 μM, n = 5, Fig 3.11*B*). To ensure this mutation was not due to the *de novo* construction of an intrasubunit Zn^{2+} binding site in the β subunit, as this β^{N130H} subunit now contained two juxtaposed histidine residues (H130 and H132), we co-expressed the β^{N130H} subunit with a GlyR $\alpha1^{H107N,\ H109F}$ double mutant and this exhibited no recovery to Zn^{2+} inhibition (IC_{50} > 1 mM, n = 4; data not shown). This strongly suggested the β subunit is indeed participating in an intersubunit site and that this contribution by the β subunit to the Zn^{2+} binding site can only be donated from the '+' face of the subunit.

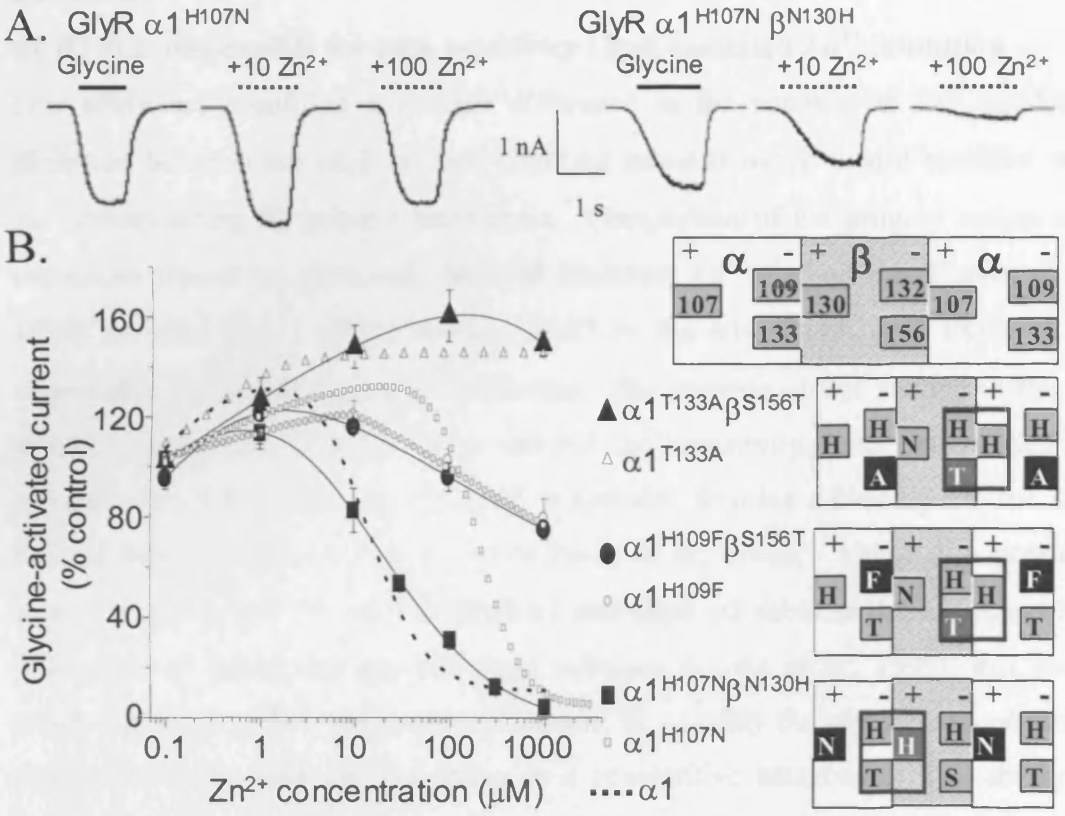

Figure 3.11 Asymmetry at the GlyR α subunit Zn^{2+} inhibitory site using β-subunit induced recovery of α subunits with perturbed Zn^{2+} sites. *A,* Raw data traces illustrating the recovery of sensitivity to Zn^{2+} inhibition at the '+' face following co-assembly of a 'corrected' β^{N130H} subunit with a defective $\alpha1^{H107N}$ subunit. *B,* Schematic cross sections of 3 of the 5 GlyR subunits in a pentamer showing the compensatory β subunits required for co-expression with GlyR α subunits lacking one component of the Zn^{2+} inhibitory site (H107, H109, or T133). Black or dark grey boxes represent the residues mutated for α1 and β subunits respectively. Red boxes occur at the αβ subunit interfaces labelled, '+' and '-' to highlight Zn^{2+} binding sites where all the binding components under examination have been restored. These sites would be restored regardless of whether the β subunits are portrayed as being separated by an α subunit (shown here) or if the β subunits are neighbours. *B,* Graph presenting assessment of Zn^{2+} inhibition in HEK cells using 15 s pre- and then co-application of Zn^{2+} with 50 % maximal glycine doses. All co-expressed heteromeric α1β receptors are predicted to reconstitute all components of the Zn^{2+} binding site at the αβ subunit interface, however, only in the case of β^{N130H} co-expressed with $\alpha1^{H107N}$ is the sensitivity to Zn^{2+} inhibition recovered (as compared to an α1 wild-type profile, dotted line, originally from Fig 3.2*D*). The inhibition curves for GlyR $\alpha1^{H107N}$, $\alpha1^{H109F}$ and $\alpha1^{T133A}$ subunits are included for comparison (data for $\alpha1^{H107N}$ and $\alpha1^{T133A}$ are taken from Figs 3.3*A* and 3.10*D*, respectively). $N = 3 - 6$.

Discussion

α1 H107 is responsible for high sensitivity GlyR mediated Zn^{2+} inhibition

This study has identified a distinct difference in the potency of Zn^{2+} mediated inhibition between the GlyR α1 and GlyR α2 subunits which is also manifest with the corresponding αβ subunit heteromers. Comparison of the primary amino acid sequences around the previously deduced inhibitory Zn^{2+} binding site (Harvey et al., 1999) revealed that a single residue, H107 in the α1 subunit, was likely to be responsible for the different Zn^{2+} potencies. The absence of this residue in the α2 subunit substantially accounts for its reduced Zn^{2+} sensitivity, further supporting the assertion that this location on the GlyR is probably forming a binding site for Zn^{2+} induced inhibition (Harvey et al., 1999;Nevin et al., 2003). Although a previous study comparing Zn^{2+} potency at GlyR α1 and GlyR α2 subunits did not report any differences in sensitivity between these subtypes (Laube et al., 1995), this could reflect the varying Zn^{2+} application protocols, or possibly the glycine concentration chosen for study since Zn^{2+} is acting as a competitive antagonist. The ability to switch the Zn^{2+} sensitivities of GlyR α1 and α2 subunits simply by point mutation ($\alpha1^{H107N}$ and $\alpha2^{N114H}$) strongly suggested that this differential effect had a molecular basis.

Zn^{2+} inhibition affects the apparent affinity of the GlyR

Despite the differential sensitivity of GlyR α1 and α2 subunits to inhibitory Zn^{2+}, both glycine concentration response curves were displaced in a parallel manner without any reduction in the maximal glycine-activated current. This is consistent with Zn^{2+} acting as a competitive inhibitor, however, this does not necessarily imply that Zn^{2+} is directly competing for the glycine recognition site, since Zn^{2+} could interact with the receptor allosteric fashion reducing the ability of glycine to bind to its entirely non-overlapping site and possibly vice-versa. Indeed, this explanation is consistent with the current views on the discrete locations of the inhibitory Zn^{2+} and agonist binding sites (Laube et al., 2002b). Prior evidence suggests that Zn^{2+} inhibition of GlyRs is largely caused by a reduction in the agonist efficacy (E; Laube et al., 2000). The values of E reported for glycine at GlyR α1 vary from, 10 - 20 (Laube et al., 2000) and 16 (Lewis et al., 2003), to 40 (Beato et al., 2004) for the higher-liganded GlyR states. By assuming a sequential ligand binding site model is

sufficient to explain GlyR activation and using this to simulate glycine dose response curves, a reduction in E alone will not produce parallel displacements in the glycine concentration response curves of the magnitude observed in our study without significant reductions in the maximum response. For example, for GlyR α1, E would need to be reduced from 40 to 0.19 to increase the glycine EC_{50} from 24 to 214 μM; however this would cause the P_o to be reduced from 0.97 to 0.15, a substantial reduction in maximum glycine current. Thus, it is highly likely that Zn^{2+} is also affecting the affinity of glycine for its recognition site. The Schild analysis here provides the first definitive measurement of Zn^{2+} affinity for the GlyR α1 (pA_2 of 4.44) and indicates that Zn^{2+} has a much lower potency (329-fold) at the glycine receptor compared to the classical competitive GlyR antagonist, strychnine (pA_2 of 7.08, K_B 83.2 nM; Saitoh et al., 1994).

To further support the mode of Zn^{2+} inhibition being the same at GlyR α1 and α2, these receptors both exhibited comparable macroscopic kinetics for the rate of onset of Zn^{2+} inhibition at activated GlyRs. The fact that there was an indistinguishable rate of onset for equipotent concentrations of inhibitory Zn^{2+} when co-applied with a 50 % maximal dose of Gly suggests that the accessibility of the site to Zn^{2+} and the rate at which Zn^{2+} mediates its effect is comparable between α1 and α2. Under these conditions the normal biphasic desensitisation of agonist currents was replaced in the presence of Zn^{2+} with a single fast decaying component. Unfortunately it is not possible to attribute this property to any effect of Zn^{2+} to alter the desensitising properties of the receptor as this may simply reflect an independent action of Zn^{2+} to inactivate the receptor via an alternative route. In addition it is not possible to accurately assess the purity of any desensitising effect mediated by inhibitory Zn^{2+} due to the competing and rapid Zn^{2+} enhancement experienced at these co-applied Zn^{2+} doses. This will increase the height of the initial response peaks and thus potentially increase the rate of desensitisation as if the receptor were effectively activated by a higher concentration of agonist.

The mechanism of Zn^{2+} inhibition

Measurements of Zn^{2+} inhibition using varying application protocols revealed that pre-equilibration of Zn^{2+} with the GlyR and subsequent co-application with agonist

incurred the highest potency for inhibition. In agreement with this, prolonged co-application of Gly and Zn^{2+} revealed a delayed onset of Zn^{2+} inhibition, which required a significant 5 – 10 second time period to reach steady-state. These observations support a hypothesis favouring Zn^{2+} binding to either a closed agonist-bound GlyR or a closed agonist-unbound GlyR or both (or the two situations may be equivalent). This dictates that Zn^{2+} would exert its greatest level of inhibition under a pre-incubation protocol as is observed here where Zn^{2+} can bind and stabilise the closed-bound/unbound receptor prior to the presence of agonist (see Smart, 1992 for a similar argument for $GABA_A$Rs). Under co-application conditions a delayed onset would be observed as some agonist will activate the receptor before Zn^{2+} can bind. Therefore as Zn^{2+} cannot bind, or binds less to the open receptor (or perhaps also to the closed receptor with agonist bound), it must wait for the receptor to close and possibly for the agonist to unbind before Zn^{2+} can coordinate and inhibit receptor reactivation during the course of the remaining agonist application. This also means that the onset of Zn^{2+} inhibition will be slower under a co-application protocol at lower Zn^{2+} concentrations because there is an increased likelihood that after the receptor has shut and/or agonist has unbound that another molecule of agonist will bind and reactivate the receptor before the Zn^{2+} can bind. This situation is represented in Fig 3.2*C,D* where despite the fact that under pre-equilibration conditions 100 and 1000 μM Zn^{2+} exert almost full inhibition at GlyR α1, under co-application (*C*, example traces) the onset of 100 μM Zn^{2+} inhibition is substantially slower than that of 1000 μM Zn^{2+}. This hypothesis also supports the apparent competitive mode of Zn^{2+} inhibition inferred by parallel dose response curve shifts with unchanged maximal agonist responses. Under these conditions when a saturating concentration of agonist is applied the receptor will effectively always have agonist bound as whenever one agonist molecule dissociates another will immediately take its place. Therefore the equilibrium between open and closed channels will be biased towards the open state, reducing the prospect of Zn^{2+} binding and causing inhibition.

This observation also has implications for the activation mechanism of the GlyR as it suggests that when agonist is bound there is a section of the receptor, encompassing as far as the Zn^{2+} binding site, that is always conformationally shifted as long as

agonist is bound. However this conformational change is not necessarily synonymous with opening of the receptor channel. The reason for this is that single channel studies clearly reveal that even in the presence of saturating agonist concentrations, i.e. effectively agonist is always bound (especially for GlyR homomers where 5 molecules of agonist can bind at any one time but only 2-3 are required to activate it; Beato et al, 2004) the receptor still flickers between open and closed states very rapidly, with occasional long closures presumably due to desensitisation. Yet Zn^{2+} does not appear to bind during these closed states as it does not reduce the Gly I_{max} suggesting part of the receptor is still in an activated conformation preventing Zn^{2+} binding to its inhibitory site.

Native GlyRs retain the sensitivity to Zn^{2+} inhibition of their recombinant counterparts

This study also revealed that a distinction between GlyR subtypes for Zn^{2+} mediated inhibition extends to a native environment where the sensitivity of a GlyR population, that is expected to be predominantly composed of α2 subunits in early spinal cord culture, demonstrates an overall low sensitivity to Zn^{2+} inhibition. More mature neurons in acute spinal cord slices, however, display a distinctly enhanced sensitivity consistent with the predicted shift to GlyR α1 receptor subtypes in adult tissues (Becker et al., 1988;Takahashi et al., 1992;Watanabe and Akagi, 1995). This suggests the physiological significance of Zn^{2+} inhibition is unlikely to be relevant at embryonic stages of development since native embryonic GlyRs require greater than 50 μM Zn^{2+} before the glycine EC_{50} response is inhibited. This result is in keeping with a previous report (Laube, 2002a) where 50 μM Zn^{2+} induced marginal inhibition of glycinergic IPSCs in spinal cord cultures. Our data, in agreement with previous immunocytochemistry (Hoch et al., 1989;Hoch et al., 1992), suggests that in spinal cord cultures the embryonic GlyR α2 remains dominant during culture maturation, regardless of the presence or absence of astrocytes, as the sensitivity to inhibitory Zn^{2+} remains low up to 14 DIV.

The properties of the β subunit support an asymmetric role for the inhibitory Zn^{2+} site

Previously, the GlyR β subunit has not been shown to exert any detectable influence on Zn^{2+} mediated inhibition at the GlyR (Bloomenthal et al., 1994;Laube et al., 1995;Nevin et al., 2003). However, this report demonstrates that in the unique instance of the α2 subtype, co-expression with the β subunit revealed an increased sensitivity to Zn^{2+} mediated inhibition. Although we were unable to attribute this effect to a specific moiety in the vicinity of the putative inhibitory Zn^{2+} binding site, as a consequence, we identified GlyR α1 T133, as a pivotal residue for Zn^{2+} inhibition. When considering the location of the intersubunit Zn^{2+} binding site, in accordance with the three-dimensional GlyR α1 model based on the AChBP, the T133 residue is predicted to lie beneath H109. This would be an ideal location for participation in the putative inhibitory Zn^{2+} binding site.

Co-expression of GlyR α subunits with complementary β subunits, designed to compensate for α subunits lacking specific components of the inhibitory Zn^{2+} binding site revealed an asymmetry of function between the opposing faces of the intersubunit binding site. Effectively knocking out either GlyR α1 H109, or T133, both predicted to be on the same '-' face of the subunit, could not be compensated by β subunits mutated to contain equivalent α subunit residues. This demonstrates that the α subunit H107 '+' face and the mutant β subunit H132/S156T '-' face cannot form a functional Zn^{2+} inhibitory site alone, when the α-subunit '-' face has been disrupted by mutation. In contrast, following knock-out of the GlyR α1 H107 on the opposing '+' face, the attenuated sensitivity to Zn^{2+} inhibition was almost fully restored by co-expression with β^{N130H} subunits. The restoration of Zn^{2+} inhibition for the GlyR α1 H107N mutant implies that such inhibition is probably mediated from either the GlyR α1 H109/T133 '-' face, or the β N130H '+' face, or both acting together. As the wild-type GlyR α1 subunit is able to mediate Zn^{2+} inhibition regardless of the removal of any inhibitory components in the β subunit this supports a hypothesis whereby the H109 and T133 '-' face of the binding site is responsible for connecting Zn^{2+} binding to an effect on receptor function (transduction). Furthermore, this transduction must be driven through the GlyR α1 subunit. In

comparison, H107 can instead be regarded as a pure binding residue, as this can be donated from a neighbouring subunit that lacks its own Zn^{2+} transduction apparatus i.e., the β subunit.

A proposed molecular basis for the action of inhibitory Zn^{2+}

The hypothesis of asymmetric transduction from the '-' face of the GlyR α1 subunit is in keeping with current perspectives of proposed structural rearrangements that occur upon receptor activation of cys-loop receptors. Intermediate resolution micrographs of the *torpedo* nAChR demonstrate that the conformation of each monomer within the pentamer is equivalent in the agonist-bound conformation of the receptor (Unwin, 1995). However, in the absence of agonist the conformation of the extracellular N-terminus for the principal nAChR agonist-binding α subunits is not equivalent to the more structural β, γ and δ subunits. In fact the β, γ and δ subunits appear to undergo only minor movements from the conformation adopted in the agonist-bound pentameric state whilst the α subunits undergo a significant conformational change to adopt a new position. Though direct structural data is lacking for the GlyR, the evidence suggests that the roles of the α and β GlyR subunits are probably equivalent to those of the nAChRs, i.e. the α subunit is the primary contributor to agonist binding whilst the β subunit acts as structural support. This is in contrast to $GABA_A$ receptors where evidence supports the converse (Amin and Weiss, 1993). Structural rearrangements in GlyRs may therefore occur in a similar manner with the agonist binding α subunit undertaking the majority of the dynamic conformational shifts, at least as far as the extracellular N-terminus is concerned. Apparent differences in the resting conformations of the α and β subunits has been recently supported (Shan et al., 2003). In this study the reactivity of cys-modifying reagents at the M2-3 linker region, a region critical for receptor activation, revealed an asymmetric contribution of α and β GlyR subunits to αβ heteromeric activation. Furthermore, mapping the AChBP onto the nAChR α-subunit in its closed and agonist-bound, presumed open, conformation, revealed that the α subunit rotated around a diagonal axis resulting in the greatest movement across the '-' side of the subunit (Unwin et al., 2002). This suggests that the GlyR '–' H109/T133 face undertakes a greater conformational shift in location compared to residues on the '+' receptor face. Here the ability of Zn^{2+} to stabilise

the closed receptor state is determined by whether or not a conformational change in response to agonist binding occurs, which would be transmitted as a conformational shift primarily across to the '-' face of the monomer i.e. a transduction route to this side of the Zn^{2+} site. The '+' H107 face by contrast is expected to undergo a smaller structural perturbation in response to activation and therefore this residue may still remain in a position where it can coordinate Zn^{2+}, thus explaining how the β subunit can donate its equivalent N130H, but not its perturbed '-' H132/S147 face, to a Zn^{2+} binding site.

Comparisons with the $GABA_AR$ family of inhibitory Zn^{2+} binding sites

Our current understanding of the molecular components required for Zn^{2+} mediated inhibition in other cys-loop ligand-gated receptors is derived from the $GABA_A$ receptor family. A recent in depth study of $GABA_A$ receptors pinpointed the sensitivity for Zn^{2+} inhibition to two separate inhibitory sites, a high potency site between two neighbouring β subunits and a lower affinity site between an α and a β subunit, rather than the single location elucidated for GlyRs (Hosie et al., 2003). This also revealed that $GABA_A$ receptors confer on the pentameric receptor varying levels of sensitivity to inhibitory Zn^{2+} by replacing one of the two neighbouring β subunits, which form a high potency intersubunit Zn^{2+} binding site, with a reduced sensitivity δ, ε or γ subunit. This means that rather than simply varying the potency of the site whilst maintaining the same mechanism of action as appears to be the case for the GlyR, $GABA_A$ receptors featuring δ, ε or γ subunits instead form a new reliance on the secondary low potency site between the α and β subunits. However, despite these initial differences, the $GABA_A$ inhibitory Zn^{2+} sites do still retain notable similarities to that predicted for the GlyR. Both the high and low potency $GABA_A$ receptor Zn^{2+} sites are proposed to be present as intersubunit sites forming a bridge between two neighbouring subunits. Furthermore both sites contain histidine residues, the most commonly occurring coordinating partner for Zn^{2+} (Vallee and Auld, 1990). In the case of the high potency site, two histidines from adjacent β subunits are proposed to form part of an intersubunit site, similar to the case for the GlyR α subunits. Only the polar hydroxyl GlyR α1 T133 identified here differs from the remaining components of the two $GABA_A$ sites, all of which are acidic residues (Hosie et al., 2003).

In view of the apparent conservation of intersubunit Zn^{2+} sites across these receptors it is tempting to postulate that the GlyR may share a similar potential mechanism of Zn^{2+} inhibition to its closest relative, the $GABA_A$ receptor. Unfortunately, alignments of the Zn^{2+} sites in $GABA_A$ and GlyRs suggest that though they may share certain chemical and structural similarities, the sites are expected to reside in different areas of the proteins, with the high potency $GABA_A$ site predicted to occupy a space at the mouth of the ion channel. In addition to this several studies investigating the properties of Zn^{2+} inhibition at $GABA_A$ receptors suggest that the high potency inhibitory component exhibits a non-competitive mode of inhibition (Smart and Constanti, 1990;Legendre and Westbrook, 1991;Gingrich and Burkat, 1998), whilst the low potency γ-subunit dependent component displays properties consistent with an apparent mixed antagonism, and also does not show the same dependence as the GlyR for pre-equilibration to ensure a high degree of inhibition (Gingrich and Burkat, 1998).

Identification of residues required for Zn^{2+} mediated inhibition in other cys-loop receptors currently extend to a histidine residue reported to be important for the $GABA_C$ receptor subtypes σ1-3 (Wang et al., 1995). Evidence to support mechanisms of actions at other cys-loop receptors varies with Zn^{2+} inhibition of $GABA_A$ ρ subtypes 1 - 3 proposed to be via an apparent mixed antagonism (Chang et al., 1995). Though there has been no molecular basis of Zn^{2+} inhibition elucidated yet for nAChRs this process does bear similarities to that of the GlyR as the sensitivity is dependent on subunit composition (Hsiao et al., 2001). In addition, the inhibition requires pre-incubation and due to its voltage independence and an apparent effect on the agonist affinity it has also been suggested to act via an apparent competitive mode either directly or through an allosteric process (Palma et al., 1998).

Conclusion

Taken overall, this study identifies Zn^{2+} as a useful pharmacological tool to distinguish between GlyR α1 and α2 or α3 subunits and identifies a new critical component in Zn^{2+} mediated inhibition, GlyR α1 T133. It also provides a rationale

by which Zn^{2+} binding initiates the transduction of Zn^{2+} mediated inhibition resulting in an effect on glycine binding to the receptor. This appears to be propagated asymmetrically from the Zn^{2+} binding site being driven from the '-' face. This phenomenon of asymmetric propagation of transduction is quite likely to be a common feature characterising the binding of ligands to many different sites on ligand-gated ion channels.

GlyR subtype	Gly EC_{50} (μM)	I_{max} (nA)	*n*	Zn^{2+} IC_{50} (μM)	*n*
α1	24 ± 5	4.5 ± 0.5	10	15 ± 2	5
α2	66 ± 6	3.7 ± 0.5	13	360 ± 40	11
α1 β	18 ± 3	4.5 ± 0.9	6	13 ± 2	3
α2 β	51 ± 4	5.6 ± 0.5	3	180 ± 30	13
$\alpha1^{H107N}$	24 ± 2	5.9 ± 0.3	4	230 ± 30	5
$\alpha1^{H109F}$	56 ± 5	5.1 ± 0.2	3	> 1 mM	3
$\alpha1^{T133A}$	64 ± 10	4.8 ±0.7	2*	> 1 mM	5
$\alpha1^{T135A}$	17 ± 2	3.3 ± 0.6	3	26 ± 6	3
$\alpha1^{H107N}\beta^{N130H}$	28 ± 8	4.8 ± 0.8	3	24 ± 3	5
$\alpha1^{H109F}\beta^{S156T}$	39 ± 4	5.2 ± 1.2	3	> 1 mM	3
$\alpha1^{T133A}\beta^{S156T}$	90 ± 16	3.2 ± 0.9	3	> 1 mM	3
$\alpha1\beta^{S156A}$	40	5.7 ± 0.8	1	17 ± 7	3
$\alpha2^{N174H}$	58 ± 3	4.2 ± 0.7	3	29 ± 2	4
$\alpha2\beta^{G128S}$	52 ± 5	5.0 ± 1.6	3	170 ± 20	4
$\alpha2\beta^{S156T}$	52 ± 2	5.2 ± 1.2	2*	210 ± 20	5
α3	48 ± 3	5.3 ± 1.3	4	150 ± 10	4
$\alpha3^{N107H}$	53 ± 12	5.3 ± 0.8	5	26 ± 7	3
sc DIV5	≈ 40	3.1 ± 0.3	12	320 ± 50	8
sc DIV7	≈ 30	4.9 ± 0.7	12	110 ± 10	8
sc DIV10-14	≈ 30	4.3 ± 0.4	8	88 ± 21	8
sc astro DIV5	≈ 30	4.3 ± 0.4	8	170 ± 50	8
sc astro DIV7	≈ 30	4.3 ± 0.4	8	170 ± 50	8

Table 3.1 GlyR sensitivities to glycine and Zn^{2+}.
The values indicate the glycine EC_{50}s for activating recombinant and native GlyRs and also the Zn^{2+} IC_{50}s for inhibiting the 50 % maximal glycine-activated responses where Zn^{2+} is first pre-equilibrated with the receptor for 15 s before an equivalent dose of Zn^{2+} is co-applied with glycine. All numbers are means ± s.e. from *n* cells. For the native GlyR in spinal cord (sc) neurons, the EC_{50}s were estimated from linear segments of the dose-response curves. I_{max} represents the maximal glycine-activated current.(* Due to an *n* of 2, these errors represent standard deviations).

Chapter 4

Evidence for an allosteric transduction pathway across the extracellular domain of the glycine receptor

Introduction

Evidence so far accrued from three independent studies provides strong support and agreement that Zn^{2+} inhibition appears to be mediated via a discrete site featuring at the very least two histidine residues GlyR α1 H107 and H109, which are presented at an intersubunit site (Harvey et al., 1999;Nevin et al., 2003;Chapter 3). Furthermore, this site appears to be distinct from the agonist-binding site as substituting these residues with alternative moieties does not exert a substantial effect on agonist potencies or their maximal responses (Harvey et al., 1999;Nevin et al., 2003;Table 3.1). These residues also differ from those previously shown to have a substantial impact on the agonist potency in a manner consistent with an effect on agonist binding. Residues implicated in agonist binding include GlyR α1 D96 to G105 (loop A;Han et al., 2001;Vafa et al., 1999), Y159 to F161 (loop B;Kuhse et al., 1990b;Schmieden et al., 1993), and C198 to C209 (loop C;Vandenberg et al., 1992a;Vandenberg et al., 1992b; Rajendra et al., 1995b). The structural homology model (Fig 4.1*A,B*) predicts the agonist-binding site and the inhibitory Zn^{2+} site occupy distinct non-overlapping locations suggesting Zn^{2+} is unable to elicit its apparent competitive inhibitory effect (Chapter 3) by direct competition to block access of the agonist to its recognition site. In addition the predicted location of the inhibitory site in relation to the ion channel suggests that Zn^{2+} is not operating as an open channel blocker on GlyRs (Fig 4.1*A,B*). This is also supported by the observation that pre-incubation of the GlyR with inhibitory concentrations of Zn^{2+} enhances the steady-state inhibition, suggesting that Zn^{2+} can access its site even when the channel is closed (Fig 3.1*A* – *D*). This is in contrast to an open channel blocker such as cyanotriphenylborate (CTB), which requires channel activation before it can inhibit the GlyR (Handford et al., 1996). Substantial parallel agonist dose-response curve displacements in the presence of inhibitory Zn^{2+}, without a reduction in the maximal agonist response, are consistent with this site exerting at least some part of its inhibition in an apparent competitive mode to reduce the

affinity of the agonist-binding site. Given the physical separation of the two sites this would therefore require allosteric communication between the two sites. From the studies in chapter 3 (Fig 3.11) the effect of Zn^{2+} binding is transduced from the H109/T133 '-' face of the Zn^{2+} binding site. Therefore, to exert an effect at the agonist-binding site would presumably require transmission through, or around, the hydrophobic core of the extracellular domain, as these two sites are on opposing sides of the extracellular domain of the protein (Fig 4.1*A,B*).

This chapter aims to investigate the consequences of disrupting potential residues that may reside on a route for signal transduction across the protein from the H109/T133 Zn^{2+} inhibitory site '-' face to the agonist-binding site. This study is of particular interest as to date there are no studies that clearly elucidate transduction pathways through cys-loop ligand-gated receptors either in terms of agonist transduction to activate the receptor or in terms of the numerous modulator sites that are present in this receptor family (Laube, 2002; Lester et al., 2004). Most likely this is a result of the complications that arise from attempting to dissect between whether particular amino acids are important for binding, or transducing, or causing an indirect structural effect on either of these properties. However, this study has several factors in its favour, firstly, through appreciation of chemistry and numerous crystal structures of Zn^{2+} binding sites (Auld, 2001), some limitation can be placed on the number and the type of residues directly contributing to Zn^{2+} binding. Secondly, several studies have already provided consistent support for the identification of a significant portion of the inhibitory Zn^{2+} binding site in the form of two histidine residues, GlyR α1 H107 and H109 (Harvey et al., 1999;Nevin et al., 2003;Chapter 3). Furthermore, evidence in Chapter 3 suggests that transduction is most likely from one side only of this site, the H109/T133 '-' face, giving a starting point for investigating any transduction routes through the protein to the agonist-binding site. Finally the model of the GlyR based on the AChBP (Brejc et al., 2001) gives a structural guide to probing any route through the protein using mutagenesis. This can also be used to then mutate residues on either side of any transduction pathway to establish the specificity of an effect, thus increasing the level of confidence in whether it is a genuine effect on receptor function rather than an indirect structural perturbation.

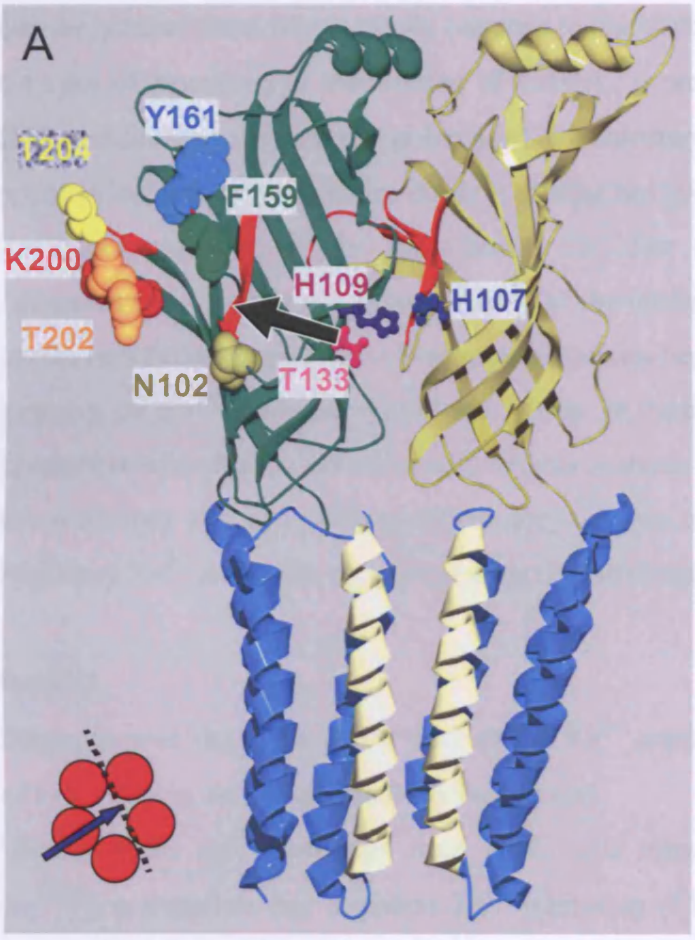

Figure 4.1 GlyR model, based on the AChBP, displaying the location of the inhibitory Zn^{2+} site viewed from the inside face of the receptor (*A*) and from above (*B*), highlighted by the small inset pictorials (red). Two neighbouring subunits from the pentameric GlyR are presented with the extracellular domains in green or yellow. Transmembrane domains are included (blue) with the pore lining M2 helix in pale yellow. The agonist binding motifs (red) and residues (bubble chains) are labelled as are the inhibitory Zn^{2+} binding site residues (thin chain). A black and white arrow marks a possible route by which the allosteric inhibitory Zn^{2+} site '-' face may transduce its effect downstream to the agonist binding site.

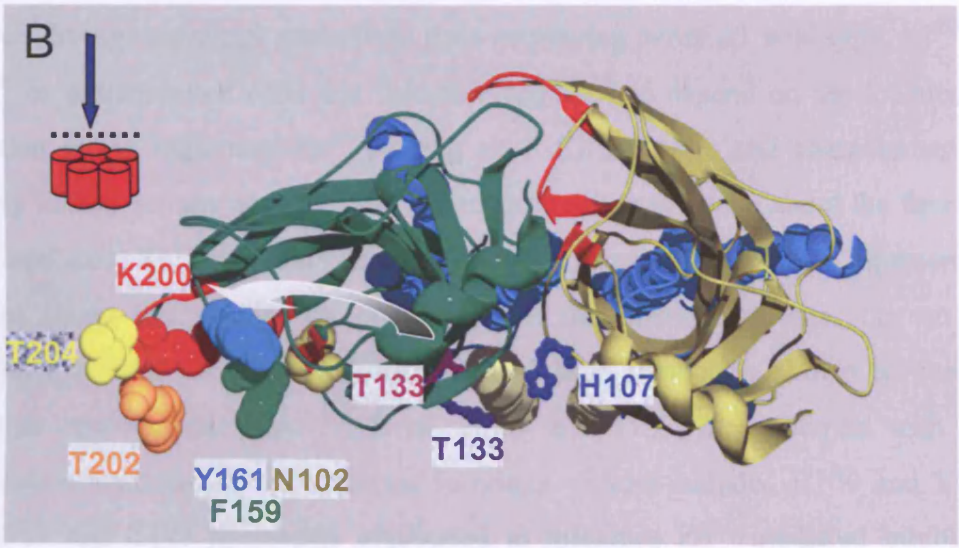

Other clues as to the genuine contribution of a residue to a transduction pathway can also be gleaned from what actually happens to the inhibitory process. For example in the case of neurosteroid modulation of $GABA_A$ ρ receptors, substitution of an M2 I307 residue can reverse the polarity of a neurosteroid effect, from inhibition to potentiation (Morris and Amin, 2004: A similar but reverse effect is also seen for the Zn^{2+} potentiation of GlyRs, see Chapter 5). The study presented here initially compared substitutions of residues at each of the inhibitory Zn^{2+} binding site faces to ascertain whether these affected receptor properties besides a simple reduction in the potency of Zn^{2+} mediated inhibition. This in turn elucidated a novel receptor phenotype whereby Zn^{2+} itself could directly activate the GlyR from the '-' face of the inhibitory site and subsequently a hydrophobic transduction pathway from the inhibitory Zn^{2+} site to the agonist-binding site was tentatively identified.

Results

Disruption of the GlyR α1 '-' face of the Zn^{2+} inhibition site generates a family of low potency Zn^{2+}-activated GlyRs (ZAGs)

During whole cell recordings from HEK cells transiently transfected with GlyR $\alpha1^{T133A}$, a mutation that impaired Zn^{2+} inhibition (Chapter 3) the appearance of a persistent but small (less than 10 % of the Gly I_{max}) inward current was observed upon pre-incubation with a high 1 mM dose of Zn^{2+}. This unexpected effect was not observed during recordings made from cells expressing either α1 wild-type, $\alpha1^{H107N}$, $\alpha1^{H109F}$, or untransfected cells and therefore appeared to depend on the location of disruption at the inhibitory Zn^{2+} binding site. To establish and characterise this property further for any possible new information this may reveal about the function of the inhibitory Zn^{2+} site, two sets of mutated α1 receptors were made representing residues lining the vicinity on either side of the intersubunit site, i.e. on the previously labelled '+' and '-' faces. The '-' face, previously shown to contain important contributions from GlyR α1 H109 and T133, was mutated with Ala substitutions individually at 5 selected locations. These included H109 and T133, also E110 and T112 previously implicated to influence Zn^{2+} mediated inhibition (Laube et al., 2000) and finally an N61 residue that resides on the next 'rung' down on β-strand 2, laying directly beneath T133 (Fig 4.2*A*). These $\alpha1^{N61A}$, $\alpha1^{H109A}$, $\alpha1^{E110A}$, $\alpha1^{T112A}$ and $\alpha1^{T133A}$ GlyRs were first characterised for their sensitivity to

Zn^{2+} mediated inhibition of glycine 50 % maximal responses. The sensitivities to inhibitory Zn^{2+} were measured by comparing the current after 4 seconds (I_4) of co-applied 50 % maximal doses of Gly plus 1000 μM Zn^{2+}, to the current of 50 % maximal Gly doses applied alone. A Zn^{2+} pre-incubation protocol was not used as GlyR $\alpha1^{N61A}$, $\alpha1^{T112A}$ and $\alpha1^{T133A}$ all exhibited significant inward currents during pre-application of Zn^{2+}, and this may partially desensitise the GlyR causing erroneous results. In the case of $\alpha1^{N61A}$, $\alpha1^{T112A}$ and $\alpha1^{T133A}$, inhibition by Zn^{2+} was completely absent even at the high 1000 μM dose tested leaving only the residual potentiating component of Zn^{2+} modulation on Gly responses apparent (Fig 4.2*C*). GlyR $\alpha1^{H109A}$ and GlyR $\alpha1^{E110A}$ by contrast were still significantly inhibited by 33 ± 6 %, (n = 4) and 97 ± 1 %, (n = 3) respectively in response to a high 1000 μM Zn^{2+} dose. Furthermore, these two receptors did not display a noticeable inward current during pre-incubation with 1000 μM Zn^{2+} and were therefore fully assessed for their sensitivity to Zn^{2+} mediated inhibition using the pre-incubation protocol. This surprisingly revealed that $\alpha1^{H109A}$ exhibits only a modest 2-fold increase in the Zn^{2+} IC_{50} to 32 ± 16 μM, (n = 5, $P < 0.05$) compared to the wild-type α1 (15 ± 2 μM, n = 5) and intriguingly reduces the maximal amount by which Zn^{2+} can inhibit Gly responses to 47 ± 7 %, (n = 5) compared to 91 ± 7 %, (n = 6) for the wild-type receptor (Fig 4.2*B*). GlyR $\alpha1^{E110A}$, by contrast, harboured a slightly more significant 4-fold reduced sensitivity to Zn^{2+} mediated inhibition (IC_{50} = 67 ± 4 μM, n = 3, $P < 0.05$) and did not affect the maximal amount of Zn^{2+} inhibition (Fig 4.2*B*).

The persistent inward current observed during pre-incubation of GlyR $\alpha1^{N61A}$, $\alpha1^{T112A}$ and $\alpha1^{T133A}$ with 1000 μM Zn^{2+} was possibly due to Zn^{2+} acting alone as a GlyR agonist. In agreement with the persistent inward current observed during pre-incubation, dose response curves for Zn^{2+} activation on the GlyR $\alpha1^{N61A}$, $\alpha1^{H109A}$ and $\alpha1^{T133A}$ mutants, representing the residues on the aligned rungs of the ladder at the '-' interface, revealed in each case, a significant but low, millimolar potency for Zn^{2+} activation. This resulted in EC_{50} values of > 10 mM, for GlyR $\alpha1^{N61A}$ and $\alpha1^{H109A}$ (n = 5 and 3 respectively) and 5.4 ± 2.5 mM, (n = 5) for $\alpha1^{T133A}$ (Fig 4.3*A,C*). Though it was not possible to obtain maximal currents for these dose response curves due to the requirement for higher doses of Zn^{2+}, the curves were

sufficient to estimate that the I_{max} for Zn^{2+} as a percentage of Gly I_{max} (i.e. relative efficacy) was greater than 30 % for GlyR $\alpha1^{N61A}$ and $\alpha1^{H109A}$ and greater than 40 % for $\alpha1^{T133A}$ (Fig 4.3*A,C*). This apparent action of Zn^{2+} as an agonist was termed 'Zn^{2+}-Activated Glycine receptor' (ZAG) activity in accordance with a cys-loop ligand-gated receptor previously identified as Zn^{2+}-activated channel (ZAC) activity, though this receptor lacked activation by a battery of agonists tested including Gly (Davies et al., 2003). In comparison, Ala substitution of the nearby E110 residue, which faces away from the site of Zn^{2+} coordination, yielded a GlyR $\alpha1^{E110A}$ with no discernable ZAG activity up to 30 mM Zn^{2+} (n = 3). However, GlyR $\alpha1^{T112A}$ produced a high sensitivity ZAG with EC_{50} = 3.5 ± 1.5 μM and a relative efficacy of 42 ± 5 % (n = 4; Fig 4.3*A,C*). As a control, a wild-type GlyR revealed no noticeable ZAG activity at Zn^{2+} concentrations up to 30 mM, (n = 3). The Zn^{2+} current traces for all four of the ZAG mutants identified revealed that the Zn^{2+} activated current was relatively slow, whether applied at maximal or submaximal doses, reaching a steady-state between 3 and 15 seconds compared to onset times of less than 2 s for a submaximal EC_{50} dose of Gly (Fig 4.3*C*). Current-voltage (IV) data accrued for each mutant using 50 % maximal responses to Zn^{2+} revealed a typical linear relationship with membrane voltage in keeping with that for Gly currents recorded from wild-type α1 GlyR (Fig 4.3*B*). Due to the small currents and extremely high concentrations of Zn^{2+} required for activation of $\alpha1^{H109A}$ an IV plot was not obtained. In addition the reversal potentials for Zn^{2+} activated currents from $\alpha1^{N61A}$, $\alpha1^{T112A}$ and $\alpha1^{T133A}$ GlyRs was close to zero (range –4 mV to 7 mV, n = 3), comparable to the predicted reversal potential for Cl^- of around 0 mV. The data was in accordance with the Zn^{2+} activated current eliciting its effect via the GlyR Cl^- channel. Furthermore, though the receptors were clearly perturbed in a manner consistent with a disruption to the transduction apparatus of the Zn^{2+} inhibitory site, the agonist activities of the receptor, via the glycine binding site, did not appear to be overtly influenced with Gly EC_{50}s remaining within 4-fold of wild-type values and maximal Gly currents not differing significantly (Table 4.1).

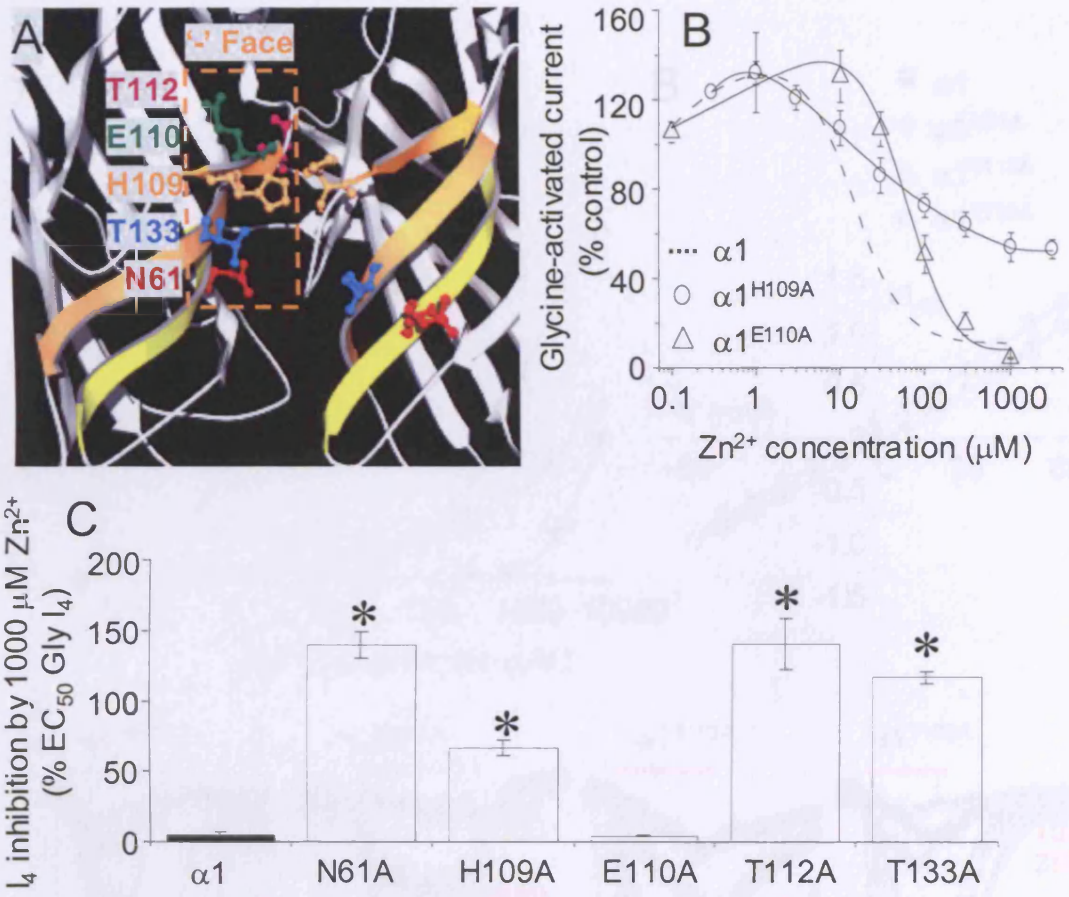

Figure 4.2 Alanine substitutions at the '-' Zn^{2+} binding site face disrupt GlyR α1 Zn^{2+} mediated inhibition. *A*, Structural homology model of GlyR α1 highlighting potential residues of interest in the '-' face of the inhibitory Zn^{2+} site, boxed orange. The orange β-strands represent the three 'ladder rungs' upon which residues were selected. *B*, Zn^{2+} dose response curves constructed using a pre-incubation protocol to measure modulation of 50 % maximal Gly-evoked responses. This was carried out for GlyR $\alpha1^{H109A}$ and $\alpha1^{E110A}$ both of which were significantly inhibited by 1000 μM Zn^{2+}. Both receptors revealed a reduced sensitivity to Zn^{2+} mediated inhibition compared to wild-type GlyR α1 (dashed line) but while $\alpha1^{E110A}$ suffered a 5-fold reduced sensitivity to Zn^{2+}, $\alpha1^{H109A}$ instead exhibited a reduced maximal level of inhibition. *C*, Current amplitude measurements at the 4-second time point (I_4) during co-application of 1000 μM Zn^{2+} with a Gly concentration corresponding to 50 % of the maximal Gly response (as a percentage of a Gly concentration causing a 50 % maximal response in the absence of Zn^{2+}). This demonstrates that Zn^{2+} mediated inhibition is completely abolished at this high concentration of Zn^{2+} for $\alpha1^{N61A}$, $\alpha1^{T112A}$ and $\alpha1^{T133A}$. Due to the discrete Zn^{2+} potentiation site these receptors retain potentiation at this concentration. Asterisks represent a significant difference from the wild-type receptor ($P < 0.05$). $N = 3$-6.

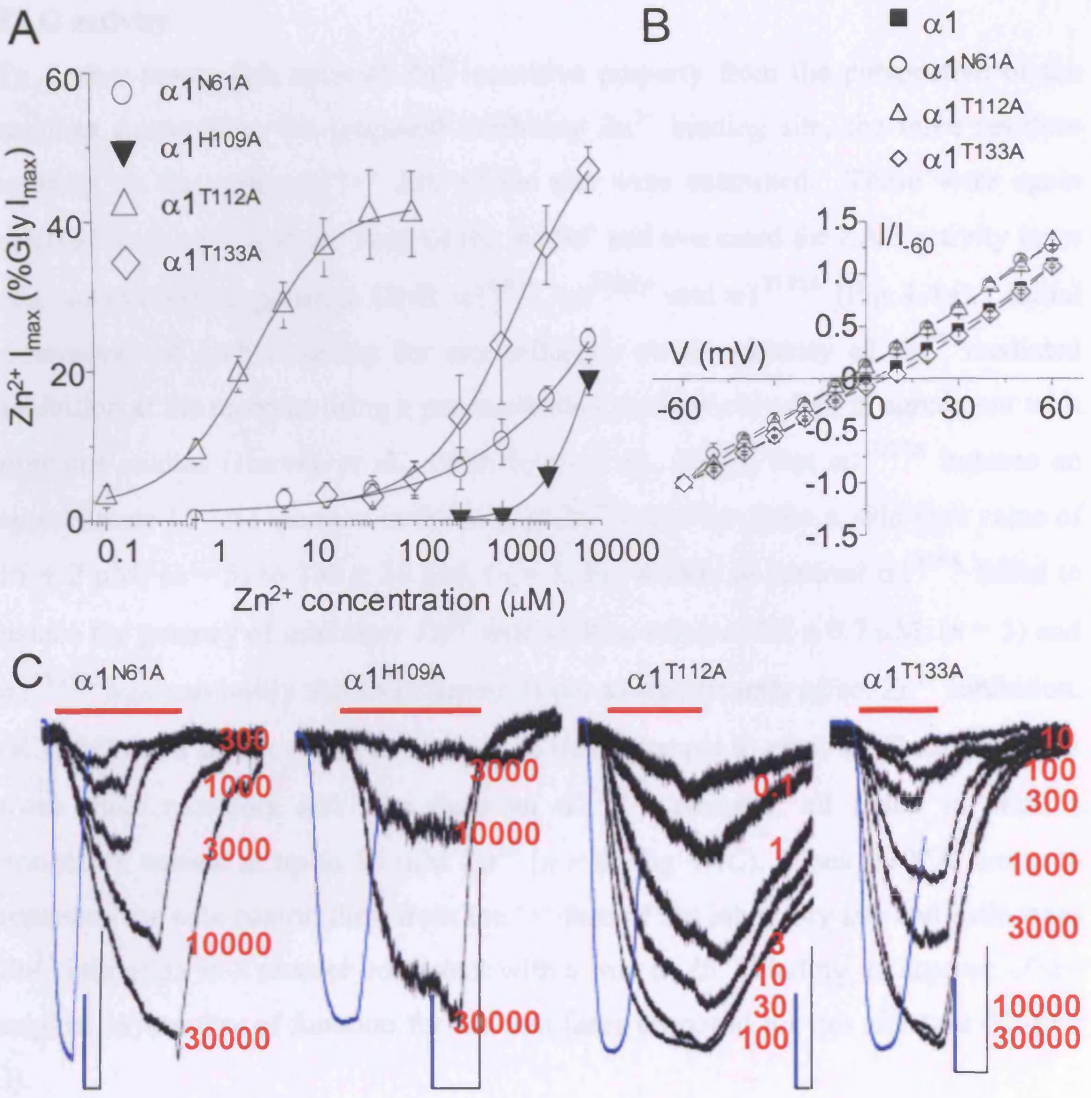

Figure 4.3 Disruption of the Zn^{2+} inhibitory site '-' face produces receptors that are sensitive to activation by Zn^{2+} acting as an agonist. *A*, Zn^{2+} dose response curves for GlyR $\alpha1^{N61A}$, $\alpha1^{H109A}$, $\alpha1^{T112A}$ and $\alpha1^{T133A}$ plotted as the percentage of a maximal response to glycine applied to the same cells. *B*, IV plots and the reversal potentials of EC_{50} Zn^{2+} activated currents for $\alpha1^{N61A}$, $\alpha1^{T112A}$, $\alpha1^{T133A}$ and EC_{50} Gly activated currents for a wild-type α1 GlyR. Due to the small currents and extremely high concentrations of Zn^{2+} required for activation of $\alpha1^{H109A}$ an IV plot was not obtained. *C*, Typical currents recorded upon Zn^{2+} activation (black traces) of GlyR $\alpha1^{N61A}$, $\alpha1^{H109A}$, $\alpha1^{T112A}$ and $\alpha1^{T133A}$. The time-scale matched doses are applied in μM (red bars). Comparative 50 % maximal glycine induced responses are displayed in blue revealing a faster activation profile than the Zn^{2+} activated currents. The doses applied are in mM (red). Scale bars represent 1 s and 1 nA respectively. $N = 3 - 6$.

Disruption of the GlyR α1 '+' face of the Zn^{2+} inhibition site does not induce ZAG activity

To further assess this unusual Zn^{2+} sensitive property from the perspective of the residues surrounding the proposed inhibitory Zn^{2+} binding site, the three residues residing on the opposing '+' face of the site were examined. These were again selected from each β-sheet 'rung of the ladder' and evaluated for ZAG activity upon Ala substitution to generate GlyR $\alpha1^{R59A}$, $\alpha1^{H107A}$ and $\alpha1^{T135A}$ (Fig 4.4*A*). Initial assessment of each mutation for any influence on the potency of Zn^{2+} mediated inhibition at the receptor using a pre-incubation protocol revealed, in agreement with previous studies (Harvey et al., 1999;Nevin et al., 2003), that $\alpha1^{H107A}$ induces an approximate 15-fold increase in the IC_{50} of Zn^{2+} inhibition from a wild-type value of 15 ± 2 μM, (n = 5) to 330 ± 30 μM, (n = 3; Fig 4.4*B*). In contrast $\alpha1^{R59A}$ failed to reduce the potency of inhibitory Zn^{2+} with an IC_{50} value of 5.2 ± 0.7 μM, (n = 3) and $\alpha1^{T135A}$ was previously shown (Chapter 3) not to significantly affect Zn^{2+} inhibition, (IC_{50} = 26 ± 6 μM, n = 3). In addition to this, attempts to elicit ZAG activity from these three receptors and also from an $\alpha1^{H107N}$ receptor, all failed to elicit a noticeable current at up to 30 mM Zn^{2+} (n = 3; Fig 4.4*C*). Thus H107A seems to represent the sole contribution from the '+' face of the inhibitory site and influences Zn^{2+} inhibition in a manner consistent with a role in Zn^{2+} binding, in support of the original asymmetry of function for the two faces proposed for this site (see Chapter 3).

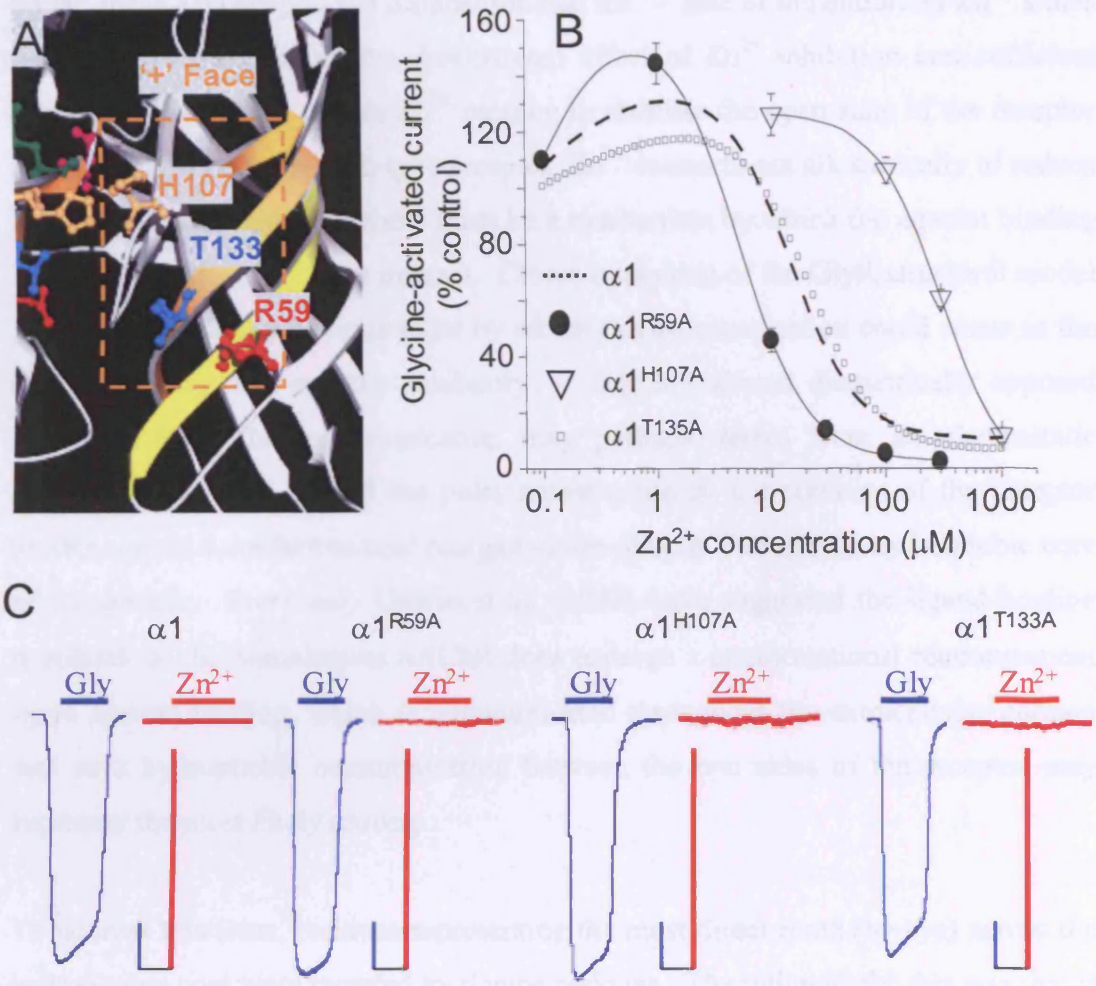

Figure 4.4 Alanine substitutions at the '+' Zn^{2+} binding site face disrupt GlyR α1 Zn^{2+} mediated inhibition only at α1 H107. *A*, Structural homology model of GlyR α1 highlighting potential residues of interest in the '+' face of the inhibitory Zn^{2+} site, boxed orange. The orange β-strands represent the three 'ladder rungs' upon which residues were selected. *B*, Zn^{2+} dose response curves using a pre-incubation protocol to measure the modulation of 50 % maximal Gly-evoked responses. Of the three residues, R59, H107 and T135, tested, only GlyR $\alpha1^{H107A}$ exhibited a reduced sensitivity to Zn^{2+} mediated inhibition with no shift in the maximal level of inhibition. GlyR $\alpha1^{R59A}$ revealed a modest 2-fold increase in the potency of Zn^{2+} mediated inhibition. *C*, Typical currents recorded upon maximal activation (blue - 500μM) demonstrating that there is no Zn^{2+} activated response for '+' face Ala substitutions when 30 mM Zn^{2+} was applied (red traces). $N = 3$. Note that GlyR α1 wild-type (dashed line) and $\alpha1^{T133A}$ (small squares) traces were taken from Fig 3.2*D* and 3.10*D*. Scale bars represent time of 0.5 s and current amplitude of 1 nA.

A putative hydrophobic transduction pathway between the Zn^{2+} inhibition and agonist-binding sites

So far, these data support the supposition that the '-' face of the inhibitory Zn^{2+} site is responsible for mediating the downstream effect of Zn^{2+} inhibition and sufficient disruption of this face causes Zn^{2+} binding to stabilise the open state of the receptor creating a ZAG. In the wild-type receptor, Zn^{2+} seems to act allosterically to reduce agonist potency suggesting there must be a mechanism by which the agonist binding and the inhibitory Zn^{2+} sites interact. Closer inspection of the GlyR structural model does not suggest any obvious route by which this communication could occur as the agonist binding site and the inhibitory '-' face are almost diametrically apposed (Fig 4.1*A,B*). This communication may perhaps derive from an electrostatic displacement passed around the polar amino acids on the outskirts of the receptor protein, or via a conformational reorganisation directly through the hydrophobic core of the protein. Previously Unwin et al, (1995) have suggested the ligand-binding α subunit of the homologous nAChR does undergo a conformational rearrangement upon agonist binding, which is communicated throughout the extracellular domain and so a hydrophobic communication between the two sides of the receptor may represent the most likely routing.

To address this issue, residues representing the most direct route (by eye) across the hydrophobic core were mutated to alanine residues. The rationale for this was that if large hydrophobic groups are required to push against each other and induce conformational change along a pathway through the centre of the protein, then at the point of Ala insertion, which is much smaller, there will be no side moiety to induce steric pressure and the communication may break down. This presumably would lead to a reduction in the efficacy of the transduction pathway, which would be manifest by a reduction in Zn^{2+} inhibition, assuming there were no indirect perturbations to the inhibitory site to affect its affinity. Initially eight hydrophobic residues were selected reflecting their prime locations to drive signal transduction from the agonist binding site to the Zn^{2+} inhibitory '-' face; L98, F99, F100, F108, I132, L134, L156 and F207 (Fig 4.5*A,B*). Amino acids L98, F99 and F100 on strand β4, L156 on β7 and F207 on β10, are spread across β-strands on the agonist-binding side of the transduction pathway (nomenclature of Brejc et al., 2001). F108 on β5

and the β6' L134 and I136 are present on β-strands alongside the Zn^{2+} inhibitory site '-' face (Fig 4.5*A,B*). These residues can be tentatively ascribed to three domains with I132 present directly on the back of the inhibitory site '-' face. F100, F108 and L134 are present in the hypothetical linker region in the pathway between the two protein domains, as are L98 and L156, though these residues are slightly to the side (Fig 4.5*A,B*). All these residues from each side of the meeting point between the two domains have their hydrophobic faces opposing each other. Finally, F99 and F207 face directly into the agonist binding site and may reflect the initiation point of any allosteric communication that is to be transmitted across the protein to or from the inhibitory site '-' face.

Disruption of the hydrophobic pathway generates spontaneously open GlyRs that are dependent on background Zn^{2+} and protons

The initial proviso was to investigate these residues with the intention of determining potential changes in the maximal inhibition by Zn^{2+}, used as an indicator of the efficacy of the inhibitory process. However initial attempts to record from some of these mutant receptors expressed in HEK cells revealed the presence of significant background leak currents in the absence of any agonist, which in the most extreme cases, declined rapidly over a 5 – 10 minute recording period making it very difficult to measure dose response curves for modulators. These persistent background inward currents could be blocked by the application of the GlyR open channel blocker cyanotriphenylborate (CTB; 20 μM) and were therefore initially proposed to be spontaneous openings of the mutant receptors. The extent of spontaneous opening was 0.5 ± 0.1 nA (7.4 %) for $\alpha1^{L98A}$, 1.4 nA ± 0.2 nA (51 %) for $\alpha1^{F99A}$, 0.3 ± 0.1 nA (7.2 %) for $\alpha1^{F108A}$ and 0.7 ± 0.1 nA (12.4 %) for $\alpha1^{L134A}$ where values represent the CTB blockable current (I_{CTB}) as a percentage of I_{CTB} plus the maximal Gly response (I_{Gly}), (n = 4 – 10; Fig 4.6*A*). Thus, percentages reflect the size of the leak current as a percentage of the maximal activatable GlyR current. All other mutated receptors exhibited a leak current of less than 2 % in the presence of CTB (data not shown; n = 4 - 5). Also a wild-type GlyR α1 exhibited only a 0.4 ± 0.1 % (n = 4) reduction in leak current following CTB application, suggesting a negligible level of spontaneous opening, in accord with single glycine channel studies (Beato et al., 2002;Beato et al., 2004). Although these mutant receptors appeared to have

spontaneously open phenotypes, in view of the ZAG channels observed earlier, these receptors were also tested for activation by contaminating background Zn^{2+} in the Krebs, which may be responsible for the observed receptor opening. Incubation of transfected HEK cells with 2.5 mM of the low affinity Zn^{2+} chelator tricine caused a significant reduction in the basal leak current of all four mutants $\alpha1^{L98A}$, $\alpha1^{F99A}$, $\alpha1^{F108A}$ and $\alpha1^{L134A}$ (Fig 4.6*A*) accounting for between 60 and 80 % of the total leak as measured by using CTB. Studies on $\alpha1^{L98A}$ and $\alpha1^{F99A}$, where the leak current was now small enough (< 0.5 nA) in the presence of tricine such that it did not rundown, showed that the remaining leak could be further attenuated by applying a more potent Zn^{2+} chelator, TPEN, presumably by chelating any remaining free Zn^{2+} (Fig 4.6*A*). This TPEN solution was applied on the tricine background but did not actually contain tricine. Using previously published K_D values of 10^{-5} for tricine and $10^{-15.6}$ for TPEN (Paoletti et al., 1997) and assuming the initial contaminating Zn^{2+} concentration in the saline solution was 0.2 μM (Wilkins and Smart, 2002) produced final predicted free contaminating Zn^{2+} concentrations of 5.42 nM in 2.5 mM tricine, reduced to 0.1 atomolar in 100 μM TPEN. Given the extremely low concentration of free Zn^{2+} in TPEN it is unlikely that the remaining leak current can be attributed to Zn^{2+}. This residual leak in TPEN was therefore most likely due to activation of these receptors by protons. This assumed that the Zn^{2+} activation was being mediated by the original Zn^{2+} inhibitory site, H109, which is also an important residue for the proton mediated inhibition of GlyRs (Chen et al., 2004) and so protons may now also be activating this new set of receptors. This was supported by the fact that applying TPEN at pH 8.4, an increase of 1 pH unit and a 10-fold decrease in the basal concentration of protons, from 39.8 nM to 3.98 nM, further reduced the residual leak current compared to that with TPEN at pH 7.4. TPEN at pH 8.4 induced an outward current (reduction in leak current) of 2.0 ± 0.8 % of the total GlyR current (measured as the Gly I_{max} + the leak current inhibited by CTB, I_{CTB}) for $\alpha1^{L98A}$ and 3.7 ± 0.6 % for $\alpha1^{F99A}$ (n = 4 - 5; Fig 4.6*B*). Furthermore, application of TPEN at pH 6.4 on a background of TPEN at the normal pH 7.4 evoked a proton-induced current of 5.3 ± 0.7 %, (n = 5) and 7.0 ± 0.6 %, (n = 4) for $\alpha1^{L98A}$ and $\alpha1^{F99A}$ respectively (Fig 4.6*B*). This increased to 10.3 ± 1.7 %, (n = 4), for $\alpha1^{F99A}$ at pH 6.0 whereas Gly α1 wild-type receptors evoked an inward current of just 0.2 ± 0.1 %, (n = 4). These measurements were from proton induced currents at steady-state 4 s time points as

HEK cells are known to possess an endogenous rapidly inactivating proton induced current,* which dropped to 0.2 ± 0.1 %, (n = 4) for wild-type GlyR transfected HEK cells in this time (Fig 4.6*B*). As 100 μM TPEN was predicted to reduce the Zn^{2+} concentration to at least 10 atomolar across the pH range 6 – 8.4 it is unlikely that the induced currents responses at variable pH values were due to changes in the efficiency with which TPEN chelates Zn^{2+}.(* Gunthorpe et al., 2001)

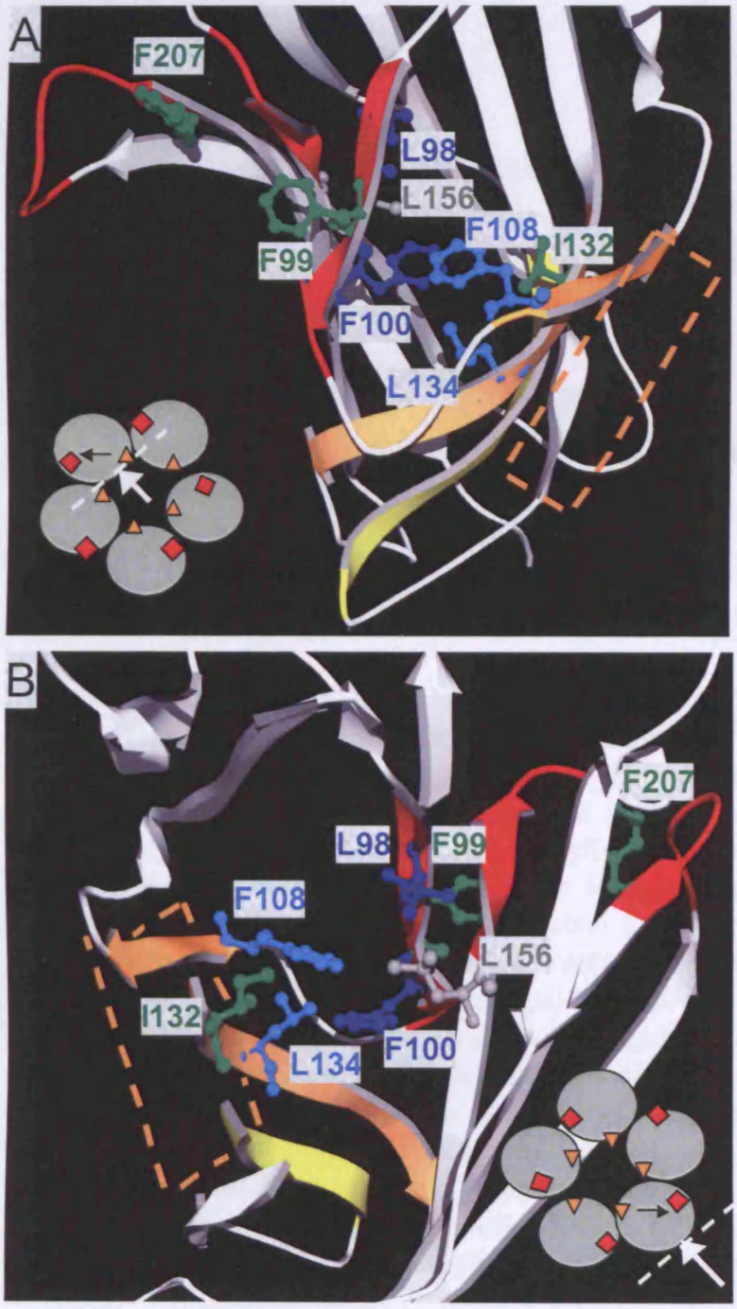

Figure 4.5 Mapping a hydrophobic pathway through the GlyR N-terminus. Close-up GlyR structural models showing a potential hydrophobic transduction pathway from the '-' face of the inhibitory Zn^{2+} site to the agonist binding site. *A*, View from the inside face and *B*, view from the outside face (see grey pictorials; Zn^{2+} site – orange triangle, agonist site – red square, white arrow shows the direction from which the subunit is being viewed, black arrow shows the predicted communication pathway). The '-' inhibition site is represented by orange β-strands and an orange box where the candidate binding residues are presented (not shown here for clarity but see Fig 4.2*A*). The agonist binding motifs are presented in red. Seven hydrophobic residues are shown as a route between the two domains with residues regarded to be at the end of the path in green and residues that are in the centre of the path shown in blue and grey. Note that some extraneous structure on the outside face is cut away from *B*, for ease of viewing.

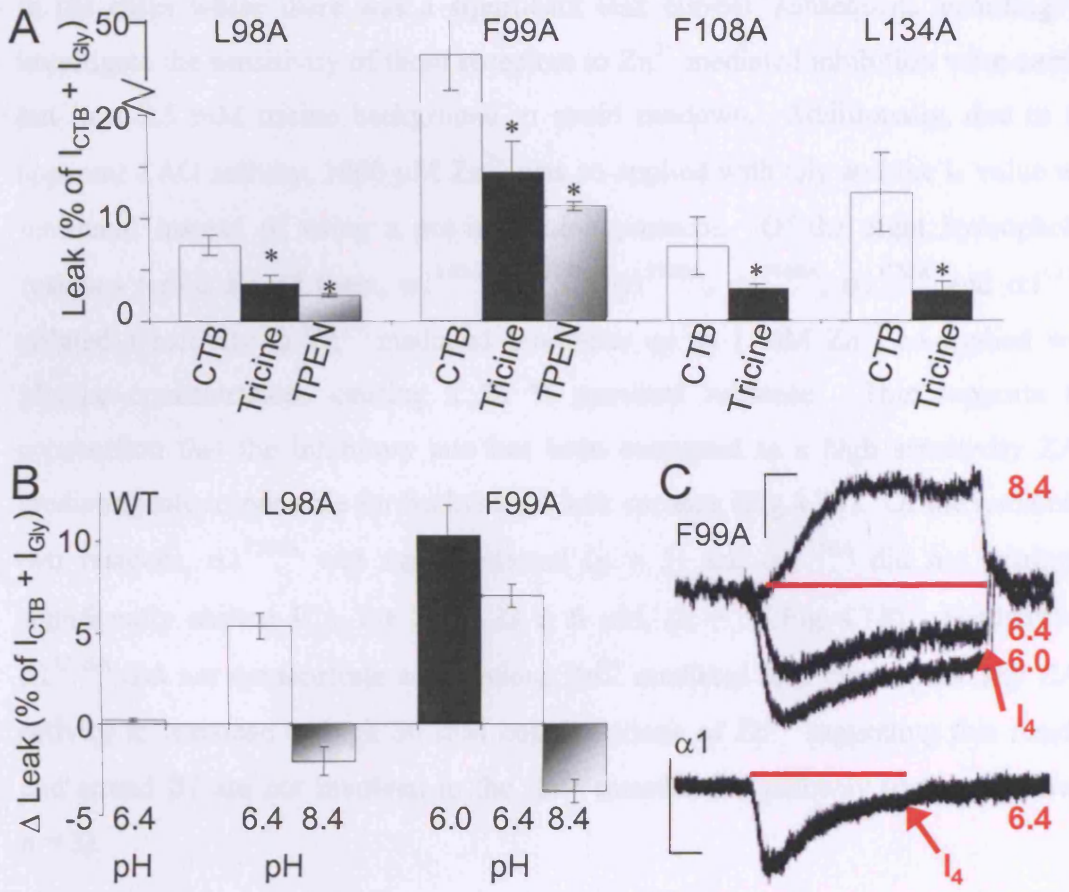

Figure 4.6 Zn^{2+} and H^+ basal leak currents in mutated GlyRs. Experiments to remove leak currents from hydrophobic mutated $\alpha1^{L98A}$, $\alpha1^{F99A}$, $\alpha1^{F108A}$ and $\alpha1^{L134A}$ receptors were carried out using Zn^{2+} chelators and external pH modulation. *A*, Leak currents were measured in terms of the background current ablated by cyanotriphenylborate (CTB) a GlyR open channel blocker (white bars). This was measured as a percentage of the total current, which is equal to the amount of CTB leak (I_{CTB}) plus the maximal glycine response (I_{Gly}). 2.5 mM tricine (black bars), a Zn^{2+} chelator, significantly (*; $P < 0.05$) reduced the leak by 50 – 80 % ($I_{tricine}/I_{CTB}+I_{leak}$ as a percentage) and 100 μM of a higher affinity Zn^{2+} chelator TPEN (shaded bars) caused a further reduction. *B*, Lowering external pH (pH 6.0 (black) and 6.4 (white)) in the presence of TPEN elicited stable currents in $\alpha1^{L98A}$ and $\alpha1^{F99A}$ GlyRs but not in wild-type α1. Removal of protons (pH 8.4 – shaded) decreased the leak on a TPEN background. *C*, Typical currents induced by increasing and reducing pH, measurements were made after 4 s (I_4) to inactivate the endogenous H^+ receptors of HEK cells (see α1 trace). Scale bars represent time of 1 s and current amplitude of 100 pA. $N = 3 – 8$.

Disruption of the hydrophobic pathway ablates Zn^{2+} mediated inhibition

In the cases where there was a significant leak current, subsequent recordings to investigate the sensitivity of these receptors to Zn^{2+} mediated inhibition were carried out in a 2.5 mM tricine background to avoid rundown. Additionally, due to the apparent ZAG activity, 1000 μM Zn^{2+} was co-applied with Gly and the I_4 value was measured instead of using a pre-incubation protocol. Of the eight hydrophobic residues tested six of them, $\alpha1^{L98A}$, $\alpha1^{F99A}$, $\alpha1^{F100A}$, $\alpha1^{F108A}$, $\alpha1^{I132A}$ and $\alpha1^{L134A}$ ablated sensitivity to Zn^{2+} mediated inhibition up to 1 mM Zn^{2+} co-applied with glycine concentrations causing a 50 % maximal response. This supports the supposition that the inhibitory site has been converted to a high sensitivity ZAG mediating site responsible for background leak currents (Fig 4.7*A*). Of the remaining two residues, $\alpha1^{F207A}$ was non-functional (n = 5) and $\alpha1^{L156A}$ did not exhibit a significantly shifted IC_{50} for Zn^{2+}, 23 ± 6 μM, (n = 3; Fig 4.7*B*). Furthermore $\alpha1^{L156A}$ did not demonstrate any obvious Zn^{2+} mediated leak current, nor any ZAG activity in response to high 30 mM concentrations of Zn^{2+} suggesting this residue and strand β7 are not involved in the Zn^{2+} transduction pathway (data not shown, n = 3).

Disruption of the hydrophobic pathway generates a family of high sensitivity ZAG receptors

To assess and correlate the sensitivities of these residues to Zn^{2+} the side chain moieties were split into two groups. One group comprised residues closest to each of the binding sites, F99 for the agonist binding site and I132 for the inhibitory Zn^{2+} binding site. The second group included residues that are present at the critical bridging region between the two sites, L98 and F100 from the agonist-binding side, and F108, L134 from the inhibitory Zn^{2+} binding '-' face (Fig 4.5*A,B*). Due to the high sensitivities of these receptors to Zn^{2+} these GlyRs were characterised for the potency of Zn^{2+} acting as an agonist alone on a 2.5 mM tricine background to reduce the amount of free Zn^{2+} and control exactly the level of free Zn^{2+}. Though TPEN could remove background Zn^{2+} more effectively, its high affinity for Zn^{2+} meant that it was unsuitable for regulating the Zn^{2+} concentration across the range required for a dose response curve. Furthermore, although there will be some small contamination from background proton activation, it was deemed more appropriate to carry out

these experiments out at physiological pH, and with the exception of $\alpha1^{F99A}$, the contribution from background protons was small, < 3 %. Dose response curves for glycine revealed that these receptors retained a sensitivity within 4-fold of the wild-type glycine EC_{50} and did not exhibit significantly different Gly I_{max} values with the exception of $\alpha1^{F99A}$, which exhibited an 8-fold increase in EC_{50} from 35 ± 3 μM, (n = 6) to 250 ± 40, (n = 4) and a two-fold reduction in I_{max} from 6.8 ± 0.5 nA, (n = 6) to 3.8 ± 0.4 nA, (n = 10; Table 4.1). This is not unexpected as the F99 moiety faces directly onto the predicted agonist-binding site (Fig 4.5*A,B*) and in addition this mutant had the largest leak currents suggesting that a portion of the $\alpha1^{F99A}$ population may already be in a desensitised state which could account for a reduction in the maximal currents attainable. By comparison to the original '-' face binding site mutations, the mutated $\alpha1^{F99A}$ GlyR exhibited a far higher sensitivity to Zn^{2+} activation with an EC_{50} of 0.13 ± 0.03 μM, (n = 5) and a higher relative efficacy of 91 ± 6 %, (n = 5) (Fig 4.8*A,C*). GlyR $\alpha1^{I132A}$ exhibited a lower potency for Zn^{2+} perhaps because it is backed onto the inhibitory '-' face and could indirectly distort the site, however, the relative efficacy was still high at 72 ± 5 %, (n = 5; Fig 4.8*A,C*). In a similar manner to the '-' face inhibitory ZAG receptors, the 50 % maximal Zn^{2+} activated currents of $\alpha1^{F99A}$ and $\alpha1^{I132A}$ also had slower onsets than that elicited by an EC_{50} dose of Gly (Fig 4.8*C*). Current-voltage (IV) relationships again revealed a comparable linear voltage dependence to that previously shown for Gly on wild-type α1 receptors and the reversal potential was close to zero consistent with the ZAG current being mediated by chloride flux through the GlyR (Fig 4.8*B*). Analysis of the residues representing the bridging region between the two sites revealed that these mutated receptors also all exhibited high sensitivities to Zn^{2+} as an agonist with EC_{50}s of 0.26 ± 0.078 μM, (n = 4) for $\alpha1^{L98A}$, 9.19 ± 0.63 μM, (n = 4) for $\alpha1^{F100A}$, 2.3 ± 0.6 uM, (n = 6) for $\alpha1^{F108}$ and 0.1 ± 0.03 μM, (n = 4) for $\alpha1^{L134A}$ (Fig 4.9*A*). In contrast though, the relative efficacy values compared to Gly for these receptors were generally lower at 49 ± 5 %, (n = 4) for GlyR $\alpha1^{L98A}$, 7.4 ± 3.8 %, (n = 4) for $\alpha1^{F100A}$, 25 ± 6 %, (n = 6) for $\alpha1^{F108A}$ and 18 ± 3 %, (n = 4) for $\alpha1^{L134A}$ (Fig 4.9*A*). Again the rates of Zn^{2+} activation for the steady-state macroscopic currents were slower compared to Gly activation, and the Zn^{2+} IV plots were comparable to those for Gly obtained for wild-type GlyR α1 (Fig 4.9*B,C*).

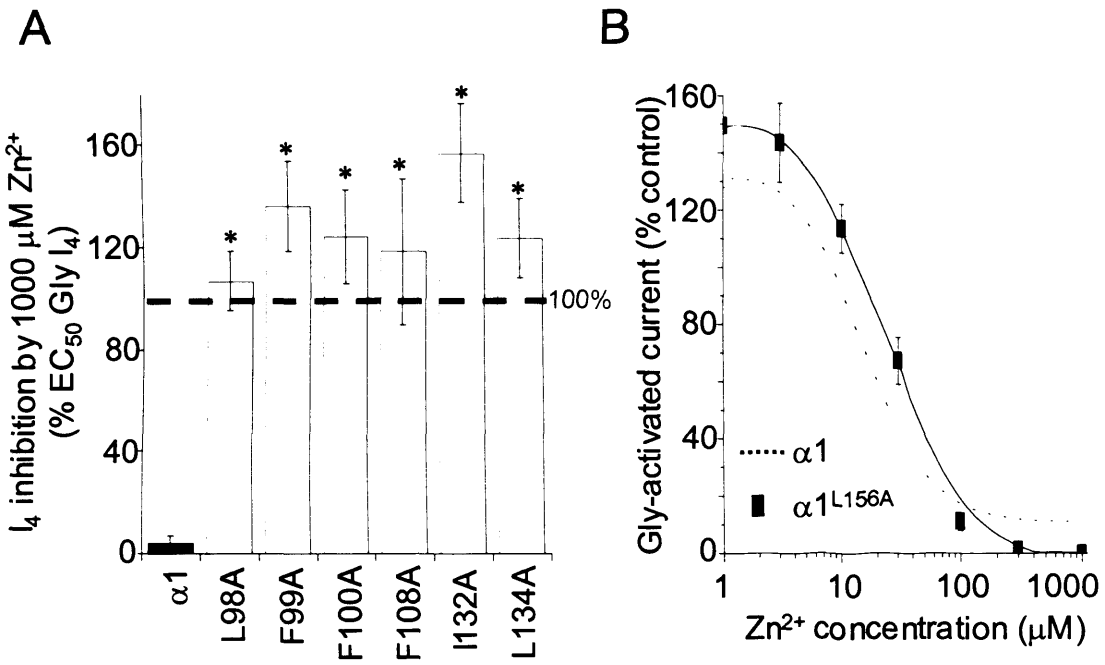

Figure 4.7 Ablation of Zn^{2+} inhibition by substitution of hydrophobic residues in the GlyR. Alanine substitutions of hydrophobic residues lining the transduction pathway between the Zn^{2+} inhibitory site '-' face and the agonist binding domain ablate GlyR α1 Zn^{2+} mediated inhibition. *A*, Measurements at the 4-second time point (I_4) during co-application of 1000 μM Zn^{2+} with a Gly concentration corresponding to 50 % of the maximal Gly response (as a percentage of a Gly concentration causing a 50 % maximal response in the absence of Zn^{2+}). Inhibition is completely abolished at this high concentration of Zn^{2+} for six hydrophobic mutated residues tested: $\alpha1^{L98A}$, $\alpha1^{F99A}$, $\alpha1^{F100A}$, $\alpha1^{F108A}$, $\alpha1^{I132A}$ and $\alpha1^{L134A}$. Due to the absence of Zn^{2+} mediated inhibition these receptors invoke currents in the presence of 1000 μM Zn^{2+} greater than 100 % possibly due to the remaining presence of Zn^{2+} potentiation. * Asterisks represent a significant difference from the wild-type receptor ($P < 0.05$). *B*, Zn^{2+} dose response curve using a pre-incubation protocol to measure modulation of 50 % maximal Gly evoked responses for the single GlyR $\alpha1^{L156A}$, which did not exhibit ablated Zn^{2+} mediated inhibition. $N = 4 - 6$. The GlyR α1 wild-type (dashed line) trace was taken from Fig 3.2*D*. Bar chart values represent mean ± s.e.

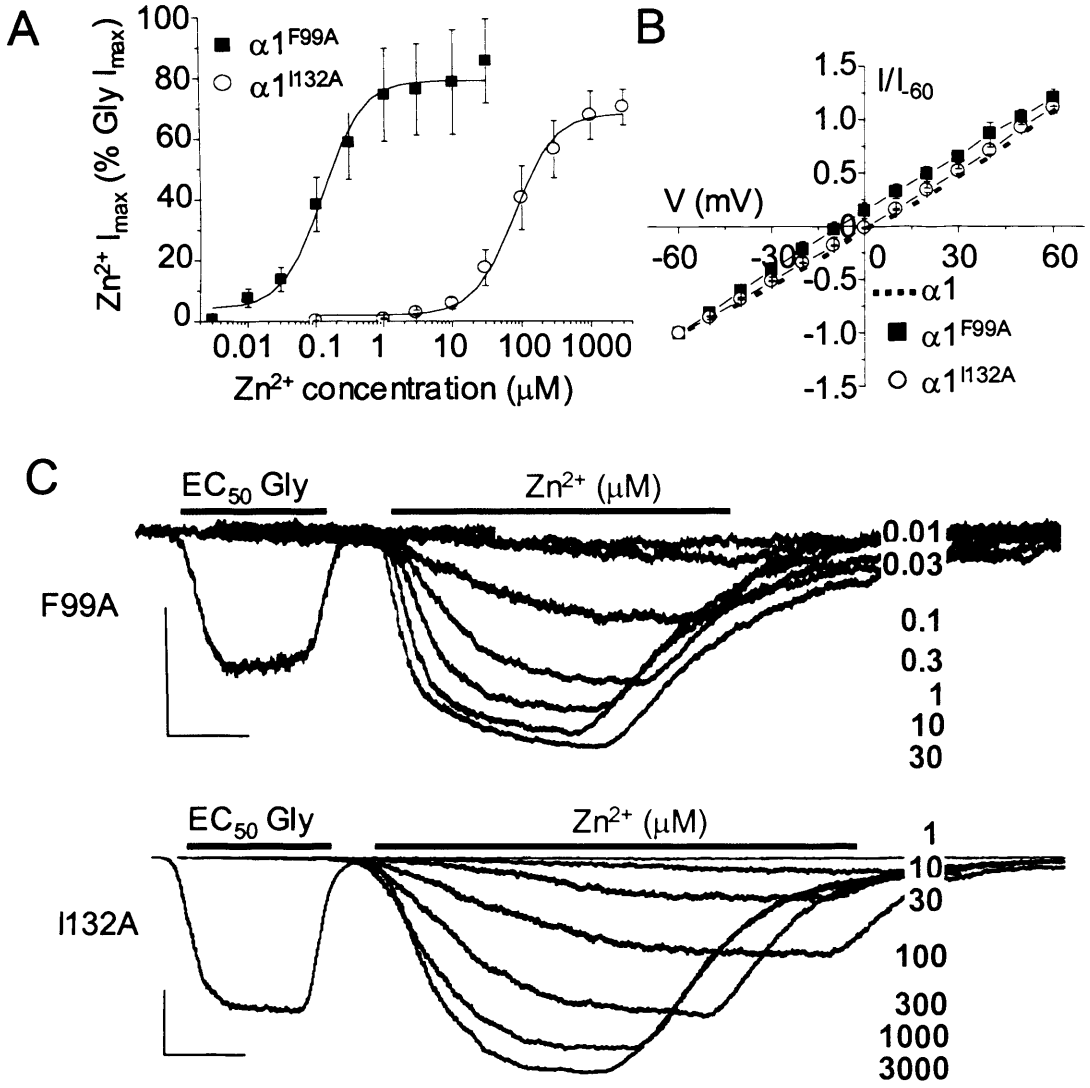

Figure 4.8 High relative efficacy ZAGs. Alanine substitutions for hydrophobic residues marking each end of the transduction pathway between the Zn^{2+} inhibitory site '-' face and the agonist binding domain produces receptors with high relative efficacies that are sensitive to direct activation by Zn^{2+}. *A*, Zn^{2+} dose response curves for GlyR $\alpha1^{F99A}$ and $\alpha1^{I132A}$ plotted as the percentage of the maximal response to glycine applied to the same cells. *B*, Current-voltage (IV) relationships and the reversal potential of EC_{50} Zn^{2+} activated currents for $\alpha1^{F99A}$ and $\alpha1^{I132A}$. These IVs are comparable with the Gly IV plot from a wild-type GlyR α1 (dashed blue line). *C*, Typical currents recorded upon Zn^{2+} activation (black) of GlyR $\alpha1^{F99A}$ and $\alpha1^{I132A}$. The time-scale matched doses applied are in μM (red bars – this represents the longest application required as the low doses took longer to reach steady-state). 50 % maximal Gly evoked responses are also included (blue) as a comparison and reveal a faster onset rate than the response matched Zn^{2+} currents. Scale bars represent 1 s and 1 nA. $N = 4 - 5$.

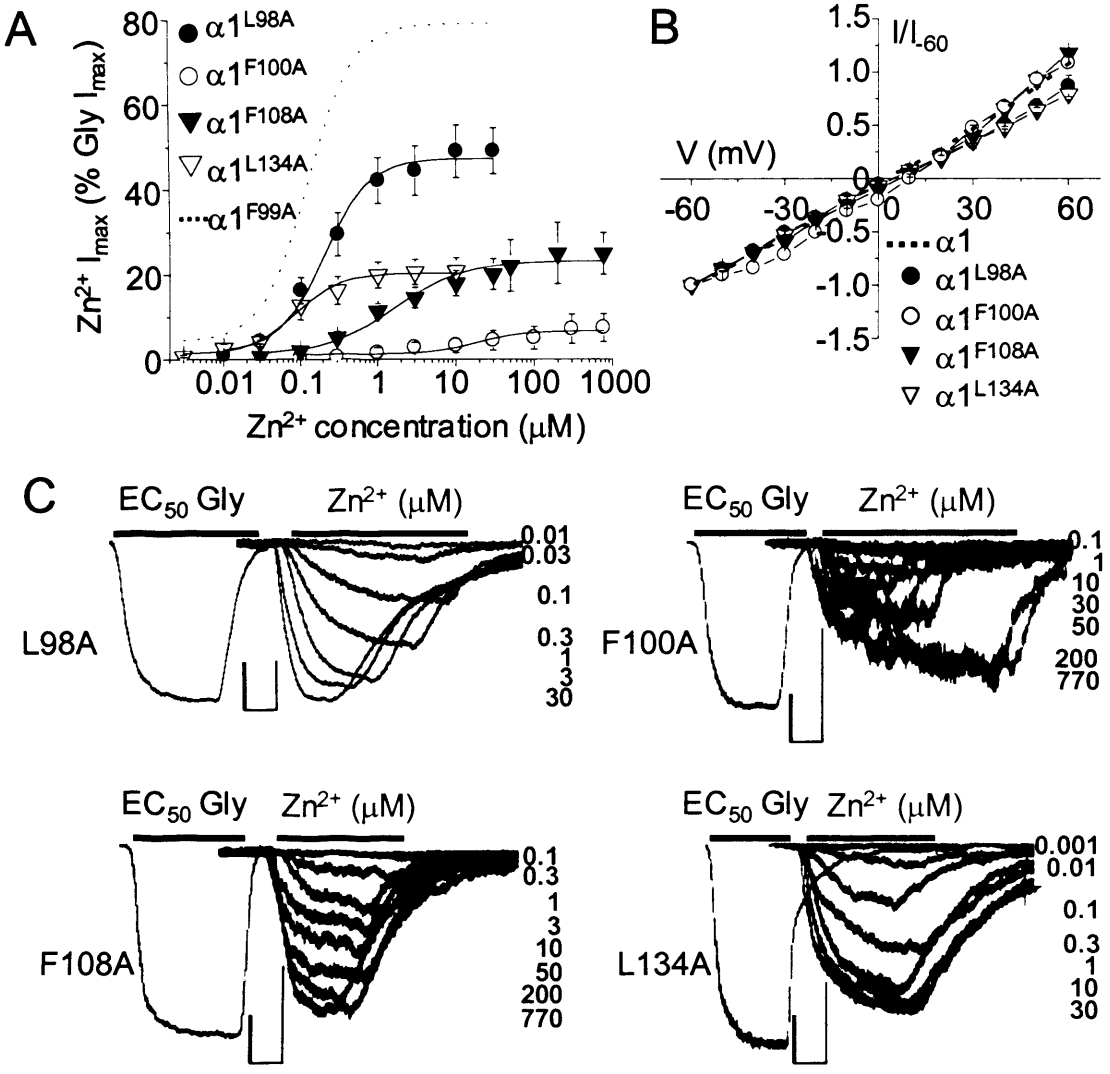

Figure 4.9 High sensitivity, low relative efficacy ZAGs. Alanine substitutions for hydrophobic residues in the bridging region between the Zn^{2+} inhibitory site '-' face and the agonist binding domain produce receptors sensitive to activation by Zn^{2+} with low relative efficacies. *A*, Zn^{2+} dose response curves for GlyR $\alpha1^{L98A}$, $\alpha1^{F100A}$, $\alpha1^{F108A}$ and $\alpha1^{L134A}$ plotted as the percentage of the maximal response to Glycine applied to the same cells. *B*, Current-voltage (IV) relationships and the reversal potential of EC_{50} Zn^{2+} activated currents for $\alpha1^{F99A}$ and $\alpha1^{I132A}$. These IVs are comparable with the EC_{50} Gly IV plot from a wild-type GlyR α1 (dashed blue line). *C*, Typical currents recorded upon Zn^{2+} activation (black) of GlyR $\alpha1^{L98A}$, $\alpha1^{F100A}$, $\alpha1^{F108A}$ and $\alpha1^{I132A}$. The time-scale matched doses applied are in μM (red bars – this represents the longest application required as the some doses took longer to reach steady-state). 50 % maximal Gly evoked responses are also included (blue) as a comparison and reveal a faster onset rate than the Zn^{2+} activated currents. Scale bars represent 1 s and 1 nA. $N = 3 - 6$.

ZAG receptors require binding components of the Zn^{2+} inhibitory site

The concomitant observations that $\alpha1^{L98A}$, $\alpha1^{F99A}$, $\alpha1^{F100A}$, $\alpha1^{F108A}$, $\alpha1^{I132A}$ and $\alpha1^{L134A}$ receptors are activated by protons and that the inhibitory Zn^{2+} site no longer functions, suggests that this ZAG activity is derived from the original inhibitory Zn^{2+} binding site. However, it also appears that there are at least two different types of ZAG site present; a high affinity site that appears in response to the hydrophobic core disruptions and a low potency site that occurs upon disruption of the '-' inhibitory binding face. The low potency ZAG site formed from the inhibitory '-' face disruptions can be explained by the fact that these receptor mutants potentially suffer disruption to the Zn^{2+} coordinating partners in the ZAG reducing the affinity of the site. In the case of the high affinity sites though the potencies for Zn^{2+} are as low as 0.1 μM compared to the potency for Zn^{2+} inhibition at wild-type receptors of approximately 20 μM, suggesting this site may have changed chemically to produce a higher affinity for Zn^{2+}. To test this hypothesis two mutated receptors, $\alpha1^{T133A}$ to represent the low potency ZAGs and $\alpha1^{F99A}$ to represent the high potency ZAGs, were compared for their dependence on residues forming the original inhibitory Zn^{2+} binding site, namely H107, H109 and T133.

GlyR $\alpha1^{T133A}$, which had a low sensitivity to Zn^{2+}, possibly due to the loss of T133 as a coordinating partner, lost almost all ZAG activity when an extra H107A, or H109F (which unlike H109A had no ZAG activity of its own; data not shown, $n = 3$) were incorporated, with 30 mM Zn^{2+} evoking currents, as a percentage of the Gly I_{max}, of only 1.8 ± 2.2 %, ($n = 3$) for $\alpha1^{T133A,\ H107A}$ and 1.4 ± 0.2 %, ($n = 3$) for $\alpha1^{T133A,\ H109F}$ (Fig 4.10*A*). By contrast, introduction of substitutions at H107 or H109 on the $\alpha1^{T133A}$ receptor only slightly affected Gly potency (Fig 4.10*B*, Table 4.1). As a further test of the criticality of H107 for Zn^{2+} coordination and induction of ZAG activity this residue was also mutated to an alternative Zn^{2+} binding moiety, Asp. The $\alpha1^{T133A,\ H107D}$ receptor retained a similar Gly potency to $\alpha1^{T133A}$, but the Zn^{2+} potency was still significantly reduced almost to the extent of $\alpha1^{T133A,H107A}$ suggesting that the exact nature of the residue at position 107 is critical, though whether this requirement is structural, chemical, or both, is unclear (Fig 4.10*A*,*B*).

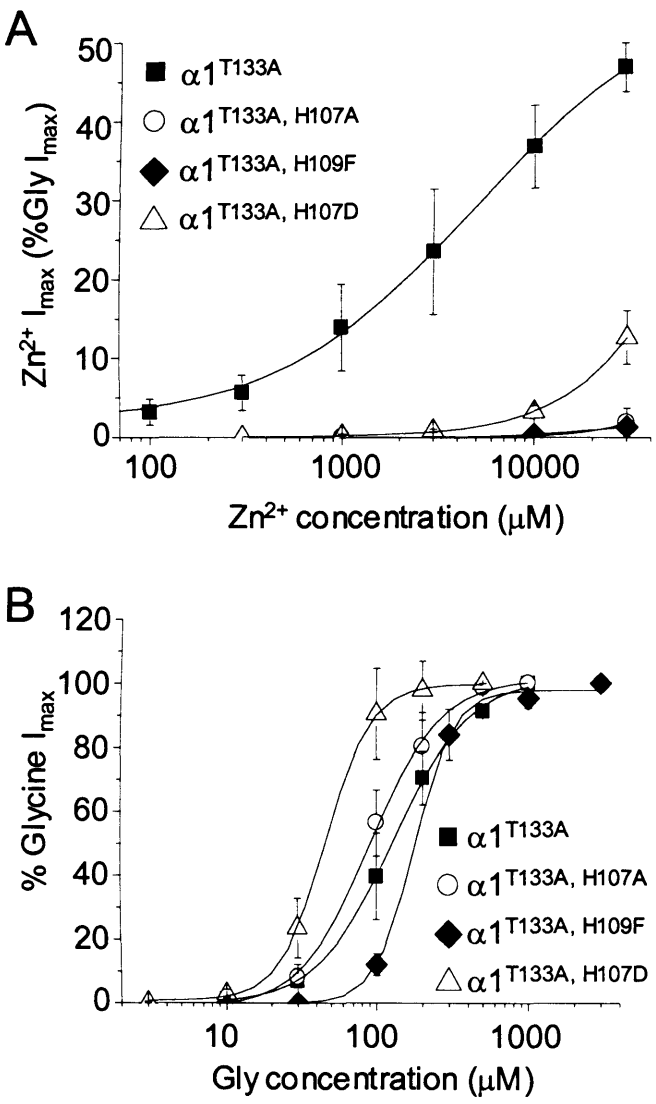

Figure 4.10 Shared Zn^{2+} binding components between Zn^{2+} inhibition and low potency ZAGs. The low potency Ala substituted ZAG receptors formed by disruption at the '-' face of the inhibitory site still require the Zn^{2+} binding residues of the inhibitory site for direct Zn^{2+} activation. *A*, Zn^{2+} dose response curves plotted as the percentage of a maximal response to Glycine applied to the same cell. For GlyR $\alpha1^{T133A}$ based mutants, the introduction of extra disruptions to the putative Zn^{2+} binding residues, H107 and H109, introduces substantial reductions in the potency of Zn^{2+}. (The $\alpha1^{T133A}$ Zn^{2+} dose response curve is taken from Figure 4.3*A*). *B*, Gly dose response curves for GlyR $\alpha1^{T133A}$ based mutants showing that introduction of extra disruptions to the putative Zn^{2+} binding residues, H107 and H109, introduces only modest shifts in Gly potency. $N = 3 - 5$.

For $\alpha1^{F99A}$, mutation of the inhibitory Zn^{2+} site residue, H109 caused a significant 10–fold reduction in the Gly potency but more substantially, virtual ablation of ZAG activity, such that a 1 mM Zn^{2+} induced a current of only 2.4 ± 2.8 %, (n = 5) for $\alpha1^{F99A, H109F}$ of the Gly I_{max} (Fig 4.11*A,B*). Intriguingly, $\alpha1^{F99A, H107A}$ and $\alpha1^{F99A, T133A}$, induced similar 10-fold reductions in Gly potency, but they only exerted modest 3 to 5-fold decreases in the sensitivity to Zn^{2+} activation with Zn^{2+} EC_{50} values increasing from 0.13 ± 0.3 μM, (n = 5) for $\alpha1^{F99A}$ to 0.4 ± 0.1, (n = 5) for $\alpha1^{F99A, H107K}$ and to 0.75 ± 0.22, (n = 4) for $\alpha1^{F99A, T133A}$ (Fig 4.11*B*). In keeping with the consistent reductions in ZAG sensitivity of these mutated receptors the level of spontaneous Zn^{2+} dependent leak was also reduced, evident from the block induced by both CTB and tricine (Fig 4.11*C*). This suggests these two residues do not have the same degree of importance as H109 for the high potency ZAG site. Further studies to attempt to elucidate alternative Zn^{2+} coordinating partners for the high potency ZAG site did not reveal any obvious candidates. The nearby residues selected were $\alpha1^{F99A, D97A}$, $\alpha1^{F99A, E103A}$, $\alpha1^{F99A, D114A}$ and $\alpha1^{F99A, E157A}$ from the '+' face and $\alpha1^{F99A, E110A}$ and $\alpha1^{F99A, T112A}$ from the '-' face, all of which failed to reduce the potency of Zn^{2+} at an $\alpha1^{F99A}$ based ZAG (Fig 4.12*A,B*). An $\alpha1^{F99A,D57A}$ receptor was also tested but this proved non-functional (n = 5).

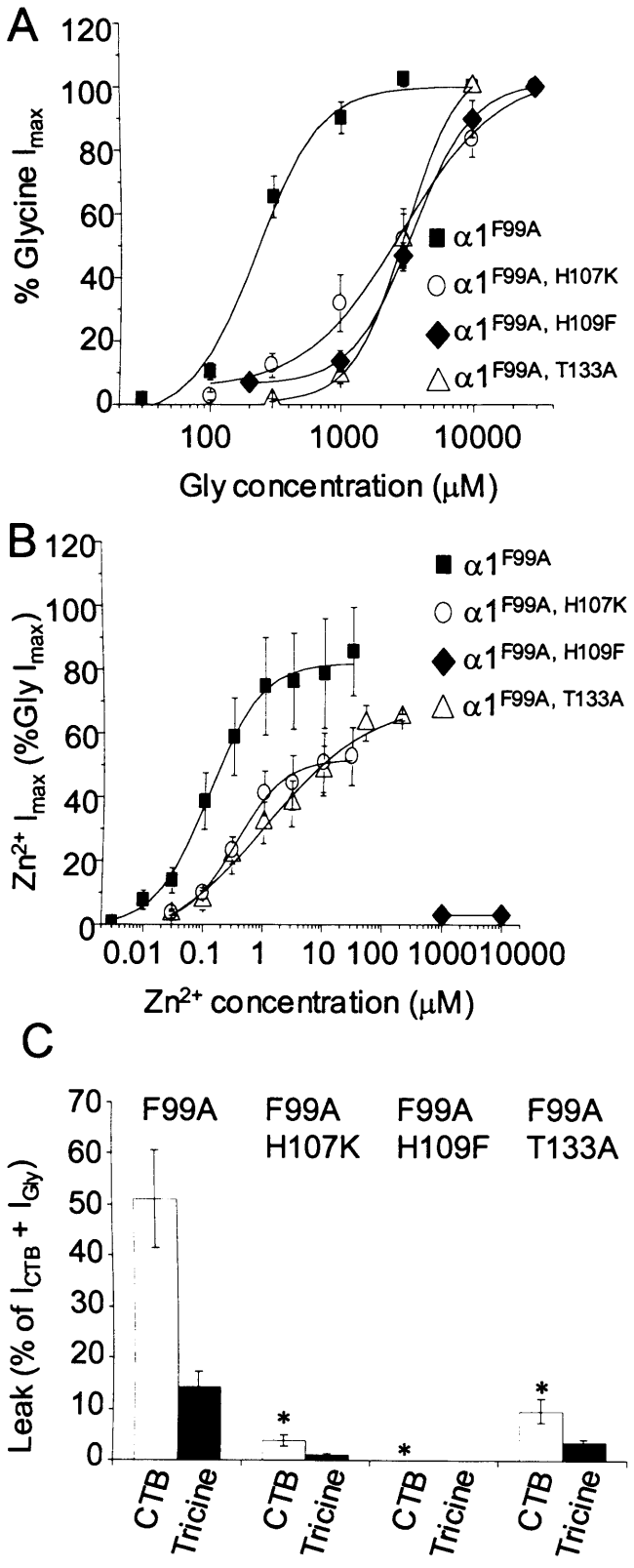

Figure 4.11 Dependence of high nM sensitivity ZAG receptors on Zn^{2+} binding residues of the original inhibitory site for direct Zn^{2+} activation. *A*, Gly dose response curves for GlyR $\alpha1^{F99A}$ based mutants showing that introduction of extra disruptions to the putative Zn^{2+} binding residues, H107, H109 and T133, introduces a consistent ten–fold reduction in the sensitivity to glycine. *B*, Zn^{2+} dose response curves plotted as the percentage of a maximal response to glycine applied to the same cell. For GlyR $\alpha1^{F99A}$ based mutants, the introduction of extra mutations to the Zn^{2+} binding residues, H107 and T133, introduces a comparable reduction in sensitivity to the agonist Zn^{2+}. However, introduction of an H109F mutation introduces a near complete ablation of ZAG activity. (The $\alpha1^{F99A}$ Zn^{2+} dose response curve is taken from Figure 4.8*A*). *C*, In keeping with the lower Zn^{2+} sensitivity of these $\alpha1^{F99A}$ receptors the leak current measured as a percentage of the total current, (I_{CTB} plus the maximal Gly response (I_{Gly})) is significantly reduced (*; $P < 0.05$, white bars) and could be further reduced by 2.5 mM tricine (black bars). $N = 4 - 5$.

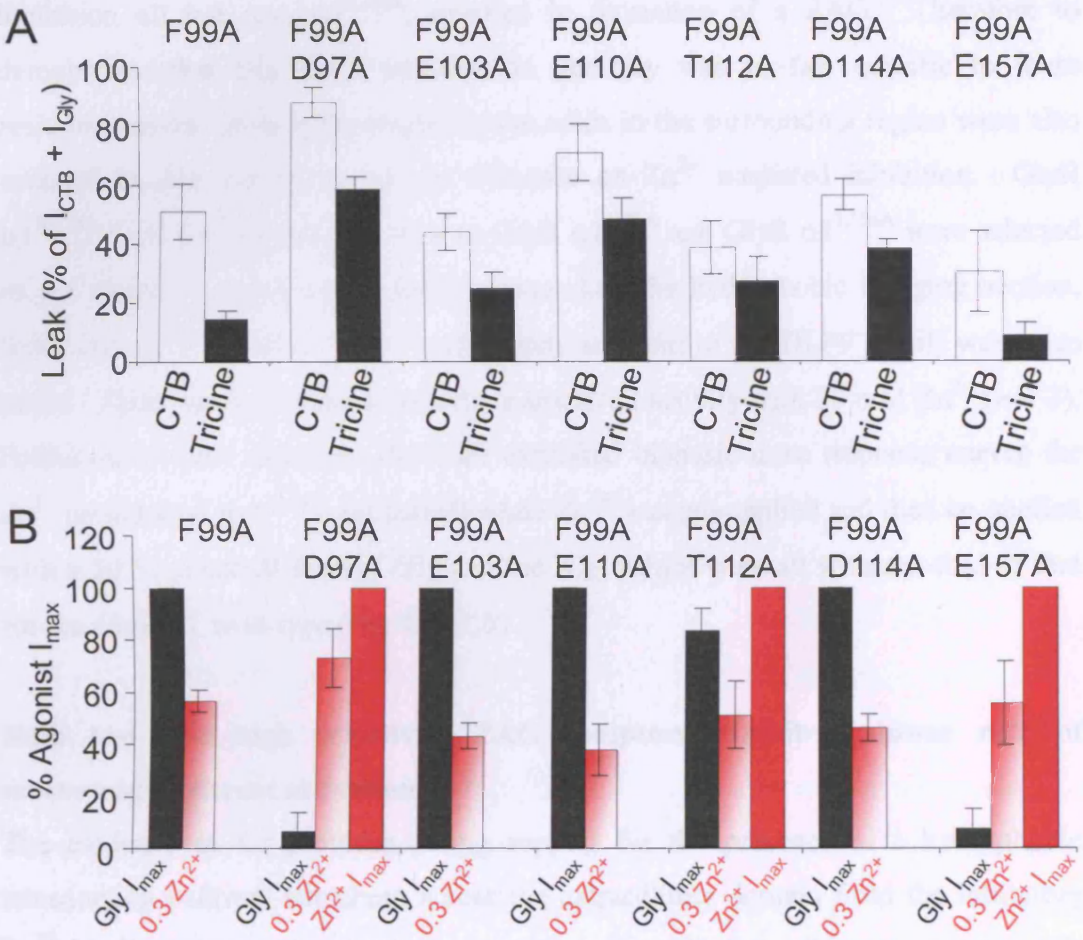

Figure 4.12 Acidic residues residing in the vicinity of the inhibitory Zn^{2+} site do not mediate Zn^{2+} binding for the high Zn^{2+} potency ZAG receptors. The ZAG sensitivity was analysed on the high sensitivity ZAG $\alpha1^{F99A}$ background in terms of the size of the leak currents (*A*) and the % maximal current evoked by a submaximal 0.3 μM dose of Zn^{2+} (*B*). *A*, Leak currents measured as a percentage of the total current, I_{CTB} plus the maximal Gly response (I_{Gly}) were not significantly reduced in any of the six potential Zn^{2+} coordinators tested when measured as the CTB blockable current (white bars) or the 2.5 mM tricine reduced current (black bars). *B*, In keeping with this, the percentage current induced by 0.3 μM Zn^{2+} (shaded red bars) was also not significantly reduced compared to the $\alpha1^{F99A}$ background when recorded as a percentage of the maximal Gly evoked response or, in cases where Gly was not the most efficacious agonist (black bars), as a percentage of the Zn^{2+} I_{max} (red bars) in the same cell. $N = 3 - 4$.

The formation of high sensitivity ZAG receptors is specific to residues of the hydrophobic transduction apparatus

From the group of residues tested for their ability to compromise Zn^{2+} mediated inhibition all but one, $\alpha1^{L156A}$, resulted in formation of a ZAG. Therefore to demonstrate that this ZAG transduction pathway was in fact specific to these residues, several other hydrophobic amino acids in the surrounding region were also mutated to Ala and tested for an influence on Zn^{2+} mediated inhibition. GlyR $\alpha1^{M154A}$ from the β7 strand as well as GlyR $\alpha1^{I130A}$ and GlyR $\alpha1^{L136A}$ were selected as the closest hydrophobic residues surrounding the hydrophobic bridging section. Also, and $\alpha1^{A101L}$ and $\alpha1^{N102A}$, immediately adjacent to the DLFF motif, were also tested. These mutations failed to induce any ZAG activity with 30 mM Zn^{2+} ($n = 3$). Furthermore these mutated GlyRs all exhibited biphasic dose response curves for Zn^{2+} modulation ($\alpha1^{N102A}$ not tested) when Zn^{2+} was pre-applied and then co-applied with a 50 % maximal dose of Gly and the IC_{50} values were all within 2-fold of that for the GlyR α1 wild-type (Fig 4.13*A*,*B*).

Both low and high sensitivity ZAG receptors exhibit a slower rate of macroscopic current activation

The evidence so far provides strong support for the presence of a hydrophobic transduction pathway stretching across the extracellular domain from the inhibitory Zn^{2+} binding site to the glycine recognition site. In the wild-type receptor this pathway presumably mediates the effect of Zn^{2+}inhibition on the agonist-binding site. However, from the data presented so far it is not obvious what function this pathway performs upon the actual binding of agonist and subsequent activation of the receptor. The Gly EC_{50}s, and I_{max} values for both the low and high potency ZAGs do not show any obvious patterns of disruption relative to the wild-type receptor (Table 4.1). It could be that this pathway exists simply to mediate a modulatory effect from Zn^{2+} during physiological processes. However it is also possible that this conformational transition from one side of the extracellular domain to the other also fulfils some other purpose in terms of receptor function. To address this issue the shapes of the macroscopic traces were analysed to measure any effects on the extent of glycine induced desensitisation, which inhibitory Zn^{2+} has been shown to influence in the NMDA receptor (Zheng et al., 2001), and also to measure

the activation rates of the receptors. In a comparable manner to the effects on glycine potencies, the desensitisation studies did not reveal any obvious disruption to this process in the ZAG receptor mutants with the wild-type receptor desensitising by 45 ± 2 %, (n = 7) during a 10 s supramaximal 10 mM glycine application (Fig 4.14*A,B*). Only GlyR $\alpha1^{L98A}$, $\alpha1^{T133A}$ and $\alpha1^{L134A}$ displayed modest increments in the extent of desensitisation with I_{gly} reducing to 36 ± 3 %, (n = 3), 44 ± 3 %, (n = 7) and 41 ± 2 %, (n = 3) of the peak current, respectively under the same conditions ($P < 0.05$; Fig 4.14*A,B*).

In contrast to the extent of desensitisation, when a single exponential was fit to the upper phase of 50 % maximal Gly currents, a significant increase in the time constant to reach steady-state was measured for all high and low potency ZAGs with the exception of GlyR $\alpha1^{F99A}$ ($P < 0.05$; Fig 4.15*A,B*). This increase in the time constant to reach steady-state peaked for the hydrophobic residues located in the bridging region with $\alpha1^{F100A}$, $\alpha1^{F108A}$ and $\alpha1^{L134A}$ having time constants of 250 ± 30 ms, (n = 8), 220 ± 30 ms, (n = 11) and 210 ± 60 ms, (n = 5) respectively, compared to GlyR α1 wild-type of 100 ± 10 ms, (n = 7). For the low potency ZAGs, the time constants were even slower with $\alpha1^{T133A}$ exhibiting the slowest time constant of 450 ± 80 ms, (n = 6). To demonstrate that this effect on receptor macroscopic rates of activation was specific to the ZAG mutants, four other nearby non-ZAG mutations, the hydrophobic $\alpha1^{I130A}$, $\alpha1^{L136A}$ and $\alpha1^{L156A}$ mutants and the '+' face mutation $\alpha1^{R59A}$ were tested. All failed to induce any change in the rate of activation values (Fig 4.15*A,B*). It should be noted that these estimations of activation rates were carried out using doses of Gly giving 50 % maximal responses in 0.25 mM tricine to remove contaminating background Zn^{2+}, which is sufficient to activate many of these receptors to a certain degree with a slower onset rate, potentially interfering with the rates of onset presented here. However $\alpha1^{F99A}$ the most sensitive and efficacious ZAG did not exhibit slower onset rates suggesting this possibility of Zn^{2+} interference was unlikely.

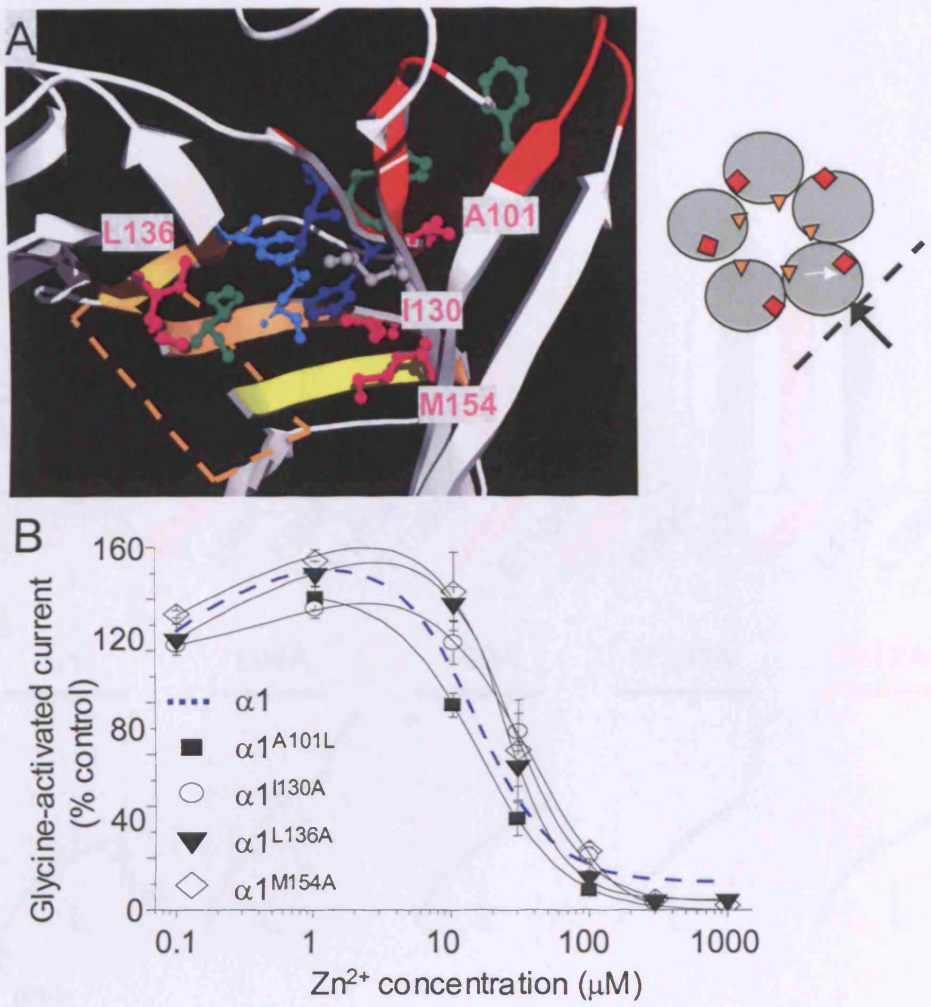

Figure 4.13 Demonstration of the specificity of the hydrophobic transduction path from the inhibitory Zn^{2+} site '-' face to the Gly binding site. *A*, View from the outside face (see grey pictorial; Zn^{2+} site – orange triangle, agonist site – red square, black arrow shows the viewing angle, white arrow - predicted transduction pathway) showing the green and blue hydrophobic residues previously demonstrated to mark a pathway between the '-' inhibition site (orange β-strands and orange box) and the agonist binding motifs (red). Residues labelled in pink are hydrophobic residues that lie just outside the predicted path of the transduction domain. Some extraneous structure is cut away for ease of viewing. *B*, Zn^{2+} dose response curves using a pre-incubation protocol for the modulation of 50 % maximal Gly evoked responses demonstrates that Ala substitution of these residues failed to reduce the sensitivity to Zn^{2+} mediated inhibition when compared to the wild-type α1 GlyR. $N = 3$.

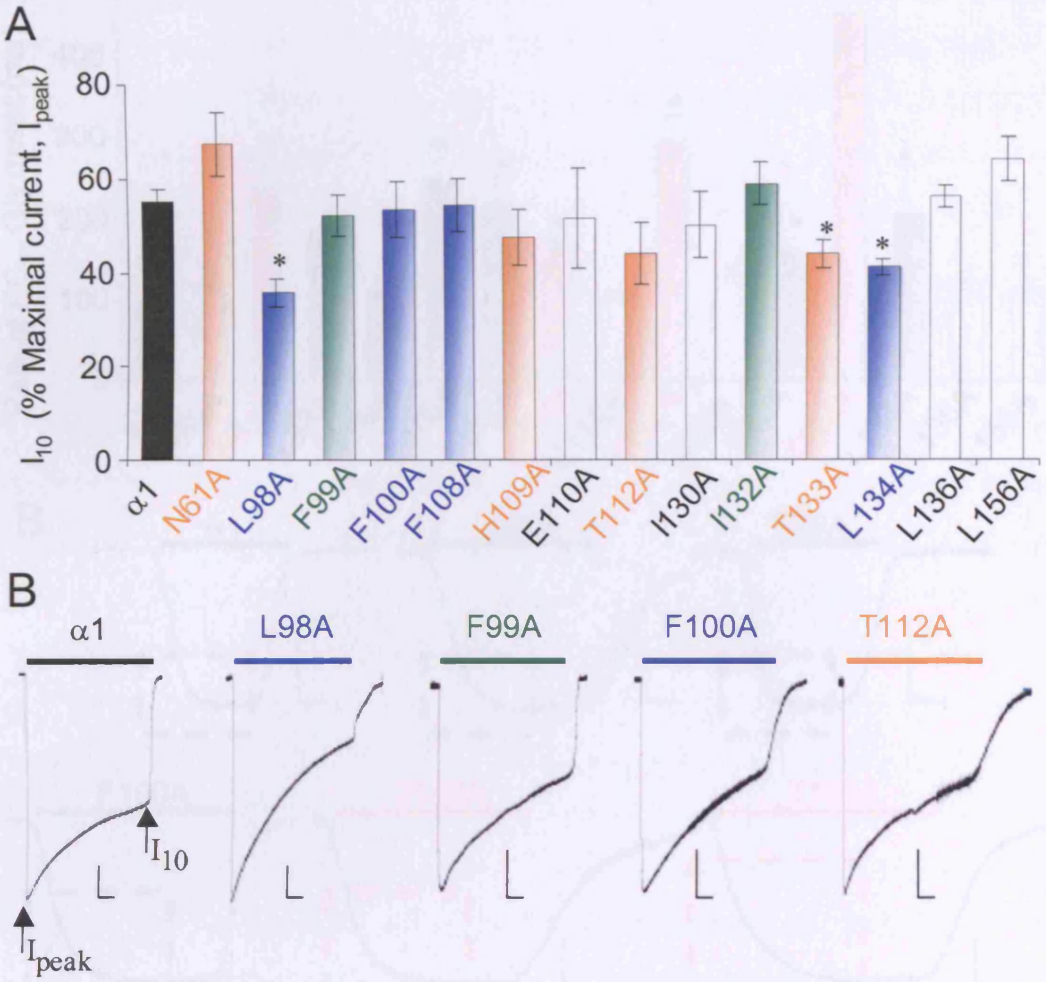

Figure 4.14 Variations in the extent of macroscopic desensitisation do not show any obvious correlation with mutations that induce the formation of ZAGs. *A*, Mean values for the extent of desensitisation of macroscopic currents measured in terms of the current amplitude after 10 seconds of supramaximal 10 mM Gly application (I_{10}) as a percentage of the peak amplitude of the same current (I_{peak}). Mutated GlyRs were compared to the wild-type α1 receptor (black bar) and were separated into categories as follows; mutated receptors that did not form ZAGs - white bars; low potency ZAGs formed through disruption of the '-' inhibitory Zn^{2+} binding site face – orange shaded bars; high relative efficacy ZAGs – green shaded bars; and high potency, low relative efficacy ZAGs – blue shaded bars. Asterisks depict mutated receptors, which reached a significantly different extent of desensitisation compared to the wild-type α1 receptor ($P < 0.05$). *B*, Typical currents showing the extent of desensitisation during 10 s applications of a supramaximal 10 mM dose of Gly. Scale bars represent 1 s and 1 nA. $N = 3 – 7$.

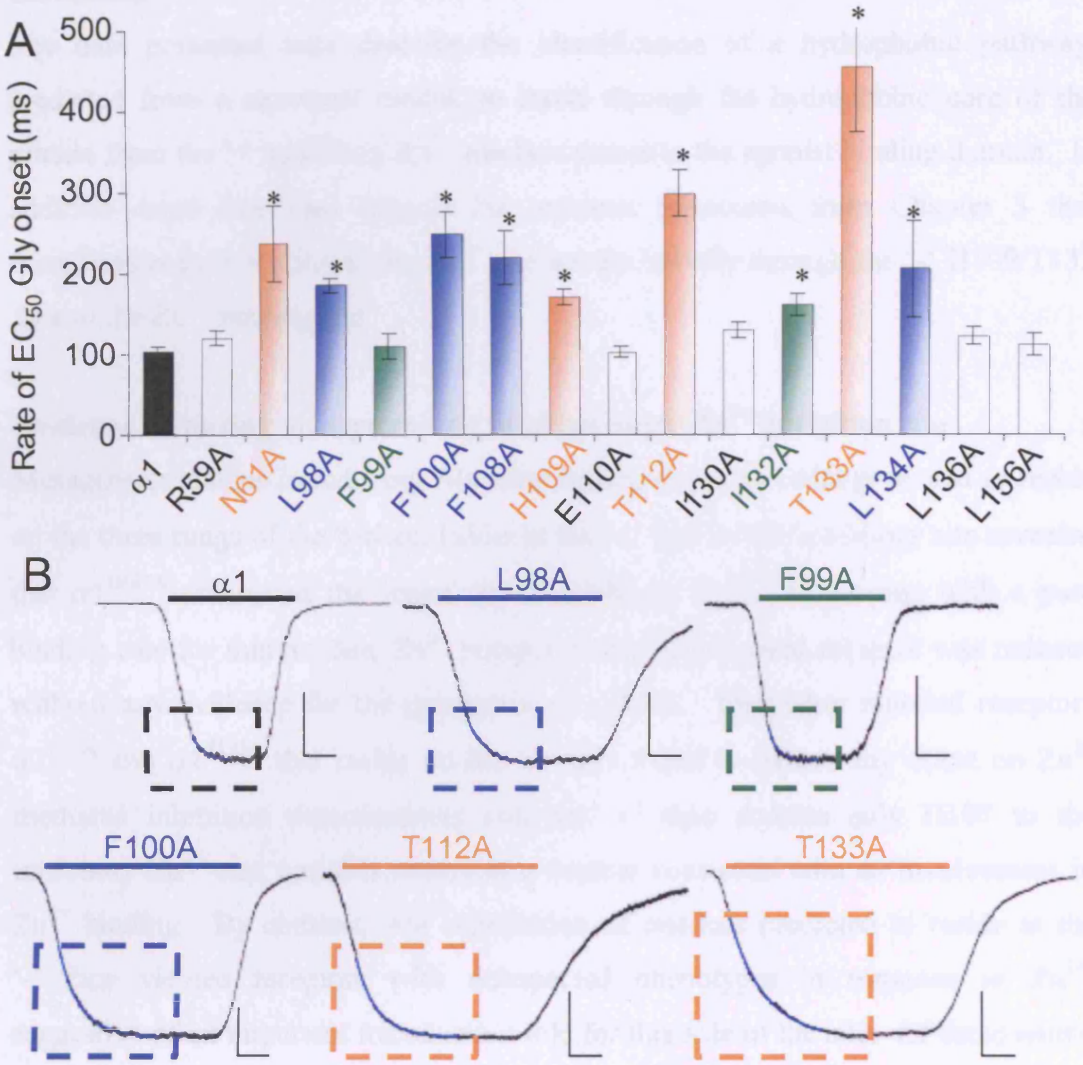

Figure 4.15 Rate of glycine current activation measured in terms of the time taken to reach steady-state, is correlated with mutations that generate ZAGs. *A*, Mean values for the rate of onset measured by fitting a monoexponential curve fit from the current onset to the time taken to reach steady-state of 50 % maximal Gly evoked responses. The wild-type α1 receptor (black bar) was compared to non-ZAG mutated receptors (white bars) and ZAG receptors with; low Zn^{2+} potency formed by disruption of the '-' inhibitory Zn^{2+} binding site face (orange bars); high relative efficacy (green bars); and high potency, low relative efficacy (blue bars). Asterisks depict a significant increase in the time constant (a decrease in the activation rate) compared to that for the wild-type α1 receptor ($P < 0.05$). *B*, Typical 50 % maximal Gly evoked currents highlighting (dashed box) the region over which the monoexponential curve fit was determined (faint blue overlay over the black trace). Scale bars represent 1 s and 1 nA. The currents presented here are timescale matched for ease of comparison. $N = 3 - 11$.

Discussion

The data presented here describe the identification of a hydrophobic pathway, predicted from a structural model, to travel through the hydrophobic core of the protein from the '-' inhibitory Zn^{2+} site face across to the agonist binding domain. In addition these data also support the previous hypothesis from Chapter 3 that transduction from the inhibitory Zn^{2+} site occurs initially through the '-' H109/T133 face of the Zn^{2+} binding site.

Evidence favouring an asymmetric function of the Zn^{2+} inhibition site

Mutagenesis studies introducing Ala substitutions to amino acids predicted to reside on the three rungs of the β-sheet ladder at the '+' face of the inhibitory site revealed that $\alpha1^{H107A}$ attenuated the sensitivity to inhibitory Zn^{2+}. In keeping with a pure binding role for this residue, Zn^{2+} potency at the Ala mutated receptor was reduced without any evidence for the generation of a ZAG. Two other mutated receptors $\alpha1^{R59A}$ and $\alpha1^{T135A}$ that reside on the '+' face failed to induce any effect on Zn^{2+} mediated inhibition demonstrating that the '+' face donates only H107 to the inhibitory Zn^{2+} site, and this occurs in a manner consistent with an involvement in Zn^{2+} binding. By contrast, Ala substitution of residues predicted to reside at the '-' face yielded receptors with unexpected phenotypes in response to Zn^{2+}, suggestive of an important transduction role for this side of the site. Of these amino acids, only disruption to an E110 residue produced an $\alpha1^{E110A}$ receptor phenotype in keeping with a possible pure binding role for this amino acid as the mutant exhibited a modest 5-fold decreased sensitivity to inhibitory Zn^{2+} without affecting the maximal limit of Zn^{2+} mediated inhibition. According to the model this residue is predicted to face away from the Zn^{2+} binding site precluding a direct role in Zn^{2+} binding, however this model is not capable of predicting the exact side chain position based on such a low primary sequence homology (approximately 20 %) and therefore in the real protein structure it may be that binding at E110 can be accommodated, or that an E110A substitution simply introduces an indirect structural perturbation. The other four mutated receptors, $\alpha1^{N61A}$, $\alpha1^{H109A}$, $\alpha1^{T112A}$ and $\alpha1^{T133A}$ all yielded either an attenuated maximal level of inhibition by Zn^{2+}, as was the case for $\alpha1^{H109A}$, or ablated Zn^{2+} mediated inhibition. Furthermore, these receptors were now susceptible to direct activation by Zn^{2+} acting as an agonist, with relative

efficacies, compared to glycine, of between 20 and 50 %. Consistent with Zn^{2+} acting as an agonist, receptor activation was concentration dependent, in a voltage-independent manner relying on transmembrane chloride flux, indicating Zn^{2+} was eliciting anionic flow via the GlyR chloride channel.

A simple hypothesis to explain ZAG formation

If Zn^{2+}, by binding to the inhibitory site, is causing channel activation in the mutated receptors, it suggests that ZAG activity involves a reorganisation of the '-' face of the inhibitory site, altering the transduction machinery of the receptor such that Zn^{2+} now activates rather than inhibits the receptor. Though it is not possible from these studies to understand exactly how such an apparently substantial phenotypic conversion could have occurred, the most likely explanation is potentially quite simple. Previous evidence (Nevin et al., 2003, Chapter 3) supports the supposition that Zn^{2+} exerts its inhibitory effect by forming a 'bridge' between two adjacent α subunits, stabilising a closed conformation of the receptor. Therefore, in order to switch this site to elicit activation, all that is needed is a disruption to the '-' face such that the bridging residues, primarily H109/T133 of the '-' face and H107 of the '+' face, are now better aligned for Zn^{2+} coordination when the receptor is activated, rather than when it is closed. This will have the resultant effect that application of Zn^{2+} to the receptor can induce activation by drawing the two faces together through coordination and subsequently, in principle, the receptor may activate. This reorganisation might not necessarily even require a substantial disruption of the '-' face as it is dependent on the size of the movement that would normally occur at this location during activation. As was previously discussed (Chapter 3) under the hypothesis that the nAChR α subunit (and therefore quite probably the GlyR α subunit also) undergoes a twist during activation (Unwin, 1995), we would expect the '-' H109/T133 region to move relative to the '+' H107 residue on the neighbouring subunit (Unwin et al., 2002) such that Zn^{2+} can no longer bind. So then, disruption to move the '-'face out of alignment could be sufficient to induce the ZAG phenotype. Though it is speculative, based on the relatively non-specific structural data currently available for GlyRs and their movements during activation, a schematic model displaying the basic tenets of such a process and the relative

simplicity by which it might arise in the context of what is expected for cys-loop receptors is presented in Fig 4.16*A,B*.

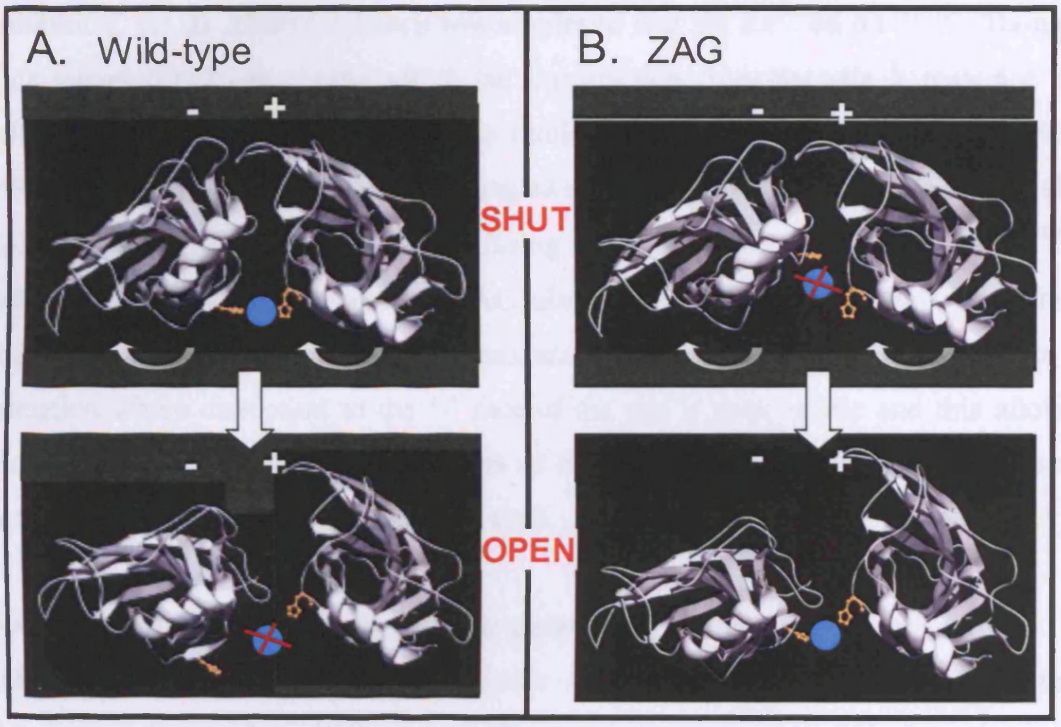

Fig 4.16 Schematic model presenting a simple mechanism for ZAG formation. *A*, Wild-type GlyR α1 can bind inhibitory Zn^{2+} (blue circle) to stabilise the closed state but not when the receptor activates (bottom). *B*, Disruption of the '-' face of the inhibitory Zn^{2+} site prevents Zn^{2+} binding in the closed state (top) but enables Zn^{2+} binding in the activated conformation (bottom) creating a ZAG receptor.

The data discussed here do, of course, assume that the Zn^{2+} site eliciting activation is in fact derived from the original Zn^{2+} inhibition site. This does seem to be the case as for all the ZAG receptors generated, Zn^{2+} mediated inhibition is ablated suggesting this functionality has been replaced by the ZAG property. Furthermore, mutation of either of the principal histidine Zn^{2+} binding residues, H107 or H109, to non-Zn^{2+} binding groups on a ZAG $\alpha1^{T133A}$ background, removed the ZAG activity suggesting this novel phenotype is still derived from the original H107/H109 based inhibitory site. Given these observations the Zn^{2+} potencies measured for the '-' face disrupted ZAGs reveals information about the nature of the residues in terms of their function at the inhibitory Zn^{2+} site. Both $\alpha1^{N61A}$, $\alpha1^{H109A}$ and $\alpha1^{T133A}$ all formed

very low potency ZAGs, suggesting the site had been disrupted such that the affinity was also reduced. However, at $\alpha1^{T112A}$, Zn^{2+} had a much higher potency for causing activation with an EC_{50} of similar magnitude to the original IC_{50} for Zn^{2+} mediated inhibition, yet its relative efficacy was similar to that for Zn^{2+} on $\alpha1^{T133A}$. Though this means T112 can clearly affect the transduction from the site it may not be affecting the potency and therefore is unlikely to have a role in binding, which concurs with its predicted location facing away from the inhibitory site (Nevin et al., 2003;Chapter 3). One potentially confusing issue remaining is the fact that $\alpha1^{H109A}$ which forms a very low potency ZAG also retains sensitivity to Zn^{2+} mediated inhibition although with a decreased maximal inhibition. This most likely reflects a situation where disruption to the '-' face of the site is more subtle and this allows Zn^{2+} to compete for two conformations of the site, one which stabilises the closed state and one which stabilises the open state.

Evidence supporting the hydrophobic pathway as a transduction pathway

The evidence so far supports an asymmetric role for the inhibitory Zn^{2+} site with the '-' face mediating the initial downstream transduction process. This hypothesis is further strengthened here by the identification of an apparent hydrophobic transduction pathway leading selectively from this '-' face of the inhibitory site across to the agonist binding site. Though it is not always possible from mutagenesis studies alone to ascribe the exact function of amino acids within the context of a binding-transduction role there are several factors elucidated here that support the assertion that this hydrophobic pathway could be a genuine transduction pathway. First and foremost is the availability of a structural model for the GlyR, which shows strong agreement with the hydrophobic residues identified here lining up to form a path between the agonist binding site and the inhibitory Zn^{2+} '-' face. This structural evidence is also supported by a previous study investigating the putative β4-strand in the homologous $GABA_A$ receptor β-subunit. The use of a cysteine accessibility reagent revealed access to residues in this domain were consistent with them adopting a β-strand structure and also showed that the $GABA_A$ receptor β subunit residue equivalent to GlyR F99 was predicted to face into the agonist binding site. This means that GlyR L98 and F100 are predicted to face into the receptor hydrophobic core (Boileau et al., 2002). Secondly, the consistent phenotypic

exchange upon distortion of the transduction pathway to create ZAGs is supportive of a transduction role since if these residues are part of a chain, as is predicted here, then disruption to any one residue within the linear chain should elicit the same phenotype. In addition to this, the substitutions introduced do not simply ablate site function, which would then preclude the dissection of whether the corresponding residues are important for transduction, binding or are causing an indirect structural perturbation. Instead, these phenotypic disruptions still retained a high potency for inhibitory Zn^{2+} suggesting that though the residues clearly influence the potency of the site they also clearly influence signal transduction from the site. As these residues are predicted to reside in the hydrophobic core of the receptor and are not considered likely Zn^{2+} binding residues, it seems reasonable to ascribe to them a pure transduction role. The only ZAG to have a low Zn^{2+} potency was I132A, which was located directly on the back of the '-' face inhibitory site. It is the best located of those hydrophobic residues to elicit a secondary indirect effect on the structure of the Zn^{2+} binding site to reduce the Zn^{2+} affinity and therefore the potency. In further support of the hydrophobic chain hypothesis was the demonstration that generation of these ZAGs was not a general side effect of disrupting the GlyR global structure. It was instead selective to the hydrophobic residues in question, as was verified by the absence of any ZAG phenotype when nearby hydrophobic residues, lying just off the hypothetical pathway, were similarly substituted with an Ala moiety.

Reliance of Zn^{2+} binding residues at the high and low potency ZAGs and the original Zn^{2+} inhibition site

As mentioned previously this transduction pathway also relies on the tenet that ZAG activity is still derived at least in part from the original Zn^{2+} inhibitory site and again this does appear to be the case. Each of the hydrophobic Ala substitutions ablated the previous Zn^{2+} mediated inhibition and replaced it with ZAG activity rather than creating a receptor with both properties as has been observed previously for a mutated nAChR (Palma et al., 1998). Secondly, and most critically, the incorporation of an H109F mutation into GlyR $\alpha1^{F99A}$ ablated the ZAG activity demonstrating that this activity still has a critical reliance on the '-' face H109 inhibitory site residue. Interestingly the potency of Zn^{2+} activating the channel is high, reaching nanomolar sensitivity compared to the original micromolar sensitivity

for Zn^{2+} inhibition. The incorporation of H107K and T133A mutations into the $\alpha1^{F99A}$ background introduced a far more modest reduction in Zn^{2+} potency for ZAG activation compared to the substantially reduced sensitivity to Zn^{2+} mediated inhibition that is induced by removing these residues. However it cannot be ruled out that these residues do have critical requirements for the high potency ZAG receptors but upon substitution another Zn^{2+} coordinating residue can step in to take their place, a point that has been raised previously (Traynelis et al., 1998) and which could not be discounted here. Though a scan of additional capable Zn^{2+} binding moieties within range of the putative ZAG site did not reveal any obvious candidates for the high sensitivity $\alpha1^{F99A}$ based ZAG. This relatively modest influence from substitutions at H107 and T133 on an $\alpha1^{F99A}$ background was perhaps not surprising as reorganisation of the '-' inhibitory site face, so that it now favours activation, would be expected to at least induce a partial shift in the emphasis placed on each of the binding residues. This, however, does not appear to be the case for the low potency ZAGs generated upon disruption to the inhibitory site '-' face as $\alpha1^{T133A}$ retained a heavy reliance on both H107 and H109. Thus the Zn^{2+} binding residues of the high and low potency ZAGs appear to differ in nature, though they do both require H109.

Consequences for the hydrophobic transduction pathway in determining macroscopic rates of receptor activation

Under the assumption that reorganisation of the hydrophobic pathway, elucidated here, does indeed represent a valid transduction pathway between the agonist-binding site and the '-' face of the GlyR, then this process may represent more than just a mechanism for allosteric modulation in response to Zn^{2+} mediated inhibition. Though this study investigated this pathway in the context of Zn^{2+} induced allostery, basic characterisation of mutated receptor properties suggested that this transduction process may be able to exert an effect over the rate of activation for the GlyR. In contrast there was no obvious correlations with the varying agonist potencies and modest effects on desensitisation measured from these Ala substituted receptors. This important influence over the rate of receptor activation could have important physiological consequences as it has been suggested that the slower macroscopic activation of the GlyR α2 subunit may reduce its efficiency as a rapid inhibitory

mediator at synapses (Mangin et al., 2003). Though the molecular basis of this slower rate of activation at the GlyR α2 subunit has not yet been dissected the pathway identified here could represent one way in which this GlyR subtype may alter its activation rate. This may also extend more generally to the variable activation rates observed throughout the cys-loop family of receptors.

The significance of related studies on ZAC formation

Unfortunately the data depicted here and the hypotheses put forward do not have much previous evidence or prior studies to draw on. Investigations tend to steer clear of perturbations to the hydrophobic core due to problems with interpreting the specificity of any downstream consequences, something that could be addressed here due to the fortuitous ZAG effect. A low potency Zn^{2+} activated channel (ZAC) has previously been reported (Davies et al., 2003) and further structure-function studies of this receptor may reveal a resemblance to the low potency ZAGs identified here, as this ZAC has a comparable low sensitivity and also retained a slow onset profile for Zn^{2+} induced currents. Though the site itself will not bear direct chemical comparison to that of the mutated GlyRs in this study, the ZAC does possess acidic residues at equivalent predicted locations to GlyR H107, E110 and T133 suggesting the site may be analogous (alignment not shown). Also of interest is a previous report identifying an M2 nAChR $\alpha7^{L247T}$ mutant that exhibited a very high nanomolar sensitivity for Zn^{2+} activation (Palma et al., 1998). However subsequent structure-function studies to elucidate the nature of this phenomenon have not been forthcoming. Furthermore such studies may be of limited relevance to the ZAG receptors discussed here as this mutation appeared to create a novel Zn^{2+} binding site rather than changing the function of a pre-existing site, as Zn^{2+} mediated inhibition was also retained in this receptor.

The rate of progress: As measured by the NMDA receptor

The data presented in this study represent a significant contribution to understanding Zn^{2+} modulation of GlyRs. As a comparison, the most intensely studied Zn^{2+} mediated process at a ligand-gated ion channel is that of Zn^{2+} inhibition of the NMDA receptor. This receptor exists as heteromers of NR1 and NR2 subunits, with inclusion of the NR2B subunit introducing a low affinity site, with sensitivity around

10 - 100 μM, and inclusion of the NR2A subunit providing a high affinity Zn^{2+} inhibitory site, with sensitivity in the range 10 – 100 nM (Paoletti et al., 1997). Though the low affinity inhibitory site remains unreported the location of the high potency site has been the subject of several studies (Choi and Lipton, 1999;Fayyazuddin et al., 2000;Paoletti et al., 2000). Candidate residues, as well as their positions, have been identified using site directed mutagenesis and a structural homology model in a similar manner to that reported here for the GlyR. Though these studies have not yet proposed any molecular basis for the transduction apparatus responsible for mediating the effects of the inhibitory Zn^{2+} binding site. Also, this unrelated receptor (to the GlyR) has not been reported to exhibit any ZAC properties despite extensive mutagenesis of potential Zn^{2+} binding site residues (Choi and Lipton, 1999;Fayyazuddin et al., 2000;Paoletti et al., 2000). This could perhaps be a consequence of the fact that the identified voltage-independent high affinity Zn^{2+} binding site of the NMDA-R is believed to act by reducing the ability of the receptor to gate rather than by reducing agonist binding (Christine and Choi, 1990;Legendre and Westbrook, 1990). In the case of the Zn^{2+} inhibitory process reported here for the GlyR, it appears the communication is an intrinsic process specific to a single globular domain of the receptor and this reduces the affinity of the protein for the agonist glycine. However in the case of the NMDA-R each subunit is split into several separate modular domains, of which the so called leucine/isoleucine/valine-binding protein (LIVBP) domain, that carries the identified high affinity voltage-independent site, is predicted to feed its transduction effect across to the gating and agonist binding modules to disrupt the communication between these two, a process which, if true, is vastly different to the unrelated GlyR (Paoletti et al., 2000). Previous studies have not attempted to discern whether Zn^{2+} inhibition elicits an effect on desensitisation in the GlyR and the studies in chapter 3, though demonstrating that Zn^{2+} can accelerate the rate of decay during co-application, which might be construed as an effect on desensitisation, are insufficient to support such a proposition. Most evidence supports an interaction of desensitisation with the GlyR ion channel domain (Breitinger et al., 2002;Breitinger et al., 2001) while Zn^{2+} inhibition appears to interact with the agonist-binding site (Chapters 3 and 4). By contrast, recent studies on the NMDA receptor suggest the main mechanism by which the high affinity Zn^{2+} inhibition site acts is by introducing

a very rapid desensitisation component into glutamate activation of NMDA receptors (Zheng et al., 2001). The two receptors are clearly separate in terms of how Zn^{2+} exerts inhibition, both in molecular and mechanistic terms, but the ability to now draw such comparisons demonstrates the progress that has now been made in these two fields of research.

Conclusion

The data here present a strong case for the presence of a hydrophobic transduction pathway across the N-terminus of the GlyR from the '-' face of the Zn^{2+} inhibition site to the β4 strand of the agonist-binding domain. Though the extent of the relevance of this communication route cannot be exactly pinpointed in the context of this work, the evidence strongly suggests that this path at the very least marks the route of allosteric communication between the inhibitory Zn^{2+} site and the agonist-binding site. Under this hypothesis agonist binding transmits a reorganisation to the '-' face of the GlyR at the location equivalent to the Zn^{2+} inhibitory site via the hydrophobic pathway such that Zn^{2+} can no longer bind and stabilise the closed state of the GlyR. From the reverse perspective, Zn^{2+} binding presumably stabilises the interface between the '-' and '+' faces of the GlyR preventing the agonist from binding and inducing reorganisation of the hydrophobic pathway to allow the receptor to open. Furthermore, due to a consistent reduction in the activation rates of the resultant ZAG receptors, this pathway may represent an important regulatory process by which cys-loop receptors can determine their intrinsic activation rates.

	Glycine			Zn^{2+} Agonist			Zn^{2+} Inhibition		
	EC_{50} (μM)	I_{max} (nA)	*n*	EC_{50} (μM)	I_{max} (% Gly I_{max})	*n*	IC_{50} (μM)	I_{min} (%)	*n*
Zn^{2+} '-' face									
α1	35 ± 3	6.7 ± 0.5	6	—	No Activation	4	15 ± 2	9 ± 7	5
$\alpha1^{N61A}$	95 ± 18	6.2 ± 0.8	4	> 10 mM	> 25 %	5	None	—	4
$\alpha1^{H109A}$	21 ± 2	5.9 ± 0.7	4	> 10 mM	> 20 %	3	33 ± 16	53 ± 7	5
$\alpha1^{E110A}$	24 ± 4	6.0 ± 1.5	3	—	No Activation	3	67 ± 4	4 ± 1	3
$\alpha1^{T112A}$	19 ± 6	5.0 ± 0.6	4	3.5 ± 1.5	42 ± 5	4	None	—	4
$\alpha1^{T133A}$	133 ± 32	5.4 ± 0.7	5	5400 ± 2500	> 45 %	5	None	—	4
$\alpha1^{T133A, H107A}$	100 ± 28	4.9 ± 0.3	3	> 10 mM	> 2 %	3	n.e	n.e	n.e
$\alpha1^{T133A, H107D}$	53 ± 15	4.4 ± 0.7	3	> 10 mM	> 12 %	3	n.e	n.e	n.e
$\alpha1^{T133A, H109F}$	180 ± 28	5.7 ± 0.8	3	> 10 mM	> 2 %	3	n.e	n.e	n.e
Zn^{2+} '+' face									
$\alpha1^{R59A}$	52 ± 5	7.3 ± 0.7	3	—	No Activation	3	5.2 ± 0.7	3 ± 3	3
$\alpha1^{H107A}$	56 ± 9	7.2 ± 0.3	3	—	No Activation	3	330 ± 30	12 ± 3	3
$\alpha1^{T135A}$	17 ± 2	3.3 ± 0.6	3	—	No Activation	3	26 ± 6	5.8 ± 0	3
Hydrophobic pathway									
$\alpha1^{L98A}$	35 ± 6	6.4 ± 0.5	6	0.26 ± 0.08	49 ± 5	4	None	—	4
$\alpha1^{F99A}$	250 ± 8	3.9 ± 0.4	4	0.13 ± 0.03	90 ± 6	5	None	—	4
$\alpha1^{F99A, H107K}$	4200 ± 1700	3.5 ± 0.6	5	0.4 ± 0.1	53 ± 12	5	n.e	n.e	n.e
$\alpha1^{F99A, H109F}$	3400 ± 330	0.5 ± 0.2	5	n.e	> 2	5	n.e	n.e	n.e
$\alpha1^{F99A, T133A}$	3300 ± 700	4.9 ± 0.9	4	0.75 ± 0.22	65 ± 4	4	n.e	n.e	n.e
$\alpha1^{F100A}$	117 ± 21	4.5 ± 0.7	6	9.19 ± 0.63	7 ± 4	4	None	—	4
$\alpha1^{F108A}$	14 ± 3	4.5 ± 0.5	5	2.3 ± 0.6	25 ± 6	6	None	—	5
$\alpha1^{I132A}$	96 ± 15	6.1 ± 0.7	6	140 ± 60	72 ± 5	5	None	—	4
$\alpha1^{L134A}$	83 ± 17	6.0 ± 0.3	7	0.1 ± 0.03	18 ± 3	4	None	—	4

Table 4.1 Summary table presenting sensitivities for the agonist Gly and where appropriate for Zn^{2+} acting as an agonist or antagonist of glycinergic currents. Values presented as means ± s.e. Definitions: n.e – not evaluated, '—' could not be evaluated as property is not present, none – property not present.

	Glycine			Zn^{2+} Inhibition		
	EC_{50} (μM)	I_{max} (nA)	*n*	IC_{50} (μM)	I_{min} (%)	*n*
Non ZAG receptors						
α1	35 ± 3	6.7 ± 0.5	6	15 ± 2	9 ± 7	5
$\alpha1^{A101L}$	430 ± 113	6.5 ± 0.8	3	18 ± 5	0.3 ± 0.3	3
$\alpha1^{I130A}$	3.4 ± 0.9	6.4 ± 0.7	4	38 ± 6	3 ± 0.9	3
$\alpha1^{L136A}$	16 ± 0.6	6.8 ± 0.8	3	22 ± 4	4 ± 0	3
$\alpha1^{M154A}$	99 ± 14	4.4 ± 1.4	3	27 ± 6	1.8 ± 0.8	3
$\alpha1^{L156A}$	105 ± 2	6.7 ± 0.7	3	23 ± 6	0.1 ± 0.1	3

Table 4.2 Summary table presenting sensitivities for the agonist Gly and the antagonist Zn^{2+} acting on GlyRs without the ZAG phenotype. Values presented as means ± s.e.

Chapter 5

Identification of a Zn^{2+} potentiation site in GlyRs and a mechanism of action involving the cys-loop gating domain

Introduction

The cys-loop family of receptors, most notably comprising nAChRs, $GABA_A$Rs, GlyRs and 5-HT_3Rs are all susceptible to Zn^{2+} mediated inhibition with varying degrees of sensitivity and selectivity (Hsiao et al., 2001*;Hubbard and Lummis, 2000;Chang et al., 1995;Smart et al., 2004). In some instances these receptors have also been shown to exhibit a more complicated biphasic modulation by Zn^{2+}, with enhancement of agonist responses occurring at low Zn^{2+} concentrations and a secondary inhibitory phase initiating at higher doses, as is the case for GlyRs, 5-HT_3Rs and certain nAChR subtypes (Bloomenthal et al., 1994;Hubbard and Lummis, 2000;Hsiao et al., 2001). Current research regarding inhibitory Zn^{2+} sites has identified discrete locations on both $GABA_A$ (Hosie et al., 2003) and GlyRs (Harvey et al., 1999;Chapter 3), but there have been no clear candidate sites elucidated for Zn^{2+} potentiation. An understanding of the molecular components and the dynamic interactions that occur during potentiation by Zn^{2+} is of importance for two reasons. Firstly, understanding the mechanism of Zn^{2+} potentiation at cys-loop receptors provides insight into how drugs can exert a positive influence on receptor function and this may be relevant to a number of other pharmacologically relevant potentiators including anaesthetics, barbiturates, benzodiazepines, ethanol and neurosteroids. Secondly, in cases where Zn^{2+} potentiation has been reported, this process occurs with higher potency than Zn^{2+} mediated inhibition and therefore may be of more relevance physiologically, where the concentrations of Zn^{2+} at a synapse are currently considered to reside in the range, 0.01 – 5 μM (Frederickson et al., 2000). (* Gill et al., 1995).

A previous study by Laube *et al*, (1995) identified a GlyR α1 D80 residue, which as well as being capable of binding Zn^{2+} also produced a receptor insensitive to Zn^{2+} enhancement of glycine-evoked responses when substituted with an Ala residue. However, a subsequent study by Lynch *et al*, (1998) demonstrated that GlyR $\alpha1^{D80A}$

ablated potentiation only of glycine mediated currents and not those elicited by taurine, another agonist of the GlyR that is also thought to bind to the glycine recognition site (Schmieden et al., 1993). This suggests either there is more than one Zn^{2+} enhancement site for each agonist, a seemingly unlikely proposition given that both agonists bind to the same receptor region and Zn^{2+} has the same potency for causing potentiation of both agonist-activated currents, or that D80A is having a complicated action on the Zn^{2+} potentiation site in a manner unrelated to the direct coordination of the cation. The study by Lynch *et al*, (1998) also identified a number of other residues all within the extracellular TM2-3 loop that attenuate Zn^{2+} induced enhancement when substituted with alanine; however the chemical nature of these residues is not consistent with Zn^{2+} coordination. Studies of other positive modulators of cys-loop receptors locate the $GABA_A$ potentiating benzodiazepines in the N-terminal extracellular domain (Sigel and Buhr, 1997), whilst anaesthetics and ethanol have been suggested to interact with the cys-loop receptor transmembrane domains (Mihic et al., 1997). Thus from current studies there are no definitive candidate regions to begin a search for a discrete Zn^{2+} potentiating site in the GlyR.

This study took advantage of an observation in chapter three that GlyR α1 and α2 appear to have subtly different sensitivities to Zn^{2+} potentiation of glycine-evoked responses (Fig 3.1*A-C*). An initial comparative scan of the GlyR α1 and α2 N-terminal domains was therefore made and substitutions to swap potential Zn^{2+} binding residues between the two receptor subtypes identified a candidate Zn^{2+} binding residue responsible for this differential sensitivity. This study used this information in combination with the AChBP structural model to characterise a discrete site for Zn^{2+} potentiation. Furthermore, it also identified an important regulatory element, which appeared to control the ability of this site to influence receptor function and attempt to explain how the site may exert a modulatory role on receptor efficacy via the cys-loop gating domain.

Results

GlyR α1 and α2 exhibit distinct sensitivities to Zn^{2+} mediated potentiation

The sensitivity of the GlyR α1 and α2 subtypes to Zn^{2+} mediated potentiation of 50 % maximal Gly responses was compared using whole-cell recordings from HEK cells. To accurately maintain low concentrations of Zn^{2+} the buffering agent tricine was used to remove interference from Zn^{2+} contamination in the external saline solution (Suwa et al., 2001). Consequently, in the presence of 10 mM tricine a significant 15-fold increase in the potentiating Zn^{2+} EC_{50} was observed from 13.9 ± 3.4 nM, (n = 4) for GlyR α1 to 203 ± 68 nM, (n = 5) for GlyR α2 ($P < 0.05$; Fig 5.1*A,C*). This distinct difference was not affected by co-expression with the GlyR ancillary β-subunit (Fig 5.1*B*), whose faithful incorporation to form αβ heteromers was ratified as before, by an approximate 20-fold shift in picrotoxin sensitivity (data not shown; Pribilla et al., 1992). The Hill slopes for Zn^{2+} mediated potentiation varied between 1.2 and 1.5 suggesting more than one Zn^{2+} ion coordinates to each receptor oligomer. To identify the determinant(s) responsible for differential Zn^{2+} sensitivity the extracellular domain was scanned for residues that differed between GlyR α1 and α2 by concentrating on classical Zn^{2+} binding substituents; Cys, Asp, Glu, and His (Auld, 2001). Three locations were identified (Fig 5.1*D*) and upon individual reconstitution of the GlyR α1 variations into α2, an $\alpha2^{E201D}$ substitution was found to be solely sufficient to recover α1 levels of sensitivity to potentiating Zn^{2+} (Fig 5.1*A,C*) with no influence observed for $\alpha2^{L178Q, S179E, D180Q}$ or $\alpha2^{E187D}$ mutated receptors (data not shown).

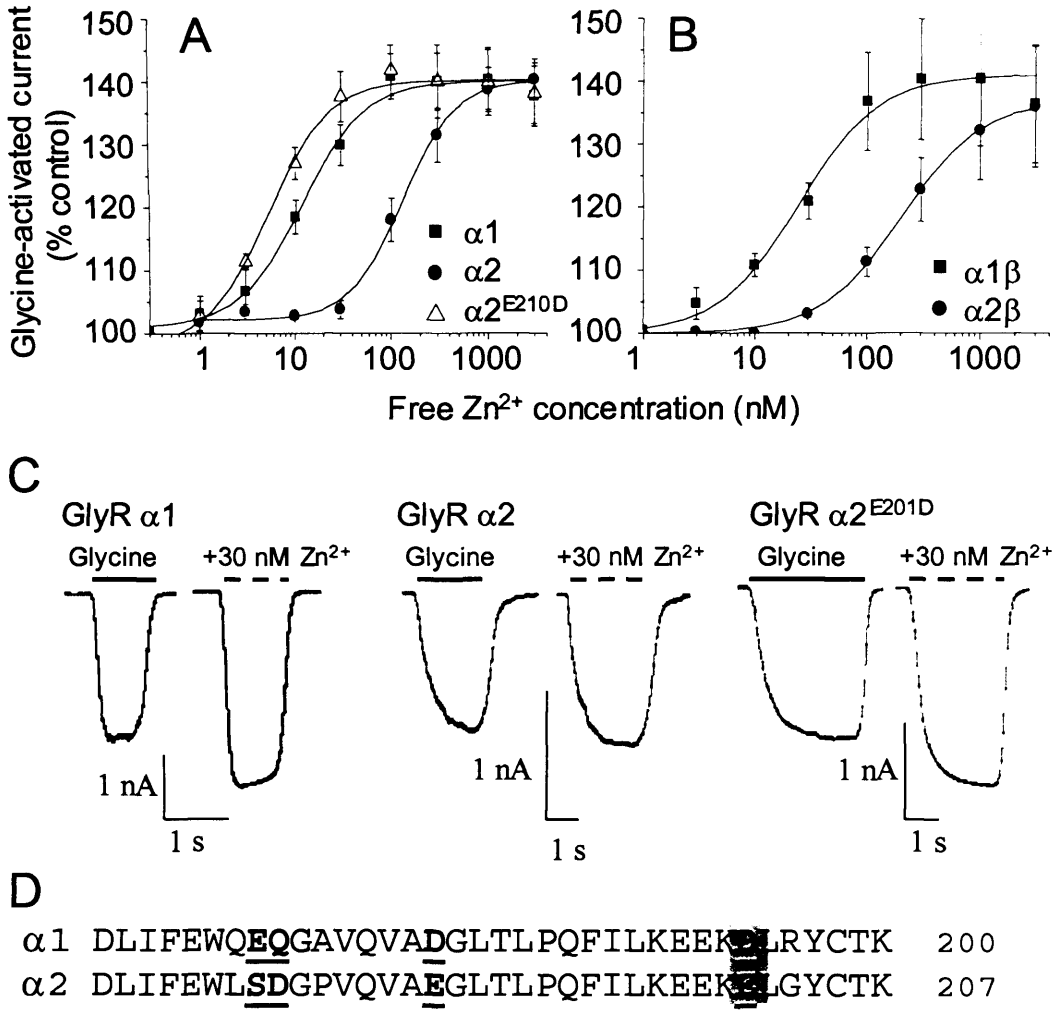

Figure 5.1 Zn^{2+} potentiation of 50 % maximal Gly responses for GlyR α1 and α2 in 10 mM tricine from whole-cell recordings in HEK cells. *A*, GlyR α2 recovers α1 levels of sensitivity to potentiating Zn^{2+} when reconstituted with the homologous residue to α1 D194, to generate $\alpha2^{E201D}$. *B*, GlyR α1β and α2β heteromers retain differential Zn^{2+} potencies for potentiation. *C*, Raw data traces of 50 % maximal glycine responses in the presence and absence of 30 nM Zn^{2+} for GlyR α1, GlyR α2 and GlyR $\alpha2^{E201D}$. *D*, Amino acid sequence alignment of GlyR α1 and GlyR α2 displaying the region of the N-terminal extracellular domain that harbours differences in potential Zn^{2+} binding residues (bold, underlined). A grey box highlights the residue responsible for the differential sensitivity to Zn^{2+} mediated potentiation between α1 and α2. $N = 4 - 6$. Maximal potentiation was normalised to 140 % at the 1 - 3 μM Zn^{2+} measurement for ease of comparison, though the maximal potentiation did not differ significantly between any individual receptor subtype (data not shown).

GlyR α1 E192, D194 and H215 are all essential for high sensitivity to potentiating Zn^{2+}

The discovery that a residue equivalent to GlyR α1 D194, a potential Zn^{2+} binding residue, is capable of influencing the potency of Zn^{2+} potentiation suggests this moiety may be an a direct contributor to Zn^{2+} binding at the potentiation site. To test this hypothesis it is necessary to remove the Zn^{2+} binding power of the Glu side chain by mutation to, for example, an inert alanine. Unfortunately due to the biphasic nature of Zn^{2+} action at the GlyR, where Zn^{2+} potentiates at low doses (0.1-10 μM) and inhibits at doses greater then 10 μM (Bloomenthal et al., 1994; Chapter 3), any attempts to measure substantial reductions in the sensitivity to Zn^{2+} enhancement will be masked by the onset of the contaminating Zn^{2+} mediated inhibition. To partially alleviate this effect, all experiments to identify the Zn^{2+} potentiation binding site were performed using an H107N background (defined as Reduced Inhibition - RI) GlyR, which exhibits a dramatically attenuated sensitivity to inhibitory Zn^{2+} without overtly affecting other receptor macroscopic properties (Table 5.1). However, it was not possible to completely remove the interfering Zn^{2+} mediated inhibition component as all other candidate residues for the inhibitory site have significant side effects on general receptor properties (as discussed in chapters 3 & 4). To further reduce the sensitivity to Zn^{2+} mediated inhibition all recordings were made using a co-application protocol for Gly plus Zn^{2+} as this favours the rapid onset of Zn^{2+} potentiation over the delayed onset of Zn^{2+} inhibition (Chapter 3). This resulted in an IC_{50} for Zn^{2+} inhibition at RIGlyR α1 of >3000 μM. In addition, potentiation was measured for two agonists, glycine and taurine, as residues that are not part of the presumed sole potentiating Zn^{2+} site have been identified that knock out enhancement of currents activated by one agonist but not the other, presumably due to an indirect affect on some downstream transduction mechanism (Lynch et al., 1998). However, Zn^{2+} potentiation of both glycine and taurine EC_{50} responses can be ablated, as demonstrated for the RI $\alpha1^{D194A}$ (Fig 5.2*A,B*). As an apparent consequence of removing Zn^{2+} enhancement the sensitivity to competing Zn^{2+} inhibition increased from > 3000 μM to 270 ± 50 μM (n = 3; Table 5.1).

To elucidate further residues capable of interacting with the putative α1 D194 based binding site, alanine point mutagenesis was carried out on classical Zn^{2+} binding

residues selected from motifs predicted to be structurally close to D194 in accordance with a GlyR structure modelled on the AChBP (See methods and Fig 5.2*C*; Brejc et al., 2001). This strategy identified two further residues, E192 and H215 that may contribute to Zn^{2+} potentiation for both Gly and taurine currents. The mutant RIGlyR $\alpha1^{E192A}$ entirely ablated Zn^{2+} potentiation, whilst RI$\alpha1^{H215A}$ dramatically reduced the potency of Zn^{2+} enhancement such that the Zn^{2+} EC_{50} for potentiation of 50 % maximal glycine responses was increased from 0.8 ± 0.2 μM, (n = 4) for RIGlyR α1 to 22 ± 4 μM, (n = 4) for the mutant ($P < 0.05$; Fig 5.2*A,B*). The results for other Ala substituted acidic residues had no effect on the potency of Zn^{2+} enhancement (Table 5.1). By removing, or reducing, Zn^{2+} enhancement the sensitivity to competing Zn^{2+} inhibition increased for both RI$\alpha1^{E192A}$ and RI$\alpha1^{H215A}$ (Fig 5.2*A, B*; Table 5.1). All three of these RI mutants, $\alpha1^{E192A}$, $\alpha1^{D194A}$ and $\alpha1^{H215A}$ did not shift the maximal responses evoked by the agonist and only RIα^{D194A} exerted a modest 3-fold shift upon the agonist EC_{50} (Table 5.1) suggesting these mutations selectively affected the Zn^{2+} potentiation binding site and do not exert a general perturbation on receptor function. Importantly, with regards to the potential of these residues to form the core of a Zn^{2+} binding site, the GlyR homology model (Fig 5.2*C*) predicts each of these residues, E192, D194 and H215 to reside in close proximity to one another and to all face the same direction pointing out into solution from the outside face of the N-terminal extracellular domain. This is in accord with the site being accessible to Zn^{2+}. To highlight the localised nature of this small domain to Zn^{2+} potentiation, alanine mutagenesis was carried out on other residues facing out into solution, selecting those residues immediately to either side of the putative Zn^{2+} binding site. These RI $\alpha1^{K190A}$, $\alpha1^{R196A}$, $\alpha1^{R213A}$ and $\alpha1^{E217A}$ mutated receptors did not have any significant shifts in Gly, taurine or Zn^{2+} EC_{50}s or in the size of maximal Zn^{2+} potentiation or maximal Gly currents (Table 5.1). In addition, co-expression of a GlyR RI$\alpha1^{E192A}$ with the β-subunit did not recover Zn^{2+} mediated potentiation suggesting the β-subunit is not an important contributor to Zn^{2+} enhancement (data not shown; n = 3).

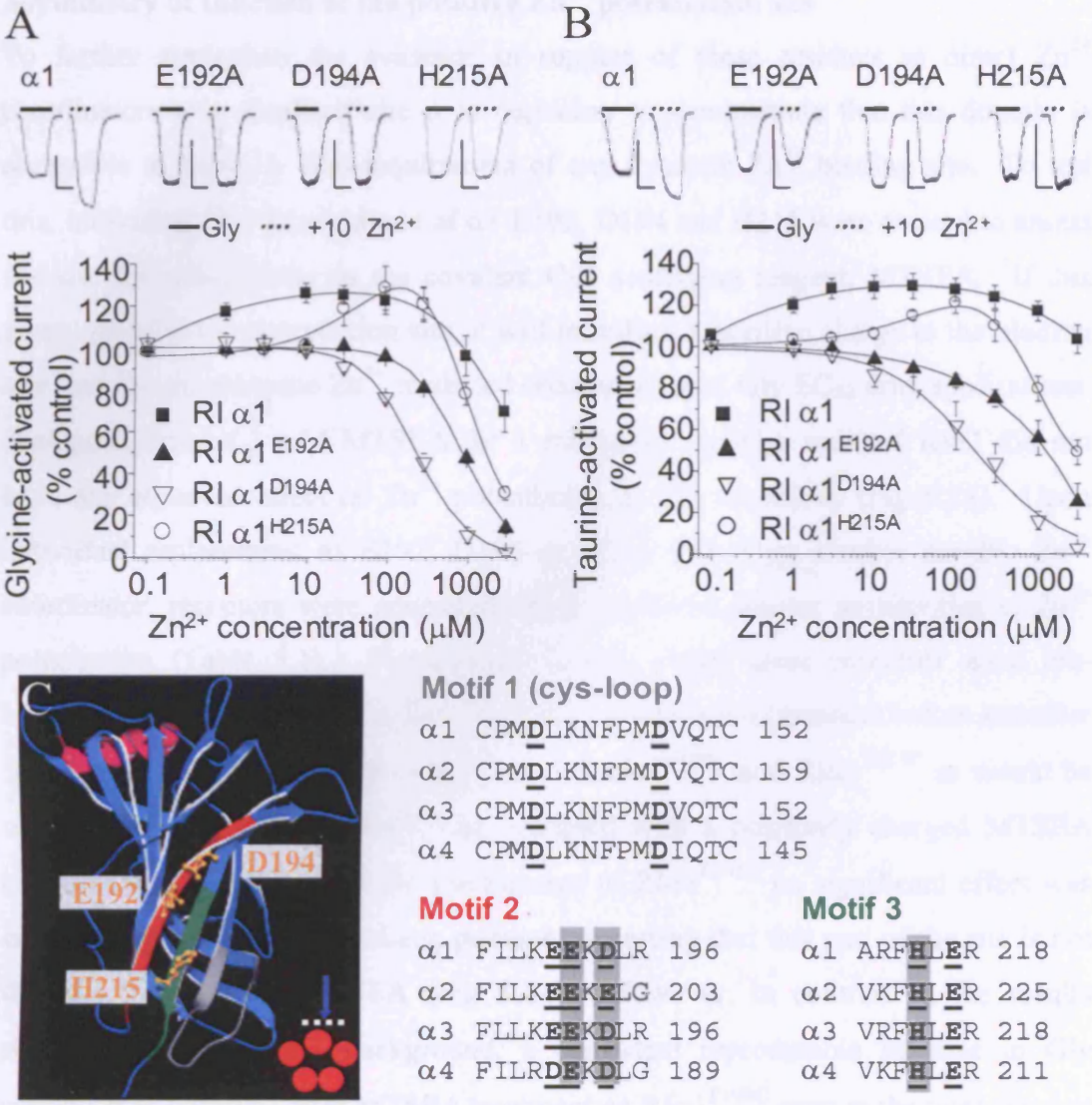

Figure 5.2 Zn^{2+} dose response curves for the modulation of 50 % maximal responses of Gly or taurine to screen for residues important in Zn^{2+} potentiation. All experiments were performed on a reduced sensitivity to Zn^{2+} inhibition background (*reduced inhibition – RI*) GlyR $\alpha1^{H107N}$. *A*, Gly and *B*, taurine both exhibit equally attenuated sensitivity to Zn^{2+} enhancement for all three candidate residues identified, RIGlyR$\alpha1^{D194A}$, RI$\alpha1^{E192A}$ and RI$\alpha1^{H215A}$ compared to RIα1. Insets represent typical raw data traces for the RIα1 background and mutants in the absence and presence of 10 μM Zn^{2+}, scale bars represent 1 nA by 1 s. *C*, Amino acid motifs in the extracellular GlyR α1 domain and homologous GlyR α counterparts that reside in close proximity to the identified $\alpha1^{D194A}$; based on the AChBP. Potential Zn^{2+} binding residues are in bold and underlined, whilst identified, important residues are highlighted in grey boxes. $N = 4 - 8$.

Asymmetry of function at the putative Zn^{2+} potentiation site

To further strengthen the evidence in support of these residues as direct Zn^{2+} coordinators at a localised site it is necessary to demonstrate that this domain is accessible to water, a vital requirement of any dynamic Zn^{2+} binding site. To test this, individual Cys substitutions of α1 E192, D194 and H215 were created to assess the site for accessibility to the covalent Cys modifying reagent, MTSEA. If this agent modifies the potentiation site, it will introduce a positive charge to the binding site that should attenuate Zn^{2+} mediated enhancement of Gly EC_{50} drug applications. Pre-application of 3 mM MTSEA for 1 minute to non-Cys mutated RIα1 did not have any observed effect on Zn^{2+} potentiation or Gly sensitivity (Fig 5.3*A*). Upon individual replacement of E192, D194 or H215 with Cys, another capable Zn^{2+} coordinator, receptors were generated which exhibited similar sensitivities to Zn^{2+} potentiation (Table 5.1). Significantly though, when these receptors were pre-incubated with 3 mM MTSEA for 1 min, Zn^{2+} potentiation (assessed before and after in the same cell) was ablated in the cases of $RI\alpha1^{D194C}$ and $RI\alpha1^{H215C}$ as would be expected if a Cys binding Zn^{2+} was occupied with a positively charged MTSEA substituent (Fig 5.3*B,C*). In the unique case of $RI\alpha1^{E192C}$ no significant effect was observed after chemical treatment, perhaps suggesting that this part of the site is not directly accessible to MTSEA (Fig 5.4*A*). However, in contrast to the results obtained with the RIα1 background, a consistent reproducible increase in Gly potency was observed after MTSEA treatment on $RI\alpha1^{E192C}$ even in the total absence of Zn^{2+}, with the 50 % maximal glycine response being potentiated by 45 ± 12 %, (n = 4; Fig 5.4*B*). This suggests the E192 location is accessible to MTSEA, as it affects the sensitivity of the receptor to Gly, but that the glutamate side chain moiety, unlike D194 and H215, is probably not necessarily a direct or major contributor to Zn^{2+} coordination.

The data so far clearly demonstrate that α1 E192, when perturbed by substitution with an Ala residue, exerts a strong influence on Zn^{2+} mediated potentiation but unlike D194 and H215 it does not exhibit properties that are entirely consistent with direct binding to Zn^{2+} via its side chain moiety. This raises the possibility that the effect elicited by E192 may be in response to a perturbation of the β-strand 9

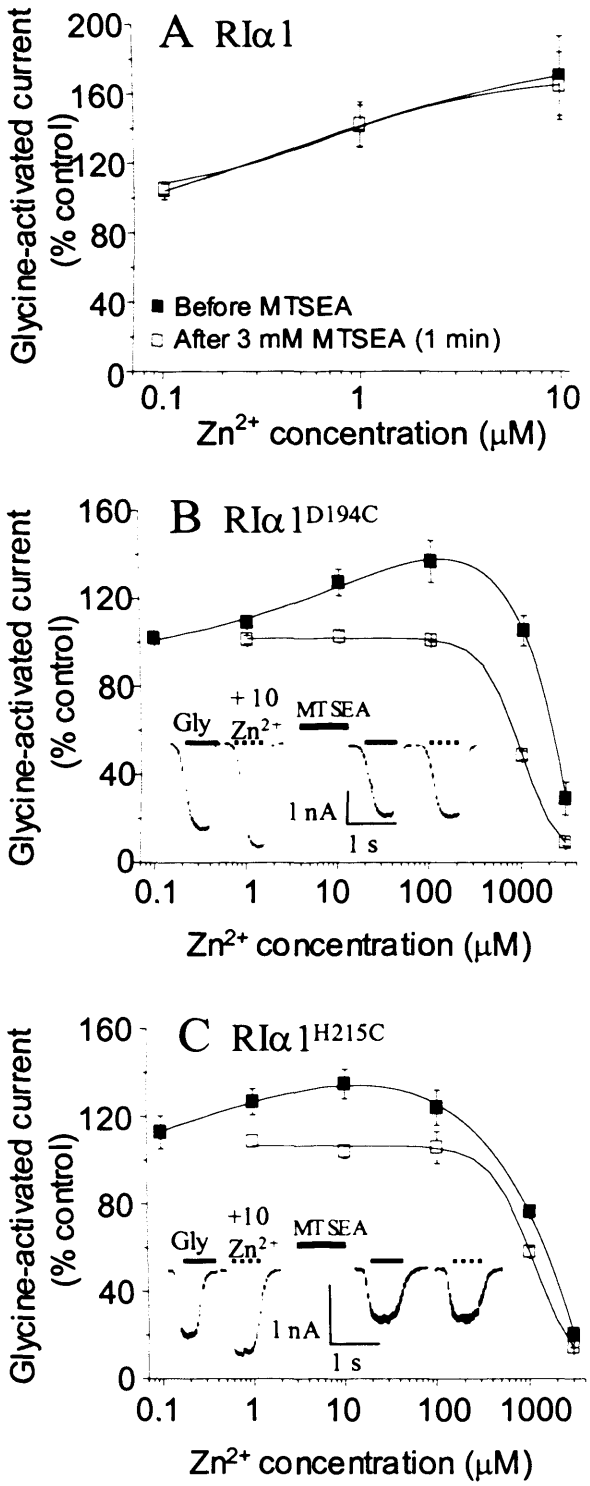

Figure 5.3 Covalent modification experiments using MTSEA to measure the accessibility of the candidate Zn^{2+} potentiation site. *A-C*, Zn^{2+} dose response curves for modulation of 50 % maximal Gly responses were measured for the sensitivity to Zn^{2+} enhancement on RIα1 and receptors mutated to incorporate Cys mutations at putative Zn^{2+} binding residues. This was assessed before and after incubation of HEK cells with 3 mM MTSEA for 1 min. *A*, RIGlyR α1 background does not exhibit any perturbed sensitivity to Zn^{2+} mediated potentiation in response to MTSEA treatment, whilst complete ablation of Zn^{2+} enhancement is observed after $RI\alpha1^{D194C}$ (*B*) and $RI\alpha1^{H215C}$ (*C*) have been exposed to the Cys covalent modifying reagent. The insets present example raw data recordings from HEK cells showing EC_{50} Gly responses ± 10 μM Zn^{2+}, before and after MTSEA incubation, for $RI\alpha1^{D194C}$ or $RI\alpha1^{H215C}$. $N = 4$ for all experiments.

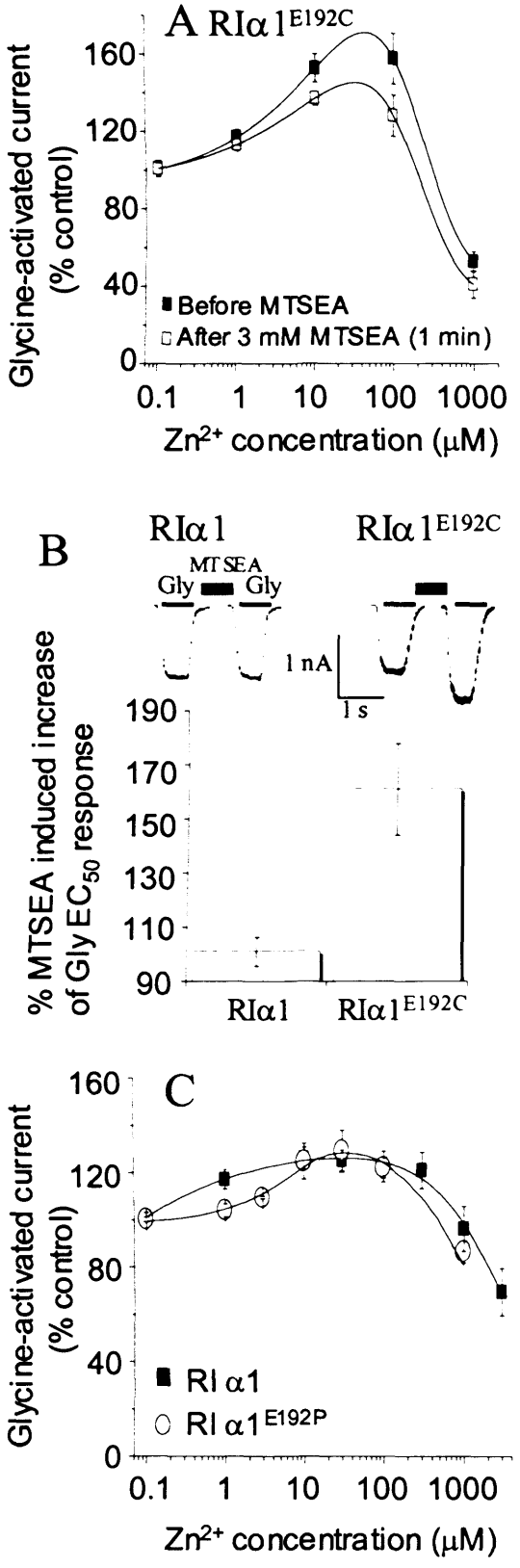

Figure 5.4 GlyR α1 E192 is unlikely to directly coordinate Zn^{2+} via the glutamate side chain. *A*, 50 % maximal Gly responses recorded from HEK cells reveal that RIα1^{E192C} shows only minor attenuation of sensitivity to Zn^{2+} enhancement in response to MTSEA treatment. *B*, Bar chart and raw data traces demonstrating that RIα1^{E192C} does appear to be modified by MTSEA treatment as an increase in sensitivity of the receptor to the agonist Gly is observed. *C*, Further evidence that E192 may influence Zn^{2+} mediated inhibition in a manner independent of its side chain moiety. Replacement with a Pro residue, typically considered to introduce rigidity to the protein backbone is incapable of supporting Zn^{2+} coordination via its side chain. Zn^{2+} dose response curves on 50 % maximal Gly responses for RIα1^{E192P} produced a receptor that retained a high sensitivity to Zn^{2+} enhancement only 5-fold less sensitive than the RIα1 background (Table 5.1). $N = 3 - 4$.

backbone (nomenclature of Brejc et al., 2001) in this region, either because the backbone indirectly disrupts the nearby Zn^{2+} potentiation site, or because the polar peptide backbone is directly contributing to Zn^{2+} coordination at this position. To address this issue an RIα1^{E192P} GlyR was generated to replace glutamate with proline, an amino acid associated with introducing an increased level of rigidity to the peptide backbone (Chou and Fasman, 1974;Yohannan et al., 2004). This might therefore prevent the same apparent disruption of the peptide backbone that is observed for RIα1^{E192A}. In this unique circumstance, potentiation was not ablated and the receptor merely experienced a subtle, reduced potency for Zn^{2+} potentiation from 0.8 ± 0.2 μM, (n = 4) for RIα1 to 4.2 ± 0.8 μM, (n = 3) for RIα1^{E192P} ($P < 0.05$; Fig 5.4*C*; Table 5.2). As the proline side chain is considered to be a poor donor for Zn^{2+} coordination this suggests that this region must retain a specific conformation at the backbone of E192 in order to retain Zn^{2+} mediated potentiation. As a control, the mutation of D194 to a Pro was found to still ablate Zn^{2+} mediated potentiation, the expected outcome if it is indeed the side chain moiety that is contributing to Zn^{2+} coordination at this position (Table 5.2; n = 3).

Comparative influence of GlyR α1 E192 and D194 on β-strand 9 with H215 of β-strand 10

In all three point mutations where Zn^{2+} potentiation is attenuated or ablated there was always an increased sensitivity to the competing Zn^{2+} inhibition. This could simply reflect an enhanced ability of Zn^{2+} to exert inhibition from the inhibitory site as competition, when the Zn^{2+} potentiating component has been removed. In this simple case, removal of a further residue at the Zn^{2+} inhibitory site should cause a direct rightward shift to reduce the sensitivity profile for inhibition of the RIα1^{E192A}, RIα1^{D194A} and RIα1^{H215A} mutants. In turn this may allow for more accurate assessment of the extent by which Zn^{2+} enhancement was ablated for RIα1^{E192A} and RIα1^{D194A} where any low sensitivity enhancement remaining is masked by the onset of inhibition. Introduction of an RIα1^{H109F} mutation, originally identified by Harvey et al, (1999), further reduced the sensitivity of Zn^{2+} mediated inhibition without affecting Zn^{2+} potentiation or overt disruption of other receptor properties (Fig 5.5*A*, Table 5.2). Evaluation of RIα1$^{H109F,\ H215A}$ did indeed generate, as predicted, a modest rightward shift to reduce the sensitivity profile of the inhibitory component

of this mutant (Fig 5.5*B*). However for both RIα1$^{H109F, E192A}$ and RIα1$^{H109F, D194A}$ there was not the expected reduction in potency of inhibitory Zn^{2+}, with RIα1$^{H109F, D194A}$ actually exhibiting evidence for a novel biphasic inhibition, suggestive of two separate inhibitory sites each with differing potencies (Fig 5.5*C,D*).

This could reflect a situation whereby the RIα1^{E192A} and RIα1^{D194A} are exerting a more complicated effect on the potentiation site, which has resulted in a reversal of the sites polarity to switch a high potency potentiation site into a novel low potency inhibitory site. Thus further ablating the original low potency inhibitory site based on H107 and H109 would not affect the receptors inhibitory profile as the inhibition now arises largely from the reversed potentiation site. To elucidate the nature of the actions of E192 and D194 on Zn^{2+} mediated potentiation more thoroughly, each of these residues was instead mutated to a non-Zn^{2+} binding residue with an extra carbon atom in the side chain, as is present on the Glu and Asp side chains, to ensure this complicating side effect of apparently converting the Zn^{2+} potentiation site to one that mediates inhibition was not specific to alanine substitution. In the case of RIα1^{E192K}, potentiation was still ablated, but consistent with the previous evidence suggesting this residue exerts a more complicated effect on the potentiation site not directly correlated with the properties of the side chain moiety, an even clearer biphasic inhibitory profile was now observed (Fig 5.6*A*, Table 5.2). This supports the supposition that disruption of E192 to an Ala residue was indeed reversing the polarity of the potentiation site to generate two separate inhibitory Zn^{2+} sites, the novel E192K based inhibitory site and the original H107/H109 based low potency inhibitory site. Conversely, the RIα1^{D194K} receptor, which also exhibited ablated Zn^{2+} potentiation, revealed less of an increased sensitivity to inhibitory Zn^{2+} compared to its RIα1^{D194A} counterpart and did not result in a biphasic inhibitory profile, raising the possibility that introduction of a Lys at D194 had perhaps not reversed the polarity of the potentiation site (Fig 5.6*B*). The modest increase in sensitivity to Zn^{2+} mediated inhibition for RIα1^{D194K} may simply reflect the removal of Zn^{2+} enhancement therefore allowing the H107/H109 based inhibitory site to manifest its effect with a monophasic profile. This was validated by evaluation of an RIα1$^{H109F, D194K}$ receptor, which demonstrated a monophasic rightward shift to reduced sensitivity for inhibitory Zn^{2+} (Fig 5.6*B*) comparable to that seen for

RIα1$^{H109F,\ H215A}$ (Fig 5.5*B*). Therefore in agreement with the MTSEA studies suggesting that D194 is a genuine Zn^{2+} coordinator at the binding site, there was no detectable functional side effect for an RIα1^{D194K} disruption on the transduction process, such as a polarity reversal of the potentiation site.

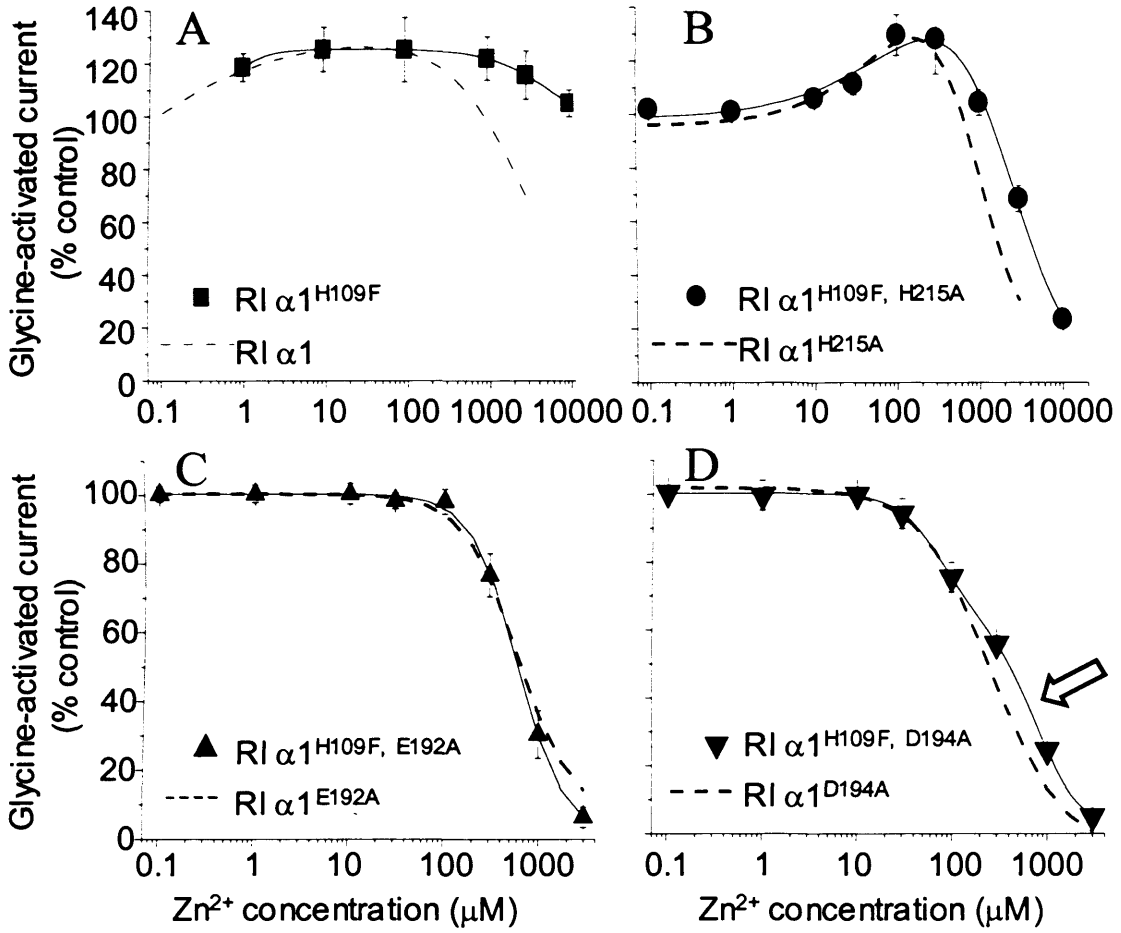

Figure 5.5 GlyR α1^{E192A} and α1^{D194A} do not exhibit pure effects on Zn^{2+} binding at the potentiation site. Introduction of an H109F mutation to attenuate the sensitivity of the H107/H109 based Zn^{2+} inhibitory site results in a clear rightward shift of the inhibitory curves for *A*, RIα1^{H109F} and *B*, RIα1$^{H109F,\ H215A}$ compared with RIα1, demonstrating that Zn^{2+} inhibition at RIα1 and RIα1^{H215A} is derived from the H107/H109 site. *C*, Introduction of an H109F mutation to create RIα1$^{H109F,\ E192A}$ does not produce any further shift of the inhibitory profile suggesting Zn^{2+} inhibition at RIα1^{E192A} is no longer derived from the H107/H109 inhibitory site and that a novel inhibitory site is probably responsible for inhibition. *D*, In the case of RIα1$^{D194A,\ H109F}$ a rightward shift of the lower phase of the inhibitory profile is evident creating a biphasic inhibition curve (arrow), supporting the presence of two inhibitory sites each with differing potencies, one derived from the H107/H109 based site and another novel inhibitory site. Most likely, E192A and D194A have reversed the 'polarity' of the potentiation site. The data for the non H109F based mutants, represented by dashed lines, are taken from Fig 5.2*A*. $N = 4 - 8$.

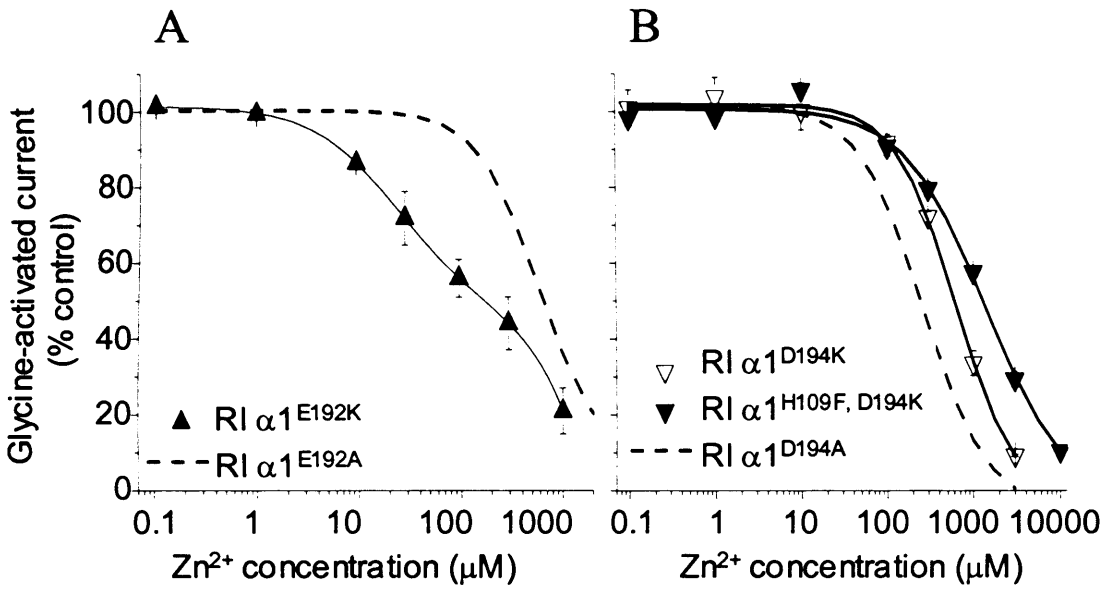

Figure 5.6 GlyR $\alpha1^{D194K}$ exhibits properties consistent with a pure effect on Zn^{2+} binding at the potentiation site. Zn^{2+} dose response curves were evaluated for the modulation of 50 % maximal glycine responses. *A*, GlyR RI$\alpha1^{E192K}$ exhibits a clear biphasic inhibitory profile consistent with this receptor ablating potentiation and generating an additional inhibitory site, most likely by reversing the polarity of the original potentiating site. *B*, GlyR RI$\alpha1^{D194K}$ shows a reduced increase in sensitivity to Zn^{2+} mediated inhibition compared to its D194A counterpart (dashed line, from Fig 5.2*A*) but still ablates the Zn^{2+} potentiation of glycine responses. Furthermore, introduction of H109F to disrupt the original H107/H109 inhibitory site decreases the sensitivity of this receptor to inhibitory Zn^{2+}. This suggests Zn^{2+} mediated inhibition in the RI$\alpha1^{D194K}$ receptor is derived from the H107/H109 site, thus D194K has not reversed the polarity of the potentiation site and may not be interfering with transduction from the Zn^{2+} site but rather is having an effect on binding at the potentiation site. $N = 3 - 6$.

GlyR α1 T151 is a critical control element for Zn^{2+} potentiation

A previously generated chimera, (Laube et al., 1995) where part of the GlyR α1 subunit was replaced by the ancillary β receptor, including a section of the cys-loop region investigated here, was reported to ablate Zn^{2+} potentiation. The two Asp residues, D141 and D148 of the Cys loop, mutated in this report, did not exert a selective effect on Zn^{2+} potentiation with D141A having no discernable affect and D148A ablating receptor function, consistent with a previous report (Schofield et al., 2003;Table 5.1). One potential unexplored candidate residue is T151, which is chemically capable of interacting with Zn^{2+} through its hydroxyl group, and is also replaced by an Arg in the β-subunit. An alanine substitution was therefore introduced at α1 T151 to generate an RIα1^{T151A} GlyR. Subsequent examination of the Zn^{2+} enhancement of 50 % maximal Gly and taurine evoked responses revealed no detectable potentiation by Zn^{2+} (Fig 5.7*A,B*). Intriguingly, although the lack of potentiation was clear, there was also an unusual additional effect revealed in the form of a novel biphasic sensitivity to Zn^{2+} inhibition, with high (IC_{50} 1.6 ± 0.6 μM, n = 5) and low potency components (IC_{50} 1040 ± 290 μM, n = 5; Table 5.3). This biphasic profile was directly comparable for taurine (IC_{50} = 3.2 ± 0.8 μM, n = 5 and 2840 ± 820 μM, n = 3; Fig 5.7*B*). The potency for the high sensitivity inhibitory component is comparable to the original Zn^{2+} IC_{50} (0.8 ± 0.2 μM, n = 4) for potentiation of RIα1 (Table 5.1) raising the possibility that the α1^{T151A} substitution converted the Zn^{2+} potentiation site to a high sensitivity Zn^{2+} inhibitory site. In support of this hypothesis the RIα1$^{T151A, E192A}$ mutant, designed to disrupt the original potentiating site, reduced the sensitivity of the high potency component of the biphasic curve (Fig 5.7*A*; Table 5.3). Whilst removal of the H107N background mutation to recover the original inhibitory Zn^{2+} site gave an α1^{T151A} receptor with an increased sensitivity for the lower potency component (Fig 5.7*A,B*; Table 5.3).

To further characterise the role of T151, this residue was mutated to its β-subunit counterpart, RIα1^{T151R}, which ablated Zn^{2+} mediated potentiation at GlyR α1 and also generated a biphasic sensitivity to inhibitory Zn^{2+} (Fig 5.7*C*). In this case, whilst the sensitivity of the high potency component was still comparable to the Zn^{2+} potentiation EC_{50} of RIα1 (RIα1^{T151R} IC_{50} = 3.6 ± 0.4 μM, n = 4) the maximal contribution of the high sensitivity inhibitory component on glycine evoked

responses was reduced to 39 ± 3 %, (n = 4), from 73 ± 8 %, (n = 4), for RIα1^{T151A} (Fig 5.7*C*, Table 5.3). Threonine 151 was further mutated to the 5-HT$_{3A}$R counterpart, Asn, as this homologous receptor is also potentiated by Zn^{2+}; however, Zn^{2+} mediated potentiation was still abolished for this mutated RIα1^{T151N} receptor. Again, though the potency of the high sensitivity inhibitory component remained similar to the original Zn^{2+} potentiation EC_{50} of RIα1 (RIα1^{T151N} IC_{50} = 1.6 ± 0.7 μM, n = 4) but the maximal contribution of this high potency inhibitory site was now even less at just 6.5 ± 0.3 %, (n = 4; Fig 5.7*C*, Table 5.3).

The 5-HT$_{3A}$R Zn^{2+} potentiation site does not operate through its GlyR T151 homologue

The data for GlyR α1^{T151N} demonstrated that this receptor was not amenable to potentiation by Zn^{2+} suggesting that this residue may not form part of the apparatus required for Zn^{2+} enhancement of the homologous cys-loop 5-HT$_{3A}$R. To validate this assertion a wild-type 5-HT$_{3A}$R and a 5-HT$_{3A}$R^{N170A} were each assessed for sensitivity to Zn^{2+} mediated potentiation of 50 % maximal serotonin induced currents. Serotonin in the presence or absence of Zn^{2+} was co-applied to receptors without Ca^{2+} or Mg^{2+} present as these cations compete with Zn^{2+} for potentiation of 5-HT$_{3A}$Rs, (Hubbard and Lummis, 2000; though Ca^{2+} and Mg^{2+} were still present in the background saline solution to maintain the health of the cells). Serotonin dose response curve analysis showed that the sensitivity of each receptor to serotonin was directly comparable (wild-type EC_{50} = 0.86 ± 0.11 μM, n = 3 and 5-HT$_{3A}$^{N170A} EC_{50} = 1.05 ± 0.25 μM, n = 3; Fig 5.8*B*). Furthermore, in agreement with the supposition that N170 does not play an equivalent role in the 5-HT$_{3A}$R to the GlyR T151 as regards Zn^{2+} potentiation, both serotonin receptors exhibited biphasic profiles in response to Zn^{2+} modulation with the sensitivity to potentiating Zn^{2+} and the maximal enhancement remaining indistinguishable (Fig 5.8*C*, n = 3).

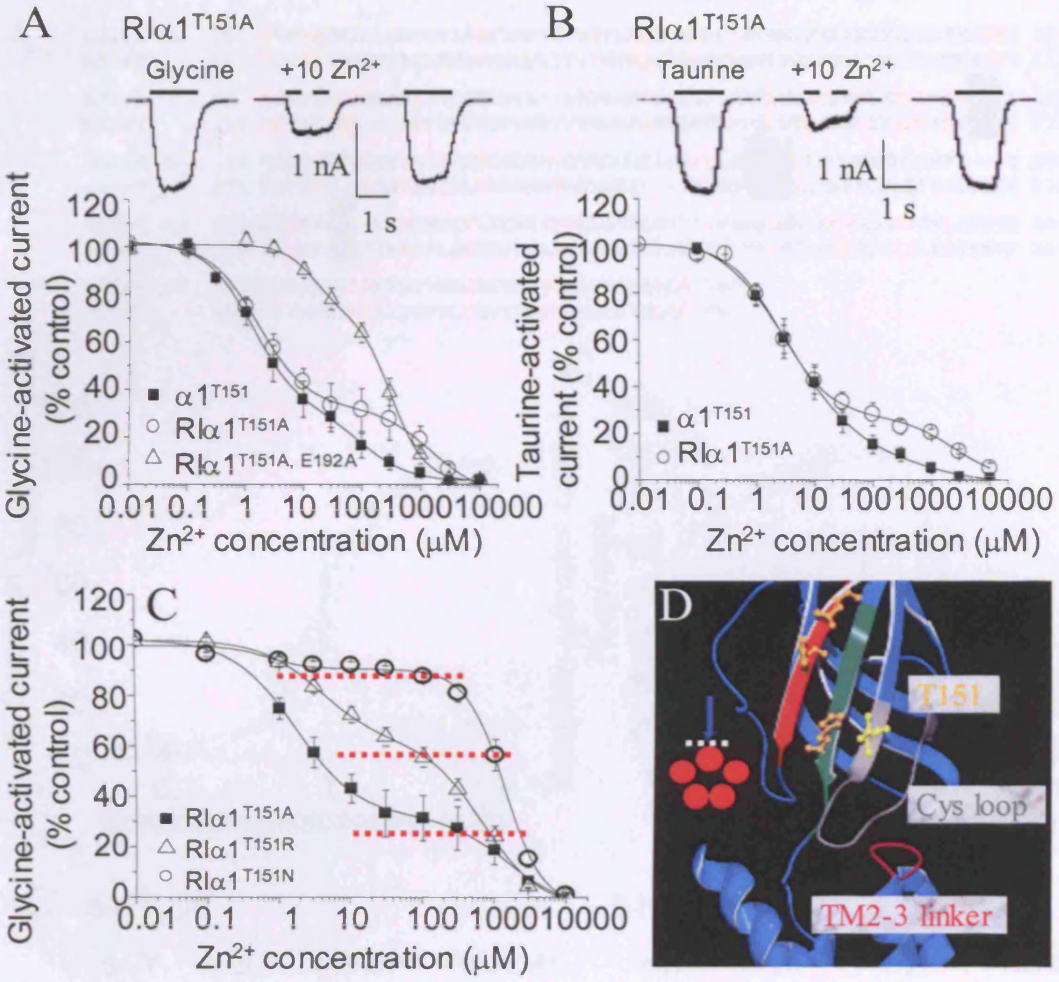

Figure 5.7 Zn^{2+} potentiation of 50 % maximal Gly or taurine responses is abolished in α1 T151 mutated receptors and replaced with a novel biphasic inhibition. $RI\alpha1^{T151A}$ exhibits biphasic inhibition for *A*, Gly and *B*, taurine. The lower potency component can be shifted to the left when the low sensitivity site residue N107 (RI) is reconstructed (N107H) to create $\alpha1^{T151A}$. Introduction of E192A to perturb the original Zn^{2+} potentiation site, by contrast, induces a reduction in the sensitivity of the high potency inhibition component of the curve on $RI\alpha1^{T151A}$. *C*, $RI\alpha1^{T151N}$ or $RI\alpha1^{T151R}$ also ablate Zn^{2+} potentiation of 50 % maximal Gly responses and introduced biphasic inhibition curves. Notably the potency of the two phases remains comparable, but the maximum inhibition (dashed red lines) for the high potency component is reduced in the order $RI\alpha1^{T151A} > RI\alpha1^{T151R} > RI\alpha1^{T151N}$. *D*, GlyR α1 extracellular domain based on AChBP, highlighting T151 (yellow) within the putative cys-loop gating domain (grey) and its proximity to another important determinant in gating, the TM2-3 linker region (pink; Lynch et al, 1997). $N = 4 - 6$.

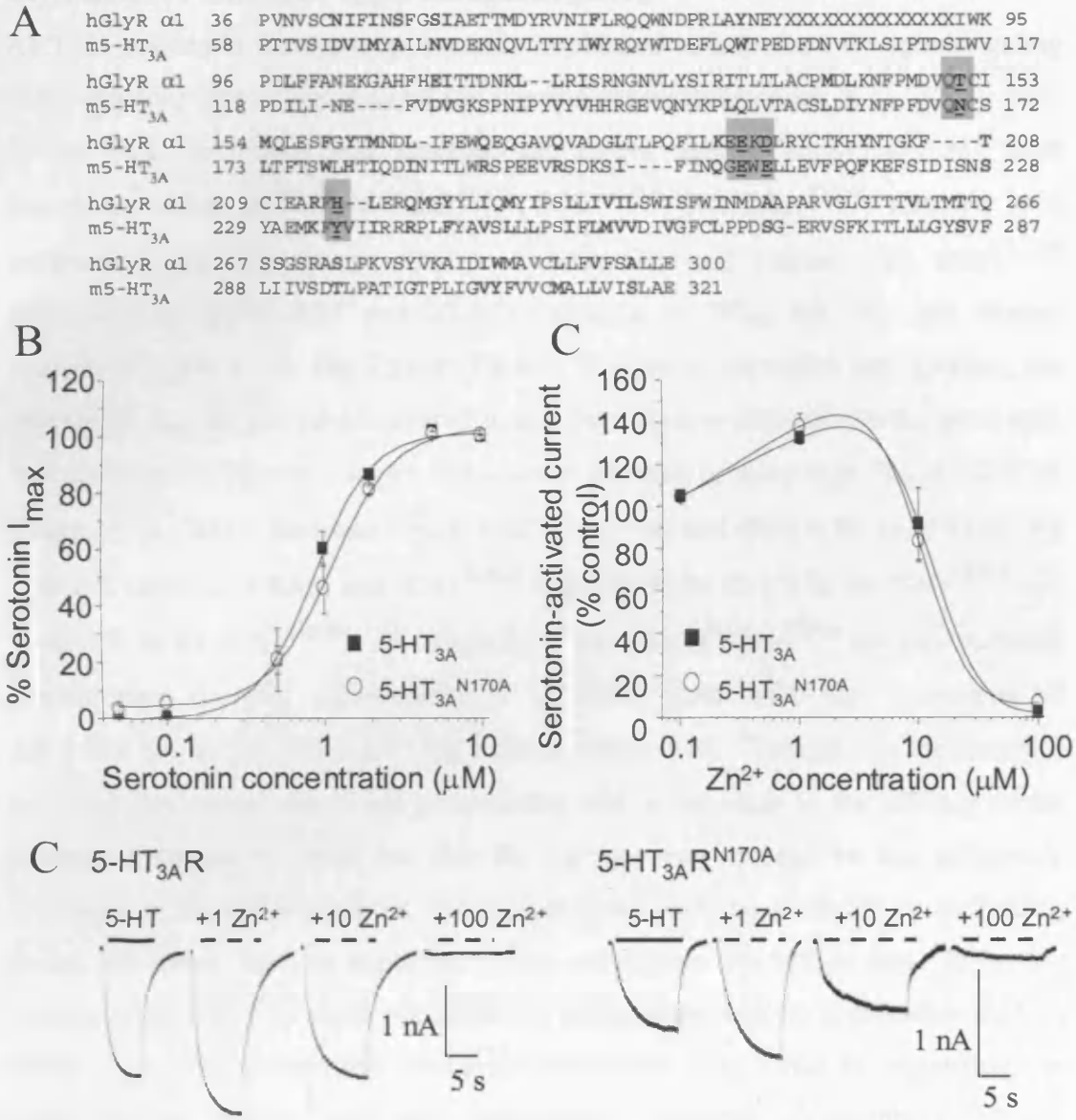

Figure 5.8 The 5-HT_{3A}R N170 homologue of GlyR α1 T151 does not influence Zn^{2+} enhancement. *A*, ClustalW protein alignment of the N-terminal extracellular domain of GlyR α1 and the 5-HT_{3A}R; identical residues – red, conserved non-identical residues – blue, T151 and potentiation site Zn^{2+} binding residues – bold, underlined on grey background. *B*, Comparable agonist dose response curves for wild-type 5-HT_{3A}R and 5-$HT_{3A}R^{N170A}$. *C*, Indistinguishable dose-response curves for co-applied Zn^{2+} modulation of 50 % maximal serotonin responses. Zn^{2+} was co-applied in the absence of Ca^{2+} and Mg^{2+}. *D*, Typical raw data traces of Zn^{2+} (1 – 100 μM) modulation profiles for wild-type 5-HT_{3A}R and 5-$HT_{3A}R^{N170A}$. $N = 3 - 4$.

GlyR α1 T151 influences apparent agonist gating

As T151 resides in the cys-loop, recently implicated as important for agonist gating in the cys-loop based ligand-gated ion channel superfamily (Kash et al., 2003), each of the T151 mutations was assessed for altered agonist potencies. All three mutations, either $\alpha1^{T151A}$ or $RI\alpha1^{T151A}$, $RI\alpha1^{T151R}$ and $RI\alpha1^{T151N}$, resulted in a progressive reduction in sensitivity to both Gly and taurine with $RI\alpha1^{T151N}$ demonstrating an 11-fold and 23-fold increase in EC_{50} for Gly and taurine respectively (n = 4 – 5; Fig 5.9*A,B*; Table 5.3). Consistent with a gating effect, the percentage I_{max} for taurine (compared to maximal glycine responses in the same cell, termed 'relative efficacy'), which has a lower absolute efficacy than Gly at GlyR α1 (Lewis et al., 2003) decreased from 100 %, (n = 4) and 97 ± 4 %, (n = 4) of Gly maximal currents in RIα1 and $RI\alpha1^{T151A}$ respectively to 93 ± 3 % for $RI\alpha1^{T151R}$ and to 46 ± 6 % for $RI\alpha1^{T151N}$. Additionally in the case of $RI\alpha1^{T151N}$ the Gly maximal current also dropped significantly ($P < 0.05$) from wild type responses of 4.5 ± 0.4 nA to 2.9 ± 0.5 nA (Fig 5.9*A-D,* Table 5.3). Though this reduction in maximal Gly current amplitude is consistent with a reduction in the efficacy of the receptor it cannot be ruled out that the receptor may instead be less efficiently expressed at the cell surface i.e. the receptor may carry an assembly or trafficking defect. However, such an explanation does not explain the taurine data. In further support of an effect by these mutations on gating there was no appreciable shift in sensitivity to the competitive antagonist strychnine (Fig 5.10*A,B*) suggesting the ligand-binding region was not substantially distorted (Vandenberg et al., 1992a;Vandenberg et al., 1992b).

To investigate further the chemical properties required by the residue at position 151 e.g. polarity and side chain volume, five other T151 mutants were generated including: $GlyR\alpha1^{T151C}$, $\alpha1^{T151D}$, $\alpha1^{T151E}$, $\alpha1^{T151F}$ and $\alpha1^{T151S}$. Glycine and taurine dose response curves for the $\alpha1^{T151C}$, $\alpha1^{T151E}$, and $\alpha1^{T151S}$ receptors all showed a significant ($P < 0.05$) but small 2 - 4 fold increase in EC_{50} for both agonists (Fig 5.10*C,D*, Table 5.3) compared to the wild-type receptor. This was comparable to the $\alpha1^{T151A}$ receptor despite the fact that these new mutations retained polar electronegative moieties at this position. Furthermore introduction of a large hydrophobic side chain at this position in the form of $\alpha1^{T151F}$ did not cause a

significantly greater ($P > 0.05$) perturbation to agonist potencies than any of the previously inserted polar substitutions (Fig 5.10*C,D*, Table 5.3). Even more intriguing was that $\alpha1^{T151D}$, which introduced another polar electronegative side chain, produced a receptor with maximal currents less than 20 pA ($n = 10$).

GlyR α1 T151 and residues in the proposed Zn^{2+} potentiation site region can interact in mutated receptors

The mutation of GlyR α1 T151 to an Ala followed by an Arg and then an Asn resulted in a progressive reduction in the ability of Zn^{2+} to interact with the receptor via the Zn^{2+} potentiation site. As the function of the potentiation site was reversed to instead elicit inhibition this progressive reduction was measured as a decreasing contribution of the high sensitivity inhibitory component to the total amount of inhibition in the biphasic inhibition profile (Fig 5.7*C*). This same series of mutations also resulted in an apparent progressive deterioration in receptor gating, in the same order of T151A < T151R < T151N, suggesting that there may be a direct link between the Zn^{2+} potentiation site and domains involved in receptor gating. To further demonstrate a potential influence of the Zn^{2+} potentiation site on receptor gating via T151 the agonist EC_{50}s of Gly and taurine along with their maximal responses were compared for RI $\alpha1^{T151A, E192A}$, $\alpha1^{T151A, D194A}$, $\alpha1^{T151A, H215A}$ to the $RI\alpha1^{T151A}$ receptor. Whilst the presence or absence of H107N does not affect agonist potency at $\alpha1^{T151A}$ mutant receptors (Fig 5.9*C,D*, Table 5.3) and E192A, D194A and H215A mutations alone introduce minimal disruption to receptor function (Table 5.1), addition of these mutations to an $RI\alpha1^{T151A}$ background did cause a synergistic disruption to receptor gating. Introduction of E192A to $RI\alpha1^{T151A}$ reduced agonist potencies in a manner consistent with a change in channel gating. Gly and taurine EC_{50}s were both 10-fold higher and the taurine maximum was reduced from 100 % ($n = 4$) to 65 ± 4.3 %, ($n = 7$) of the Gly maximal response. Again the maximal Gly responses were also reduced from 4.0 ± 0.4 nA, ($n = 5$) for $RI\alpha1^{T151A}$ to 1.9 ± 0.5 nA, ($n = 7$) for $RI\alpha1^{T151A, E192A}$, consistent with a decrease in the efficiency of channel gating, assembly or trafficking. The strychnine sensitivity remained at wild-type levels suggesting the agonist-binding site retained the characteristics required for agonist binding (Fig 5.10*A,B*). In comparison to the dual mutation of T151 and E192, the strongest candidates for direct Zn^{2+} coordination,

RIα1$^{T151A,\ D194A}$ and RIα1$^{T151A,\ H215A}$ showed a more dramatic phenotype with Gly currents significantly reduced to 150 ± 70 pA, (n = 8 from 27) for RIα1$^{T151A,\ D194A}$ and 40 ± 10 pA, (n = 7 from 23) for RIα1$^{T151A,\ H215A}$ (Fig 5.11*A-C*). Once more the Gly EC_{50} increased significantly in a comparable fashion to RIα1$^{T151A,\ E192A}$ with a 14- and 24-fold increase to 220 ± 20 μM, (n = 4 from 24) and 370 ± 30 μM, (n = 2 from 23) for RIα1$^{T151A,\ D194A}$ and α1$^{T151A,\ H215A}$ respectively. The relative efficacy of taurine was also substantially reduced to 33 ± 6 %, (n = 3 from 24) for RIα1$^{T151A,\ D194A}$ and 40 ± 10 %, (n = 7 from 23) for RIα1$^{T151A,\ H215A}$ (Fig 5.11*A-C*). Thus D194 and H215, the strongest candidates for Zn^{2+} potentiation binding site residues, also have the strongest influence on receptor function when mutated in combination with T151A.

Further studies, mutating residues immediately surrounding the proposed Zn^{2+} binding site and which are presented on the same side of the β-strands, revealed that RI α1$^{T151A,\ K190A,}$ α1$^{T151A,\ R196A,}$ α1$^{T151A,\ R213A}$ and α1 $^{T151A,\ E217A}$ all exacerbated the properties of the RI α1^{T151A} mutation in a comparable way to the RIα1$^{T151A,\ E192A}$ mutation. This is despite the fact that individually these K190A, R196A, R213A and E217A mutations do not influence GlyR agonist properties (Table 5.1). The Gly and taurine EC_{50}s were increased in each case, whilst the maximal glycinergic response was reduced and taurine was reduced to a partial agonist with maximal taurine currents varying between 30 and 85 % of the maximal glycine response (Fig 5.11*A-C*, Table 5.3). This synergistic disruption to receptor function, especially at the core of the proposed Zn^{2+} potentiating binding site (D194 and H215), suggests this region is capable of interacting with T151.

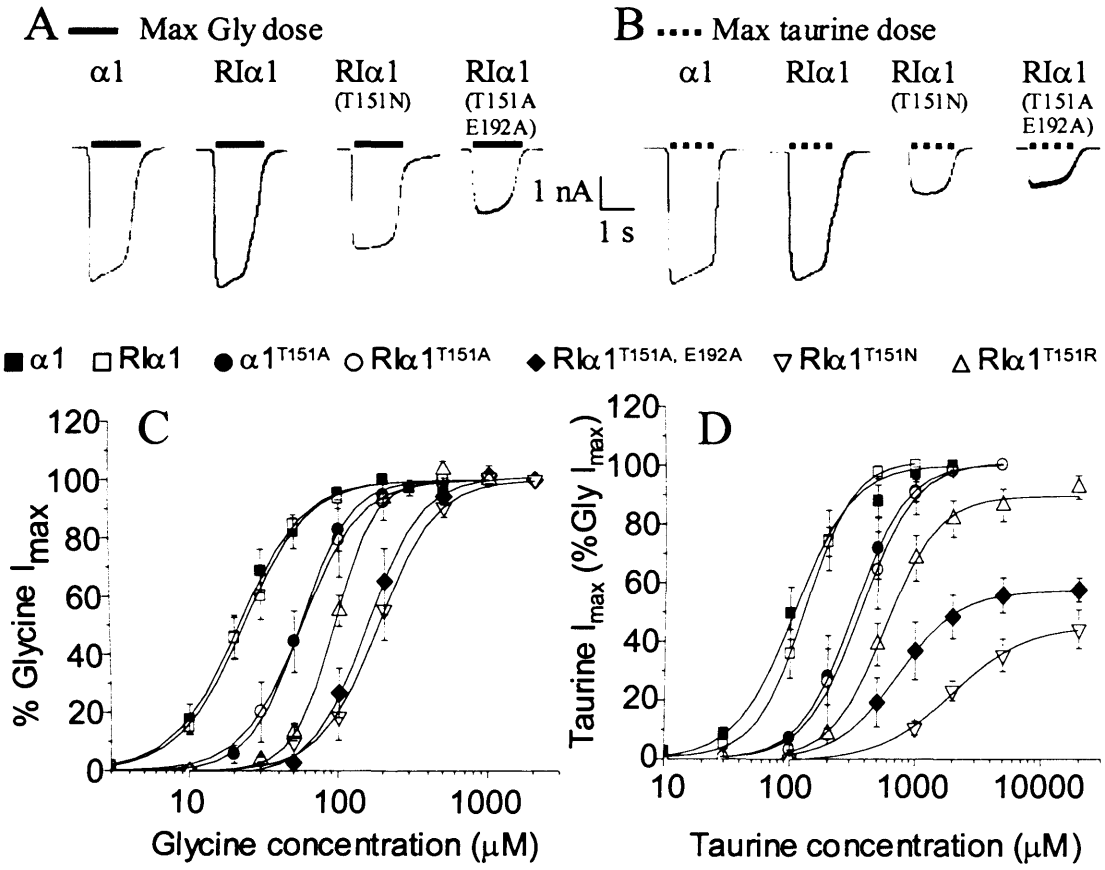

Figure 5.9 T151 mutated GlyR α1 receptors exhibit altered agonist activation properties consistent with changes to channel gating. Representative raw data traces showing maximal evoked responses to *A*, Gly, and then in the same cell *B*, taurine revealing the maxima for both agonists was reduced in $RI\alpha1^{T151N}$ and $RI\alpha1^{T151A,E192A}$ though to a greater degree for the less efficacious and potent agonist taurine. *C*, and *D*, Corresponding dose response curves to demonstrate decreased potency of agonists in a series of α1 T151 mutants; α1 » RIα1 > $\alpha1^{T151A}$ » $RI\alpha1^{T151A}$ > $RI\alpha1^{T151R}$ > $RI\alpha1^{T151N}$ » $RI\alpha1^{T151A,E192A}$ are shown for Gly (*C*) and taurine (D). Taurine I_{max} data were always measured as a percentage of the maximal Gly response in the same cell. $N = 4 - 11$.

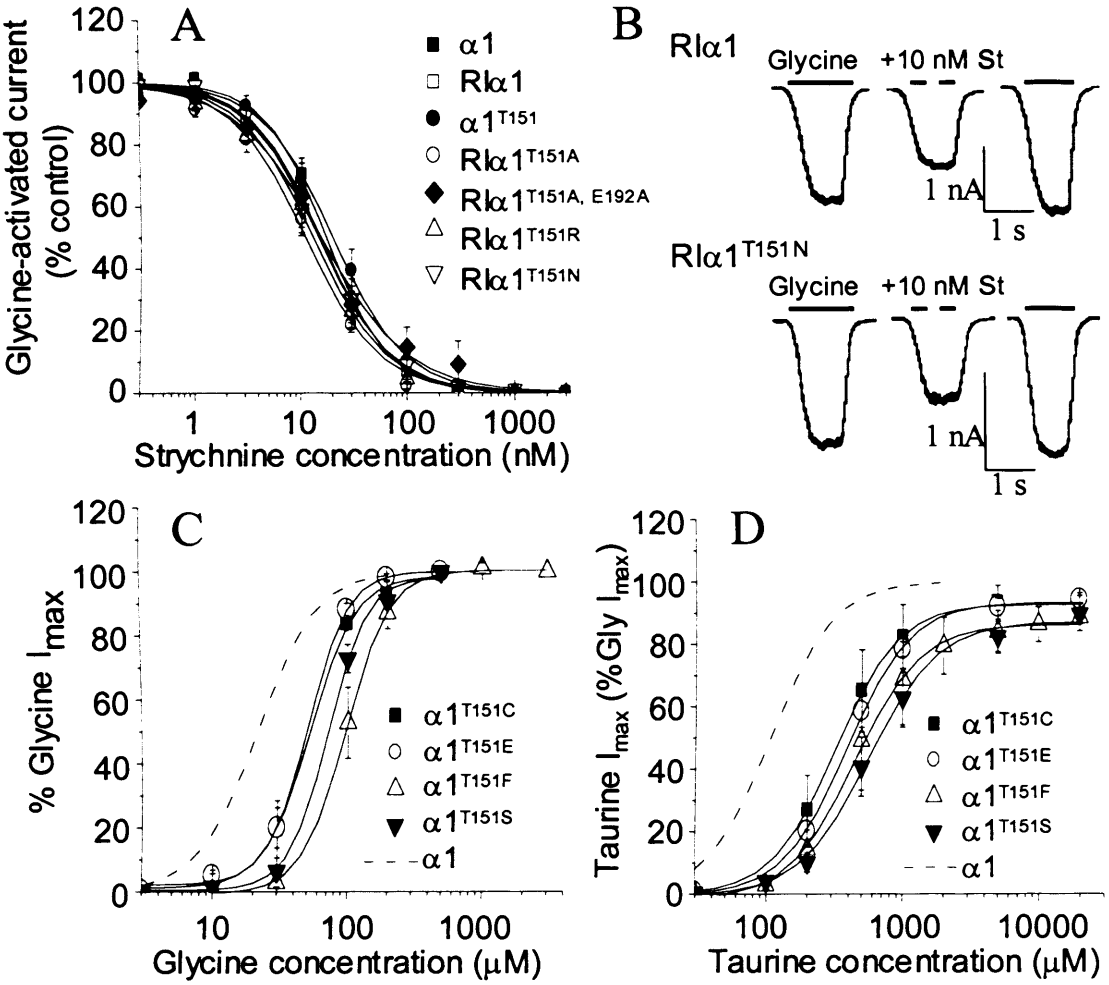

Figure 5.10 Further studies on T151 mutated GlyR α1 receptors. *A*, Sensitivity to inhibition by the competitive antagonist strychnine of 50 % maximal Gly responses remained comparable across a series of α1 T151 mutants. *B*, Typical 50 % maximal glycine responses in the absence and presence of 10 nM strychnine (St) and after recovery for RIα1 and RIα1^{T151N}. Further characterisation of the effect of T151 mutated receptors on dose response curves for *C*, glycine and *D*, taurine for α1^{T151C}, α1^{T151E}, α1^{T151F} and α1^{T151S} mutated GlyRs. Despite retaining polar electronegative groups at α1^{T151C}, α1^{T151E} and α1^{T151S}, all three receptors exhibited a 2 – 4 fold increase in EC_{50} for both agonists and a minor reduction in taurine relative efficacy, assessed in comparison to the maximal Gly response in the same cell. Introduction of a large hydrophobic group in the form of an α1^{T151F} did not cause a further increase in agonist EC_{50}s relative to its polar electronegative counterparts. $N = 3 - 4$.

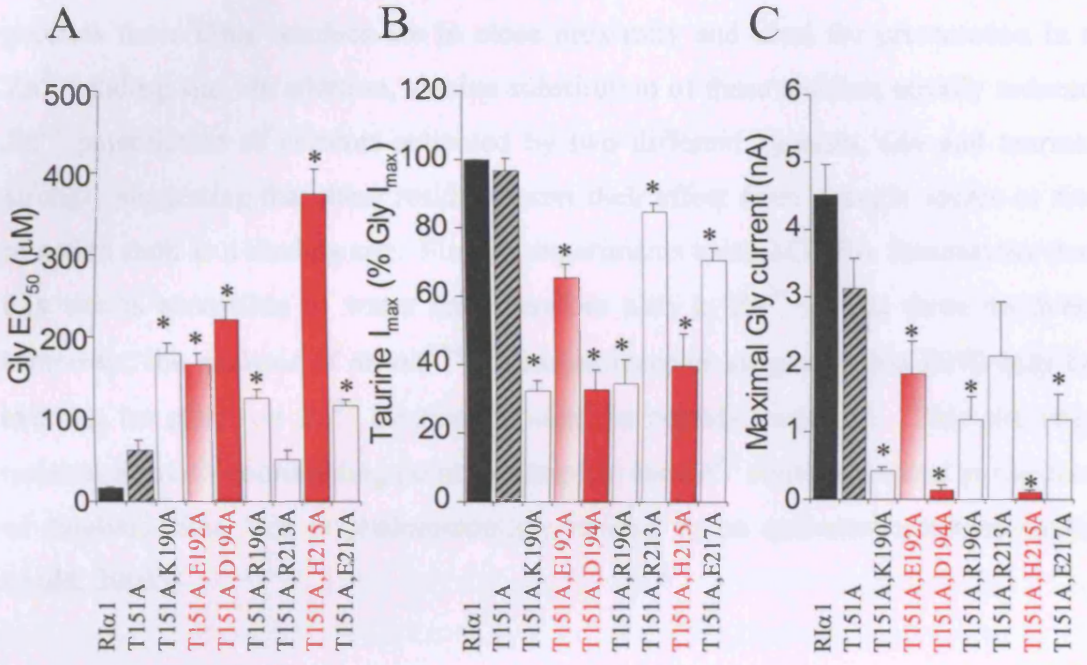

Figure 5.11 Agonist properties for Gly and taurine activating $RI\alpha1^{T151A}$ receptors carrying additional mutations in the nearby potentiating Zn^{2+} binding site region. *A*, Gly EC_{50} values increased and taurine efficacy *B*, and Gly maximal currents *C*, were both decreased when mutations from the Zn^{2+} binding region were introduced into $RI\alpha1^{T151A}$. The greatest perturbation to receptor function coincided with the axis of the predicted Zn^{2+} binding site with $RI\alpha1^{T151A, D194A}$ and $RI\alpha1^{T151A, H215A}$ producing effectively non-functional receptors with Gly maximal currents less than 200 pA. Asterisks (*) denote significant ($P < 0.05$) divergence in receptor property from $RI\alpha1^{T151A}$. $N = 4 - 7$.

Discussion

Evidence for a discrete Zn^{2+} potentiation site in GlyR α1

The Zn^{2+} potentiation site elucidated here in the form of GlyR α1 D194, H215 and E192 fits the criteria for a Zn^{2+} binding site. Each of these residues is chemically adept at interacting with Zn^{2+}, and the structural GlyR α1 model, based on AChBP, predicts these three residues are in close proximity and ideal for presentation in a Zn^{2+} binding site. In addition, alanine substitution of these residues equally reduced Zn^{2+} potentiation of currents activated by two different agonists, Gly and taurine, strongly suggesting that these residues exert their effect from a single source or site of action such as a binding site. Finally, experiments using MTSEA demonstrate that this site is accessible to water and therefore also to Zn^{2+} via all three residues. Moreover, the analysis of an $\alpha1^{E192P}$ mutated receptor suggested that E192 may be exerting its effect on Zn^{2+} binding through the peptide backbone. This site only requires a fourth coordinating point to complete the Zn^{2+} binding site and in the case of catalytic sites, this is predominantly provided by an activated water molecule (Auld, 2001).

Comparison of the GlyR α1 inhibition and potentiation sites

This potentiation site features a histidine residue as a likely Zn^{2+} coordinating partner and thus has some similarity with the GlyR inhibitory site. However, even without a precise atomic structural guide for the potentiating site it is still possible to predict that the exact chemical nature and structural properties of this site will be quite different from the Zn^{2+} inhibitory site. This is because the other main candidate residue for Zn^{2+} coordination features an acidic carboxylic acid group donated by an Asp, a residue not present in the inhibitory site. In addition there may be an unusual contribution to Zn^{2+} coordination, at the potentiation site, from the peptide backbone, the organisation of which is important for Zn^{2+} sensitivity. These coordinating groups could account for the higher sensitivity of the potentiation site to Zn^{2+} ($EC_{50} \approx 1$ μM) compared with the inhibitory site ($IC_{50} \approx 20$ μM), as acidic groups are stronger Zn^{2+} coordinators than polar hydroxyl groups such as those of the inhibitory site, e.g. α1 T133 (Auld, 2001). Finally, this potentiation site differs critically from the inhibitory site in that its predicted location suggests the site exists as a discrete unit on each subunit rather than as a cross-bridge between adjacent subunit

interfaces. This means that in contrast to the mechanism of action of the inhibitory site, which could act by stabilising communication between two neighbouring subunits and preventing the subunits rotating to activate the receptor (Chapter 3), each potentiation site must communicate its effect initially within the confines of a single subunit before any downstream global consequences on receptor function could be imposed.

Transduction roles for residues at the GlyR α1 Zn^{2+} potentiation site

Although the three residues identified here, GlyR α1 E192, D194 and H215, are all potential contributors to the potentiating Zn^{2+} site, it appears that the contribution of these residues to the site is not equal, as was previously shown to be the case for residues at the GlyR α1 inhibitory site (Chapter 3 - 4). In the case of an H215 substitution, an Ala residue attenuated but did not ablate the sensitivity to potentiating Zn^{2+}. The $\alpha1^{H215A}$ receptor also did not have any obvious effect on the maximum level of Zn^{2+} enhancement or alter the function of the potentiating site. This suggested that H215 may contribute a pure binding role to the potentiating site. In contrast, introduction of Ala at either E192 or D194 produced a receptor with no detectable Zn^{2+} enhancement. Furthermore these substitutions appeared to create an extra Zn^{2+} inhibition site suggesting this region could influence the function and transduction of potentiation. However, in accord with a role in direct cation coordination for E192 and D194 the potency of Zn^{2+} at the new inhibitory site was always of the order 15 – 50 fold less than at the original potentiation site. Substitution of the prime Zn^{2+} coordinating candidate D194 with a Lys residue, also a non-Zn^{2+} binding moiety but of larger volume than Ala, still ablated potentiation but did not induce any secondary functional effects. It is conceivable that the effect of $\alpha1^{D194A}$ on transduction may simply be due to the insertion of an alanine at this position. In the case of E192 this residue does appear to be able to specifically influence the transduction that is induced from the potentiating site. The data support the supposition that the organisation of the backbone at this locus is critical both for the potency of the site and also for the polarity of the site. In order for Zn^{2+} to bind and potentiate glycine currents, it must increase the propensity of the receptor to open in response to agonist binding. From the evidence presented here and given that the region surrounding the E192/D194/H215 site did not influence Zn^{2+}

potentiation, it can be speculated that the movement required is most likely linked to the backbone region at E192, though this cannot be validated without thermodynamic and structural data.

A link between the GlyR α1 Zn^{2+} potentiation site and the channel gating domain

In addition to those residues thought to line the Zn^{2+} binding site, T151 was also identified as a vital 'control element' for this site. Threonine 151 appears to be an important transduction component since its replacement by other residues altered the phenotype of the potentiation site reversing its polarity to create a high sensitivity inhibitory site. More profoundly, the sensitivity of the novel inhibitory site was comparable to that of the original potentiating site for Zn^{2+}, suggesting this residue was not affecting the affinity of the site. Instead the alternative residues inserted at position 151 varied the extent of inhibition in agreement with a transduction role. Threonine 151, located in the critical cys-loop gating domain (Kash et al., 2003;Schofield et al., 2003;Schofield et al., 2004), was also important in determining agonist potencies since mutation to Ala, Arg and Asn reduced the GlyR sensitivity to agonists. This clear dual function of T151 suggested a mechanism of action for the Zn^{2+} potentiation site. The effect of Zn^{2+} binding appears to communicate downstream to T151 to increase the efficacy of the agonist-induced channel opening. This is supported by mutations introduced in the extracellular domain outer face around the Zn^{2+} binding site, which compounded the effect on agonist potencies of $\alpha1^{T151A}$ mutated receptors, even though these mutations alone were innocuous. Importantly, the putative Zn^{2+} binding locus, E192, D194 and H215, when replaced with Ala residues, all strongly reduced agonist relative efficacies on the $\alpha1^{T151A}$ background. This supported the supposition that for the wild-type receptor, Zn^{2+} binding at this location could induce a downstream effect onto the cys-loop at T151 enabling potentiation. In accordance with Zn^{2+} potentiation increasing agonist efficacy, the partial agonism of taurine on GlyR α1 in oocytes is enhanced to nearly a full agonist by potentiating doses of Zn^{2+} (Laube et al., 2000). Furthermore, residues located in the M2-3 extracellular loop, which are predicted to be closely opposed and to interact with the cys-loop gating domain (Brejc et al.,

2001;Miyazawa et al., 2003), also affect Zn^{2+} mediated potentiation (Lynch et al., 1998) as would be expected if there is interplay between these two domains.

Recently it has been shown that in the case of anaesthetics operating on GlyRs perturbation of a selection of residues in the proposed cys-loop domain, not only reduced glycine potency but also diminished the potentiation caused by certain anaesthetics (Schofield et al., 2004). Though T151 was not one of the residues concerned, the authors did replicate a reduction in agonist potency for a GlyR $\alpha1^{T151A}$ mutation as is reported here. This supports a potential scheme in which positive modulators that increase the receptor efficacy may operate by feeding into the critical receptor gating domain comprising the cys-loop and M2-3 loop, even if originally the input is derived from distinct sources such as the extracellular or transmembrane domains. Also of interest is the recent observation that when I307 in the TM2 domain of the $GABA_A$ ρ receptor is substituted with a Gln residue the polarity of an inhibitory 5β-pregnane-3α-ol-20-one neurosteroid is reversed to now induce potentiation (Morris and Amin, 2004). This is comparable to the reversal of the Zn^{2+} potentiation site polarity observed here upon perturbation of α1 E192 or T151 suggesting that modulation site polarity reversals may be a common side effect of interfering with the transduction machinery of a binding site.

Implications for Zn^{2+} potentiation at other GlyR subtypes

The structure-function study reported here focused primarily on determinants of Zn^{2+} mediated potentiation in GlyR α1. However the implications for properties of Zn^{2+} enhancement at GlyR α2-4, GlyR β and the $5\text{-}HT_{3A}$ receptor were also investigated. Accurate comparisons of the potency of potentiating Zn^{2+} at GlyR α1 and α2 and their respective heteromers revealed that both receptors have a submicromolar high sensitivity to Zn^{2+} enhancement, though the potency is 10 – fold less for α2 due to a subsitution at the Zn^{2+} binding residue, α1 D194, with another acidic moiety, α2 E201. The remaining two residues α1 E192 and H215 as well as the control element T151 all remain the same in α2 (Fig 5.2*C*) suggesting the properties of Zn^{2+} potentiation at the α2 subtype have the same molecular basis. Though no studies were carried out to measure the potency of Zn^{2+} enhancement at GlyR α3 and 4 these two receptors retain the exact same molecular composition as α1 for Zn^{2+}

potentiation and are therefore likely to retain comparable properties, an assumption supported by a significant potentiation of GlyR α3 by 1 μM Zn^{2+} (Chapter 3).

Studies to investigate a contribution from the β-subunit to Zn^{2+} potentiation suggested its role is unimportant in this process. Incorporation of the β subunit forming heteromeric GlyR α1β and α2β did not in any way influence the potency of Zn^{2+} enhancement and co-expression of the β-subunit with an $\alpha1^{E192A}$ mutant devoid of Zn^{2+} potentiation did not enable the recovery of a positive allosteric action by Zn^{2+}. The molecular basis of this apparent lack of sensitivity to Zn^{2+} enhancement by the β-subunit could be attributed at least in part to the identification of a variant residue at the equivalent position to α1 T151. Introduction of the corresponding β-subunit residue, an Arg, into the GlyR rendered the $\alpha1^{T151R}$ mutant insensitive to Zn^{2+} enhancement such that the potentiating site now seemed to support an inhibitory influence. This is supported by a previous observation where an α1 chimera that suffered a partial replacement of the region encoding the cys-loop and therefore T151 with the β-subunit sequence also generated a GlyR α1 subunit insensitive to Zn^{2+} potentiation (Laube et al., 1995).

Implications for Zn^{2+} enhancement of 5-HT_{3A}Rs and nAChRs

Characterisation of the 5-HT_{3A}R for modulation by Zn^{2+} has also previously revealed a biphasic profile with comparable sensitivities for Zn^{2+} potentiation and inhibition to those measured for the GlyR (Hubbard and Lummis, 2000). The possibility though that these two receptors share the same molecular basis for Zn^{2+} potentiation now seems unlikely as replacing GlyR α1 T151 with the Asn present in the 5-HT_{3A}R did not retain Zn^{2+} potentiation at the GlyR. In addition substitution of the 5-HT_{3A}R Asn residue with an Ala, which when introduced to create GlyR $\alpha1^{T151A}$ ablates enhancement, did not cause any apparent effect on Zn^{2+} potentiation at 5-HT_{3A}Rs. Though the other specific molecular correlates of the GlyR α1 binding site E192, D194 and H215 did align with potential Zn^{2+} binding partners in the mouse 5-HT_{3A}R variant tested here (Fig 5.8*A*), alignment analysis with the human 5-HT_{3A}R did not provide the same results (data not shown). As the regions around the actual Zn^{2+} binding site residues are poorly conserved between GlyRs and the 5-HT_{3A}R it was not possible to gage whether these acidic residues in the 5-HT_{3A}R were homologous

to those of the GlyR and an in depth structure-function study to investigate this was not undertaken. Overall the evidence presented here suggests that the 5-HT_{3A}R is unlikely to possess a homologous Zn^{2+} potentiation site compared to that of the GlyR. This is further supported by the fact that the 5-HT_{3A}R does not maintain the same degree of specificity for cation enhancement (Hubbard and Lummis, 2000). At 5-HT_{3A}Rs the Zn^{2+} enhancement effect can be displaced by other cations including Ca^{2+} and Mg^{2+} making it necessary to carry out the Zn^{2+} modulation curves in the absence of these ions, which is not required when measuring Zn^{2+} enhancement at the GlyR.

There is also no molecular basis for the potentiation by Zn^{2+} of some subtypes of the nAChR (Hsiao et al., 2001). Though it may be possible that nAChRs retain a comparable site for Zn^{2+} enhancement to the GlyR, the properties of this nAChR site(s), are likely to be quite different. Whilst Zn^{2+} potentiation of GlyRs is a very robust process occurring with comparable sensitivities and maximal enhancements across GlyR α1-3 and their respective αβ heteromers, Zn^{2+} potentiation at various nAChRs is more complex. Both the subtype of the α and β-subunit are able to influence the extent and maximal level of Zn^{2+} mediated potentiation at nAChRs (Hsiao et al., 2001). Furthermore the sensitivity to Zn^{2+} enhancement in normal saline across all these nAChR variants, α2-4 and β2 and β4, was substantially lower with EC_{50}s in the range 15 – 100 μM compared to the 0.8 μM value reported here for GlyR α1.

The nAChR potentiation site does however share a higher level of selectivity like the GlyR (Laube et al., 1995) when compared to the 5-HT_{3A}R, with significant Zn^{2+} potentiation occurring even in the presence of Ca^{2+} and Mg^{2+} ions and only Cd^{2+} being able to partially compensate for Zn^{2+} enhancement (Hsiao et al., 2001). A study using chimeras has demonstrated that the most important contribution to Zn^{2+} mediated potentiation in nAChRs comes from the extracellular N-terminal domain of the receptor similar to the GlyR. However, there are no obvious correlates between the GlyR residues, T151, E192, D194 and H215, in the nAChR α and β subunits (alignment not shown) that could account for Zn^{2+} modulation.

Physiological significance of GlyR Zn^{2+} potentiation

The high sensitivity to Zn^{2+} enhancement reported here for homomeric α1 and 2 and heteromeric α1β and α2β GlyRs, along with the rapid onset of Zn^{2+} potentiation previously reported (Chapter 3), make Zn^{2+} an ideal endogenous co-modulator at glycinergic synapses. This is relevant especially as Zn^{2+} is concentrated into selected nerve terminals and packaged into synaptic vesicles throughout the CNS including those present within glycinergic boutons of the spinal cord (Birinyi et al., 2001;Jo et al., 2000;Velazquez et al., 1999;Wang et al., 2001). Additionally, Zn^{2+} ions may be released into the synaptic cleft or from a thin Zn^{2+} veneer following nerve fibre stimulation (Assaf and Chung, 1984;Howell et al., 1984;Kay, 2003) resulting in multiple effects on neuronal excitability by modulating ligand-gated and voltage-operated ion channels (Smart et al., 1994;Harrison and Gibbons, 1994). Experiments measuring zebrafish glycinergic IPSC kinetics in the presence and absence of the Zn^{2+} chelators, tricine and TPEN, revealed that these synaptic receptors are sensitive enough to be potentiated even by Zn^{2+} contamination in the extracellular saline solution (Suwa et al., 2001). Thus it would appear likely that GlyRs can at least undergo a basal level of modulation by released Zn^{2+} though whether this extends to the specific action of Zn^{2+} as a rapidly released and removed synaptic co-modulator will require further studies.

Conclusion

I report here the identification of the Zn^{2+} potentiation site for the GlyR and a possible mechanism of action for Zn^{2+} potentiation via the cys-loop channel-gating domain. This site has a high sensitivity to Zn^{2+}, with the EC_{50} estimated at less than 1 μM, well within the current range of estimates for putative physiological levels of released Zn^{2+} (Frederickson et al., 2000). Importantly, this mutagenesis study supports the supposition that the AChBP is a powerful model for use in GlyR structure-function studies and strengthens the recent precedent linking the GlyR cys-loop region to channel gating (Kash et al., 2003;Schofield et al., 2003;Schofield et al., 2004), by identifying a novel regulatory component in GlyR function in the form of T151. This study provides novel insight into the function of a cys-loop ligand-gated ion channel Zn^{2+} binding site.

	Glycine			Taurine			Zn^{2+} (on Gly)			
	Max current (nA)	EC_{50} (μM)	*n*	EC_{50} (μM)	I_{max} (% Gly I_{max})	*n*	EC_{50} (μM)	Max (%) increase*	IC_{50} (μM)	*n*
Zn^{2+} binding residues										
α1	4.5 ± 0.5	16 ± 2	5	90 ± 10	~100	5	0.8 ± 0.3	39 ± 8	20 ± 5	4
RIα1	5.9 ± 0.3	25 ± 4	4	130 ± 30	~100	4	0.8 ± 0.2	42 ± 6	> 3000	4
$RI\alpha1^{E192A}$	3.6 ± 0.7	19 ± 4	3	190 ± 60	~100	3	None	None	710 ± 100	7
$RI\alpha1^{D194A}$	4.8 ± 0.4	48 ± 4	3	310 ± 70	~100	3	None	None	270 ± 50	3
$RI\alpha1^{H215A}$	3.7 ± 0.2	21 ± 3	3	100 ± 30	~100	3	22 ± 4	28 ± 12	1320 ± 210	4
Acidic non-binding residues										
$RI\alpha1^{D141A}$	2.9 ± 1.1	46 ± 7	2	240 ± 80	~100	2*[1]	0.5 ± 0.2	41 ± 21	> 3000	3
$RI\alpha1^{D148A}$	< 0.04	—	10	—	—	3	—	—	—	—
$RI\alpha1^{E191A}$	4.8 ± 0.6	22 ± 5	3	190 ± 40	~100	3	0.8 ± 0.4	80 ± 50	> 3000	3
Residues surrounding Zn^{2+} binding site										
$RI\alpha1^{K190A}$	4.5 ± 0.3	9 ± 2	3	80 ± 20	~100	3	0.9 ± 0.7	29 ± 6	n.e	3
$RI\alpha1^{R196A}$	5.0 ± 0.5	27 ± 6	4	150 ± 50	~100	4	0.6 ± 0.1	34 ± 7	n.e	4
$RI\alpha1^{R213A}$	5.3 ± 0.2	9 ± 7	3	60 ± 10	~100	3	0.5 ± 0.3	58 ± 30	n.e	3
$RI\alpha1^{E217A}$	4.2 ± 0.8	21 ± 5	3	120 ± 50	~100	3	0.9 ± 0.3	37 ± 3	n.e	4
Cys mutated receptors										
$RI\alpha1^{E192C}$	5.8 ± 0.8	110 ± 10	4	n.e	n.e		1.9 ± 0.2	59 ± 15	~ 1000	4
$RI\alpha1^{D194C}$	5.6 ± 0.8	99 ± 24	4	n.e	n.e		3.6 ± 0.6	40 ± 12	2000 ± 300	5
$RI\alpha1^{H215C}$	4.0 ± 0.6	71 ± 10	3	n.e	n.e		0.44	35 ± 8	1100	2
$RI\alpha1^{E192C, H215C}$	< 0.1	—	6	—	—		—	—	—	—
$RI\alpha1^{D194C, H215C}$	< 0.1	—	6	—	—		—	—	—	—

Table 5.1 Agonist potency data and Zn^{2+} modulation data for mutagenesis studies to elucidate the Zn^{2+} potentiation site of GlyR α1.

Definitions: n.e. – not evaluated, '—' represents receptors where maximal Gly currents were too small to accurately evaluate Zn^{2+} modulation, none – denotes circumstances where the attribute under evaluation was not present.

* The maximum percentage increase of a 50 % maximal agonist induced response. *[1] – This error is a standard deviation.

	Glycine			Zn^{2+} (on Gly)			
	Max current (nA)	EC_{50} (μM)	*n*	EC_{50} (μM)	Max (%)* increase	IC_{50} (μM)	*n*
H109F mutated receptors							
RIα1	5.9 ± 0.3	25 ± 4	4	0.8 ± 0.2	42 ± 6	> 3000	4
$RI\alpha1^{H109F}$	5.1 ± 0.2	28 ± 5	3	~1	67 ± 14	> 10000	7
$RI\alpha1^{E192A}$	3.6 ± 0.7	19 ± 4	3	None	None	710 ± 100	6
$RI\alpha1^{H109F, E192A}$	6.0 ± 0.5	51 ± 4	4	None	None	660 ± 90	4
$RI\alpha1^{H215A}$	3.7 ± 0.2	21 ± 3	3	22 ± 4	28 ± 12	1320 ± 210	4
$RI\alpha1^{H109F, H215A}$	1.2 ± 0.3	150 ± 15	3	40 ± 11	34 ± 11	3200 ± 600	4
Pro & Lys mutated receptors							
$RI\alpha1^{E192P}$	7.0 ± 0.2	48 ± 4	3	4.2 ± 0.8	50 ± 11	> 1000	3
$RI\alpha1^{D194K}$	6.4 ± 0.8	140 ± 30	6	None	None	640 ± 80	6
$RI\alpha1^{H109F, D194K}$	1.9 ± 0.5	200 ± 30	3	None	None	1270 ± 110	6
				Zn^{2+} $IC_{50}A$*[1] (μM)	$IC_{50}A$ Max*[2] (%) inhibition	Zn^{2+} $IC_{50}B$*[3] (μM)	*n*
H109F mutated receptors (biphasic inhibition)							
$RI\alpha1^{D194A}$	4.8 ± 0.4	48 ± 4	3	270 ± 50	100	n.a.	3
$RI\alpha1^{H109F, D194A}$	2.5 ± 0.6	290 ± 70	3	79 ± 28	45 ± 4	820 ± 80	4
Pro & Lys mutated receptors (biphasic inhibition)							
$RI\alpha1^{E192K}$	7.0 ± 0.2	60 ± 6	3	32 ± 14	52 ± 8	1000 ± 100	3
$RI\alpha1^{D194P}$	5.2 ± 0.9	43 ± 9	4	8.2 ± 1.3	42 ± 7	150 ± 28	3

Table 5.2 Agonist potency data and Zn^{2+} modulation data for mutagenesis studies to determine effects on transduction from the Zn^{2+} potentiation site.

Definitions: n.a. – not applicable as this receptor exhibited only one distinguishable inhibitory phase, none – denotes circumstances where the attribute under evaluation was not present.

* The maximum percentage increase of a 50 % maximal agonist induced response.

*[1] First high sensitivity IC_{50} component, *[2] Maximum achievable percentage reduction by the first inhibitory component of 50 % maximal Gly responses, *[3] Second low sensitivity IC_{50} component.

	Glycine			Taurine			Zn^{2+} (on Gly)			
	Max current (nA)	EC_{50} (μM)	*n*	EC_{50} (μM)	I_{max} (% Gly I_{max})	*n*	Zn^{2+} $IC_{50}A$*1 (μM)	$IC_{50}A$ Max*2 (%) inhibition	Zn^{2+} $IC_{50}B$*3 (μM)	*n*
Agonist and Zn^{2+} transduction T151 residue mutations										
$\alpha1^{T151A}$	4.7 ± 0.6	53 ± 9	4	330 ± 60	~100	4	2.9 ± 2.0	68 ± 7	160 ± 60	4
$R\alpha1^{T151A}$	4.0 ± 0.4	63 ± 12	5	380 ± 80	97 ± 4	4	1.6 ± 0.6	73 ± 8	1040 ± 290	5
$R\alpha1^{T151N}$	2.9 ± 0.5	180 ± 30	7	2060 ± 230	46 ± 6	5	1.6 ± 0.7	7 ± 0.4	1410 ± 210	4
$R\alpha1^{T151R}$	3.8 ± 0.9	95 ± 7	3	560 ± 130	93 ± 3	4	3.6 ± 0.4	39 ± 3	710 ± 130	4
T151 combined with residues both within and surrounding the Zn^{2+} binding site										
$R\alpha1^{T151A,\ K190A}$	0.4 ± 0.1	180 ± 10	4	1810 ± 140	32 ± 3	4	n.e	n.e	n.e	
$R\alpha1^{T151A,\ E192A}$	1.9 ± 0.5	170 ± 10	7	960 ± 160	65 ± 4	7	16 ± 3	32 ± 4	390 ± 60	3
$R\alpha1^{T151A,\ D194A}$	0.15 ± 0.07	220 ± 20	20	n.e	33 ± 6	20	n.e	n.e	n.e	
$R\alpha1^{T151A,\ R196A}$	1.2 ± 0.3	130 ± 10	4	1810 ± 450	35 ± 7	4	n.e	n.e	n.e	
$R\alpha1^{T151A,\ R213A}$	2.1 ± 0.8	52 ± 10	5	400 ± 120	85 ± 2	5	n.e	n.e	n.e	
$R\alpha1^{T151A,\ H215A}$	0.1 ± 0.04	380 ± 30	15	n.e	40 ± 10	15	n.e	n.e	n.e	
$R\alpha1^{T151A,\ E217A}$	1.2 ± 0.4	120 ± 6	4	900 ± 70	71 ± 3	3	n.e	n.e	n.e	
Further T151 residue mutations										
$R\alpha1^{T151C}$	4.6 ± 1.6	52 ± 8	3	370 ± 130	94 ± 4	3	n.e	n.e	n.e	
$R\alpha1^{T151D}$	< 0.05	n.e	10	< 0.05	n.e	10	n.e	n.e	n.e	
$R\alpha1^{T151E}$	5.0 ± 1.5	50 ± 7	3	390 ± 70	94 ± 1	3	n.e	n.e	n.e	
$R\alpha1^{T151F}$	5.7 ± 0.6	100 ± 20	4	600 ± 240	88 ± 5	4	n.e	n.e	n.e	
$R\alpha1^{T151S}$	5.3 ± 0.8	73 ± 7	3	620 ± 190	90 ± 4	3	n.e	n.e	n.e	

Table 5.3 Glycine, taurine and Zn^{2+} potencies for GlyR α1 carrying mutations at threonine 151.

Definitions: n.e. – not evaluated, '—' represents receptors where maximal Gly currents were too small to accurately evaluate Zn^{2+} modulation.

*1 First high sensitivity IC_{50} component, *2 Maximum achievable percentage reduction by the first inhibitory component of 50 % maximal Gly responses, *3 Second low sensitivity IC_{50} component.

Chapter 6

Summary and Final Thoughts

The 1960s represented a critical landmark in the optimisation of techniques to elucidate protein structure. This holy grail was of fundamental importance as scientists believed that knowledge of a protein's structure was key to its functional secrets. Clearly, since the deduction of crystal structures such as insulin and haemoglobin, this has proved to be an unfounded assumption, largely because the structure of a protein is not the sole source of functional information. Another vital component is also required, that of protein dynamics. In contrast to structural techniques, such as NMR and X-ray crystallography, there is as yet no formal process for obtaining the dynamic information possessed by a protein. Strategies to monitor real-time equilibrium fluctuations within a protein's structure and to measure the movements that are undertaken in response to 'stimuli', i.e. binding events, will be key to determining this information. The standardisation of such techniques, however, is most likely decades away and in the mean-time functional diagnoses rely predominantly on covalent modifications, whether this be in the form of site-directed mutagenesis or covalent labelling strategies.

The work described in this thesis demonstrates that with appropriate interpretation, covalent modification is remarkably powerful at determining the locations involved in binding events and even at elucidating potential mechanisms of communication between different protein domains. The data presented reveal that an unequivocal picture of amino acid function is almost never forthcoming. This supports the assertion above that a protein is not merely a static image where residues can be pigeon-holed into their specific functional roles, but that instead a protein is a dynamic structure, constantly in a state of physical flux, where amino acids contribute to multiple processes and work together as an inseparable team. Even attempts to assess the importance of residues at potential Zn^{2+} binding sites, where the coordinating moieties can be chemically predicted and might be expected to have a fairly specific role in coordination, proved remarkably complex with a wide range of functional consequences for the GlyR. The functional interpretations of such data

are beyond that which can be determined from the structural model alone and instead require an appreciation of, as yet, completely absent dynamic information.

Previous studies on GlyR α1 pointed to four residues with a potential involvement in Zn^{2+} coordination at the inhibitory Zn^{2+} binding site, H107 from the subunit '+' face and H109, E110 and T112 from the '-' face of a neighbouring subunit (Harvey et al., 1999;Laube et al., 2000; Fig 6.1). The work here identifies two further polar residues exposed at the surface of the GlyR α1 Zn^{2+} inhibitory '-' face, which also influence Zn^{2+} mediated inhibition, N61 and T133 (Fig 6.1). All these residues are predicted to reside in the same region and therefore may influence Zn^{2+} coordination at the predicted inhibitory site, either directly or indirectly. The primary sequence arrangement for the original three identified residues on the Zn^{2+} inhibitory site '-' face means that these residues are all spatially close to one another. However given that H109 marks the end of the predicted β-sheet 5 with its immediate neighbour E110 marking the start of a loop region it is unlikely that the peptide psi bond angles would permit both residues to be similarly orientated to contribute to Zn^{2+} coordination (Auld, 2001;Vallee and Auld, 1990). Such a situation where two neighbouring residues on a β-strand contribute to Zn^{2+} coordination of the same ion has not yet been reported (Auld, 2001;Vallee and Auld, 1990). Furthermore, GlyR α1 N61 and T133, which from a structural perspective are predicted to reside on two separate nearby loops ideal for contributing to Zn^{2+} binding, represent relatively less favoured Zn^{2+} binding moieties (Auld, 2001;Vallee and Auld, 1990). The results from the functional site-directed mutagenesis studies were also not unequivocal. The evidence for H107 as a direct binding partner in the site is the strongest, as ablation of the Zn^{2+} coordination property of this residue gives a dramatic reduction in the potency of Zn^{2+} inhibition without affecting the efficacy (maximal level of inhibition) or inducing other Zn^{2+} related phenomena such as ZAG activity. Furthermore, only the residue at the equivalent position to H107 can be donated from what is considered to be a neighbouring non-functional β-subunit and return functionality to the inhibitory site. The data suggest that this is because the inhibitory signal can then be mediated through the α subunit '-' face, therefore suggesting that the '+' face H107 is required for binding but not transduction. Perhaps also of consequence, the data presented here reveal that the H107 equivalent

is also responsible for differential sensitivity to Zn^{2+} inhibition between GlyR subtypes. From an evolutionary perspective, if it were desirable to select for receptors with varying sensitivities to Zn^{2+} then it would be most effective to target a residue with a pure role in Zn^{2+} coordination so as not to induce other effects on the properties of the receptor.

Concerning the residues residing on the inhibitory Zn^{2+} site '-' face it is more difficult to distinguish specific roles for each moiety. Previous data and the evidence presented in this report favours Zn^{2+} binding at the intersubunit interface, between the '+' and '-' subunit domains, to stabilise the receptor in a closed conformation (Nevin et al., 2003). From this standpoint H109 and E110 chemically represent the strongest candidates to mediate the Zn^{2+} binding process at the '-' interface. However alanine substitution of E110 induced a relatively small 5-fold reduction in the potency of Zn^{2+} mediated inhibition, while an $\alpha1^{H109A}$ mutated GlyR has an even smaller reduction in potency, just 2-fold, and also affects the efficacy of this process by reducing the maximal amount of inhibition that Zn^{2+} can induce. The structural model of the GlyR presents H109 in a more favourable orientation for direct coordination with Zn^{2+} across to H107. However the AChBP has a low sequence homology with GlyRs (approximately 20 %) and the region for H109 and E110 falls across the start of a peptide loop within the receptor, which classically retains the least structural similarity between homologues. Therefore, it is not possible to place complete confidence in this prediction that H109 is the primary '-' face Zn^{2+} coordinating partner. The remaining three residues, N61, T112 and T133 do not represent classical Zn^{2+} coordination partners, though these moieties have been reported as binding partners in some instances (Auld, 2001). All three of these residues, along with H109, can clearly influence Zn^{2+} transduction when substituted with alanines, as Zn^{2+} mediated inhibition is ablated and ZAG activity is conferred. Plus these residues exert other complicating effects on GlyR properties, including some modest reductions in the potency of glycine and a decrease in the macroscopic activation rates by non-saturating doses of glycine. The clear similarities exhibited between these residues, despite their discrete locations along the primary sequence, demonstrates the usefulness of the structural model as a reliable predictor of approximate amino acid positions. It is also worth mentioning that alanine

substitution at N61, H109 and T133 generated low potency ZAGs but at T112, high potency ZAG activity was induced, not dissimilar in sensitivity to the original potency of Zn^{2+} mediated inhibition. As the evidence suggests the ZAG induced by disruption at the subunit '-' face, relies on the same Zn^{2+} binding components as the original Zn^{2+} inhibitory site this implies that disruption at N61, H109 and T133 affects the site potency whilst disruption at T112 affects only the transduction. This would agree with previous studies where substitutions of T112 have induced effects on the relative efficacy of partial agonists and so T112 may have a general role in multiple aspects of GlyR function (Schmieden et al., 1999), rather than a specific role in Zn^{2+} coordination.

This report also identified a novel site for Zn^{2+} potentiation. The evidence for residues specifically involved in direct coordination of Zn^{2+} at this location is clearer perhaps due to its predicted intrasubunit nature. Site directed mutagenesis studies identified a discrete region, composed of three residues, GlyR α1 E192, D194 and H215 (Fig 6.2) that when substituted with alanine either ablated, or reduced, sensitivity to Zn^{2+} enhancement. Other potential Zn^{2+} coordinating amino acids in the vicinity and neighbouring residues did not exert any influence over Zn^{2+} potentiation when substituted, demonstrating the specificity of this location. Furthermore, the evidence that two of these residues, D194 and H215, were direct coordinators of Zn^{2+} was strengthened by demonstrating their apparent accessible nature at the surface of the protein using a cys-modifying reagent, a requirement for any dynamic Zn^{2+} binding site. As with the studies on the Zn^{2+} inhibitory site, the results were not always unequivocal. The alanine substitution at E192 ablated Zn^{2+} potentiation but also induced the formation of a low potency Zn^{2+} inhibition site. The evidence indicated that this occurred through a reversal of the function of the potentiation site suggesting E192 can influence transduction from this site. The inhibition was also of a lower potency than the original potentiation implying that manipulation of E192 also reduced the affinity of the site, though decreasing the efficiency of transduction can also cause such an effect. Interestingly, side chain modification of E192 using a cys-modifying reagent did not ablate potentiation. Furthermore substitution with a proline, known to influence the peptide backbone geometry (Chou and Fasman, 1974;Yohannan et al., 2004), also retained the capacity

for Zn^{2+} potentiation with only a modest reduction in potency. This suggests it is the trajectory of the backbone at this loci that is of vital consequence for Zn^{2+} potentiation rather than the side chain identity. It was not possible from these studies to determine if the peptide backbone is involved directly in binding, but dynamic Zn^{2+} binding sites are predicted to retain at least three coordinating residues and an activated water molecule (Auld, 2001). As there are no other obvious candidate binding residue for the third coordinating partner in this region, then currently, the peptide backbone presents the most plausible explanation.

The mutagenesis experiments presented in this report not only investigated the relatively simple prospect of dissecting true components of Zn^{2+} binding but also attempted to divulge possible mechanisms by which the two sites could propagate their effects. This strategy proved surprisingly powerful in divulging useful information regarding such transduction mechanisms. In the case of Zn^{2+} potentiation, an element in the cys-loop gating domain of the GlyR, T151, was isolated that could determine the extent by which the potentiation site was able to exert an effect on receptor function. This suggested that Zn^{2+} might exert potentiation by acting on the gating process, a hypothesis also supported by the synergistic effect that disrupting the gating element, T151, in combination with residues in the vicinity of the Zn^{2+} potentiation site had on reducing the efficacy of agonist action. Such synergy was not observed between T151 and H107 at the inhibitory site suggesting this effect is selective to the region of Zn^{2+} enhancement. A previous study in oocytes also showed that Zn^{2+} increased the relative efficacy of the partial agonist taurine (Laube et al., 2000). Furthermore, certain residues in the M2-3 loop, an important component of the gating process (Lynch et al., 1997) ablate Zn^{2+} potentiation (Lynch et al., 1998) as would be expected if Zn^{2+} potentiation interacts with this process. Though this study has not proved that T151 is the exclusive element from the cys-loop in order for the Zn^{2+} potentiation site to mediate its effect, disruption of two acidic residues, and Q150 in this domain, did not affect enhancement by Zn^{2+}. Moreover C152, an immediate neighbour of T151, is involved in formation of the cys-loop bridge, critical for receptor gating and assembly, making it an unlikely mediator in the Zn^{2+} enhancement process. Thus T151 would appear to be a specific control element that transduces the binding of Zn^{2+} at the potentiation site to increase the efficacy of the receptor.

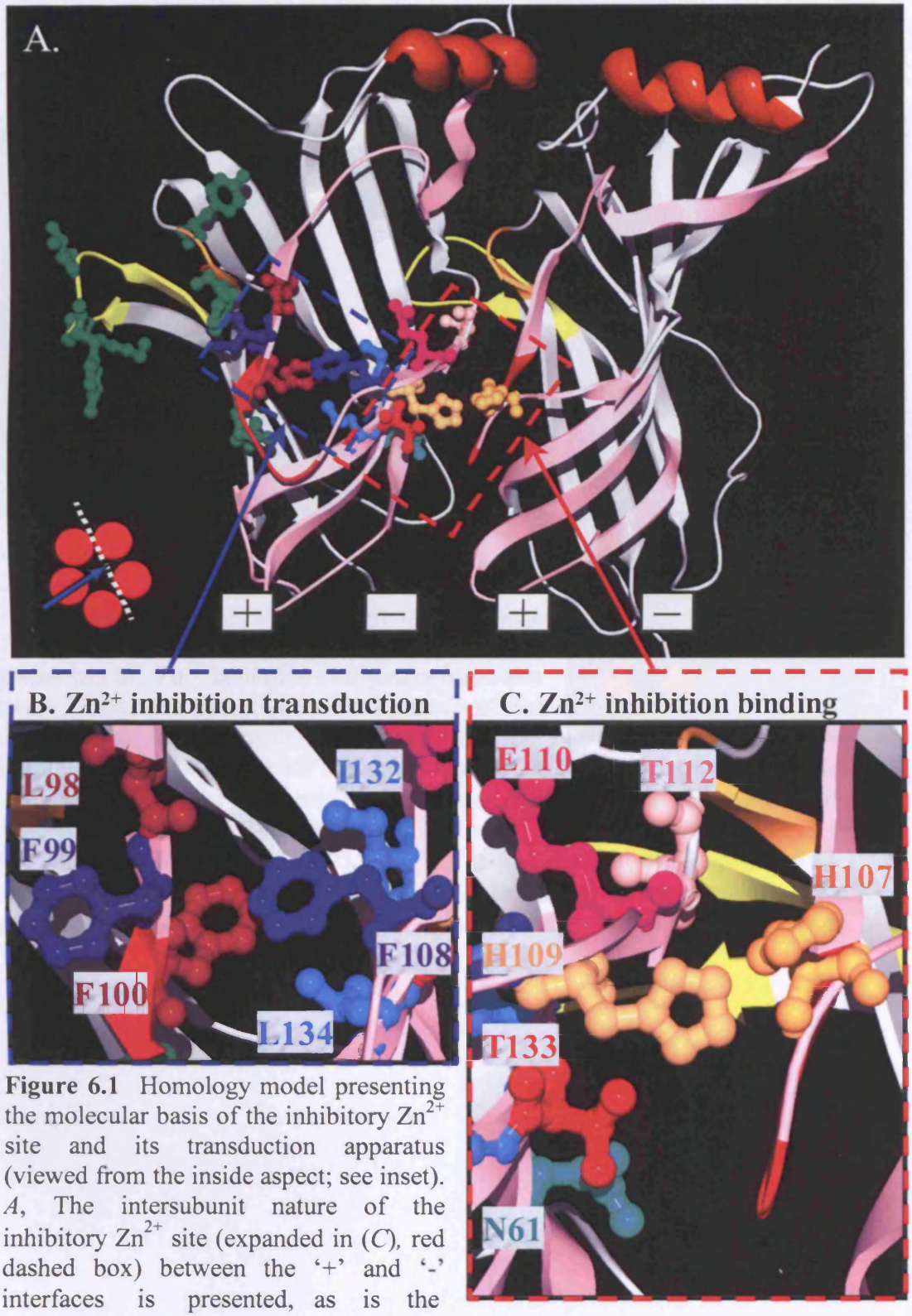

Figure 6.1 Homology model presenting the molecular basis of the inhibitory Zn^{2+} site and its transduction apparatus (viewed from the inside aspect; see inset). *A*, The intersubunit nature of the inhibitory Zn^{2+} site (expanded in (*C*), red dashed box) between the '+' and '-' interfaces is presented, as is the hydrophobic Zn^{2+} inhibition transduction domain (expanded in (*B*), blue dashed box), which leads to the agonist binding site (Top picture, green residues. A more in depth view of the proposed agonist binding site can be viewed in Fig 1.6*B,C*).

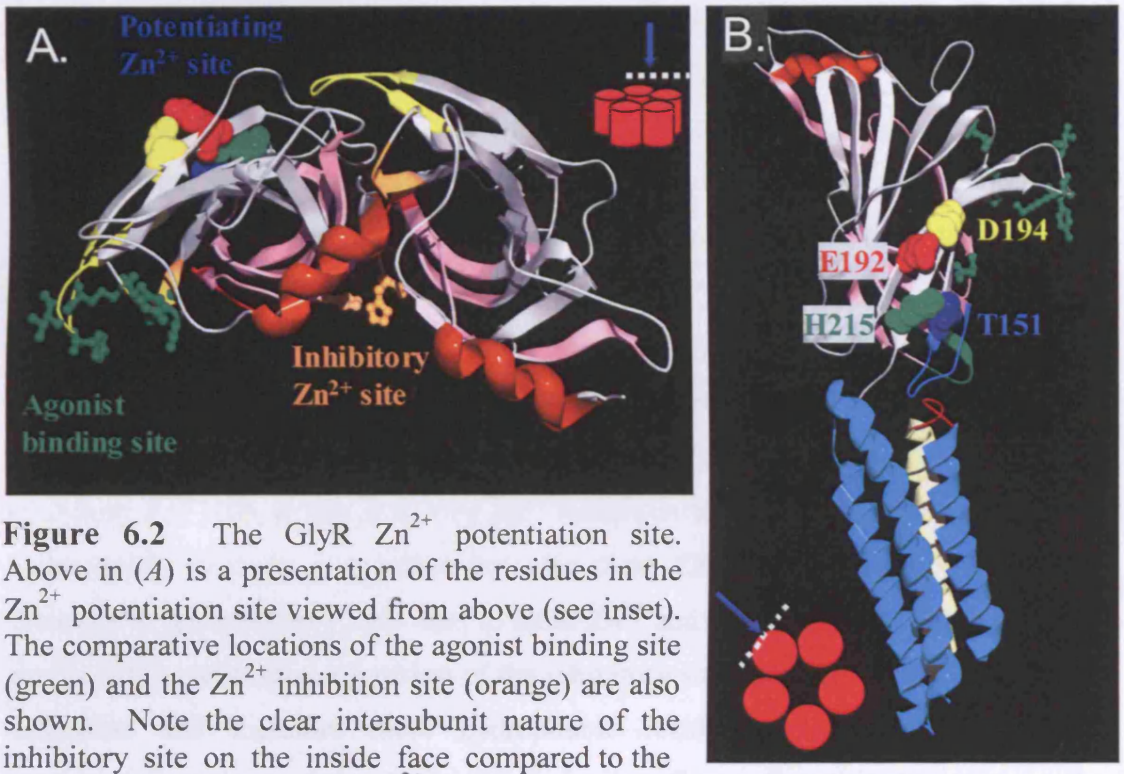

Figure 6.2 The GlyR Zn^{2+} potentiation site. Above in (*A*) is a presentation of the residues in the Zn^{2+} potentiation site viewed from above (see inset). The comparative locations of the agonist binding site (green) and the Zn^{2+} inhibition site (orange) are also shown. Note the clear intersubunit nature of the inhibitory site on the inside face compared to the intrasubunit location of the Zn^{2+} potentiation site on the external face. *B*, Side view (see inset) of the Zn^{2+} potentiation site with labels for the three potential Zn^{2+} coordinating residues, E192, D194 and H215 and the control element T151 (blue). This highlights the location of T151 on the gating element cys-loop (blue) in close proximity to the β1-2 loop (green) and M2-3 loop (red) gating elements. The four transmembrane domains are also shown, with the pore lining helix, M2, in yellow.

Perhaps the most revelatory discovery to result from the site directed mutagenesis studies reported here, was the determination of an entire hydrophobic transduction pathway required for allosteric interplay between the Zn^{2+} inhibition site and the agonist binding site. The ability to determine a genuine and selective role for these residues in transduction, something that is notoriously hard to do, was a fortuitous consequence of ZAG induction (Chapter 4) upon substitution of hydrophobic residues, L98, F99, F100, F108, I132 and L134 with alanine. These residues were all predicted from the structural GlyR model to line up in a pathway from the inhibitory Zn^{2+} site '-' face across to the agonist-binding site (Fig 6.1). Other hydrophobic residues surrounding the pathway did not induce such an effect. Previously, transduction had been predicted to occur from the '-' face of the Zn^{2+} inhibition site due to the unique ability of the GlyR β subunit to only donate a Zn^{2+} binding site residue from its '+' face (Chapter 3). This ZAG formation was linked to the original inhibitory Zn^{2+} site, as not only was Zn^{2+} inhibition ablated upon substitution of the hydrophobic residues in question but also these ZAG receptors relied on H109, formerly of the inhibitory Zn^{2+} site, to elicit Zn^{2+} activated currents. This suggested that in ZAG receptors the function of the inhibitory site had been switched to induce activation and therefore these hydrophobic residues were important in the transduction process of the Zn^{2+} inhibition site. To confirm this discovery really requires dynamic protein data. In this case, the dynamic data was elucidated using functional mutagenesis studies to modify the protein, and therefore its energetics, then observe the consequences. Though this pathway marks an apparent allosteric transduction route across the protein, it may be that such a communication event also represents a more significant role in the general function of the receptor itself. Despite a model structure of the extracellular domain of cys-loop receptors, based on AChBP, it has, as yet, not proved possible to decipher the order and importance of downstream transduction events that mediate the communication between the agonist binding loops and the three base loops, the β1-2 loop, cys-loop and the β8-9 loop so that agonist binding can induce channel opening. The mechanism of action of the inhibitory Zn^{2+} site clearly suggests that Zn^{2+} stabilises the closed conformation of the receptor by fixing the inhibitory site '-' face in a set orientation with the inhibitory site '+' face of a neighbouring subunit (Chapter 3). Clearly then, binding of agonist to open the receptor results in movement of the inhibitory site '-' face such

that Zn^{2+} can no longer bind and inhibit the receptor, a process that the evidence reported here suggests is mediated via a hydrophobic transduction domain. Reorganisation of the receptor's hydrophobic pathway and inhibitory Zn^{2+} site '-' face may therefore be part of the GlyR activation procedure. How important this event is in activation of the receptor, i.e. whether it is a driving force for receptor activation or a side effect of receptor activation, remains to be seen, but undoubtedly this will come under scrutiny in the near future.

The data presented in this study represents a significant contribution to understanding the molecular basis of Zn^{2+} modulation of GlyRs. Where an understanding is currently lacking is in the appreciation of any physiological role Zn^{2+} may be exerting over GlyRs. The hippocampus, an ideal preparation to study NMDA receptors, is also the favoured preparation for research on synaptic Zn^{2+} release and several studies have attained indirect evidence that Zn^{2+} can endogenously modulate NMDA receptors (Ueno et al., 2002;Vogt et al., 2000). Furthermore pathways by which Zn^{2+} can be released in the hippocampus have been characterised (Frederickson et al., 2000) and due to the very high affinity of NR2A containing NMDA receptors it would seem likely that these receptors experience a significant level of background modulation by Zn^{2+} (Paoletti et al., 1997). Unfortunately the hippocampus appears to express only extrasynaptic GlyRs (Mori et al., 2002) and these are less prominent than NMDA and $GABA_A$Rs, therefore limiting the extent to which studies, especially dynamic endogenous Zn^{2+} modulation studies on GlyRs, can be carried out. Spinal cord, the ideal preparation to acquire information about synaptic GlyR modulation, has yet to become the subject of any study addressing endogenous release of Zn^{2+} as a neuromodulator. Though studies in Xenopus do suggest that background concentrations of Zn^{2+} may be sufficient to elicit potentiation of GlyRs and therefore have physiological significance (Suwa et al., 2001). With regards to future progress in this field it may prove possible to use the high potency ZAG receptors developed in this report as probes for Zn^{2+} release. Transfection of such receptors into neuronal preparations to be expressed at synapses could provide an exciting opportunity, to detect for the first time, direct release of Zn^{2+} at the synapse.

In conclusion, the data reported here provide a tantalising insight into some of the complex interactions that can occur in the extracellular portion of the GlyR. To dissect the processes that occur in a novel protein merely from a structural image is as futile as attempting to appreciate the picture of a face without any understanding of expressions. The dynamic information dissected in this report offer a glimpse into two expressions, Zn^{2+} potentiation and inhibition, available to the GlyR during the course of its routine role to process activation in response to the binding of an agonist.

Acknowledgments

Ahhhhhhh finally, it took ages to get his far, and now the final curtain. Firstly, the boss, Trevor Smart, to whom I am most in debted. I would like to thank Trevor for always giving me the freedom to pursue my own ideas, whilst steering me enough to keep me on the correct course of action. Secondly I have to show my gratitude to Alastair Hosie. Without his insight, advice and knowledge close at hand I never would have got so far so fast. I also need to state my deep appreciation to Philip Thomas. Someone I regard as a special individual and a real altruist, as well as a comedian. Philip has given me much technical help and advice during my PhD consistently demonstrating patience beyond the bounds of reason. To the lab technician Helena Da Silva, I am also most grateful for the many tasks she has fulfilled to make my life that bit easier and for the challenging debates she has always been happy to initiate. Others, whose daily presence has encouraged and motivated me onto greater things and to whom I am grateful include, Megan Wilkins, Ian Duguid, Martin Mortensen and Catriona Houston. I would also like to thank Marco beato, for agreeing to help me complete the functional characterisation of a GlyR developmental shift, and Robert Harvey and Paul Groot-Kormelink for advice and GlyR clones. Finally I need to thank my girlfriend Roshni Bhuva and my parents for their continued support during this most enjoyable of endeavours for me. THANK YOU ALL.

This work would not have been possible without the generous support of the MRC and the Wellcome Trust.

Reference List

Absalom NL, Lewis TM, Kaplan W, Pierce KD, Schofield PR (2003) Role of charged residues in coupling ligand binding and channel activation in the extracellular domain of the glycine receptor. J Biol Chem. 278: 50151-7

Ahmadi S, Lippross S, Neuhuber WL, Zeilhofer HU (2002) PGE(2) selectively blocks inhibitory glycinergic neurotransmission onto rat superficial dorsal horn neurons. Nat Neurosci 5: 34-40.

Amin J, Weiss DS (1993) $GABA_A$ receptor needs two homologous domains of the beta-subunit for activation by GABA but not by pentobarbital. Nature 366: 565-569.

Andermann F, Andermann E (1988) Startle disorders of man: hyperekplexia, jumping and startle epilepsy. Brain Dev 10: 213-222.

Aprison MH, Shank RP, Davidoff R, Werman RA (1968) The distribution of glycine, a neurotransmitter suspect in the central nervous system of several vertebrate species. Life Sci. 7:583-590.

Aprison MH (1970a) Evidence of the release of glycine from hemisectioned toad spinal cord with dorsal root stimulation. Pharmacologist 12:222

Aprison MH (1970b) Studies on the release of glycine in the isolated spinal cord of the toad. Trans. Am. Soc. Neurochem. 1:25

Aprison MH, McBride WJ (1973) Evidence for the net accumulation of glycine into a synaptosomal fraction isolated from the telencephalon and spinal cord of the rat. Life Sci I 12: 449-458.

Aprison MH, Shank RP, Davidoff RA (1969) A comparison of the concentration of glycine, a transmitter suspect, in different areas of the brain and spinal cord in seven different vertebrates. Comp Biochem Physiol 28: 1345-1355.

Aprison MH, Werman R (1965) The distribution of glycine in cat spinal cord and roots. Life Sci 4: 2075-2083.

Aprison MH, Lipkowitz KB, Simon JR (1987) Identification of a glycine-like fragment on the strychnine molecule. J Neurosci Res 17: 209-213.

Arunlakshana O, Schild HO (1959) Some quantitative uses of drug antagonists. Br J Pharmacol 14: 48-58.

Assaf SY, Chung SH (1984) Release of endogenous Zn^{2+} from brain tissue during activity. Nature 308: 734-736.

Auld DS (2001) Zinc coordination sphere in biochemical zinc sites. Biometals 14: 271-313.

Banker G, Goslin K (1998) Culturing Nerve Cells, 2nd edition, pp 346.

Basbaum AI (1999) Spinal mechanisms of acute and persistent pain. Reg Anesth Pain Med 24: 59-67.

Baulac S, Huberfeld G, Gourfinkel-An I, Mitropoulou G, Beranger A, Prud'homme JF, Baulac M, Brice A, Bruzzone R, LeGuern E (2001) First genetic evidence of $GABA_A$ receptor dysfunction in epilepsy: a mutation in the γ2-subunit gene. Nat Genet 28: 46-48.

Beato M, Groot-Kormelink PJ, Colquhoun D, Sivilotti LG (2002) Openings of the rat recombinant alpha 1 homomeric glycine receptor as a function of the number of agonist molecules bound. J Gen Physiol 119: 443-466.

Beato M, Groot-Kormelink PJ, Colquhoun D, Sivilotti LG (2004) The activation mechanism of α1 homomeric glycine receptors. J Neurosci 24: 895-906.

Becker CM, Hoch W, Betz H (1988) Glycine receptor heterogeneity in rat spinal cord during postnatal development. EMBO J 7: 3717-3726.

Belachew S, Rogister B, Rigo JM, Malgrange B, Mazy-Servais C, Xhauflaire G, Coucke P, Moonen G (1998) Cultured oligodendrocyte progenitors derived from cerebral cortex express a glycine receptor which is pharmacologically distinct from the neuronal isoform. Eur J Neurosci 10: 3556-3564.

Belelli D, Herd MB (2003) The contraceptive agent Provera enhances $GABA_A$ receptor-mediated inhibitory neurotransmission in the rat hippocampus: evidence for endogenous neurosteroids? J Neurosci 23: 10013-10020.

Birinyi A, Parker D, Antal M, Shupliakov O (2001) Zinc co-localizes with GABA and glycine in synapses in the lamprey spinal cord. J Comp Neurol 433: 208-221.

Bloomenthal AB, Goldwater E, Pritchett DB, Harrison NL (1994) Biphasic modulation of the strychnine-sensitive glycine receptor by Zn^{2+}. Mol Pharmacol 46: 1156-1159.

Boileau AJ, Newell JG, Czajkowski C (2002) $GABA_A$ receptor β2 Tyr97 and Leu99 line the GABA-binding site. Insights into mechanisms of agonist and antagonist actions. J Biol Chem 277: 2931-2937.

Bormann J, Hamill OP, Sakmann B (1987) Mechanism of anion permeation through channels gated by glycine and gamma-aminobutyric acid in mouse cultured spinal neurones. J Physiol 385: 243-286.

Bormann J, Rundstrom N, Betz H, Langosch D (1993) Residues within transmembrane segment M2 determine chloride conductance of glycine receptor homo- and hetero-oligomers. EMBO J 12: 3729-3737.

Bouzat C, Gumilar F, Spitzmaul G, Wang HL, Rayes D, Hansen SB, Taylor P, Sine SM (2004) Coupling of agonist binding to channel gating in an ACh-binding protein linked to an ion channel. Nature 430: 896-900.

Breitinger HG, Villmann C, Becker K, Becker CM (2001) Opposing effects of molecular volume and charge at the hyperekplexia site alpha 1(P250) govern glycine receptor activation and desensitization. J Biol Chem 276: 29657-29663.

Breitinger HG, Villmann C, Rennert J, Ballhausen D, Becker CM (2002) Hydroxylated residues influence desensitization behaviour of recombinant alpha3 glycine receptor channels. J Neurochem 83: 30-36.

Brejc K, van Dijk WJ, Klaassen RV, Schuurmans M, van Der OJ, Smit AB, Sixma TK (2001) Crystal structure of an ACh-binding protein reveals the ligand-binding domain of nicotinic receptors. Nature 411: 269-276.

Brickley SG, Cull-Candy SG, Farrant M (1999) Single-channel properties of synaptic and extrasynaptic $GABA_A$ receptors suggest differential targeting of receptor subtypes. J Neurosci 19: 2960-2973.

Buckwalter MS, Cook SA, Davisson MT, White WF, Camper SA (1994) A frameshift mutation in the mouse alpha 1 glycine receptor gene (Glra1) results in progressive neurological symptoms and juvenile death. Hum Mol Genet 3: 2025-2030.

Budde T, Minta A, White JA, Kay AR (1997) Imaging free zinc in synaptic terminals in live hippocampal slices. Neuroscience 79: 347-358.

Burkat PM, Yang J, Gingrich KJ (2001) Dominant gating governing transient $GABA_A$ receptor activity: a first latency and Po/o analysis. J Neurosci 21: 7026-7036.

Campos-Caro A, Sala S, Ballesta JJ, Vicente-Agullo F, Criado M, Sala F (1996) A single residue in the M2-M3 loop is a major determinant of coupling between binding and gating in neuronal nicotinic receptors. Proc Natl Acad Sci U S A 93: 6118-6123.

Caraiscos VB, Mihic SJ, MacDonald JF, Orser BA (2002) Tyrosine kinases enhance the function of glycine receptors in rat hippocampal neurons and human $\alpha(1)\beta$ glycine receptors. J Physiol 539: 495-502.

Celie PH, Rossum-Fikkert SE, van Dijk WJ, Brejc K, Smit AB, Sixma TK (2004) Nicotine and carbamylcholine binding to nicotinic acetylcholine receptors as studied in AChBP crystal structures. Neuron 41: 907-914.

Chakrapani S, Bailey TD, Auerbach A (2003) The role of loop 5 in acetylcholine receptor channel gating. J Gen Physiol 122: 521-539.

Chang Y, Amin J, Weiss DS (1995) Zinc is a mixed antagonist of homomeric rho 1 gamma-aminobutyric acid-activated channels. Mol Pharmacol 47: 595-602.

Chen Z, Dillon GH, Huang R (2004) Molecular determinants of proton modulation of glycine receptors. J Biol Chem 279: 876-883.

Chery N, de Koninck Y (1999) Junctional versus extrajunctional glycine and $GABA_A$ receptor-mediated IPSCs in identified lamina I neurons of the adult rat spinal cord. J Neurosci 19: 7342-7355.

Choi YB, Lipton SA (1999) Identification and mechanism of action of two histidine residues underlying high-affinity Zn^{2+} inhibition of the NMDA receptor. Neuron 23: 171-180.

Chou PY, Fasman GD (1974) Conformational parameters for amino acids in helical, beta-sheet, and random coil regions calculated from proteins. Biochemistry 13: 211-222.

Christine CW, Choi DW (1990) Effect of zinc on NMDA receptor-mediated channel currents in cortical neurons. J Neurosci 10: 108-116.

Cohen JB, Sharp SD, Liu WS (1991) Structure of the agonist-binding site of the nicotinic acetylcholine receptor. [^{3}H]acetylcholine mustard identifies residues in the cation-binding subsite. J Biol Chem 266: 23354-23364.

Cole TB, Martyanova A, Palmiter RD (2001) Removing zinc from synaptic vesicles does not impair spatial learning, memory, or sensorimotor functions in the mouse. Brain Res 891: 253-265.

Cole TB, Robbins CA, Wenzel HJ, Schwartzkroin PA, Palmiter RD (2000) Seizures and neuronal damage in mice lacking vesicular zinc. Epilepsy Res 39: 153-169.

Cole TB, Wenzel HJ, Kafer KE, Schwartzkroin PA, Palmiter RD (1999) Elimination of zinc from synaptic vesicles in the intact mouse brain by disruption of the ZnT3 gene. Proc Natl Acad Sci U S A 96: 1716-1721.

Colvin RA, Davis N, Nipper RW, Carter PA (2000a) Evidence for a zinc/proton antiporter in rat brain. Neurochem Int 36: 539-547.

Colvin RA, Davis N, Nipper RW, Carter PA (2000b) Zinc transport in the brain: routes of zinc influx and efflux in neurons. J Nutr 130: 1484S-1487S.

Corsi M, Fina P, Trist DG (1996) Co-agonism in drug-receptor interaction: illustrated by the NMDA receptors. Trends Pharmacol Sci 17: 220-222.

Coull JA, Boudreau D, Bachand K, Prescott SA, Nault F, Sik A, De Koninck P, de Koninck Y (2003) Trans-synaptic shift in anion gradient in spinal lamina I neurons as a mechanism of neuropathic pain. Nature 424: 938-942.

Cromer BA, Morton CJ, Parker MW (2002) Anxiety over $GABA_A$ receptor structure relieved by AChBP. Trends Biochem Sci 27: 280-287.

Crawford IL, Connor JD (1972) Zinc in maturing rat brain: hippocampal concentration and localization. J Neurochem 19: 1451-1458.

Curtis DR, Duggan AW, Johnston GA (1971) The specificity of strychnine as a glycine antagonist in the mammalian spinal cord. Exp Brain Res 12: 547-565.

Curtis DR, Hosli L, Johnston GA (1968) A pharmacological study of the depression of spinal neurones by glycine and related amino acids. Exp Brain Res 6: 1-18.

Dahan DS, Dibas MI, Petersson EJ, Auyeung VC, Chanda B, Bezanilla F, Dougherty DA, Lester HA (2004) A fluorophore attached to nicotinic acetylcholine receptor β M2 detects productive binding of agonist to the α δ site. Proc Natl Acad Sci U S A 101: 10195-10200.

Danober L, Pape HC (1998) Strychnine-sensitive glycine responses in neurons of the lateral amygdala: an electrophysiological and immunocytochemical characterization. Neuroscience 85: 427-441.

Danscher G (1981) Histochemical demonstration of heavy metals. A revised version of the sulphide silver method suitable for both light and electronmicroscopy. Histochemistry 71: 1-16.

Danscher G (1982) Exogenous selenium in the brain. A histochemical technique for light and electron microscopical localization of catalytic selenium bonds. Histochemistry 76: 281-293.

Danscher G (1984) Autometallography. A new technique for light and electron microscopic visualization of metals in biological tissues (gold, silver, metal sulphides and metal selenides). Histochemistry 81: 331-335.

Danscher G (1996) The autometallographic zinc-sulphide method. A new approach involving in vivo creation of nanometer-sized zinc sulphide crystal lattices in zinc-enriched synaptic and secretory vesicles. Histochem J 28: 361-373.

Danscher G, Howell G, Perez-Clausell J, Hertel N (1985) The dithizone, Timm's sulphide silver and the selenium methods demonstrate a chelatable pool of zinc in CNS. A proton activation (PIXE) analysis of carbon tetrachloride extracts from rat brains and spinal cords intravitally treated with dithizone. Histochemistry 83: 419-422.

Davidoff RA, Aprison MH, Werman R (1969) The effects of strychnine on the inhibition of interneurons by glycine and γ-aminobutyric acid. Int J Neuropharmacol 8: 191-194.

Davidoff RA, Graham LT, Jr., Shank RP, Werman R, Aprison MH (1967a) Changes in amino acid concentrations associated with loss of spinal interneurons. J Neurochem 14: 1025-1031.

Davidoff RA, Shank RP, Graham LT, Jr., Aprison MH, Werman R (1967b) Association of glycine with spinal interneurones. Nature 214: 680-681.

Davies PA, Wang W, Hales TG, Kirkness EF (2003) A novel class of ligand-gated ion channel is activated by Zn^{2+}. J Biol Chem 278: 712-717.

Dennis M, Giraudat J, Kotzyba-Hibert F, Goeldner M, Hirth C, Chang JY, Lazure C, Chretien M, Changeux JP (1988) Amino acids of the Torpedo marmorata acetylcholine receptor alpha subunit labeled by a photoaffinity ligand for the acetylcholine binding site. Biochemistry 27: 2346-2357.

Devillers-Thiery A, Galzi JL, Eisele JL, Bertrand S, Bertrand D, Changeux JP (1993) Functional architecture of the nicotinic acetylcholine receptor: a prototype of ligand-gated ion channels. J Membr Biol 136: 97-112.

Dieudonne S (1995) Glycinergic synaptic currents in Golgi cells of the rat cerebellum. Proc Natl Acad Sci U S A 92: 1441-1445.

Donato R, Nistri A (2000) Relative contribution by GABA or glycine to Cl^--mediated synaptic transmission on rat hypoglossal motoneurons in vitro. J Neurophysiol 84: 2715-2724.

* Draguhn A, Verdorn TA, Ewert M, Seeburg PH, Sakmann B (1990) Functional and molecular distinction between recombinant rat $GABA_A$ receptor subtypes by Zn^{2+}. Neuron 5: 781-788.

Dumoulin A, Triller A, Dieudonne S (2001) IPSC kinetics at identified GABAergic and mixed GABAergic and glycinergic synapses onto cerebellar Golgi cells. J Neurosci 21: 6045-6057.

Duncalfe LL, Carpenter MR, Smillie LB, Martin IL, Dunn SM (1996) The major site of photoaffinity labeling of the gamma-aminobutyric acid type A receptor by [^{3}H]flunitrazepam is histidine 102 of the alpha subunit. J Biol Chem 271: 9209-9214.

Fayyazuddin A, Villarroel A, Le Goff A, Lerma J, Neyton J (2000) Four residues of the extracellular N-terminal domain of the NR2A subunit control high-affinity Zn^{2+} binding to NMDA receptors. Neuron 25: 683-694.

Feng G, Tintrup H, Kirsch J, Nichol MC, Kuhse J, Betz H, Sanes JR (1998) Dual requirement for gephyrin in glycine receptor clustering and molybdoenzyme activity. Science 282: 1321-1324.

ffrench-Constant RH, Rocheleau TA, Steichen JC, Chalmers AE (1993) A point mutation in a Drosophila GABA receptor confers insecticide resistance. Nature 363: 449-451.

Findlay GS, Phelan R, Roberts MT, Homanics GE, Bergeson SE, Lopreato GF, Mihic SJ, Blednov YA, Harris RA (2003) Glycine receptor knock-in mice and hyperekplexia-like phenotypes: comparisons with the null mutant. J Neurosci 23: 8051-8059.

Flint AC, Liu X, Kriegstein AR (1998) Nonsynaptic glycine receptor activation during early neocortical development. Neuron 20: 43-53.

Frederickson CJ (1989) Neurobiology of zinc and zinc-containing neurons. Int Rev Neurobiol 31: 145-238.

Frederickson CJ, Howell GA, Haigh MD, Danscher G (1988) Zinc-containing fiber systems in the cochlear nuclei of the rat and mouse. Hear Res 36: 203-211.

* Downie DL, Hall AC, Lieb WR, Franks NP (1996) Effects of inhalational general anaesthetics on native glycine receptors in rat medullary neurones and recombinant glycine receptors in Xenopus oocytes. Br J Pharmacol 118: 493-502.

Frederickson CJ, Kasarskis EJ, Ringo D, Frederickson RE (1987) A quinoline fluorescence method for visualizing and assaying the histochemically reactive zinc (bouton zinc) in the brain. J Neurosci Methods 20: 91-103.

Frederickson CJ, Rampy BA, Reamy-Rampy S, Howell GA (1992) Distribution of histochemically reactive zinc in the forebrain of the rat. J Chem Neuroanat 5: 521-530.

Frederickson CJ, Suh SW, Silva D, Frederickson CJ, Thompson RB (2000) Importance of zinc in the central nervous system: the zinc-containing neuron. J Nutr 130: 1471S-1483S.

Fu DX, Sine SM (1996) Asymmetric contribution of the conserved disulfide loop to subunit oligomerization and assembly of the nicotinic acetylcholine receptor. J Biol Chem 271: 31479-31484.

Fucile S, de Saint JD, David-Watine B, Korn H, Bregestovski P (1999) Comparison of glycine and GABA actions on the zebrafish homomeric glycine receptor. J Physiol 517 (Pt 2): 369-383.

Fucile S, de Saint JD, de Carvalho LP, Bregestovski P (2000) Fast potentiation of glycine receptor channels of intracellular calcium in neurons and transfected cells. Neuron 28: 571-583.

Galindo A, Krnjevic K, Schwartz S (1967) Micro-iontophoretic studies on neurones in the cuneate nucleus. J Physiol 192: 359-377.

Galzi JL, Bertrand D, Devillers-Thiery A, Revah F, Bertrand S, Changeux JP (1991b) Functional significance of aromatic amino acids from three peptide loops of the α 7 neuronal nicotinic receptor site investigated by site-directed mutagenesis. FEBS Lett 294: 198-202.

Galzi JL, Devillers-Thiery A, Hussy N, Bertrand S, Changeux JP, Bertrand D (1992) Mutations in the channel domain of a neuronal nicotinic receptor convert ion selectivity from cationic to anionic. Nature 359: 500-505.

Galzi JL, Revah F, Black D, Goeldner M, Hirth C, Changeux JP (1990) Identification of a novel amino acid α-tyrosine 93 within the cholinergic ligands-binding sites of the acetylcholine receptor by photoaffinity labeling. Additional evidence for a three-loop model of the cholinergic ligands-binding sites. J Biol Chem 265: 10430-10437.

Galzi JL, Revah F, Bouet F, Menez A, Goeldner M, Hirth C, Changeux JP (1991a) Allosteric transitions of the acetylcholine receptor probed at the amino acid level with a photolabile cholinergic ligand. Proc Natl Acad Sci U S A 88: 5051-5055.

Gentet LJ, Clements JD (2002) Binding site stoichiometry and the effects of phosphorylation on human α1 homomeric glycine receptors. J Physiol 544: 97-106.

Gill CH, Peters JA, Lambert JJ (1995) An electrophysiological investigation of the properties of a murine recombinant 5-HT3 receptor stably expressed in HEK 293 cells. Br J Pharmacol 114: 1211-1221.

Gingrich KJ, Burkat PM (1998) Zn^{2+} inhibition of recombinant $GABA_A$ receptors: an allosteric, state-dependent mechanism determined by the γ-subunit. J Physiol 506 (Pt 3): 609-625.

Graham D, Pfeiffer F, Betz H (1983) Photoaffinity-labelling of the glycine receptor of rat spinal cord. Eur J Biochem 131: 519-525.

Graham LT, Jr., Aprison MH (1966) Fluorometric determination of aspartate, glutamate, and γ-aminobutyrate in nerve tissue using enzymic methods. Anal Biochem 15: 487-497.

Greferath U, Brandstatter JH, Wassle H, Kirsch J, Kuhse J, Grunert U (1994) Differential expression of glycine receptor subunits in the retina of the rat: a study using immunohistochemistry and in situ hybridization. Vis Neurosci 11: 721-729.

Grenningloh G, Gundelfinger E, Schmitt B, Betz H, Darlison MG, Barnard EA, Schofield PR, Seeburg PH (1987a) Glycine vs GABA receptors. Nature 330: 25-26.

Grenningloh G, Rienitz A, Schmitt B, Methfessel C, Zensen M, Beyreuther K, Gundelfinger ED, Betz H (1987b) The strychnine-binding subunit of the glycine receptor shows homology with nicotinic acetylcholine receptors. Nature 328: 215-220.

Grenningloh G, Schmieden V, Schofield PR, Seeburg PH, Siddique T, Mohandas TK, Becker CM, Betz H (1990a) α subunit variants of the human glycine receptor: primary structures, functional expression and chromosomal localization of the corresponding genes. EMBO J 9: 771-776.

Grenningloh G, Pribilla I, Prior P, Multhaup G, Beyreuther K, Taleb O, Betz H (1990b) Cloning and expression of the 58 kd β subunit of the inhibitory glycine receptor. Neuron 4: 963-970.

Grewer C (1999) Investigation of the α(1)-glycine receptor channel-opening kinetics in the submillisecond time domain. Biophys J 77: 727-738.

Guastella J, Brecha N, Weigmann C, Lester HA, Davidson N (1992) Cloning, expression, and localization of a rat brain high-affinity glycine transporter. Proc Natl Acad Sci U S A 89: 7189-7193.

Gundlach AL, Dodd PR, Grabara CS, Watson WE, Johnston GA, Harper PA, Dennis JA, Healy PJ (1988) Deficit of spinal cord glycine/strychnine receptors in inherited myoclonus of Poll Hereford calves. Science 241: 1807-1810.

Gundlach AL, Kortz G, Burazin TC, Madigan J, Higgins RJ (1993) Deficit of inhibitory glycine receptors in spinal cord from Peruvian Pasos: evidence for an equine form of inherited myoclonus. Brain Res 628: 263-270.

Gurley D, Amin J, Ross PC, Weiss DS, White G (1995) Point mutations in the M2 region of the α, beta, or gamma subunit of the $GABA_A$ channel that abolish block by picrotoxin. Receptors Channels 3: 13-20.

Gunthorpe MJ, Smith GD, Davis JB, Randall AD (2001) Characterisation of a human acid-sensing ion channel (hASIC1a) endogenously expressed in HEK293 cells. Pflugers Arch 442: 668-674.

Hamill OP, Bormann J, Sakmann B (1983) Activation of multiple-conductance state chloride channels in spinal neurones by glycine and GABA. Nature 305: 805-808.

Han NL, Haddrill JL, Lynch JW (2001) Characterization of a glycine receptor domain that controls the binding and gating mechanisms of the β-amino acid agonist, taurine. J Neurochem 79: 636-647.

Han Y, Wu SM (1999) Modulation of glycine receptors in retinal ganglion cells by zinc. Proc Natl Acad Sci U S A 96: 3234-3238.

Handford CA, Lynch JW, Baker E, Webb GC, Ford JH, Sutherland GR, Schofield PR (1996) The human glycine receptor β subunit: primary structure, functional characterisation and chromosomal localisation of the human and murine genes. Brain Res Mol Brain Res 35: 211-219.

Harrison NL, Gibbons SJ (1994) Zn^{2+}: an endogenous modulator of ligand- and voltage-gated ion channels. Neuropharmacology 33: 935-952.

Harvey RJ, Depner UB, Wassle H, Ahmadi S, Heindl C, Reinold H, Smart TG, Harvey K, Schutz B, Abo-Salem OM, Zimmer A, Poisbeau P, Welzl H, Wolfer DP, Betz H, Zeilhofer HU, Muller U (2004) GlyR α3: an essential target for spinal PGE2-mediated inflammatory pain sensitization. Science 304: 884-887.

Harvey RJ, Schmieden V, Von Holst A, Laube B, Rohrer H, Betz H (2000) Glycine receptors containing the α4 subunit in the embryonic sympathetic nervous system, spinal cord and male genital ridge. Eur J Neurosci 12: 994-1001.

Harvey RJ, Thomas P, James CH, Wilderspin A, Smart TG (1999) Identification of an inhibitory Zn^{2+} binding site on the human glycine receptor α1 subunit. J Physiol 520: 53-64.

Haug FM, Blackstad TW, Simonsen AH, Zimmer J (1971) Timm's sulfide silver reaction for zinc during experimental anterograde degeneration of hippocampal mossy fibers. J Comp Neurol 142: 23-31.

Haverkamp S, Muller U, Harvey K, Harvey RJ, Betz H, Wassle H (2003) Diversity of glycine receptors in the mouse retina: localization of the α3 subunit. J Comp Neurol 465: 524-539.

Hoch W, Betz H, Becker CM (1989) Primary cultures of mouse spinal cord express the neonatal isoform of the inhibitory glycine receptor. Neuron 3: 339-348.

Hoch W, Betz H, Schramm M, Wolters I, Becker CM (1992) Modulation by NMDA Receptor Antagonists of Glycine Receptor Isoform Expression in Cultured Spinal Cord Neurons. Eur J Neurosci 4: 389-395.

Hokfelt T, Ljungdahl A (1971) Light and electron microscopic autoradiography on spinal cord slices after incubation with labeled glycine. Brain Res 32: 189-194.

Holland JM, Davis WC, Prieur DJ, Collins GH (1970) Lafora's disease in the dog. A comparative study. Am J Pathol 58: 509-530.

Hosie AM, Aronstein K, Sattelle DB, ffrench-Constant RH (1997) Molecular biology of insect neuronal GABA receptors. Trends Neurosci 20: 578-583.

Hosie AM, Dunne EL, Harvey RJ, Smart TG (2003) Zinc-mediated inhibition of $GABA_A$ receptors: discrete binding sites underlie subtype specificity. Nat Neurosci 6: 362-369.

Howell GA, Welch MG, Frederickson CJ (1984) Stimulation-induced uptake and release of zinc in hippocampal slices. Nature 308: 736-738.

Hsiao B, Dweck D, Luetje CW (2001) Subunit-dependent modulation of neuronal nicotinic receptors by zinc. J Neurosci 21: 1848-1856.

Hubbard PC, Lummis SC (2000) Zn^{2+} enhancement of the recombinant 5-HT(3) receptor is modulated by divalent cations. Eur J Pharmacol 394: 189-197.

Imboden M, Devignot V, Goblet C (2001) Phylogenetic relationships and chromosomal location of five distinct glycine receptor subunit genes in the teleost Danio rerio. Dev Genes Evol 211: 415-422.

Jensen KB, Dredge BK, Stefani G, Zhong R, Buckanovich RJ, Okano HJ, Yang YY, Darnell RB (2000) Nova-1 regulates neuron-specific alternative splicing and is essential for neuronal viability. Neuron 25: 359-371.

Jeong HJ, Jang IS, Moorhouse AJ, Akaike N (2003) Activation of presynaptic glycine receptors facilitates glycine release from presynaptic terminals synapsing onto rat spinal sacral dorsal commissural nucleus neurons. J Physiol.

Ji RR, Befort K, Brenner GJ, Woolf CJ (2002) ERK MAP kinase activation in superficial spinal cord neurons induces prodynorphin and NK-1 upregulation and contributes to persistent inflammatory pain hypersensitivity. J Neurosci 22: 478-485.

Jo SM, Danscher G, Daa SH, Won MH, Cole TB (2000) Zinc-enriched (ZEN) terminals in mouse spinal cord: immunohistochemistry and autometallography. Brain Res 870: 163-169.

Johnson JW, Ascher P (1987) Glycine potentiates the NMDA response in cultured mouse brain neurons. Nature 325: 529-531.

Johnston GA (1968) The intraspinal distribution of some depressant amino acids. J Neurochem 15: 1013-1017.

Johnston GA, Iversen LL (1971) Glycine uptake in rat central nervous system slices and homogenates: evidence for different uptake systems in spinal cord and cerebral cortex. J Neurochem 18: 1951-1961.

Jonas P, Bischofberger J, Sandkuhler J (1998) Corelease of two fast neurotransmitters at a central synapse. Science 281: 419-424.

Kandel ER, Schwartz JH, Jessell TM (2000) Spinal reflex. In: Kandel ER, Schwartz JH, Jessell TM (eds). Principles of Neuronal Science, pp.713-736, McGraw-Hill. New York.

Kapfer C, Seidl AH, Schweizer H, Grothe B (2002) Experience-dependent refinement of inhibitory inputs to auditory coincidence-detector neurons. Nat Neurosci 5: 247-253.

Karlin A, Akabas MH (1995) Toward a structural basis for the function of nicotinic acetylcholine receptors and their cousins. Neuron 15: 1231-1244.

Kash TL, Dizon MJ, Trudell JR, Harrison NL (2003b) Charged residues in the $GABA_A$ receptor β-2 subunit are crucial for efficient receptor activation. J Biol Chem.

Kash TL, Jenkins A, Kelley JC, Trudell JR, Harrison NL (2003a) Coupling of agonist binding to channel gating in the $GABA_A$ receptor. Nature 421: 272-275.

Katsurabayashi S, Kubota H, Wang ZM, Rhee JS, Akaike N (2001) cAMP-dependent presynaptic regulation of spontaneous glycinergic IPSCs in mechanically dissociated rat spinal cord neurons. J Neurophysiol 85: 332-340.

Kay AR (2003) Evidence for chelatable zinc in the extracellular space of the hippocampus, but little evidence for synaptic release of Zn^{2+}. J Neurosci 23: 6847-6855.

Keller AF, Coull JA, Chery N, Poisbeau P, de Koninck Y (2001) Region-specific developmental specialization of GABA-glycine cosynapses in laminas I-II of the rat spinal dorsal horn. J Neurosci 21: 7871-7880.

Kelley SP, Dunlop JI, Kirkness EF, Lambert JJ, Peters JA (2003) A cytoplasmic region determines single-channel conductance in $5\text{-}HT_3$ receptors. Nature 424: 321-324.

Kelly JS, Krnjevic K (1969) The action of glycine on cortical neurones. Exp Brain Res 9: 155-163.

Keramidas A, Moorhouse AJ, French CR, Schofield PR, Barry PH (2000) M2 pore mutations convert the glycine receptor channel from being anion- to cation-selective. Biophys J 79: 247-259.

Kim G, Kandler K (2003) Elimination and strengthening of glycinergic/GABAergic connections during tonotopic map formation. Nat Neurosci 6: 282-290.

Kim KM, Kingsmore SF, Han H, Yang-Feng TL, Godinot N, Seldin MF, Caron MG, Giros B (1994) Cloning of the human glycine transporter type 1: molecular and pharmacological characterization of novel isoform variants and chromosomal localization of the gene in the human and mouse genomes. Mol Pharmacol 45: 608-617.

Kirsch J, Betz H (1993) Widespread expression of gephyrin, a putative glycine receptor-tubulin linker protein, in rat brain. Brain Res 621: 301-310.

Kneussel M, Hermann A, Kirsch J, Betz H (1999) Hydrophobic interactions mediate binding of the glycine receptor β-subunit to gephyrin. J Neurochem 72: 1323-1326.

Korpi ER, Seeburg PH (1993) Natural mutation of $GABA_A$ receptor α 6 subunit alters benzodiazepine affinity but not allosteric GABA effects. Eur J Pharmacol 247: 23-27.

Kuhse J, Kuryatov A, Maulet Y, Malosio ML, Schmieden V, Betz H (1991) Alternative splicing generates two isoforms of the α 2 subunit of the inhibitory glycine receptor. FEBS Lett 283: 73-77.

Kuhse J, Schmieden V, Betz H (1990b) A single amino acid exchange alters the pharmacology of neonatal rat glycine receptor subunit. Neuron 5: 867-873.

Kuhse J, Schmieden V, Betz H (1990a) Identification and functional expression of a novel ligand binding subunit of the inhibitory glycine receptor. J Biol Chem 265: 22317-22320.

Kullmann PH, Ene FA, Kandler K (2002) Glycinergic and GABAergic calcium responses in the developing lateral superior olive. Eur J Neurosci 15: 1093-1104.

Kungel M, Friauf E (1997) Physiology and pharmacology of native glycine receptors in developing rat auditory brainstem neurons. Brain Res Dev Brain Res 102: 157-165.

Kusama T, Wang JB, Spivak CE, Uhl GR (1994) Mutagenesis of the GABA ρ 1 receptor alters agonist affinity and channel gating. Neuroreport 5: 1209-1212.

Labarca C, Nowak MW, Zhang H, Tang L, Deshpande P, Lester HA (1995) Channel gating governed symmetrically by conserved leucine residues in the M2 domain of nicotinic receptors. Nature 376: 514-516.

Lambert JJ, Belelli D, Peden DR, Vardy AW, Peters JA (2003) Neurosteroid modulation of GABAA receptors. Prog Neurobiol 71: 67-80.

Lane PW, Ganser AL, Kerner AL, White WF (1987) Spasmodic, a mutation on chromosome 11 in the mouse. J Hered 78: 353-356.

Langosch D, Laube B, Rundstrom N, Schmieden V, Bormann J, Betz H (1994) Decreased agonist affinity and chloride conductance of mutant glycine receptors associated with human hereditary hyperekplexia. EMBO J 13: 4223-4228.

Laube B (2002a) Potentiation of inhibitory glycinergic neurotransmission by Zn^{2+}: a synergistic interplay between presynaptic $P2X_2$ and postsynaptic glycine receptors. Eur J Neurosci 16: 1025-1036.

Laube B, Kuhse J, Betz H (2000) Kinetic and mutational analysis of Zn^{2+} modulation of recombinant human inhibitory glycine receptors. J Physiol 522 Pt 2: 215-230.

Laube B, Kuhse J, Rundstrom N, Kirsch J, Schmieden V, Betz H (1995) Modulation by zinc ions of native rat and recombinant human inhibitory glycine receptors. J Physiol 483 (Pt 3): 613-619.

Laube B, Maksay G, Schemm R, Betz H (2002b) Modulation of glycine receptor function: a novel approach for therapeutic intervention at inhibitory synapses? Trends Pharmacol Sci 23: 519-527.

Laube B, Maksay G, Schemm R, Betz H (2002b) Modulation of glycine receptor function: a novel approach for therapeutic intervention at inhibitory synapses? Trends Pharmacol Sci 23: 519-527.

Legendre P (1997) Pharmacological evidence for two types of postsynaptic glycinergic receptors on the Mauthner cell of 52-h-old zebrafish larvae. J Neurophysiol 77: 2400-2415.

Legendre P (1998) A reluctant gating mode of glycine receptor channels determines the time course of inhibitory miniature synaptic events in zebrafish hindbrain neurons. J Neurosci 18: 2856-2870.

Legendre P (2001) The glycinergic inhibitory synapse. Cell Mol Life Sci 58: 760-793.

Legendre P, Muller E, Badiu CI, Meier J, Vannier C, Triller A (2002) Desensitization of homomeric $\alpha 1$ glycine receptor increases with receptor density. Mol Pharmacol 62: 817-827.

Legendre P, Westbrook GL (1991) Noncompetitive inhibition of gamma-aminobutyric $acid_A$ channels by Zn. Mol Pharmacol 39: 267-274.

Legendre P, Westbrook GL (1990) The inhibition of single N-methyl-D-aspartate-activated channels by zinc ions on cultured rat neurones. J Physiol 429: 429-449.

Lester HA, Dibas MI, Dahan DS, Leite JF, Dougherty DA (2004) Cys-loop receptors: new twists and turns. Trends Neurosci 27: 329-336.

Lewis TM, Schofield PR, McClellan AM (2003) Kinetic determinants of agonist action at the recombinant human glycine receptor. J Physiol 549: 361-374.

Li P, Yang XL (1999) Zn_{2+} differentially modulates glycine receptors versus GABA receptors in isolated carp retinal third-order neurons. Neurosci Lett 269: 75-78.

Li Y, Hough CJ, Suh SW, Sarvey JM, Frederickson CJ (2001) Rapid translocation of Zn^{2+} from presynaptic terminals into postsynaptic hippocampal neurons after physiological stimulation. J Neurophysiol 86: 2597-2604.

Li Y, Wu LJ, Legendre P, Xu TL (2003) Asymmetric Cross-inhibition between $GABA_A$ and Glycine Receptors in Rat Spinal Dorsal Horn Neurons. J Biol Chem 278: 38637-38645.

Li YX, Schaffner AE, Barker JL (1999) Astrocytes regulate the developmental appearance of GABAergic and glutamatergic postsynaptic currents in cultured embryonic rat spinal neurons. Eur J Neurosci 11: 2537-2551.

Lim R, Alvarez FJ, Walmsley B (2000) GABA mediates presynaptic inhibition at glycinergic synapses in a rat auditory brainstem nucleus. J Physiol 525 Pt 2: 447-459.

Liu QR, Lopez-Corcuera B, Mandiyan S, Nelson H, Nelson N (1993) Cloning and expression of a spinal cord- and brain-specific glycine transporter with novel structural features. J Biol Chem 268: 22802-22808.

Ljungdahl A, Hokfelt T (1973) Autoradiographic uptake patterns of (^{3}H)GABA and (^{3}H)glycine in central nervous tissues with special reference to the cat spinal cord. Brain Res 62: 587-595.

Lobo IA, Mascia MP, Trudell JR, Harris RA (2004) Channel gating of the glycine receptor changes accessibility to residues implicated in receptor potentiation by alcohols and anesthetics. J Biol Chem 279: 33919-33927.

Lodge D, Curtis DR, Brand SJ (1977) A pharmacological study of the inhibition of ventral group Ia-excited spinal interneurones. Exp Brain Res 29: 97-105.

Logan WJ, Snyder SH (1972) High affinity uptake systems for glycine, glutamic and aspaspartic acids in synaptosomes of rat central nervous tissues. Brain Res 42: 413-431.

Lynch JW (2004) Molecular structure and function of the glycine receptor chloride channel. Physiol Rev 84: 1051-1095.

Lynch JW, Jacques P, Pierce KD, Schofield PR (1998) Zinc potentiation of the glycine receptor chloride channel is mediated by allosteric pathways. J Neurochem 71: 2159-2168.

Lynch JW, Rajendra S, Barry PH, Schofield PR (1995) Mutations affecting the glycine receptor agonist transduction mechanism convert the competitive antagonist, picrotoxin, into an allosteric potentiator. J Biol Chem 270: 13799-13806.

Lynch JW, Rajendra S, Pierce KD, Handford CA, Barry PH, Schofield PR (1997) Identification of intracellular and extracellular domains mediating signal transduction in the inhibitory glycine receptor chloride channel. EMBO J 16: 110-120.

Malosio ML, Grenningloh G, Kuhse J, Schmieden V, Schmitt B, Prior P, Betz H (1991b) Alternative splicing generates two variants of the α 1 subunit of the inhibitory glycine receptor. J Biol Chem 266: 2048-2053.

Malosio ML, Marqueze-Pouey B, Kuhse J, Betz H (1991a) Widespread expression of glycine receptor subunit mRNAs in the adult and developing rat brain. EMBO J 10: 2401-2409.

Mangin JM, Baloul M, Prado DC, Rogister B, Rigo JM, Legendre P (2003) Kinetic properties of the α2 homo-oligomeric glycine receptor impairs a proper synaptic functioning. J Physiol 553: 369-386.

Mangin JM, Guyon A, Eugene D, Paupardin-Tritsch D, Legendre P (2002) Functional glycine receptor maturation in the absence of glycinergic input in dopaminergic neurones of the rat substantia nigra. J Physiol 542: 685-697.

Mascia MP, Machu TK, Harris RA (1996) Enhancement of homomeric glycine receptor function by long-chain alcohols and anaesthetics. Br J Pharmacol 119: 1331-1336.

Matus AI, Dennison ME (1971) Autoradiographic localisation of tritiated glycine at 'flat-vesicle' synapses in spinal cord. Brain Res 32: 195-197.

Mayer ML, Armstrong N (2004) Structure and function of glutamate receptor ion channels. Annu Rev Physiol 66: 161-181.

McCool BA, Farroni JS (2001) Subunit composition of strychnine-sensitive glycine receptors expressed by adult rat basolateral amygdala neurons. Eur J Neurosci 14: 1082-1090.

Meier J, De Chaldee M, Triller A, Vannier C (2000) Functional heterogeneity of gephyrins. Mol Cell Neurosci 16: 566-577.

Mengual E, Casanovas-Aguilar C, Perez-Clausell J, Gimenez-Amaya JM (2001) Thalamic distribution of zinc-rich terminal fields and neurons of origin in the rat. Neuroscience 102: 863-884.

Meyer G, Kirsch J, Betz H, Langosch D (1995) Identification of a gephyrin binding motif on the glycine receptor β subunit. Neuron 15: 563-572.

Mihic SJ, Harris RA (1996) Inhibition of ρ1 receptor GABAergic currents by alcohols and volatile anesthetics. J Pharmacol Exp Ther 277: 411-416.

Mihic SJ, Ye Q, Wick MJ, Koltchine VV, Krasowski MD, Finn SE, Mascia MP, Valenzuela CF, Hanson KK, Greenblatt EP, Harris RA, Harrison NL (1997) Sites of alcohol and volatile anaesthetic action on $GABA_A$ and glycine receptors. Nature 389: 385-389.

Miller PS, Harvey RJ, Smart TG (2004) Differential agonist sensitivity of glycine receptor α2 subunit splice variants. Br J Pharmacol 143: 19-26.

Miyazawa A, Fujiyoshi Y, Stowell M, Unwin N (1999) Nicotinic acetylcholine receptor at 4.6 A resolution: transverse tunnels in the channel wall. J Mol Biol 288: 765-786.

Miyazawa A, Fujiyoshi Y, Unwin N (2003) Structure and gating mechanism of the acetylcholine receptor pore. Nature 424: 949-955.

Mohammadi B, Krampfl K, Cetinkaya C, Moschref H, Grosskreutz J, Dengler R, Bufler J (2003) Kinetic analysis of recombinant mammalian α(1) and α(1)beta glycine receptor channels. Eur Biophys J 32: 529-536.

Moorhouse AJ, Jacques P, Barry PH, Schofield PR (1999) The startle disease mutation Q266H, in the second transmembrane domain of the human glycine receptor, impairs channel gating. Mol Pharmacol 55: 386-395.

Mori M, Gahwiler BH, Gerber U (2002) β-alanine and taurine as endogenous agonists at glycine receptors in rat hippocampus in vitro. J Physiol 539: 191-200.

Morris KD, Amin J (2004) Insight into the mechanism of action of neuroactive steroids. Mol Pharmacol 66: 56-69.

Moss SJ, Smart TG (2001) Constructing inhibitory synapses. Nat Rev Neurosci 2: 240-250.

Mu TW, Lester HA, Dougherty DA (2003) Different binding orientations for the same agonist at homologous receptors: a lock and key or a simple wedge? J Am Chem Soc 125: 6850-6851.

Mulder AH, Snyder SH (1974) Potassium-induced release of amino acids from cerebral cortex and spinal cord slices of the rat. Brain Res 76: 297-308.

Neal MJ (1969) Uptake of [^{14}C]-glycine by rat spinal cord. Br J Pharmacol 36: 205P.

Nevin ST, Cromer BA, Haddrill JL, Morton CJ, Parker MW, Lynch JW (2003) Insights into the structural basis for zinc inhibition of the glycine receptor. J Biol Chem 278: 28985-28992.

Nicoll RA (1988) The coupling of neurotransmitter receptors to ion channels in the brain. Science 241: 545-551.

Nikolic Z, Laube B, Weber RG, Lichter P, Kioschis P, Poustka A, Mulhardt C, Becker CM (1998) The human glycine receptor subunit α3. Glra3 gene structure, chromosomal localization, and functional characterization of alternative transcripts. J Biol Chem 273: 19708-19714.

O'Brien JA, Berger AJ (1999) Cotransmission of GABA and glycine to brain stem motoneurons. J Neurophysiol 82: 1638-1641.

Okabe A, Kilb W, Shimizu-Okabe C, Hanganu IL, Fukuda A, Luhmann HJ (2004) Homogenous glycine receptor expression in cortical plate neurons and Cajal-Retzius cells of neonatal rat cerebral cortex. Neuroscience 123: 715-724.

Osborne RH, Bradford HF, Jones DG (1973) Patterns of amino acid release from nerve-endings isolated from spinal cord and medulla. J Neurochem 21: 407-419.

Ottersen OP, Storm-Mathisen J, (1990) Glycine neurotransmission. 1-23. John Wiley & Sons Ltd.

Palma E, Maggi L, Miledi R, Eusebi F (1998) Effects of Zn^{2+} on wild and mutant neuronal α7 nicotinic receptors. Proc Natl Acad Sci U S A 95: 10246-10250.

Palmiter RD, Cole TB, Quaife CJ, Findley SD (1996) ZnT-3, a putative transporter of zinc into synaptic vesicles. Proc Natl Acad Sci U S A 93: 14934-14939.

Paoletti P, Ascher P, Neyton J (1997) High-affinity zinc inhibition of NMDA NR1-NR2A receptors. J Neurosci 17: 5711-5725.

Paoletti P, Perin-Dureau F, Fayyazuddin A, Le Goff A, Callebaut I, Neyton J (2000) Molecular organization of a zinc binding n-terminal modulatory domain in a NMDA receptor subunit. Neuron 28: 911-925.

Perez-Clausell J (1996) Distribution of terminal fields stained for zinc in the neocortex of the rat. J Chem Neuroanat 11: 99-111.

Perez-Clausell J, Frederickson CJ, Danscher G (1989) Amygdaloid efferents through the stria terminalis in the rat give origin to zinc-containing boutons. J Comp Neurol 290: 201-212.

Pfeiffer F, Graham D, Betz H (1982) Purification by affinity chromatography of the glycine receptor of rat spinal cord. J Biol Chem 257: 9389-9393.

Pidoplichko VI, DeBiasi M, Williams JT, Dani JA (1997) Nicotine activates and desensitizes midbrain dopamine neurons. Nature 390: 401-404.

Pribilla I, Takagi T, Langosch D, Bormann J, Betz H (1992) The atypical M2 segment of the β subunit confers picrotoxinin resistance to inhibitory glycine receptor channels. EMBO J 11: 4305-4311.

Price DL, Stocks A, Griffin JW, Young A, Peck K (1976) Glycine-specific synapses in rat spinal cord. Identification by electron microscope autoradiography. J Cell Biol 68: 389-395.

Prior P, Schmitt B, Grenningloh G, Pribilla I, Multhaup G, Beyreuther K, Maulet Y, Werner P, Langosch D, Kirsch J, . (1992) Primary structure and alternative splice variants of gephyrin, a putative glycine receptor-tubulin linker protein. Neuron 8: 1161-1170.

Protti DA, Gerschenfeld HM, Llano I (1997) GABAergic and glycinergic IPSCs in ganglion cells of rat retinal slices. J Neurosci 17: 6075-6085.

Rajendra S, Lynch JW, Pierce KD, French CR, Barry PH, Schofield PR (1995c) Mutation of an arginine residue in the human glycine receptor transforms β - alanine and taurine from agonists into competitive antagonists. Neuron 14: 169-175.

Rajendra S, Schofield PR (1995a) Molecular mechanisms of inherited startle syndromes. Trends Neurosci 18: 80-82.

Rajendra S, Vandenberg RJ, Pierce KD, Cunningham AM, French PW, Barry PH, Schofield PR (1995b) The unique extracellular disulfide loop of the glycine receptor is a principal ligand binding element. EMBO J 14: 2987-2998.

Rajendra S, Lynch JW, Schofield PR (1997) The glycine receptor. Pharmacol Ther 73: 121-146.

Ramming M, Kins S, Werner N, Hermann A, Betz H, Kirsch J (2000) Diversity and phylogeny of gephyrin: tissue-specific splice variants, gene structure, and sequence similarities to molybdenum cofactor-synthesizing and cytoskeleton-associated proteins. Proc Natl Acad Sci U S A 97: 10266-10271.

Rees MI, Andrew M, Jawad S, Owen MJ (1994) Evidence for recessive as well as dominant forms of startle disease (hyperekplexia) caused by mutations in the α 1 subunit of the inhibitory glycine receptor. Hum Mol Genet 3: 2175-2179.

Rees MI, Harvey K, Ward H, White JH, Evans L, Duguid IC, Hsu CC, Coleman SL, Miller J, Baer K, Waldvogel HJ, Gibbon F, Smart TG, Owen MJ, Harvey RJ, Snell RG (2003) Isoform heterogeneity of the human gephyrin gene (GPHN), binding domains to the glycine receptor, and mutation analysis in hyperekplexia. J Biol Chem 278: 24688-24696.

Reeves DC, Sayed MF, Chau PL, Price KL, Lummis SC (2003) Prediction of 5-HT3 receptor agonist-binding residues using homology modeling. Biophys J 84: 2338-2344.

Roberts PJ, Mitchell JF (1972) The release of amino acids from the hemisected spinal cord during stimulation. J Neurochem 19: 2473-2481.

Rocha E Silva, Schild HO (1949) The release of histamine by d-tubocurarine from the isolated diaphragm of the rat. J Physiol 109: 448-458.

Ruiz A, Walker MC, Fabian-Fine R, Kullmann DM (2003) Endogenous zinc inhibits $GABA_A$ receptors in a hippocampal pathway. J Neurophysiol.

Ruiz-Gomez A, Morato E, Garcia-Calvo M, Valdivieso F, Mayor F, Jr. (1990) Localization of the strychnine binding site on the 48-kilodalton subunit of the glycine receptor. Biochemistry 29: 7033-7040.

Ruiz-Gomez A, Vaello ML, Valdivieso F, Mayor F, Jr. (1991) Phosphorylation of the 48-kDa subunit of the glycine receptor by protein kinase C. J Biol Chem 266: 559-566.

Rundstrom N, Schmieden V, Betz H, Bormann J, Langosch D (1994) Cyanotriphenylborate: subtype-specific blocker of glycine receptor chloride channels. Proc Natl Acad Sci U S A 91: 8950-8954.

Russier M, Kopysova IL, Ankri N, Ferrand N, Debanne D (2002) GABA and glycine co-release optimizes functional inhibition in rat brainstem motoneurons in vitro. J Physiol 541: 123-137.

Ryan SG, Buckwalter MS, Lynch JW, Handford CA, Segura L, Shiang R, Wasmuth JJ, Camper SA, Schofield P, O'Connell P (1994) A missense mutation in the gene encoding the alpha 1 subunit of the inhibitory glycine receptor in the spasmodic mouse. Nat Genet 7: 131-135.

Sabatini DM, Barrow RK, Blackshaw S, Burnett PE, Lai MM, Field ME, Bahr BA, Kirsch J, Betz H, Snyder SH (1999) Interaction of RAFT1 with gephyrin required for rapamycin-sensitive signaling. Science 284: 1161-1164.

Saitoh T, Ishida M, Maruyama M, Shinozaki H (1994) A novel antagonist, phenylbenzene omega-phosphono-alpha-amino acid, for strychnine-sensitive glycine receptors in the rat spinal cord. Br J Pharmacol 113: 165-170.

Saul B, Schmieden V, Kling C, Mulhardt C, Gass P, Kuhse J, Becker CM (1994) Point mutation of glycine receptor α 1 subunit in the spasmodic mouse affects agonist responses. FEBS Lett 350: 71-76.

Schmieden V, Kuhse J, Betz H (1993) Mutation of glycine receptor subunit creates β-alanine receptor responsive to GABA. Science 262: 256-258.

Schofield CM, Jenkins A, Harrison NL (2003) A highly conserved aspartic acid residue in the signature disulfide loop of the α 1 subunit is a determinant of gating in the glycine receptor. J Biol Chem 278: 34079-34083.

Schofield CM, Trudell JR, Harrison NL (2004) Alanine-scanning mutagenesis in the signature disulfide loop of the glycine receptor α 1 subunit: critical residues for activation and modulation. Biochemistry 43: 10058-10063.

Shan Q, Nevin ST, Haddrill JL, Lynch JW (2003) Asymmetric contribution of α and β subunits to the activation of αβ heteromeric glycine receptors. J Neurochem 86: 498-507.

Sigel E, Buhr A (1997) The benzodiazepine binding site of $GABA_A$ receptors. Trends Pharmacol Sci 18: 425-429.

Sigel E, Buhr A, Baur R (1999) Role of the conserved lysine residue in the middle of the predicted extracellular loop between M2 and M3 in the $GABA_A$ receptor. J Neurochem 73: 1758-1764.

Simons TJ (1991) Intracellular free zinc and zinc buffering in human red blood cells. J Membr Biol 123: 63-71.

Slomianka L (1992) Neurons of origin of zinc-containing pathways and the distribution of zinc-containing boutons in the hippocampal region of the rat. Neuroscience 48: 325-352.

Smart TG (1992) A novel modulatory binding site for zinc on the $GABA_A$ receptor complex in cultured rat neurones. J Physiol 447: 587-625.

Smart TG, Constanti A (1990) Differential effect of zinc on the vertebrate $GABA_A$-receptor complex. Br J Pharmacol 99: 643-654.

Smart TG, Hosie AM, Miller PS (2004) Zn^{2+} ions: modulators of excitatory and inhibitory synaptic activity. Neuroscientist 10: 432-442.

Smart TG, Moss SJ, Xie X, Huganir RL (1991) $GABA_A$ receptors are differentially sensitive to zinc: dependence on subunit composition. Br J Pharmacol 103: 1837-1839.

Smith AJ, Owens S, Forsythe ID (2000) Characterisation of inhibitory and excitatory postsynaptic currents of the rat medial superior olive. J Physiol 529 Pt 3: 681-698.

Song YM, Huang LY (1990) Modulation of glycine receptor chloride channels by cAMP-dependent protein kinase in spinal trigeminal neurons. Nature 348: 242-245.

Stell BM, Brickley SG, Tang CY, Farrant M, Mody I (2003) Neuroactive steroids reduce neuronal excitability by selectively enhancing tonic inhibition mediated by delta subunit-containing $GABA_A$ receptors. Proc Natl Acad Sci U S A 100: 14439-14444.

Sturman JA (1986) Nutritional taurine and central nervous system development. Ann N Y Acad Sci 477: 196-213.

Sullivan DA, Cohen JB (2000) Mapping the agonist binding site of the nicotinic acetylcholine receptor. Orientation requirements for activation by covalent agonist. J Biol Chem 275: 12651-12660.

Suwa H, Saint-Amant L, Triller A, Drapeau P, Legendre P (2001) High-affinity zinc potentiation of inhibitory postsynaptic glycinergic currents in the zebrafish hindbrain. J Neurophysiol 85: 912-925.

Takahashi T, Momiyama A, Hirai K, Hishinuma F, Akagi H (1992) Functional correlation of fetal and adult forms of glycine receptors with developmental changes in inhibitory synaptic receptor channels. Neuron 9: 1155-1161.

Tapia JC, Mentis GZ, Navarrete R, Nualart F, Figueroa E, Sanchez A, Aguayo LG (2001) Early expression of glycine and $GABA_A$ receptors in developing spinal cord neurons. Effects on neurite outgrowth. Neuroscience 108: 493-506.

ten Bruggencate G, Sonnhof U (1972) Effects of glycine and GABA, and blocking actions of strychnine and picrotoxin in the hypoglossus nucleus. Pflugers Arch 334: 240-252.

Thompson RB, Whetsell WO, Jr., Maliwal BP, Fierke CA, Frederickson CJ (2000) Fluorescence microscopy of stimulated Zn(II) release from organotypic cultures of mammalian hippocampus using a carbonic anhydrase-based biosensor system. J Neurosci Methods 96: 35-45.

Tian N, Hwang TN, Copenhagen DR (1998) Analysis of excitatory and inhibitory spontaneous synaptic activity in mouse retinal ganglion cells. J Neurophysiol 80: 1327-1340.

Traynelis SF, Burgess MF, Zheng F, Lyuboslavsky P, Powers JL (1998) Control of voltage-independent zinc inhibition of NMDA receptors by the NR1 subunit. J Neurosci 18: 6163-6175.

Twyman RE, Macdonald RL (1991) Kinetic properties of the glycine receptor main- and sub-conductance states of mouse spinal cord neurones in culture. J Physiol 435: 303-331.

Ueno S, Tsukamoto M, Hirano T, Kikuchi K, Yamada MK, Nishiyama N, Nagano T, Matsuki N, Ikegaya Y (2002) Mossy fiber Zn^{2+} spillover modulates heterosynaptic N-methyl-D-aspartate receptor activity in hippocampal CA3 circuits. J Cell Biol 158: 215-220.

Ule J, Jensen KB, Ruggiu M, Mele A, Ule A, Darnell RB (2003) CLIP identifies Nova-regulated RNA networks in the brain. Science 302: 1212-1215.

Unwin N (1993) Nicotinic acetylcholine receptor at 9 A resolution. J Mol Biol 229: 1101-1124.

Unwin N (1995) Acetylcholine receptor channel imaged in the open state. Nature 373: 37-43.

Unwin N, Miyazawa A, Li J, Fujiyoshi Y (2002) Activation of the nicotinic acetylcholine receptor involves a switch in conformation of the alpha subunits. J Mol Biol 319: 1165-1176.

Vafa B, Lewis TM, Cunningham AM, Jacques P, Lynch JW, Schofield PR (1999) Identification of a new ligand binding domain in the α1 subunit of the inhibitory glycine receptor. J Neurochem 73: 2158-2166.

Vallee BL, Auld DS (1990) Zinc coordination, function, and structure of zinc enzymes and other proteins. Biochemistry 29: 5647-5659.

Vandenberg RJ, French CR, Barry PH, Shine J, Schofield PR (1992a) Antagonism of ligand-gated ion channel receptors: two domains of the glycine receptor α subunit form the strychnine-binding site. Proc Natl Acad Sci U S A 89: 1765-1769.

Vandenberg RJ, Handford CA, Schofield PR (1992b) Distinct agonist- and antagonist-binding sites on the glycine receptor. Neuron 9: 491-496.

Varea E, Ponsoda X, Molowny A, Danscher G, Lopez-Garcia C (2001) Imaging synaptic zinc release in living nervous tissue. J Neurosci Methods 110: 57-63.

Velazquez RA, Cai Y, Shi Q, Larson AA (1999) The distribution of zinc selenite and expression of metallothionein-III mRNA in the spinal cord and dorsal root ganglia of the rat suggest a role for zinc in sensory transmission. J Neurosci 19: 2288-2300.

Voet D, Voet JG (1996) Biochemistry.

Vogt K, Mellor J, Tong G, Nicoll R (2000) The actions of synaptically released zinc at hippocampal mossy fiber synapses. Neuron 26: 187-196.

Walstrom KM, Hess GP (1994) Mechanism for the channel-opening reaction of strychnine-sensitive glycine receptors on cultured embryonic mouse spinal cord cells. Biochemistry 33: 7718-7730.

Wang TL, Hackam A, Guggino WB, Cutting GR (1995) A single histidine residue is essential for zinc inhibition of GABA ρ 1 receptors. J Neurosci 15: 7684-7691.

Wang Z, Li JY, Dahlstrom A, Danscher G (2001) Zinc-enriched GABAergic terminals in mouse spinal cord. Brain Res 921: 165-172.

Watanabe E, Akagi H (1995) Distribution patterns of mRNAs encoding glycine receptor channels in the developing rat spinal cord. Neurosci Res 23: 377-382.

Wensink J, Molenaar AJ, Woroniecka UD, Van den Hamer CJ (1988) Zinc uptake into synaptosomes. J Neurochem 50: 782-789.

Wenzel HJ, Cole TB, Born DE, Schwartzkroin PA, Palmiter RD (1997) Ultrastructural localization of zinc transporter-3 (ZnT-3) to synaptic vesicle membranes within mossy fiber boutons in the hippocampus of mouse and monkey. Proc Natl Acad Sci U S A 94: 12676-12681.

Werman R, Davidoff RA, Aprison MH (1967) Inhibition of motoneurones by iontophoresis of glycine. Nature 214: 681-683.

Werman R, Davidoff RA, Aprison MH (1968) Inhibition of glycine on spinal neurons in the cat. J Neurophysiol 31: 81-95.

Wick MJ, Mihic SJ, Ueno S, Mascia MP, Trudell JR, Brozowski SJ, Ye Q, Harrison NL, Harris RA (1998) Mutations of gamma-aminobutyric acid and glycine receptors change alcohol cutoff: evidence for an alcohol receptor? Proc Natl Acad Sci U S A 95: 6504-6509.

Wieland HA, Luddens H, Seeburg PH (1992) A single histidine in $GABA_A$ receptors is essential for benzodiazepine agonist binding. J Biol Chem 267: 1426-1429.

Wilkins ME, Smart TG (2002) Redox modulation of GABAA receptors obscured by Zn^{2+} complexation. Neuropharmacology 43: 938-944.

Wu WL, Ziskind-Conhaim L, Sweet MA (1992) Early development of glycine- and GABA-mediated synapses in rat spinal cord. J Neurosci 12: 3935-3945.

Xu M, Covey DF, Akabas MH (1995) Interaction of picrotoxin with $GABA_A$ receptor channel-lining residues probed in cysteine mutants. Biophys J 69: 1858-1867.

Xu TL, Li JS, Jin YH, Akaike N (1999) Modulation of the glycine response by Ca^{2+}-permeable AMPA receptors in rat spinal neurones. J Physiol 514 (Pt 3): 701-711.

Yevenes GE, Peoples RW, Tapia JC, Parodi J, Soto X, Olate J, Aguayo LG (2003) Modulation of glycine-activated ion channel function by G-protein $\beta\gamma$ subunits. Nat Neurosci 6: 819-824.

Yohannan S, Yang D, Faham S, Boulting G, Whitelegge J, Bowie JU (2004) Proline substitutions are not easily accommodated in a membrane protein. J Mol Biol 341: 1-6.

Young AB, Snyder SH (1973) Strychnine binding associated with glycine receptors of the central nervous system. Proc Natl Acad Sci U S A 70: 2832-2836.

Young AB, Snyder SH (1974) The glycine synaptic receptor: evidence that strychnine binding is associated with the ionic conductance mechanism. Proc Natl Acad Sci U S A 71: 4002-4005.

Young TL, Cepko CL (2004) A role for ligand-gated ion channels in rod photoreceptor development. Neuron 41: 867-879.

Zafra F, Gomeza J, Olivares L, Aragon C, Gimenez C (1995) Regional distribution and developmental variation of the glycine transporters GLYT1 and GLYT2 in the rat CNS. Eur J Neurosci 7: 1342-1352.

Zhang HG, ffrench-Constant RH, Jackson MB (1994) A unique amino acid of the Drosophila GABA receptor with influence on drug sensitivity by two mechanisms. J Physiol 479 (Pt 1): 65-75.

Zheng F, Erreger K, Low CM, Banke T, Lee CJ, Conn PJ, Traynelis SF (2001) Allosteric interaction between the amino terminal domain and the ligand binding domain of NR2A. Nat Neurosci 4: 894-901.

Zhou L, Chillag KL, Nigro MA (2002) Hyperekplexia: a treatable neurogenetic disease. Brain Dev 24: 669-674.

Zhou ZJ (2001) A critical role of the strychnine-sensitive glycinergic system in spontaneous retinal waves of the developing rabbit. J Neurosci 21: 5158-5168.